THE
PHYSICAL REVIEW

A journal of experimental and theoretical physics established by E. L. Nichols in 1893

SECOND SERIES, VOL. 73, NO. 12 JUNE 15, 1948

Compact Electrostatic Generator for the Production of Positive Ions*

W. E. DANFORTH, E. L. HUDSPETH, C. E. MANDEVILLE, AND C. P. SWANN
Bartol Research Foundation of the Franklin Institute, Swarthmore, Pennsylvania

(Received March 4, 1948)

The design and operational characteristics of a compact pressurized electrostatic generator are described. The machine is operated in a pressure vessel with an over-all height of 13 feet, and positive ions have been accelerated to energies up to 1.75 Mev through a tube 5 feet long. The potential gradient thus achieved along the tube is 350 kv/ft., which is considerably greater than the average value achieved by other positive ion accelerators thus far reported. It is believed that even the present voltage limitation can be extended.

I. INTRODUCTION

IN the summer of 1939 plans were formulated for the construction at the Bartol Foundation of a compact electrostatic generator ("statitron") for the acceleration of positive ions. The basic design was completed by one of us (WED) after a consideration of published reports,[1] supplemented by discussions with persons who have had experience with high voltage machines. By 1941[2] the machine had been assembled in rudimentary form, but the beginning of the war forced us to abandon this work temporarily. In August, 1946, the work was resumed by the three last named authors toward further development of the machine, and, in particular, of those features having to do with the acceleration of positive ions.

Difficulty was encountered in maintaining, during summer weather, a humidity low enough so that the insulating material of the generator, if exposed for a few hours or days to moist air, would dry out again in a reasonable time when the pressure vessel was put over the machine and dry air circulated through it. (Humidity control equipment was not available at the time.) The insulation problem became progressively more acute, and was aggravated by such sparking as did occur during operation; our voltage limitation dropped to about 800 kilovolts. It was decided, therefore, to change insulating materials and to make other rather extensive improvements which our experience indicated as desirable, and in the summer of 1947 two of us (ELH and CPS) accordingly began this work.

The results reported in this paper represent the total of the effort which has been made to develop this generator to its present operating condition.

* The work reported herein has been assisted by the Office of Naval Research since June 1946. The basic parts of the machine were fabricated through the use of Bartol funds.

[1] R. G. Herb, D. B. Parkinson, and D. W. Kerst, Phys. Rev. **51**, 75 (1937); J. G. Trump and R. J. Van de Graaff, Phys. Rev. **55**, 1160 (1939); W. H. Wells, R. O. Haxby, W. E. Stephens, and W. E. Shoupp, Phys. Rev. **58**, 162 (1940); I. A. Getting, J. B. Fisk, and H. G. Vogt, Phys. Rev. **56**, 1098 (1939); T. Lauritsen, C. C. Lauritsen, and W. A. Fowler, Phys. Rev. **59**, 241 (1940); J. H. Williams, L. H. Rumbaugh, and J. T. Tate, Rev. Sci. Inst. **13**, 202 (1942).

[2] W. E. Danforth and E. L. Hudspeth, Phys. Rev. **60**, 170 (1941).

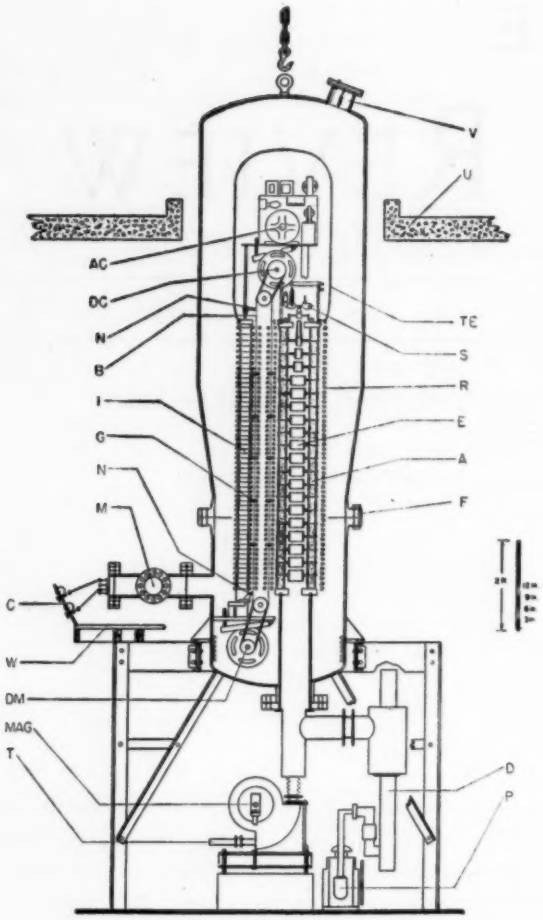

FIG. 1. Sectional view of the Bartol generator. The belt *B* is driven by a 10-horsepower motor *DM*. Charge is sprayed on and subsequently removed through corona needles *N*, *N*. The upper pulley is coupled by a V-belt to a 1.5-kw d.c. generator which supplies current for the arc of an ion source *S* and also drives an a.c. converter. The upper assembly is covered by a terminal electrode, *TE*, which was spun from copper. The belt itself is centered by guards *G*. The supporting structure consists of 52 equipotential rings *R*, separated by Textolite insulators *I*. The accelerating tube is built up of porcelains, *A*, which support electrodes, *E*, and which are evacuated through pumps *D* and *P*. The positive ion beam is resolved by use of the magnet *MAG* and the selected component impinges on target *T*. The energy of the bombarding particles is measured by the voltmeter *V* (which is at present of the generating type). The controls *C* pass from the outside of the tank to the terminal electrode through suitable shafting and insulating rods. Internal leads are brought in through the manifold *M*. The pressure vessel is separable at flange *F*, and the equipment inside the tank is then accessible from platform *W*. The tank, when raised, may be moved along the upper floor *U*, thus permitting use of the hoist for disassembly and replacement of other component parts of the generator.

II. GENERAL NATURE OF THE DESIGN

It was our purpose to build a pressure-insulated generator of compact design, utilizing a low voltage arc to produce positive ions which are homogeneous in energy to a hundred volts or so. The space available indicated the desirability of constructing a vertical machine in a pressure chamber which would occupy the lower floor of our building, with provision for removing the pressure cap through a hole in the ceiling (see Fig. 1). The vertical dimensions of the machine were therefore set by the distance from the floor of the first story of the building to the ceiling of the second floor. After allowing room for removal of the pressure cap as a single unit and additional room beneath the vessel for the analysis of the emergent ion beam, it appeared that the over-all height of the tank should be about 13 feet. The apparatus at the terminal electrode was to be housed in a spinning of vertical height of about four feet, clearance for the belt drive-motor and associated equipment was nearly two feet, and the space required for insulation between the terminal electrode and the wall of the pressure vessel was estimated to be something over one foot. This left approximately five feet for the maximum length of our accelerating tube, and it was hoped that it would withstand a potential difference of at least 1.5-million volts between its ends. Using 1.5-million volts as a rough working limit for the generator, the remainder of the dimensions were adjusted and a final design was formulated. The various components of the generator and something of the operation of the completed unit will be described in the following sections.

III. PRESSURE VESSEL AND STORAGE TANKS

The pressure vessel was constructed in two parts, separable at a flange which accommodates 36 $1\frac{1}{4}$ in. bolts. Removal of the upper section exposes nearly all of the internal parts of the generator. This section can be lifted by an electric hoist in about five minutes, and provision is made for rolling it along the second floor for storage; the hoist may then be used to raise the terminal electrode assembly, or, if necessary, the entire column or bottom motor plate. The general dimensions of the tank may be gauged from Fig. 1; it is 44-in. in maximum diameter and has a wall thickness of $\frac{7}{16}$ in. The tank may be evacuated completely, and it has an internal

working pressure of 200 pounds per square inch. Its volume is 110 cubic feet.

Since we planned originally to use compressed air in the generator, no provision was made for gas storage. One fire and the danger of additional fires proved to us the desirability of using gases which would not support combustion, but the cost of likely gases (nitrogen and freon) was too great unless storage could be provided. We accordingly made use of four tanks (of the type used for oxygen storage on submarines) for gas storage; the generator tank may be exhausted into these tanks, and the stored gas subsequently pumped again into the generator.

IV. SUPPORTING COLUMN AND EQUIPOTENTIAL RINGS

We adopted the design of Herb and his collaborators[3] as regards the use of equipotential rings for controlling voltage gradients. Fifty-two rings, made of $\frac{3}{4}$-in. brass tubing and 24 in. in diameter, are built up with three insulators made of corrugated Textolite between adjacent rings.[4] The potential difference between the rings is established by placing a 500-megohm resistance between them, and the total resistance of our column is hence approximately 2.5×10^{10} ohms.

The insulating Textolite supports for the rings snap into place as the rings are placed on top of one another, and each ring also supports a removable belt guard of the type described by Trump and Van de Graaff.[4] These guards have effectively shielded the belt up to our maximum operating voltage. Because of the importance of keeping the belt well centered between the guards, we have installed guides on both the inside and outside of the belt; these are placed on every tenth ring, the design of which was copied from Trump. Each guide consists simply of a glass rod set in a machined groove in an aluminum rod. The belt just touches the surface of the rods, and many hours of running have shown no appreciable wear. Guides of Textolite and hard rubber tubing were also tested, but the glass guides were much more satisfactory.

[3] R. G. Herb *et al.*, reference 1, and subsequent papers from the University of Wisconsin.

[4] J. G. Trump and R. J. Van de Graaff, reference 1.

V. ACCELERATING TUBE

The accelerating tube was made up of 20 corrugated porcelains, each of which was $3\frac{1}{8}$ in. high, $6\frac{1}{2}$ in. I.D., and 11 in. O.D. It would doubtless be worth while to use more[5] procelain sections—probably one should be associated with each equipotential ring. However, these porcelains were available at the time and it was felt originally that the upper limit of voltage on the generator would not be set by tube breakdown. The porcelains were heated and cemented to stainless steel electrode supports with Apiezon W (mixed with a small amount of pump oil). The column has been quite vacuum tight except for a slight amount of initial difficulty. The electrodes inside the accelerating tube are made of cylinders, rounded on the ends, and each $2\frac{3}{4}$ in. in height and $4\frac{1}{2}$ in. in mean diameter. The electrodes nearest the ion source, however, are graded in diameter from about 1 in. to this maximum size.

VI. BELT, DRIVE MOTOR, AND CHARGING SYSTEM

The charging belt is driven by a 10-horsepower motor which is placed in the bottom of the pressure vessel. Charge is sprayed onto the belt from a series of corona needles which are fed by a 50,000-volt adjustable supply. The lower pulley is insulated from ground through a microammeter, and we are thus able to measure leakage of the belt and to observe direct sparking to the pulley. The belt runs at 3800 ft./sec. over balanced pulleys, each 4 in. in diameter, and drives a belt which is 13 in. wide.

Both rubberized fabric belts and a Tilton endless woven cotton belt have been tried. The Tilton belt is much smoother in operation, as others have also observed, and is now used. The cotton belt does not now constitute a fire hazard (in a nitrogen-freon atmosphere), but we understand that coated cotton belts which are fire resistant can be obtained.

The spray-on voltage required to attain a given potential on the terminal electrode is, of course, a function of the pressure and nature of the gas in the tank, the distance from the needles to the surface of the belt, and the value of the tube current. Charge from the belt is drawn off

[5] Lauritsen *et al.*, reference 1.

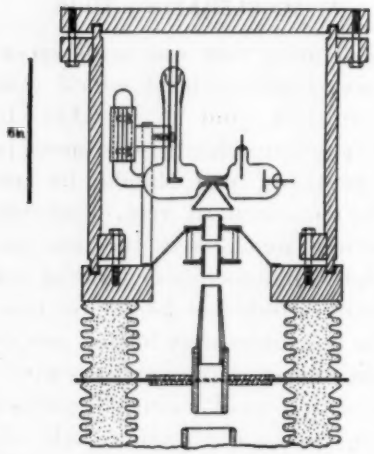

FIG. 2. This drawing shows the ion source, which was constructed of glass, in position at the top of the accelerating tube. The focusing electrodes are shown beneath the cone-shaped electrode which protrudes into the glass capillary. Electrical leads are brought in through tungsten rods set in glass grinds.

at the terminal electrode by a set of needles similar to those used for spray-on; return charge can be drawn from the terminal electrode by charging still another set of needles by induction (the upper pulley being insulated), but the voltage has not been as steady under these conditions and this plan was abandoned. In neither case is the upper limit on voltage which the generator will achieve set by any lack of charge carrying capacity of the belt, since a single run of belt will carry several hundred microamperes.

VII. TERMINAL ELECTRODE AND ION SOURCE

All equipment at the high potential end of the column is housed inside a large copper spinning. This equipment includes a 120-volt, 2-kw d.c. generator, driven from the upper pulley of the generator. This furnishes d.c. power for a low voltage capillary arc (see Fig. 2) and also drives a 1-kw d.c.-a.c. converter. The 110-volts a.c. from this converter supplies, through Variacs and suitable associated circuits, the power for (a) a "tickler" voltage of 800-volts a.c. for initiating the discharge in the ion source, (b) a variable voltage—300 volts negative to 100 volts positive—which may be applied to a cone-shaped (see Fig. 2) electrode for the purpose of obtaining initial focusing of the ion beam, (c) a focusing voltage of 0 to 4000 volts negative on the electrode just beneath the cone, and (d) another focusing voltage of 0 to 15,000 volts negative on the next electrode. Power is also supplied for (e) heating a palladium leak which regulates the flow of hydrogen, and (f) the cathode of the ion source. Both oxide-coated cathodes and thoria-coated cathodes have been used; either is satisfactory, although the former are subject to "poisoning" and the latter dissipate considerable heat. About 15 watts are required for the oxide-coated cathode and nearly 50 watts for the thoria-coated cathodes, with an emission in each case in excess of 500 milliamperes.

It was observed, with compressed air in the pressure tank, that the d.c. generator often failed to deliver current. Various types of brushes were tried, but no reliable performance was attained under pressure. This trouble vanished, however, when the gas in the tank was changed to a nitrogen-freon mixture, and it has not recurred.

VIII. CONTROL SYSTEM

The circuits enumerated in the previous section may be controlled as follows: Steel rods pass through suitable glands in a pressure-tight manifold. These rods are then individually connected through flexible shafting to a gear box located at the bottom of the lowest equipotential ring. Control is then carried to the terminal electrode through lengths of Pyrex rod; these rods terminate in another gear box which connects flexible shafting to the Variacs or potentiometers which must be adjusted. The system has been quite reliable, and calibrated dials on a panel outside the generator enable us to determine the settings of the circuits inside the terminal electrode. Flashlight bulbs associated with various circuit elements were used, together with a suitable lens system and photoelectric cells at the base of the column, to determine the actual functioning of the circuits. These were not found to be necessary, however, and their use was discontinued before the system was really perfected.

The Pyrex rods which are now used in our control system were installed after Textolite tubes had caused a fire in the generator when it was operating in compressed air. The fire melted solder on some of the equipotential rings and we were forced to recement our accelerating

tube. No really major damage was inflicted, but the control rods were changed to Pyrex. Pyrex tubes were also tested, but were not satisfactory because of the discharges which occurred inside the tubes, and which limited the voltage which the set could generate.

IX. COOLING SYSTEM AND DRYING OF GAS

During operation of the set the power dissipated in the pressure vessel amounts to about 8 kilowatts, most of which is expended in driving the belt. In order to prevent excessive heating of the equipment, water is circulated through eight coils of copper tubing which are wound around the inside of the tank at about the height of the motor.

It is, of course, necessary to maintain a low relative humidity inside the tank. When air was used in the vessel, it was pumped in through a drying agent, and the air could be further dried by use of a blower which pulled it over potassium hydroxide sticks. At present the tank is dried by simply evacuating it, then admitting dry gas.

The relative humidity rises to values around 80 percent or more in the Philadelphia area during the summer, and if the tank is open to room air for a few hours during such weather, it may be several days before it can be dried out sufficiently to operate at high voltages again. In any case, humid air on the outside of the tank has caused trouble with spray-on leads and with other equipment which is used with the generator. It is highly desirable to provide suitable control of humidity. As a temporary measure we have, on occasion during humid weather, simply blown the room air over calcium chloride crystals (used commercially as ice cream salt), thus lowering the humidity to a point where tests and preliminary adjustments on the machine could be conducted in the air (without putting on the pressure cap).

X. OPERATION OF THE GENERATOR

The generator has been operated with a positive ion beam from 150 kev to 1750 kev. The beam is analyzed by means of a magnet (see Fig. 1) which bends the selected component through a right angle, sending it onto a target about 20 in. above the floor of the room. The total positive ion current has been as great as 40 microamperes or more, but in such cases focusing has been poor and operation of the set correspondingly erratic. This condition was improved by placing a small diaphragm in one of the focusing electrodes. Although the current was considerably diminished, operation of the set was quite steady. We obtain about 0.1 to 2 or more microamperes of resolved beam; the atomic beam is sometimes nearly as intense as the molecular beam, but the latter is more often 50 percent greater. It is known that we could substantially increase our beam current, but it has not thus far proved necessary to have greater currents. It would seem, from the reported experience of others, that we should extend our focusing control to at least one more accelerating electrode, and this can be readily done.

Voltage on the terminal electrode is measured by a generating voltmeter (which replaced the electrostatic instrument shown in Fig. 1) of a previously tested design.[6] Current from this voltmeter is balanced by a calibrated cell and a decade resistance box, and fluctuations are observed as a galvanometer deflection. Within observational limits imposed by a 3-second galvanometer period, our set is steady to somewhat less than $\frac{1}{4}$ percent for periods of half a minute or so; a fine-control adjusts spray-on current to compensate for voltage fluctuations on the terminal electrode, and a system of highly stabilized voltage control will be installed when experiments requiring it are undertaken. Magnet current is held constant during a run by a highly accurate control system which will be suitable in its present form for high resolution of the ion beam. The low voltage spread of our beam as it emerges from the ion source should be of particular advantage for this type of work.

Current may be drawn from the terminal electrode through a small metal rod (probe) which passes through the pressure vessel and whose distance from the electrode is adjustable. This probe may be used for voltage changes, and it serves to stabilize the set when large currents are drawn down the tube. Its function in this respect is apparently not so important as in the case of generators which utilize corona discharge instead of resistors between equipotential rings.

[6] J. G. Trump, F. J. Safford, and R. J. Van der Graaff, Rev. Sci. Inst. **11**, 54 (1940).

Incidentally, the current flowing through these resistances can be observed, and gives an indication of the voltage on the terminal electrode. This current, at a given set voltage, appears quite steady after the generator has become well dried out, but we rely on the generating voltmeter for voltage measurements.

The maximum voltage at which we can operate at present is limited by sparking inside the accelerating tube; with about 10 pounds of freon and 70 pounds of nitrogen inside the pressure vessel, sparking from the terminal electrode and between equipotential rings was eliminated. No difficulty with sparking down the cotton belt has yet been observed, although a temporary difficulty was once experienced with a rubber fabric belt.

Although tube breakdown limits the maximum voltage which we can obtain with this generator, the potential gradient which has been achieved with the present tube is substantially larger than has been generally achieved heretofore. Breakdown occurs at 350 kilovolts per foot of tube in this generator, whereas 200 kilovolts per foot is an approximate average of performance thus far reported in the literature of positive-ion generators. Several generators reported were not limited by tube breakdown, however, and hence no direct comparison of limiting tube gradients is possible.

It would seem advisable to increase the number of porcelain sections in order to establish smaller potential drops per section, and this will probably be done in the future. The ultimate voltage should exceed 2 Mev, and this limit will probably be again set (judging also by experience of the M.I.T. group) by the accelerating tube.

ACKNOWLEDGMENTS

The fabrication of component parts for the generator has been performed wherever possible within the Bartol Foundation. The services of the head of our shops, Mr. R. C. Pfeiffer, and of the chief glassblower, Mr. Austin Nester, and the technical assistance of Mr. E. T. Kurtzner and Mr. J. T. Peoples are all gratefully acknowledged. Mr. J. F. Marshall and Mr. Wayne Lees also gave valuable assistance in early stages of the work prior to the war.

We are particularly indebted to other experimenters for their comments and advice at various times during the design and construction of the generator. Drs. M. A. Tuve, I. A. Getting, E. S. Lamar, J. G. Trump, R. J. Van de Graaff, and W. W.. Buechner have been particularly helpful in this respect.

It is a pleasure to acknowledge the helpful interest of Dr. W. F. G. Swann, Director of this Foundation, during the entire course of this undertaking.

Cosmic-Ray Investigations on Mt. McKinley*

THOMAS D. CARR, MARCEL SCHEIN, AND IAN BARBOUR
Department of Physics, University of Chicago, Chicago, Illinois
(Received March 11, 1948)

Three cosmic-ray experiments were carried out on Mt. McKinley (Alaska) at an altitude of 18,100 feet. The first experiment measures the absorption curve of penetrating particles in Pb thicknesses up to 50 cm. A large number of slow mesotrons of energies around 200 Mev was found. From the measured mesotron energy spectrum on Mt. McKinley a calculation was made to determine the spectrum which would be anticipated at 14,250 feet (Mt. Evans, Colorado). The result is compared with experimental data obtained on Mt. Evans. The discrepancy between the two curves strongly indicates that an additional production of mesotrons of energies less than 400 Mev takes place in the atmosphere between these altitudes. The other two experiments at 18,100 feet investigate the production of penetrating particles by ionizing and non-ionizing radiation in lead and paraffin.

DURING the Spring of 1947 there was organized an expedition to Mt. McKinley, Alaska, one objective of which was to undertake cosmic-ray investigations at an altitude previously attainable only in short-duration plane flights. Since the conditions under which observations were made were very difficult, it was necessary to make the equipment as simple as possible. The apparatus was all assembled at the University of Chicago and dropped by parachute from an airplane at Denali Pass between the two peaks of Mt. McKinley where the high altitude camp was established. Here, H. T. Victoreen, who was in charge of the experiment, carried out the actual measurements in a hut which was located at an altitude of 18,100 feet. The temperature in the hut was kept within 3° of 10°C, despite extremely low temperatures outside.

EXPERIMENT I: ABSORPTION OF PENETRATING PARTICLES

Figure 1 shows the geometry of the first counter experiment in which the intensity of penetrating radiation at 18,100 feet was investigated. Recording apparatus measured counts from (a) the upper telescope (fourfold coincidences 1–2–3–4), (b) the lower telescope (fourfold coincidences 2–3–4–5), and (c) showers (fourfolds from the out-of-line system 1–6–3–4). The resolving time of the coincidence sets was 20 microseconds. All counters had the same dimensions, 7 in.×1 in. In successive ten-hour recording intervals various thicknesses of lead were placed at positions A, B, and C; a narrow ($1\frac{7}{8}$″) vertical column of lead plates was used to minimize scattering. The fact that the recording rate for a given total thickness of lead in a telescope remained uniform and did not depend on how that thickness was distributed between the positions A, B, and C strongly indicates that scattering played a negligible role in this experiment. The shower rate, about 6 per hour, showed little variation with the thickness or position of

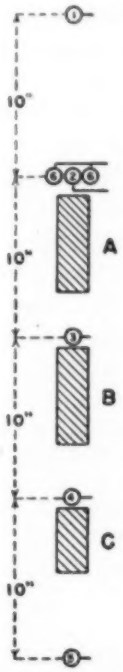

Expt. I

FIG. 1.

* This research was supported in part by Navy Contract N6ori-20, Task Order XVIII.

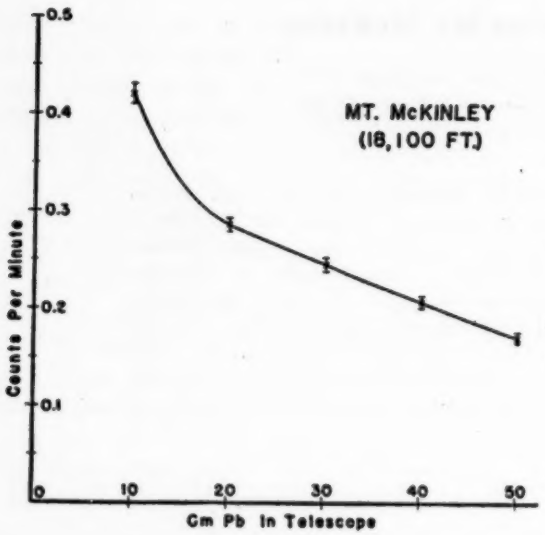

FIG. 2.

the lead plates. The counting rate of the *upper* telescope, averaged over recording intervals when it included a given total thickness of Pb, agreed in all cases within statistical error with the average rate of the *lower* telescope during recording intervals when it included the same total thickness of Pb. The intensity of penetrating particles was obtained by averaging the coincidence rate of the upper (a) and lower (b) telescopes for each case in which the thickness of lead included in the telescopes was the same, and then subtracting showers (c). The results are shown in Table I. The counts per minute are plotted in Fig. 2 against the total thickness of Pb in the telescope. The ratio of intensity through 18-cm Pb at McKinley to that in initial tests at Chicago near sea level is 3.0. This may be compared with data from balloon flights by Schein and others,[1] who find the intensity through 18-cm Pb increases by a factor of 3.1 between sea level and 18,000 feet.

EXPERIMENT II: PRODUCTION OF MESOTRONS BY NON-IONIZING RADIATION

The apparatus for direct investigation of production of penetrating particles by non-ionizing radiation in lead and paraffin is shown in the left portion of Fig. 3. It is designed to give information about radiation which is non-ionizing when incident on the apparatus from above and hence does not actuate the upper three anticoincidence counters 5, but which in interacting with the matter placed at *D* gives rise to a penetrating ionizing particle capable of actuating the telescope 1–2–3–4 containing 10 cm of Pb. Two anticoincidence counters are also placed on either side of the counter 1 to give additional protection against showers. Counters 1, 2, 3, and 4 are 1 in.×7 in.; all the counters 5 are 1 in.×17 in. The inefficiency of the anticoincidence arrangement was measured at Chicago to be 0.5 percent. However, initial tests at Chicago with a radium source increasing the total background rate by a factor of 12 (giving single-tube counting rates comparable to those at McKinley) indicated an inefficiency of 1.2 percent under those conditions. The counts recorded on Mt. McKinley are listed in Table II. The first entry, "mesotrons," is the number of fourfold coincidences of the telescope 1–2–3–4 with all the anticoincidence counters 5 removed, and represents the intensity of particles penetrating 10-cm Pb within the solid angle of the telescope. A recording interval (4.70 hours), equal to the time in which 1000 counts were thus registered with the anticoincidence counters removed, was used in all subsequent runs so that the resulting data can easily be read as percentage of the mesotron intensity. With various thicknesses of lead and paraffin inserted at *D*, the number of counts of counters 1–2–3–4 in coincidence and counters 5 in anticoincidence found during each interval are shown. Repeated values represent duplicate runs under the same conditions. The counts (about 2 percent of the total mesotron intensity) recorded with no material in position *D* are most probably attributable to inefficiency, since the solid angle of the telescope was completely covered by the anticoincidence counters and the chances are practically negligible for either (a) showers which could strike 1, 2, 3, 4, and none of the counters 5, or (b) mesotron production in

TABLE I.

Cm Pb	10	20	30	40	50
Counts/min.	0.420	0.285	0.244	0.206	0.170
Prob. error	±0.010	±0.007	±0.007	±0.006	±0.005

[1] Marcel Schein and D. J. Montgomery, *Problems in Cosmic Ray Research* (Princeton University Press, Princeton, New Jersey, 1946).

he counter walls or in the air gap at D. Introduction of either lead or paraffin at D changes the counting rate by an insignificantly small amount. Allowing for the statistical errors of the experiment, it can be stated that any production by non-ionizing radiation of mesotrons capable of penetrating 10-cm Pb, at a rate greater than 3 percent of the total mesotron intensity, certainly could not have escaped detection. Hence, for the number of mesotrons capable of penetrating 10-cm Pb produced by non-ionizing radiation in up to 6 cm of Pb and paraffin at 18,100 feet, we may set an upper limit of 3 percent of the total mesotron intensity through 10-cm Pb.

Two additional runs were carried out to investigate multiple production of mesotrons by non-ionizing radiation. With 6-cm Pb at D in Experiment II, the two counters 6 connected in parallel were added as shown below the bottom absorber, and counts with 1–2–3–4–6 in coincidence and counters 5 in anticoincidence were recorded. The very low counting rate (7 and 1 counts per 4.7 hour interval, respectively) under these conditions indicates the excellent shower-protecting ability of the anticoincidence arrangement. In view of the results above in which single particles were recorded, it is not surprising that no measurable effect of multiple production was found.

EXPERIMENT III: PRODUCTION OF MESOTRONS BY IONIZING RADIATION

The apparatus designed to investigate the production of mesotrons by ionizing radiation is shown in the right section of Fig. 3. The two counters 3 and 4 on either side are just clear of the line of counters 1, 2, and 5 so that it is impossible for one or even two particles traveling in a straight line to activate all the counters. All five counters can be activated, however, by an incident ionizing particle which, in addition to being able either itself to penetrate the block E plus 10-cm Pb or to give rise in the block E to an ionizing particle capable of penetrating 10-cm Pb, can *also* produce in the block E at least two ionizing particles with an angular spread suitable to actuate counters 3 and 4. Since there is no shower protection, a shower of five particles can also cause a coincidence of all five counters. The fivefold coincidences 1–2–3–4–5 recorded with various thicknesses of lead and paraffin at E are shown in Table III. The counts for each thickness of absorber cover a ten-hour period during which about 780 penetrating particles would have passed through the vertical telescope 1–2–5. Comparison with the shower rate in Experiment I leads one to expect here a shower rate of the same order of magnitude as

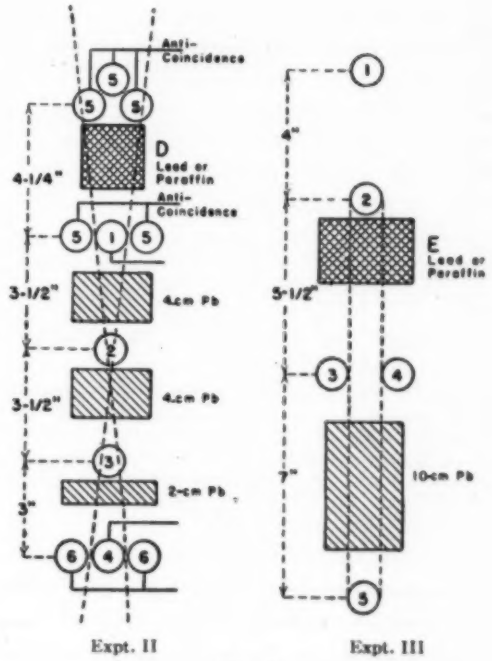

FIG. 3.

TABLE II.

("mesotrons" Absorber at D	Counts (4.7 hrs.) 1000)
No absorber	18, 21
1-cm Pb	17
2-cm Pb	17, 20
6-cm Pb	24, 24
3-cm paraffin	21
6-cm paraffin	22

TABLE III.

Absorber at E	Counts (10 hrs.)
No absorber	49
1-cm Pb	71
2-cm Pb	56
5-cm Pb	46
No absorber	43
2.5-cm paraffin	45
5-cm paraffin	51

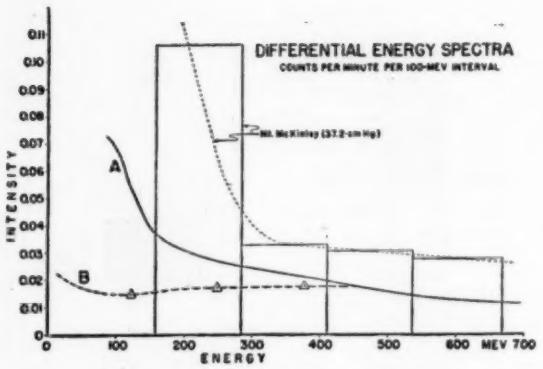

FIG. 4. The blocks and dotted curve represent the differential mesotron energy spectrum obtained on Mt. McKinley. Curve *A* is the Mt. Evans (45.7-cm Hg) spectrum from data of D. Hall. Curve *B* is the spectrum anticipated at 45.7-cm Hg, calculated by the diffusion of the mesotrons of the McKinley spectrum.

the rates recorded in Table III. The rates (49, 43) with no absorber at *E* must have been entirely due to showers, and the rates when an absorber was introduced can probably be attributed to the same cause.

DIFFERENTIAL ENERGY SPECTRUM

From the absorption curve of Experiment I one can obtain a differential energy spectrum for the penetrating radiation. Only a negligible number of electrons can have been included in the curve of Fig. 2. Electrons of energy sufficient to penetrate 10-cm Pb or more should occur at this altitude predominantly in the core of air showers which are dense enough so that if they actuated circuit (*a*) or (*b*) they would also have tripped the shower circuit (*c*). The shower rate was subtracted before the absorption curve was plotted. A check on the absence of an appreciable high energy electron component was afforded by the other two experiments. In Experiment III above, electrons able to penetrate 10-cm Pb would in passing through the block *E* have given rise to other ionizing particles with a probability high enough to have been detected; in Experiment II, photons, which would be in approximate equilibrium with any high energy electron component, would have created in a narrow lead plate at *D* electrons that would have recorded in the lower telescope. Neglecting any appreciable contribution to the counting rate by high energy protons, which cloud-chamber[2] work at similar altitudes has shown to be small in the same energy range, it has been assumed that the radiation producing our absorption curve consists predominantly of mesotrons. Range-energy relationships for ionization losses of mesotrons assumed to have mass 200 m_e make possible the calculation[3] of the number of mesotrons having energies sufficient to penetrate 10-, 20-, 30-, 40-, and 50-cm Pb. From the differences between values for these successive thicknesses a differential energy spectrum of the mesotrons has been obtained. This block spectrum is plotted in Fig. 4; the height of each block represents the number of counts (per min. per 100-Mev interval) produced by mesotrons traversing the telescope with energies in the energy range indicated by the base of the block.

On the basis of the McKinley spectrum at 37.2-cm Hg, calculations have been carried out to obtain the mesotron spectrum which would be expected at the elevation of Mt. Evans, 45.7-cm Hg, on the following assumptions: (a) the mesotrons with which we are concerned lose energy predominantly by ionization; (b) they have a rest mass of 200 m_e and a mean life at rest of 2.1 microseconds; (c) their latitude effect between McKinley and Mt. Evans is negligible; and (d) no additional mesotrons are produced between these two altitudes. A formula in which ionization loss and mesotron decay are combined gives the diffusion of mesotrons. According to these calculations the McKinley mesotron spectrum will give rise to a spectrum at the altitude of Mt. Evans, as shown by the curve *B*. (The points indicated by triangles were obtained from the midpoints of the three blocks in the right portion of the McKinley spectrum. The dashed curve *B* is obtained by using the dotted curve above drawn to fit the blocks of the McKinley spectrum.)

For comparison, there is also plotted in Fig. 4 the differential mesotron energy spectrum *A* from the experimental data obtained on Mt. Evans by Hall.[4] We have normalized his data to ours by using the ratio of mesotron intensity through 167 g/cm² Pb between Mt. Evans and sea level found by Greisen.[5]

[2] W. M. Powell, Phys. Rev. **69**, 385 (1946).

[3] We are indebted to Dr. John A. Wheeler for the use of energy-range curves calculated at Princeton.

[4] D. Hall, Phys. Rev. **66**, 325 (1944).

[5] K. Greisen, Phys. Rev. **61**, 212 (1942).

DISCUSSION OF SLOW MESOTRON INTENSITIES

The large discrepancy between the experimental curve *A* and the curve *B* predicted on the basis of the McKinley spectrum, strongly indicates that considerably more mesotrons of energy less than 400 Mev are found on Mt. Evans than could, according to our assumptions, have diffused to that point from higher altitudes. It seems difficult to account for this discrepancy except by the production of mesotrons in the atmosphere between the two elevations, 18,100 and 14,250 feet. The difference between curves *A* and *B* between 80 and 400 Mev represents a production of mesotrons totaling about 0.06 counts per minute in the McKinley telescope (or equivalent to 0.17 mesotrons per min. per unit solid angle per cm²), which corresponds to 14 percent of the McKinley mesotron intensity through 10-cm Pb. This production must have taken place between McKinley and Mt. Evans altitudes in a layer of air of mass 115 g/cm². Furthermore, it is very difficult to imagine that the lower energy ranges of the McKinley mesotron spectrum itself could have been produced solely by the diffusion of mesotrons from near the top of the atmosphere; this large increase at low energies seems another direct indication of some secondary process. A remarkably large intensity of mesotrons at this same altitude and energy (200 Mev) has also been reported from airplane cloud-chamber investigations by Moore and Brode.[6]

Production of mesotrons has been previously investigated by several authors. On Mt. Evans, Tabin[7] and Rossi and Regener[8] found that production of penetrating particles by non-ionizing radiation in thicknesses up to 124 g/cm² Pb and 9 g/cm² paraffin was not greater than 1 percent of the Mt. Evans mesotron intensity through 10-cm Pb. However, a considerable production was reported above 25,000 feet by Schein and Wilson.[9] The results in our Experiments II and III on the production of mesotrons by ionizing and non-ionizing radiation in thicknesses up to 68 g/cm² Pb and 5 g/cm² paraffin at 18,100 feet have been presented. Although adverse weather conditions cut down the recording time and hence the accuracy of these experiments, no positive evidence for any production effect in matter was found, and it appears that any production in excess of three percent of the total mesotron intensity could not have escaped detection. The calculated production effect of 14 percent of the McKinley mesotron intensity, in the layer of air of 115 g/cm², seems larger than can be accounted for by the results of the experiments on Mt. McKinley with solid matter. Further experiments of higher precision should clearly demonstrate whether production of mesotrons in matter is frequent enough to account for the large number of slow mesotrons, or whether some other process may be involved. The decay of a neutral particle (such as that reported by Rochester[10]) into positive and negative mesotrons, for example, while escaping detection in experiments with small layers of Pb and paraffin, could in traversing a long path in air give rise to an appreciable number of slow mesotrons.

We wish to thank Bradford Washburn, Director of the Boston Museum of Natural History, for his excellent leadership and cooperation during the whole expedition. It is a special pleasure to acknowledge the fortitude and skill of Mr. H. T. Victoreen in the actual operation of the equipment on the mountain under extremely rigorous conditions. General Carl A. Spaatz kindly made arrangements with the Army Air Forces to drop the apparatus by parachute at Denali Pass, which greatly facilitated carrying out the experiments.

[6] D. C. Moore and R. B. Brode, Phys. Rev. **73**, 532 (1948).
[7] J. Tabin, Phys. Rev. **66**, 86 (1944).
[8] B. Rossi and V. Regener, Phys. Rev. **58**, 83 (1940).
[9] Marcel Schein and V. C. Wilson, Phys. Rev. **54**, 304 (1938).
[10] G. D. Rochester and C. C. Butler, Nature **160**, 854 (1947).

The Beta- and Gamma-Rays of Ga^{72}

ALLAN C. G. MITCHELL, DANIEL J. ZAFFARANO, AND BERNARD D. KERN
Indiana University, Bloomington, Indiana

(Received March 2, 1948)

The beta- and gamma-ray spectra of Ga^{72} (14.1 hours) have been measured in a magnetic lens spectrometer. Measurement of the energies of photoelectrons produced in a thin lead radiator gave lines corresponding to gamma-rays of energies 0.631, 0.835, 1.05, 2.18, and 2.50 Mev, and indications of weaker lines at 1.30, 1.47, 1.57, and 1.81 Mev. An internal conversion line, produced by a gamma-ray of 0.691-Mev energy, was also found.

The beta-ray spectrum was found to be highly complex. It is possible to resolve the spectrum into seven groups with end-point energies at 3.17, 2.57, 1.74, 1.45, 1.00, 0.74, and 0.56 Mev.

I. INTRODUCTION

THE beta- and gamma-ray spectra of gallium 72 (14.1 hours) have been investigated with the help of a magnetic lens spectrometer.[1] Gallium exists as two stable isotopes, Ga^{69} and Ga^{71}, from which two radioactive species, Ga^{70}, half-life 20 min., and Ga^{72}, half-life 14.1 hours, have been shown to be formed by neutron capture.[2–4]

Some preliminary results on the spectrum of Ga^{72} have been known for some time,[5,6] but no detailed study has been made until recently. The distribution of Compton electrons produced by the gamma-rays in a metallic radiator was studied by Mandeville.[7] He used a small 180° type spectrometer and concluded that the spectrum consists of two equally intense gamma-rays of energies 1.17 ± 0.02 and 2.65 ± 0.06 Mev. Siegel and Glendenin[8] found, by absorption techniques, beta-group end points of 0.8 and 3.1 Mev, and one gamma-ray of 2.1 Mev energy. Recently Mitchell, Jurney, and Ramsey[9] made a study of the radiations from Ga^{72} by the use of coincidence counting methods. The beta-ray end point was determined by absorption to be 2.3 Mev. The most energetic gamma-ray, determined by coincidence absorption of the Compton electrons, appeared to have an energy of 2.4 Mev. Finally, measurement of gamma-gamma coincidences showed that there are several gamma-rays per disintegration. Measurements on beta-gamma coincidences as a function of the range of the beta-particles indicated that the beta-ray spectrum is complex and that a strong group of beta-rays with an end-point energy of approximately 0.8 Mev is also present. Later Mandeville and Scherb[10] made a similar study using these techniques with essentially the same results.

A determination of the gamma-ray spectrum, with the help of a magnetic lens spectrometer, was made by Miller and Curtiss,[11] who found gamma-rays at 0.64, 0.84, and 2.25 Mev. Finally, while the present authors' work was nearing completion, a report of an investigation of both the beta- and gamma-ray spectra was published by Haynes[12] with results quite similar to those to be given here.

II. APPARATUS AND PREPARATION OF SOURCES

The apparatus used in this investigation was a magnetic lens spectrometer of conventional design. The general details of the instrument have been described elsewhere[13] and need not be repeated here. An end window counter served as the detector of beta-particles in the instrument

[1] A. C. G. Mitchell, B. D. Kern, and D. J. Zaffarano, Phys. Rev. **73**, 1220 (1948).
[2] E. Amaldi, O. D'Agostino, E. Fermi, B. Pontecorvo, F. Rasetti, and E. Segrè, Proc. Roy. Soc. **A149**, 522 (1935).
[3] R. Sagane, Phys. Rev. **53**, 212 (1938); Phys. Rev. **55**, 31 (1939).
[4] J. J. Livingood and G. T. Seaborg, Phys. Rev. **54**, 51 (1938).
[5] R. Sagane, S. Kojima, and G. Miyamoto, Proc. Phys.-Math. Soc. Jap. **21**, 728 (1939).
[6] J. J. Livingood and G. T. Seaborg, Rev. Mod. Phys. **12**, 30 (1940).
[7] C. E. Mandeville, Phys. Rev. **64**, 147 (1943).
[8] J. M. Siegel and L. E. Glendenin, Rev. Mod. Phys. **18**, 513 (1946); Plutonium Project Reports **9B**, 7.1 (1946).
[9] A. C. G. Mitchell, E. T. Jurney, and M. Ramsey, Phys. Rev. **71**, 324 (1947).
[10] C. E. Mandeville and M. Scherb, Phys. Rev. **72**, 520 (1947).
[11] L. E. Miller and L. F. Curtiss, Phys. Rev. **70**, 983 (1946).
[12] S. K. Haynes, Phys. Rev. **73**, 187 (1948).
[13] B. D. Kern, D. J. Zaffarano, and Allan C. G. Mitchell, Phys. Rev. **73**, 1142 (1948).

and throughout these experiments it was fitted with a mica window of 4 mg/cm² surface density.

The sources were prepared by bombarding gallium oxide (Ga_2O_3) targets with 11.5 Mev deuterons in the Indiana University cyclotron. Bombardments ranging from 150–450 microampere hours were used.

The source was purified chemically in the following manner. The oxide was dissolved off the copper target plate with 12*N* HCl and the solution evaporated to dryness. A small amount of copper carrier was added, the solution was diluted to 100 cc, the hydrogen ion concentration adjusted to 3 normal, and the copper was precipitated as copper sulfide by H_2S. The filtrate was evaporated to a small volume and an ether extraction was made of the $GaCl_3$. The source was finally brought down as $Ga(OH)_3$ and converted to Ga_2O_3 by heating. The period of the active source was measured and only the 14.1 hour period of Ga^{72} was found. The twenty-minute period had, of course, disappeared by the time the chemistry was completed.

When the gamma-rays of gallium were to be investigated, the gallium oxide was placed in a cylindrical copper capsule, 1 cm outside diameter, with walls and end just thick enough to stop all beta-rays. If the distribution of photoelectrons was to be observed, a lead radiator, 1 cm in diameter and of 26 mg/cm² surface density (in some cases 75 mg/cm²) covered the end of the capsule. If, on the other hand, the distribution of Compton electrons was to be studied, no additional radiator was used. The preparation of the beta-ray sources will be described later.

III. THE GAMMA-RAY SPECTRUM

The distribution of photoelectrons ejected from a thin lead radiator by gamma-radiation from Ga^{72} was examined in the lens. A number of strong lines appeared corresponding to gamma-ray energies of 0.631, 0.835, 2.18, and 2.50 Mev. In addition, a careful search showed a weak gamma-ray at 1.05 Mev and a number of irregularities in the distribution of the photoelectrons apparently caused by the presence of weaker gamma-rays. In order to investigate these weak lines, a lead radiator of 75 mg/cm²

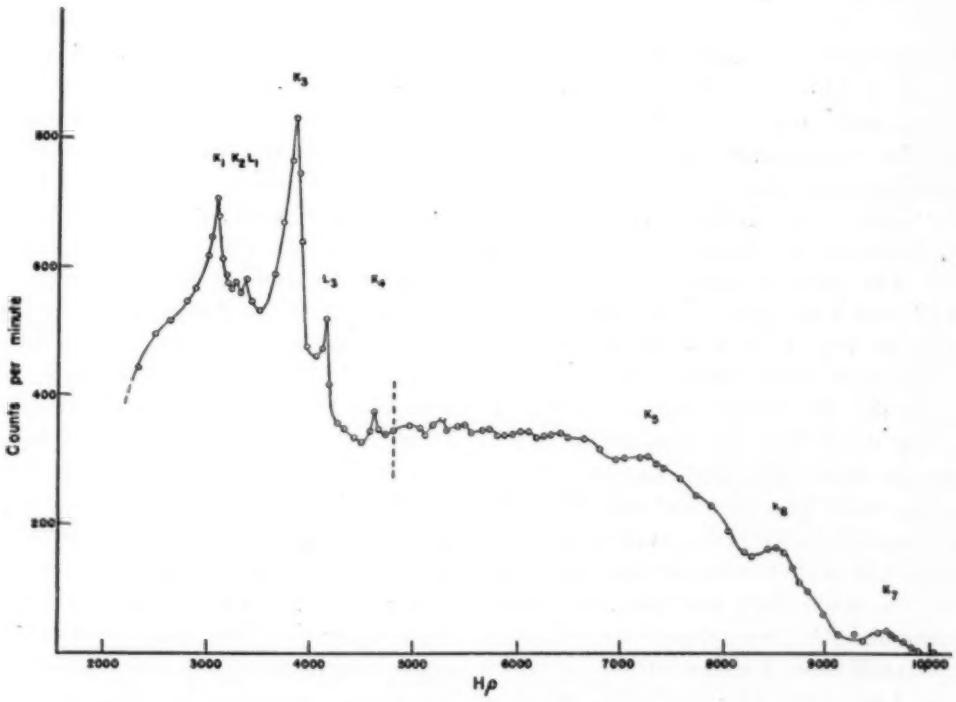

FIG. 1. Spectrum of photoelectrons ejected from lead by the gamma-rays of Ga^{72}. Below 4800 Hρ the lead radiator used had a surface density of 26 mg/cm²; above 4800 Hρ, 75 mg/cm². The gamma-ray energies are, respectively: K_1, L_1, 0.631 Mev; K_2, 0.676 Mev; K_3, L_3, 0.835 Mev; K_4, 1.05 Mev; K_5, 1.81 Mev; K_6, 2.18 Mev; K_7, 2.50 Mev.

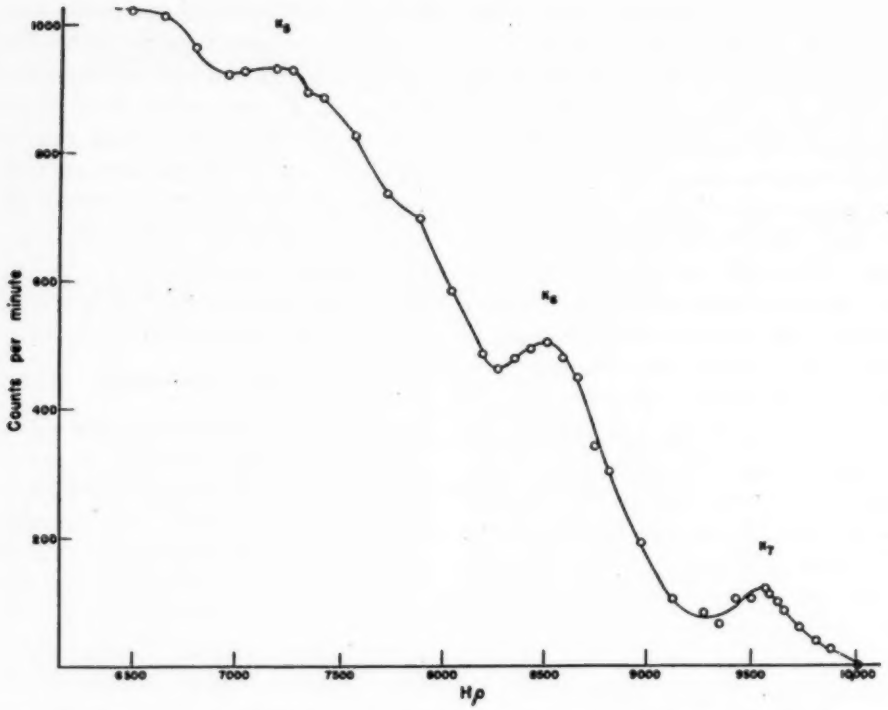

FIG. 2. Spectrum of photoelectrons ejected from lead by the higher energy gamma-rays of Ga^{72}. The lead radiator used had a surface density of 75 mg/cm². The gamma-ray energies are, respectively: K_5, 1.81 Mev; K_6, 2.18 Mev; K_7, 2.50 Mev.

surface density was used and the region from approximately 1 Mev to 3 Mev was carefully studied. This study brought to light a weaker line at 1.81 Mev. A composite curve of the photoelectron distribution is shown in Fig. 1, in which the various peaks are labelled. Figure 2 gives the enlarged view of the distribution at the high energy end. The peaks caused by gamma-rays at 1.81, 2.18, and 2.50 Mev can be clearly seen.

Returning to Fig. 1, it is evident that the strongest and most easily identifiable peaks on the curve, in the low energy region, are the K peak from the 0.631-Mev line and the K and L peaks from the 0.835 Mev line. Between the K peak from the 0.631 Mev line and that from the 0.835-Mev line will be seen two small peaks. The higher energy one of these two corresponds to the L peak of the 0.631-Mev line and the other, barely distinguishable, corresponds to a K peak for a line at 0.676 Mev. Farther out on the curve the lines at 1.05, 1.81, 2.18, and 2.50 Mev are clearly seen.

In order to get confirmation of the existence of these lines and to obtain an estimate of their relative intensities, the distribution of the Compton electrons from a copper radiator was studied. Figure 3 shows the results of this investigation. Here the number of counts per minute is plotted as ordinate against $H\rho$ (gauss-cm) as abscissa. The results confirm the existence of the gamma-rays at 2.50, 2.18, and 1.81 Mev, together with most of those of lower energy. In addition, there is some evidence for the existence of a gamma-ray at 0.691 Mev, and additional lines at 1.57, 1.47, and 1.30 Mev. The line at 0.69 Mev, if present, is quite weak. An estimate of the relative intensities of the stronger lines was obtained by using a method developed by Siegbahn.[14] In this method an "empirically-determined shape" is fitted to the data in Fig. 3. The higher energy components are fitted first, and the lower energy ones are then determined by subtraction. The areas under the individual curves are then calculated by integration and the intensities estimated by applying a correction for the efficiency of production of Compton elec-

[14] K. Siegbahn, Proc. Roy. Soc. **A188**, 541 (1947).

trons as a function of energy. The weak lines are taken together in one group. These results are shown in Table I. Since the intensities of the lower energy lines are determined by subtracting off the contributions from the higher energy lines, they are subject to rather large errors.

IV. THE BETA-RAY SPECTRUM

For the measurement of the beta-ray spectrum sources of high specific activity were used. In general, these required a bombardment of about 400 microampere hours of 11.5–Mev deuterons. The beta-ray sources were prepared by dissolving the active purified $Ga(OH)_3$ in HCl and evaporating a small drop of this solution on a thin Zapon film, approximately 0.1 mg/cm² surface density, or on an aluminum foil of surface density 1 mg/cm². These sources were approximately circular and varied in size from 0.5 cm to 1.0 cm in diameter. The surface density of the sources varied from 0.15 to 5.0 mg/cm².

Several determinations of the beta-ray spectrum were made. A plot of the spectrum is shown in Fig. 4. Here the number of counts per minute, corrected for decay, is plotted as ordinate against $H\rho$ (gauss-cm) as abscissa. Many points were taken, close together, and each point

TABLE I. Energies and relative abundances of beta- and gamma-rays from Ga^{72}.

Gamma-rays			
$H\rho$ of electrons	Energy of gamma-ray	Percent abundance	Evidence
9620	2.50 Mev	6 percent	K photo line
8520	2.18	13	K photo line
7260	1.81	4	K photo line
5970	1.57	9	Compton electrons; weak
5510	1.47		
5060	1.30		
4610	1.05	6	K photo line
3833	0.835	39	K photo line
3245	0.676*	2	K photo line; very weak
——	0.691*	—	Internal conversion
3075	0.631	21	K photo line

Beta-rays	
Group end-point energy	Percent abundance
3.17 Mev	8 percent
2.57	8
1.74	3
1.45	7
1.00	26
0.74	23
0.56	25

Internal conversion electrons		
$H\rho$ of electrons	Energy of electrons	Energy of gamma-ray
3585	0.680 Mev	0.691 Mev

* Probably both are due to the same gamma-ray (0.691 Mev); the internal conversion electron determination is more accurate.

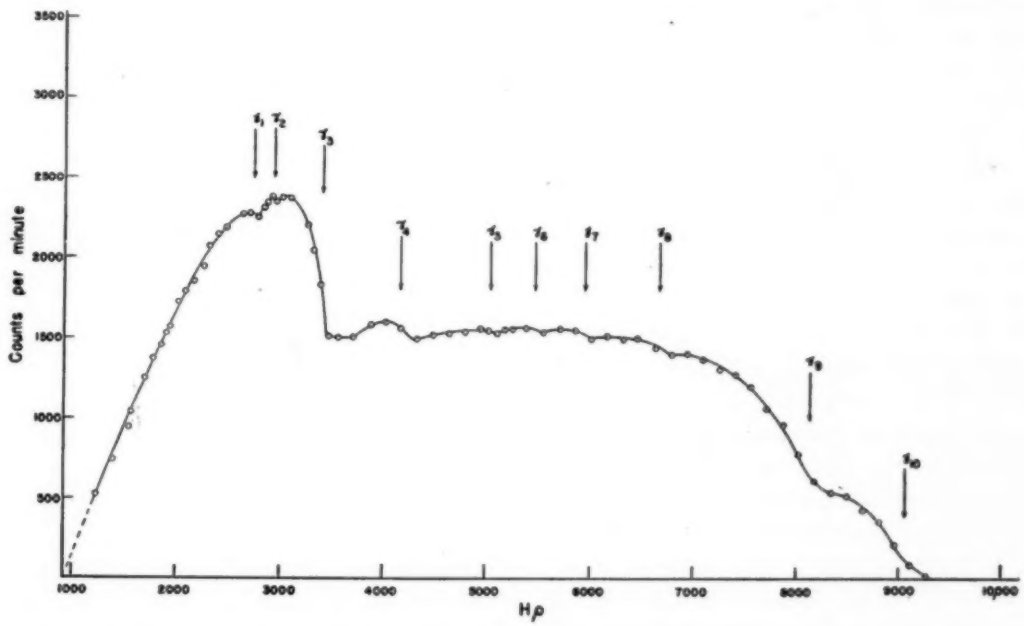

FIG. 3. Spectrum of Compton electrons ejected from copper by the gamma-rays of Ga^{72}. The gamma-ray energies are, respectively: γ_1, 0.631 Mev; γ_2, 0.691 Mev; γ_3, 0.835 Mev; γ_4, 1.05 Mev; γ_5, 1.30 Mev; γ_6, 1.47 Mev; γ_7, 1.57 Mev; γ_8, 1.81 Mev; γ_9, 2.18 Mev; γ_{10}, 2.50 Mev.

represents not less than 10,000 counts. From a casual inspection of this curve it is readily seen that the spectrum is highly complex. Even without the construction of a Fermi plot, it is evident that there are several groups of electrons. In addition, there is an internal conversion line at 3585 gauss-cm.

An analysis of the beta-ray data was made with the help of the Fermi theory. The data may be resolved into seven groups with end points and relative intensities as shown in Table I. Of the various groups, those at 1.74, 1.45, and 0.56 are probably the least certain; the first two because they are weak, the last because of the many subtractions which have to be made before arriving at this group. The groups at 3.17, 2.57, 1.00, and 0.74 Mev are more easily determined by virtue of either their position or intensity. The possibility of groups of lower energy than 0.56 Mev is not precluded.

The *ft.* values for each group have been calculated. The groups with end points at 3.17, 2.57, 1.74, and 1.45 Mev belong to the second forbidden class, and those with end points at 1.00, 0.74, and 0.56 Mev are first forbidden.

The internal conversion electrons which appear at 3585 gauss-cm have an energy of 0.680 Mev. If it be assumed that these electrons are produced by internal conversion in the *K*-shell of Ge^{72}, the energy of the gamma-ray which is internally converted is 0.691 Mev. The ratio of the number of internal conversion electrons to the total number of disintegration electrons is 0.005. It is not definitely known where this internally converted transition occurs in the disintegration scheme, hence it is not possible to calculate an internal conversion coefficient for this process.

Recently Bowe, Goldhaber, Hill, Meyerhoff, and Sala[15] have measured delayed coincidences between the internal conversion electrons men-

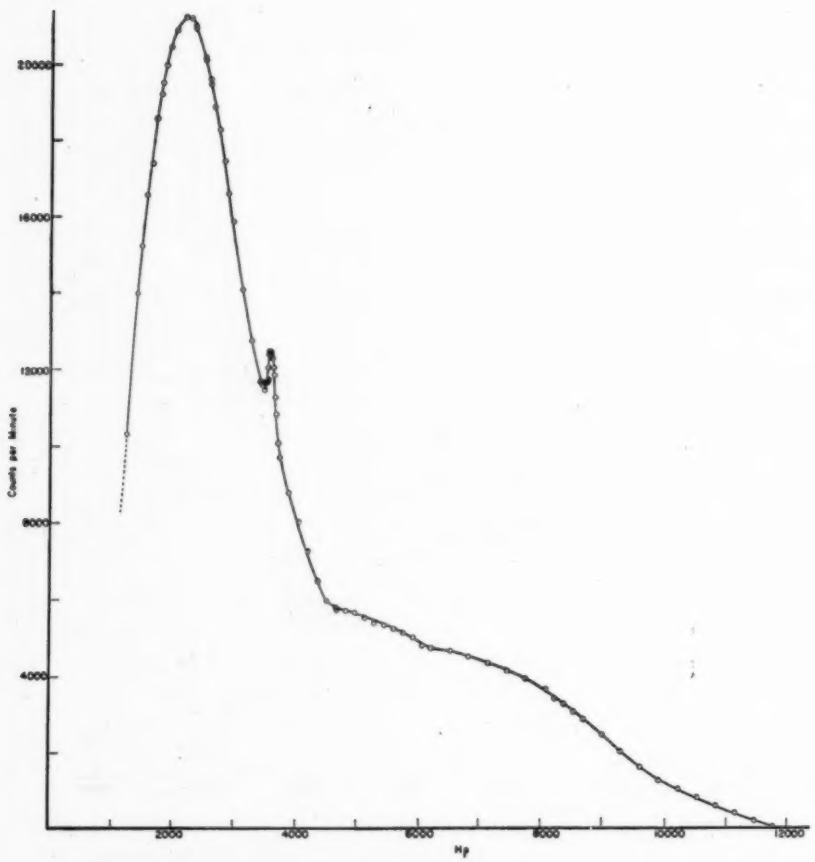

FIG. 4. The beta-ray spectrum of Ga^{72}.

[15] J. C. Bowe, M. Goldhaber, R. D. Hill, W. E. Meyerhoff, and O. Sala, Bull. Am. Phys. Soc. **22**, No. 6, 6 (1947).

tioned above and the disintegration electrons. They concluded that the internal conversion electrons come from a metastable level of about 30 microseconds' half-life, which follows a low intensity beta-transition of energy 1.5 Mev. Moreover, they could find no delayed gamma-rays, from which they concluded that the gamma-ray associated with this transition must be almost completely internally converted. They suppose that the transition involved is one in which both the initial and final level have spin $i=0$.

V. DISCUSSION

It is probably not possible to give a complete decay scheme for Ga^{72} since this seems to be extremely complicated. Some of the gamma-rays are so weak as to make one skeptical of their existence. However, these weak gamma-rays are seen on each run and appear not to be caused by impurities.

The most striking feature of the spectrum is the high intensity of the line at 0.835 Mev. The intensity of this line is sufficiently high so that it may be assumed that practically all transitions lead through it to the ground state of Ge^{72}. The next most intense gamma-ray is that at 0.631 Mev, and it would appear that this line must be in series with several other gamma-rays. The line at 2.18 Mev is the third strongest line of the spectrum but, being a high energy line, its intensity probably comes about because it follows a beta-ray transition of rather high intensity. With these ideas as a foundation, a tenetative disintegration scheme is given in Fig. 5. In this diagram, the levels of Ge^{72} which are determined by the analysis of the beta-ray spectrum are shown slightly separated from and to the left of those determined with the help of the gamma-ray data. This is done purposely to show the order of magnitude of the discrepancies found. The worst discrepancy found seems to be of the order of 3 percent. The gamma-ray lines which appear to be certain are shown as solid lines, the others as dotted lines. Using the three better-known lines together with the associated beta-ray transitions as shown in the diagram, the energy of Ga^{72} above the ground state of Ge^{72} is found to be 4.01, 4.04, and 4.02 Mev, which shows that this part of the scheme is internally

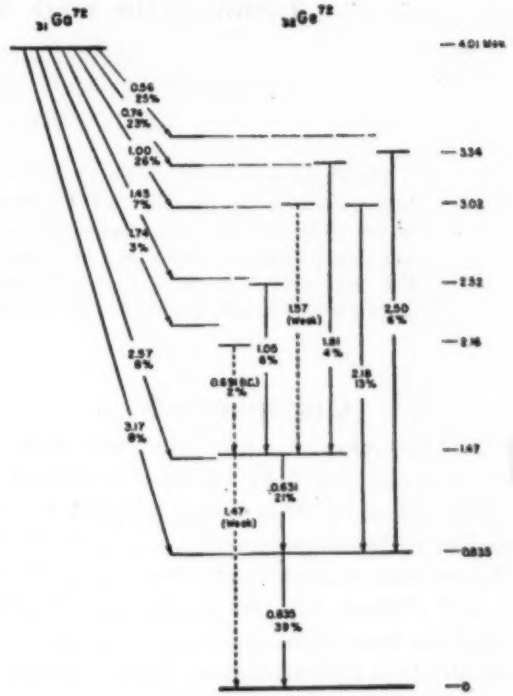

FIG. 5. Tentative energy level diagram for the disintegration of Ga^{72}.

consistent to better than one percent. In addition, the energies of the two gamma-rays at 0.631 and 1.57 Mev add up approximately to that of the gamma-ray of energy 2.18 Mev. The 2.50-Mev line probably follows the 0.56-Mev beta-ray transition and leads to the 0.835-Mev level. The energy of Ga^{72} calculated via this route is $0.835+2.50+0.56=3.90$ Mev, which agrees with the other values for that energy to 2.5 percent. The remaining weak lines are placed in the scheme where they seem to fit from energy considerations. The line at 0.691 Mev is placed following the 1.74-Mev beta-transition and in a position in which it does not lead to the ground state, in spite of the fact that it is internally converted and has been shown by Bowe *et al.*[15] to be a delayed transition. From energetic considerations, there seems to be no other place in the scheme into which this line will fit.

The authors wish to express their thanks to Dr. M. B. Sampson and the cyclotron group for making the sources used in these experiments. This research was supported by the Office of Naval Research under Contract Ori N6-48.

A Note on the Stark Effect in Diatomic Molecules

W. A. NIERENBERG, I. I. RABI, AND M. SLOTNICK
Department of Physics, Columbia University, New York, New York
(Received March 9, 1948)

The hyperfine splitting of the energy levels of a polar diatomic molecule in a constant electric field caused by the presence of $\mathbf{I}\cdot\mathbf{J}$ interactions between each nucleus and the other charges of the molecule and a quadrupole interaction involving one of the nuclei is calculated. The calculation explains recent measurements of Trischka on molecular beams of CsF and KF. For weak fields a method is given for computing the fine structure splitting resulting from any form of interaction, provided one nucleus interacts more strongly than the other.

I. INTRODUCTION

THE behavior of a polar diatomic molecule in an electric field has been examined by several authors.[1,2] The model adopted for the molecule in these treatments is a rigid rotator with moments of inertia zero about its symmetry axis and A about a perpendicular axis. Hughes[3] studied the transitions induced in a beam of CsF molecules by a radiofrequency electric field while the molecules were subjected to a constant electric field. His experiments allowed him to verify the applicability of the above model and to measure A as well as the molecular dipole moment μ. In more recent experiments of Trischka[4] with CsF and other diatomic molecules, these transitions were examined with much higher resolution, and a detailed study of their fine structure was made. Similar experiments with molecules in magnetic fields[5–7] have been made, and the fine structure of the lines successfully explained by assuming the existence of two interactions: (a) A coupling between the electric quadrupole moment of the nucleus and the electrostatic field of the remaining charges. (The theory for the magnetic case was given by KRRZ.[5] The extension to the case of polar diatomic molecules in an electric field is due to Fano.[8]) (b) An interaction of the form $c\mathbf{I}\cdot\mathbf{J}$, where $\mathbf{I}$ is the nuclear spin and $\mathbf{J}$ is the rotational angular momentum. (All angular momenta will be expressed in units of $\hbar$.) The influence of this term in the Hamiltonian will be shown to lead to modifications of Fano's results that are required to explain the spectra observed by Trischka.

II. ENERGY LEVELS AND EIGENFUNCTIONS IN WEAK ELECTRIC FIELDS

In the absence of an external field, the Hamiltonian, in general, may be written as

$$\mathcal{H}=(\hbar^2/2A)\mathbf{J}^2+f_1(\mathbf{I}_1\cdot\mathbf{J})+f_2(\mathbf{I}_2\cdot\mathbf{J}), \quad (1)$$

where $\mathbf{I}_1$, $\mathbf{I}_2$ are the spins of the nuclei and $\mathbf{J}$ is the angular momentum of rotation. The f_i are polynomials in $\mathbf{I}_i\cdot\mathbf{J}$ of degree no higher than $2I_i$, or $2J$, whichever is smaller.[9] If $I_2=0$ (or if the coefficients of f_2 vanish), the energy levels are

$$W_{J,F_1,m}=(\hbar^2/2A)J(J+1)+f_1(\tfrac{1}{2}K_1), \quad (2)$$

where

$$K_1=F_1(F_1+1)-I_1(I_1+1)-J(J+1);$$
$$F_1=I_1+J;(F_1=I_1+J,I_1+J-1,\cdots,|I_1-J|),$$

and $m=m_{F_1}=m_1+m_J$. If $f_2(\mathbf{I}_2\cdot\mathbf{J})$ is treated as a small perturbation, the energy levels will be roots of a secular equation of degree $2I_2+1$, and each F_1 level (assume each $F_1\geqslant I_2$) will be split

[1] P. Debye, *Polar Molecules* (Dover Publications, New York, 1945).
[2] F. Brouwer, Dissertation, Amsterdam 1930.
[3] H. K. Hughes, Phys. Rev. **72**, 614 (1947).
[4] These results, not yet published, were kindly made available to us by Dr. Trischka.
[5] J. M. B. Kellogg, I. I. Rabi, N. F. Ramsey, Jr., and J. R. Zacharias, Phys. Rev. **57**, 677 (1940).
[6] N. F. Ramsey, Jr., Phys. Rev. **58**, 226 (1940).
[7] W. A. Nierenberg and N. F. Ramsey, Phys. Rev. **72**, 1075 (1947).
[8] U. Fano, J. Research Nat. Bur. Stand. **40**, RP 1866 (1948).

[9] (a) The simplest way of demonstrating this property is to consider that the submatrix of $\mathbf{I}\cdot\mathbf{J}$ which is diagonal in m_I+m_J satisfies its own characteristic equation and, therefore, that $(\mathbf{I}\cdot\mathbf{J})^{2I+1}$ may be expressed as a linear combination of lesser powers of $\mathbf{I}\cdot\mathbf{J}$. Therefore, at most $2I$ coefficients are needed to describe the Hamiltonian, the additional constant term having no significance for term differences. (b) This simple expression also depends on the assumption that J is a good quantum number, that is, that the term splitting involved in introducing the f_i's are small compared to $\hbar^2/(2A)$ and therefore only that part of the interaction diagonal in J need be included.

into $2I_2+1$ levels. The correct unperturbed eigenfunctions are obtained from linear combinations of the product representation of $\phi_{J,\,F_1,\,m}$ and χ_{m_2} (the wave function of nucleus 2) and are denoted by $\psi_{J,\,F_1,\,M,\,i}$. Solution of the secular equation yields

$$\psi_{J,\,F_1,\,M,\,i}=\sum_{m_2=-I_2}^{I_2} a_{im_2}{}^{M}\phi_{J,\,F_1,\,M-m_2}\chi_{m_2}$$
$$(i=-I_2,\ -I_2+1,\ \cdots,\ I_2) \quad (3)$$

and the term splitting energy $W'_{J,\,F_1,\,M,\,i}$. These wave functions may now be used to compute the additional splitting of the levels on the application of a weak electric field $\mathcal{E}$. The additional term in the Hamiltonian is $-\boldsymbol{\mu}\cdot\mathcal{E}$. A weak field exists if the interaction of the external field with the molecule is much less than the interaction of $\mathbf{I}_2$ and $\mathbf{J}$. (I.e., if a cosine coupling $c\mathbf{I}_2\cdot\mathbf{J}$ exists, then $c\gg\mu^2\mathcal{E}^2/(h^2/2A)$.) Fano[8] has calculated this term splitting for a diatomic molecule where $I_2=0$. If $E_{J,\,F_1,\,m}$ denote these electrical energies, then the new electrical terms are given by

$$W''_{J,\,F_1,\,M,\,i}=\sum_{m_2=-I_2}^{I_2}|a_{im_2}{}^{M}|^2E_{J,\,F_1,\,M-m_2}$$
$$(i=-I_2,\ -I_2+1,\ \cdots,\ I_2). \quad (4)$$

These calculations have been completed for the case $f_2(\mathbf{I}_2\cdot\mathbf{J})=c\mathbf{I}_2\cdot\mathbf{J}$. The results are:

$$W'_{J,\,F_1,\,M,\,i}=\tfrac{1}{2}cgK, \quad (5)$$

where

$$K=F(F+1)-F_1(F_1+1)-I_2(I_2+1);$$

$F=F_1+F_2-i$,[10] and

$$g=\frac{F_1(F_1+1)+J(J+1)-I_1(J_1+1)}{2F_1(F_1+1)}.$$

The coefficients $a^{M}_{F,\,m_2}$ are

$$a^{M}_{F,\,m_2}=\frac{((F+F_1-I_2)!(F-F_1+I_2)!(F_1+I_2-F)!(F+M)!(F-M)!)^{\frac{1}{2}}}{((F+F_1+I_2+1)!(F_1-M+m_2)!(F_1+M-m_2)!(F_2-m_2)!(F_2+m_2)!)^{\frac{1}{2}}}$$
$$\times\sum_{\kappa}\frac{(-1)^{\kappa+I_2+m_2}(2F+1)^{\frac{1}{2}}(F+I_2+M-m_2-\kappa)!(F_1-M+m_2+\kappa)!}{(F-F_1+I_2-\kappa)!(F+M-\kappa)!\kappa!(\kappa+F_1-I_2-M)!}. \quad (6)$$

These coefficients are those derived by Wigner.[11]

The alkali-fluorides are treated as an example. The Hamiltonian is

$$\mathcal{H}=\frac{h^2}{2A}\mathbf{J}^2-\boldsymbol{\mu}\cdot\mathcal{E}-\frac{e^2q_1'Q_1}{J_1(2I_1-1)(2J-1)(2J+3)}\{3(\mathbf{I}_1\cdot\mathbf{J})^2+\tfrac{3}{2}(\mathbf{I}_1\cdot\mathbf{J})-\mathbf{I}_1{}^2\mathbf{J}^2\}+c_1\mathbf{I}_1\cdot\mathbf{J}+c_2\mathbf{I}_2\cdot\mathbf{J} \quad (7)$$

and $I_2=\frac{1}{2}$. The third term is due to the quadrupole coupling of the alkali and the molecule. The molecular q' and the nuclear Q are defined in references 5 and 12. The cosine interactions are discussed in references 7, 13, and 14.

The energy levels for weak fields are

$$W_{J,\,F_1,\,M,\,F_1\pm\frac{1}{2}}=\frac{h^2}{2A}J(J+1)-\frac{e^2q_1'Q_1}{(2J-1)(2J+3)I_1(2I_1-1)}\{\tfrac{3}{4}K_1(K_1+1)-I_1(I_1+1)J(J+1)\}$$
$$+\frac{c_1}{2}K_1\pm c_2\frac{F_1(F_1+1)+J(J+1)-I_1(I+1)}{4F_1(F_1+1)}(F_1+\tfrac{1}{2}\mp\tfrac{1}{2})$$
$$-\frac{\alpha^2\dfrac{h^2}{2A}\left[3\left(M^2+\tfrac{1}{4}\right)\mp\dfrac{6M^2}{2F_1+1}-F_1(F_1+1)\right][3K_1(K_1-1)-F_1(F_1+1)J(J+1)]}{2J(J+1)(2J-1)(2J+3)2F_1(F_1+1)(2F_1-1)(2F_1+3)}, \quad (8)$$

$$\alpha=\mu\mathcal{E}/(h^2/2A).$$

[10] $\mathbf{F}=\mathbf{F}_1+\mathbf{I}_2=\mathbf{I}_1+\mathbf{I}_2+\mathbf{J}$ is the total angular momentum of the system. The index i will be replaced by $F-F_1-I_2$.

[11] E. Wigner, *Gruppentheorie*, p. 206, Viewlg, 1931.

[12] A. Nordsieck, Phys. Rev. **58**, 310 (1940).

[13] H. M. Foley, Phys. Rev. **72**, 504 (1947).

[14] G. C. Wick, Phys. Rev. **73**, 51 (1948).

The more general case of $f_2(\mathbf{I}_2\cdot\mathbf{J})$ has not yet successfully yielded any general formulae. However, the first-order energies can be found by a subtraction process described in an appendix.

III. STRONG ELECTRIC FIELDS

The term "strong field" is used to describe conditions when $e^2q'Q \ll \mu^2\mathcal{E}^2/(\hbar^2/2A)$, that is, when the interaction with the external field is much greater than the quadrupole interaction. In this calculation, the eigenstates of the external interaction are used as the zero-order wave functions while the quadrupole and cosine interactions are treated as perturbations. The unperturbed eigenfunctions satisfy the Schrödinger equation:

$$\left(\frac{\hbar^2}{2A}\mathbf{J}^2-\mu\mathcal{E}\cos\vartheta_R-W\right)\psi(\vartheta_R,\varphi_R)=0, \quad (9)$$

where ϑ_R and φ_R are the polar and azimuth angles of the symmetry axis with respect to the electric field. These eigenfunctions are labeled by the quantum numbers n and m_J.[8] n ($n\rightarrow J$ for $\mathcal{E}\rightarrow 0$) may assume all positive integral values. The corresponding energy levels are W_{n,m_J} ($W_{n,m_J}=W_{n,-m_J}$); the eigenfunctions ψ_{n,m_J}. The correct matrix elements of the quadrupole interaction are no longer given by KRRZ[5] but have been computed by Fano and are functions of the field $\mathcal{E}$. They may be written as

$$(nm_Jm_1m_2|\mathcal{H}_{Q_1}|n'm_J'm_1'm_2') = \delta_{m_2m_2'}\delta_{mm'}\frac{e^2q_1'Q_1}{2I_1(2I_1-1)}(-1)^{m_J-m_J'} \times R_{nm_J}^{n'm_J'}d(I_1)_{m-m_J}^{m-m_J'}, \quad (10)$$

where $m=m_1+m_J$. The $R_{nm_J}^{n'm_J'}$ are functions of $\mu\mathcal{E}/(\hbar^2/2A)$, while $d(I_1)_r^s$ are numerical coefficients that vanish unless r and s differ by 0, 1, or 2. There is a similar expression for $\mathcal{H}_{Q_2}$.

The interaction between the nuclear magnetic moment and the magnetic field of the molecule is of the form $c\mathbf{I}\cdot\mathbf{J}$, where c is assumed to vary negligibly with J. Since

$$(nm_Jm_I|\mathbf{I}\cdot\mathbf{J}|nm_J'm_I)=cm_Im_J,$$

the mixing of J states has no effect on the diagonal elements of this interaction in the Hamiltonian. Similarly, it is clear that the selection rules $\Delta m_J=0,\ \pm1,\ \Delta(m_I+m_J)=0$ still hold for the matrix elements of this interaction in this representation. It will be seen later that only the diagonal elements of this perturbation are involved in the perturbed levels, so that this perturbation can be treated, to the approximation that c is independent of J, as completely independent of the mixing of J-states.

Since $W_{n,m_J}=W_{n,-m_J}$, states of fixed n, $\pm m_J$, and all m_1 and m_2 are degenerate. If the Hamiltonian includes interactions of order no higher than quadrupolar, only two cases need be considered:

$|m_J|\neq 1$: There are no off-diagonal elements connecting degenerate states and

$$W_{n,m_J,m_1,m_2}=W_{n,m_J} + \frac{e^2q_1'Q_1}{2I_1(2I_1-1)}R_{n,m_J}^{n,m_J}[3m_1^2-I_1(I_1+1)] + \frac{e^2q_2'Q_2}{2I_2(2I_2-1)}R_{n,m_J}^{n,m_J}[3m_2^2-I_2(I_2+1)] + c_1m_1m_J+c_2m_2m_J \ (|m_J|\neq 1), \quad (11)$$

$|m_J|=1$. There are no off-diagonal elements connecting degenerate states resulting from the cosine interaction, but there are such elements due to both $\mathcal{H}_{Q_1}$ and $\mathcal{H}_{Q_2}$. There remains two matrices of at most $2I+1$ dimensions (where I is the smaller spin) to be diagonalized. If one of the two nuclei has no quadrupole moment, a general expression can be derived. The functions $R_{n,m_J}^{n,m_J}=R_{n,-m_J}^{n,-m_J}$ will be abbreviated to $R(n,m_J)$ and $R_{n,1}^{n,-1}=R_{n,-1}^{n,1}$ will be denoted by $S(n)$. The energy levels are

$$W_{n,|m_J|=1,m,m_2,\pm}=W_{n,1}+\frac{e^2q_1'Q_1}{2I_1(2I_1-1)}R(n,1)[3(m^2+1)-I_1(I_1+1)]-c_1 \pm\left(\left(c_1m+c_2m_2-\frac{3e^2q_1'Q_1}{I_1(2I_1-1)}R(n,1)m\right)+\frac{3}{2}\left(\frac{e^2q_1'Q_1}{I_1(2I_1-1)}S(n)\right)^2\{(I_1+1)^2-m^2\}\{I_1^2-m^2\}\right)^{\frac{1}{2}}, \quad (12)$$

for $|m|<I_1$. If $|m|=I_1$ or I_1+1, Eq. (11) applies. Equations (11) and (12) are valid for all fields for which the electrical energy is much greater than the quadrupole and cosine energies. However, for moderately strong fields, where the electrical energy is much larger than the nuclear orientation-dependent interactions but much smaller than the rotational energy of the molecule [i.e. $e^2q'Q/(\hbar^2/2A)\ll(\mu\mathcal{E}/(\hbar^2/2A))^2\ll 1$, a condition easily obtained in practice], Eqs. (11) and (12) are simplified to the extent that J may be considered a good quantum number and

$$R(n, m_J)\cong\frac{[n(n+1)-3m_J^2]}{(2n-1)(2n+3)},$$

$$S(n)\cong-\left(\frac{3}{2}\right)^{\frac{1}{2}}\frac{n(n+1)}{(2n-1)(2n+3)}, \quad (13)$$

and

$$W_{n,\,m_J}\cong\frac{\hbar^2}{2A}\left\{n(n+1)+\alpha^2\left[\frac{n^2-m_J^2}{2n(2n-1)(2n+1)}-\frac{(n+1)^2-m_J^2}{2(n+1)(2n+1)(2n+3)}\right]\right\}.$$

Stated differently, the approximation ignores the mixing of J states caused by the field, and therefore the matrix elements of the quadrupole interaction are independent of the field and are essentially those of Casimir's operator.[5]

APPENDIX

The first-order energies of $f_2(\mathbf{I}_2\cdot\mathbf{J})$ can be found by a subtraction process along the diagonal. Each original F_1 level is split into $2I_2+1$ levels, numbered according to the index i, by the perturbation. Each of these levels is still $2(F_1+i)+1$ times degenerate in the total quantum number M. Since that level of F_1 corresponding to $M=F_1+I_2$ has no matrix elements connecting this state and any other of the same F_1 in the representation, the corresponding energy is $(J, F_1, F_1, I_2|f_2(\mathbf{I}_2\cdot\mathbf{J})|J, F_1, F_1, I_2)$. This state is $2(F_1+I_2)+1$ fold degenerate. Therefore, this energy must be one of the eigenvalues of the submatrix on the diagonal corresponding to F_1 and $M=F_1+I_2-1$. This matrix is two by two and the next energy ($i=I_2-1$) can be found by subtracting the eigenvalue already found from the spur of the 2×2 matrix. This root is $2(F_1+I_2-1)+1$ fold degenerate, and therefore this process can be repeated until all the splittings of the level F_1 are determined. The transformation amplitudes a_{im_2} may now be found in each case.

Let the matrix $\mathbf{I}_2\cdot\mathbf{J}$ be chosen to illustrate the method. The diagonal matrix elements of $I_2\cdot J$ in the F_1, M, m_2 representation are

$$(F_1, M-m_2, m_2|\mathbf{I}_2\cdot\mathbf{J}|F_1, M-m_2, m_2)=gm_2(M-m_2),$$

and g is defined with Eq. (5). If $M=F_1+I_2$ and $m_2=I_2$, there is no matrix elements connecting this state with any other of the same F_1. Therefore, $W'_{F_1,\,F_1+I_2,\,I_2}=gI_2F_1$. The diagonal submatrix F_1, $M=F_1+I_2-1$, and $m_2=I_2$, I_2-1 is 2×2 with no matrix elements connecting it and any other state of the same F_1. Its spur is $gI_2(F_1-1)+g(I_2-1)F_1$. The additional root is

$$W'_{F_1,\,F_1+I_2-1}=gI_2(F_1-1)g(I_2-1)F_1-gI_2F_1=g(I_2F_1-I_2-F_1).$$

In general, the energy level is given by

$$\tfrac{1}{2}g\{(F_1+I_2-i+1)(F_1+I_2-i)-F_1(F_1+1)-I_2(I_2+1)\},$$

which is the result previously obtained (Eq. (5)).

A Study of the Radiations from Iridium (194), Iridium (192), Lanthanum (140), Antimony (124), and Zirconium (95)*

C. E. MANDEVILLE AND M. V. SCHERB
Bartol Research Foundation of the Franklin Institute, Swarthmore, Pennsylvania

(Received March 10, 1948)

The beta- and gamma-radiations of radioactive isotopes of iridium, lanthanum, antimony, and zirconium, prepared by slow neutron bombardment in the Clinton pile, have been investigated by absorption and coincidence methods. The results are given in summary below.

(1) Iridium (194): The beta-gamma coincidence rate decreases from 0.06×10^{-3} coincidence per beta-ray at zero absorber thickness to zero at 0.150 g/cm², corresponding to 0.48 Mev, indicating a soft beta-ray spectrum of low intensity, and that the hard beta-rays of energy 2.2 Mev are non-coincident with gamma-radiation. The gamma-gamma coincidence rate is $(0.54\pm0.05)\times10^{-3}$ coincidence per gamma-ray, indicative of cascade emission of gamma-rays in the nineteen-hour period. Coincidence absorption experiments revealed the presence of a gamma-ray of quantum energy 1.43 Mev. The momentum distribution of secondary electrons ejected from a thick aluminum radiator in a magnetic spectrograph gives an energy of 1.35 ± 0.03 Mev. A disintegration scheme is given for Ir^{194}.

(2) Iridium (192): The beta-rays have a maximum energy of 0.56 Mev as measured by absorption in aluminum and Feather analysis. The beta-gamma coincidence rate is 0.41×10^{-3} coincidence per beta-ray, independent of the beta-ray energy, suggesting a simple spectrum. The gamma-gamma coincidence rate is $(0.23\pm0.01)\times10^{-3}$ coincidence per gamma-ray recorded in the gamma-ray counter. The coincidence experiments show that on the average, each beta-ray is followed by 0.6 Mev of gamma-radiation.

(3) Lanthanum (140): The beta-gamma coincidence rate is 1.63×10^{-3} coincidence per beta-ray and seems to be independent of the beta-ray energy. A strong gamma-gamma coincidence rate, $(0.85\pm0.03)\times10^{-3}$ coincidence per gamma-ray, was also observed. The coincidence experiments show that gamma-rays are emitted in cascade and that 2.3 Mev of gamma-radiation follow each beta-ray.

(4) Antimony (124): Coincidence experiments show a decrease in the beta-gamma coincidence rate from 0.92×10^{-3} coincidence per beta-ray at zero absorber thickness to 0.38×10^{-3} coincidence per beta-ray at 0.110 g/cm². Beyond that point, the coincidence rate remains constant. A gamma-gamma coincidence rate of $(0.59\pm0.03)\times10^{-3}$ coincidence per gamma-ray was also observed. From the coincidence rates it may be concluded that gamma-rays are in cascade and that the high energy beta-rays are followed by 0.55 Mev of gamma-radiation.

(5) Zirconium (95): The 63-day activity was found to emit 0.40-Mev beta-rays. The maximum energy of the gamma-rays was 0.91 Mev as measured by coincidence absorption. The beta-gamma coincidence rate was 0.21×10^{-3} coincidence per beta-ray, independent of the beta-ray energy. The gamma-gamma coincidence rate, greater than the beta-gamma coincidence rate, was $(0.29\pm0.02)\times10^{-3}$ coincidence per gamma-ray. The coincidence experiments suggest that the 0.91-Mev gamma-ray is non-coincident with the beta-rays and may be related to some other decay process.

Chemical purification was carried out in all cases, except that of antimony (124). The calibration curve for the coincidence absorption counting set is given as well as a short discussion of some previously measured beta-ray spectra.

1. INTRODUCTION

THE characteristic radiations of a number of activities prepared at the Clinton pile have been investigated by absorption and coincidence methods. Beta-ray energies were measured by inserting aluminum foils before a single G-M counter, while the gamma-ray measurements were carried out with the aid of a calibrated coincidence counting set, using the method of coincidence absorption.

In all cases beta-gamma and gamma-gamma coincidence measurements were made. A general description of the counters and the procedure of the experiments has been given previously.[1]

2. IRIDIUM (194)

The nineteen-hour activity has long been known to emit hard beta-rays and gamma-rays.[2-6] In addition to the high energy beta-rays

* Assisted by the Office of Naval Research.

[1] C. E. Mandeville and M. V. Scherb, Phys. Rev. **73**, 141 (1948).
[2] A. I. Alichanian, A. I. Alichanow, and B. S. Dzelepow, Physik. Zeits. Sowjetunion **10**, 78 (1936).
[3] E. McMillan, M. Kamen, and S. Ruben, Phys. Rev. **52**, 375 (1937).
[4] C. M. Witcher, Phys. Rev. **60**, 32 (1941).
[5] C. E. Mandeville and H. W. Fulbright, Phys. Rev. **64**, 265 (1943).
[6] L. J. Goodman and M. L. Pool, Phys. Rev. **71**, 288 (1947).

of energy 2.2 Mev,[2,4] indications of a spectrum of lower energy have been obtained also. Witcher,[4] using a thick magnetic lens spectrometer, has concluded that the end point of the low energy beta-ray group lies between $3000H\rho$ and $3500H\rho$. The gamma rays of Ir^{191} were reported to have an energy of 1.35 Mev by Mandeville and Fulbright[5] who took this value from the end point of a momentum distribution of secondary electrons ejected from a thick aluminum radiator in a semicircular, focusing magnetic spectrograph. In a recent paper by Goodman and Pool,[6] Ir^{194} was shown to emit gamma-rays having energies of 0.38 and 1.65 Mev, as determined by absorption in lead. The 0.38-Mev gamma-ray would not have been detected in the apparatus of Mandeville and Fulbright because the spectrograph was unsatisfactory for the measurement of gamma-ray energies less than 0.5 Mev.

IrO_2 was irradiated by slow neutrons for 30 minutes in the Clinton pile. The short exposure time made the 19-hour activity large as compared to the 68-day period. Measurements were commenced about twenty hours after removal of the isotope from the pile.

A coincidence absorption experiment, carried out with a calibrated double coincidence counter

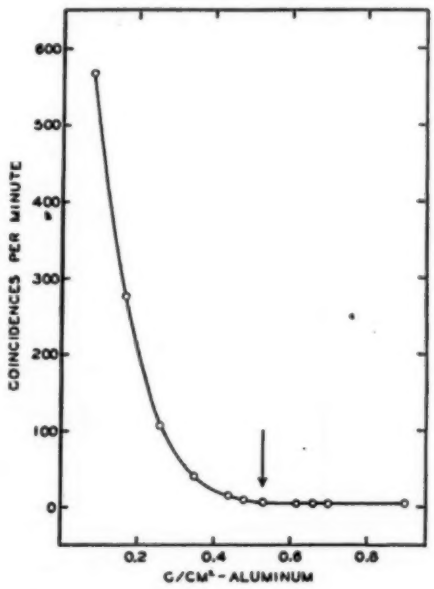

FIG. 1. Coincidence absorption of the secondary electrons of the gamma-rays from Ir^{194}. The end point corresponds to a quantum energy of 1.43 ± 0.05 Mev.

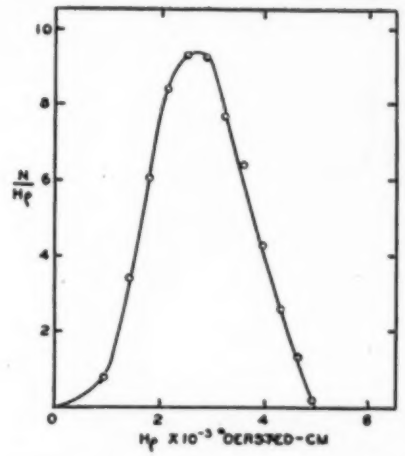

FIG. 2. Momentum distribution of the secondary electrons ejected from a thick aluminum radiator by the gamma-rays of the nineteen-hour Ir^{194}.

set, revealed the presence of a high energy gamma-ray having an energy of 1.43 ± 0.05 Mev. The plot of these data is given in Fig. 1. This value is to be compared with 1.35 ± 0.03 Mev, as calculated from the end point of the curve[7] of Fig. 2. This is a momentum distribution of secondary electrons knocked out of a thick aluminum radiator. Both of the values quoted above would indicate that the 1.65-Mev estimate of the Ohio State University group is somewhat high.

A thin source of chemically purified IrO_2 was placed between two G-M counters in coincidence, and the beta-gamma and gamma-gamma coincidence rates were measured. The beta-gamma coincidence rate is shown in Fig. 3 as a function of the surface density of aluminum absorber placed before the beta-ray counter. The curve of Fig. 3 was taken about 24 hours after the radioactive material was removed from the pile. The beta-gamma coincidence rate is seen to decrease from 0.09×10^{-3} coincidence per beta-ray at zero absorber thickness to zero at 0.150 g/cm². These data were later corrected for the presence of the 68-day Ir^{192} and are plotted in Fig. 4. From these measurements it may be concluded that in addition to the spectrum of maximum energy

[7] This distribution, previously unpublished, was observed in the semi-circular focusing spectrograph at the Rice Institute in April, 1943. As mentioned in the text, the quantum energy taken from the end point is calculated to be 1.35 ± 0.03 Mev and was so quoted a number of years ago (see reference 5).

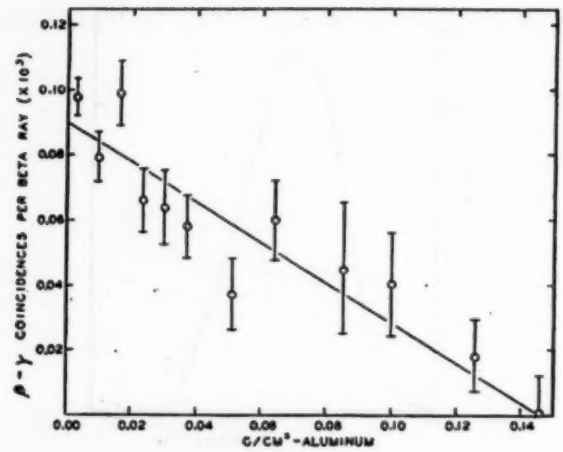

FIG. 3. Beta-gamma coincidence rate of Ir^{194} as a function of the surface density of aluminum inserted before the beta-ray counter.

2.2 Mev, a second spectrum, coupled with gamma-radiation, is present, having an end point at 0.150 g/cm². This corresponds to an energy of 0.48 Mev.[8] It is also clear that no gamma-rays are coupled with the spectrum of maximum energy 2.2 Mev. The high energy spectrum then leads to the ground state of the Pt^{194} residual nucleus. Gamma-gamma coincidences indicating cascade emission of gamma-rays were found in the nineteen-hour period and when corrected for the presence of Ir^{192}, give a gamma-gamma coincidence rate of $(0.54\pm0.05)\times10^{-3}$ coincidence per gamma-ray.

The measurements of this paper, coupled with those of reference 4 and reference 6, make it possible to construct the level diagram of Fig. 5.

3. IRIDIUM (192)

The beta-rays of the 68-day activity were found to have a visual absorption limit at 0.160 g/cm², or 0.50 Mev. This is shown in Fig. 6. Feather analysis, given in Fig. 7, results in an end point at 0.56 Mev. The values reported previously were 0.67 Mev[9] and 0.617 Mev[10].

The beta-gamma coincidence rate, shown in Fig. 8, is clearly independent of the beta-ray energy, in agreement with the findings of Wiedenbeck and Chu.[11] This suggests a simple beta-ray spectrum. According to the calibrated gamma-ray counter of the beta-gamma coincidence counting set, the beta-gamma coincidence rate of 0.41×10^{-3} coincidence per beta-ray indicates

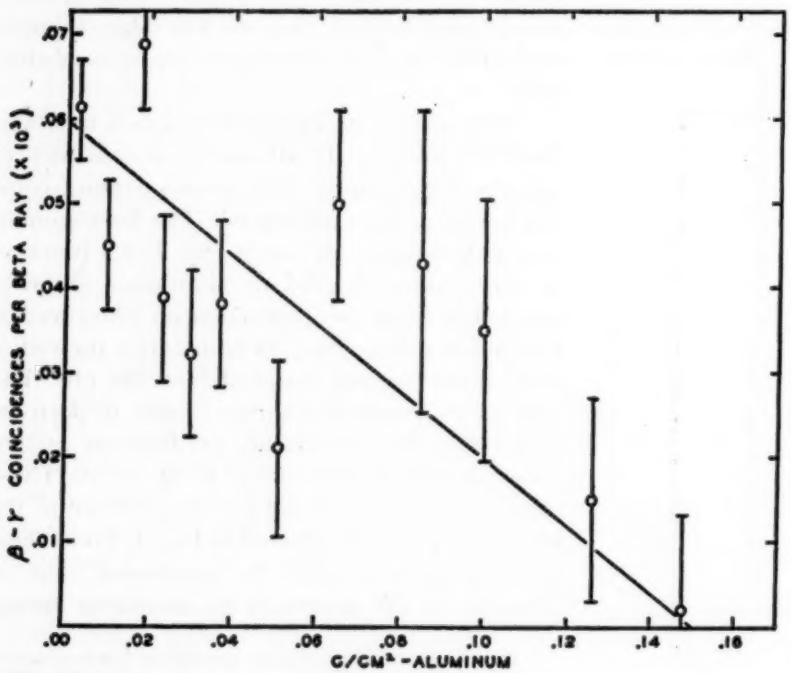

FIG. 4. Beta-gamma coincidence rate of Ir^{194} corrected for the presence of Ir^{192}.

[8] L. E. Glendenin, Nucleonics 2, No. 1, 12 (1948).
[9] P. W. Levy, Phys. Rev. 72, 352 (1947).
[10] Swami Jnanananda, Phys. Rev. 72, 1124 (1947).
[11] M. L. Wiedenbeck and K. Y. Chu, Phys. Rev. 72, 1164 (1947).

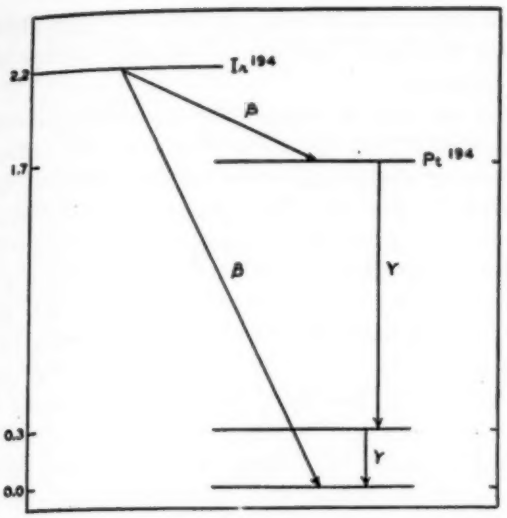

FIG. 5. Proposed disintegration scheme for Ir^{194}.

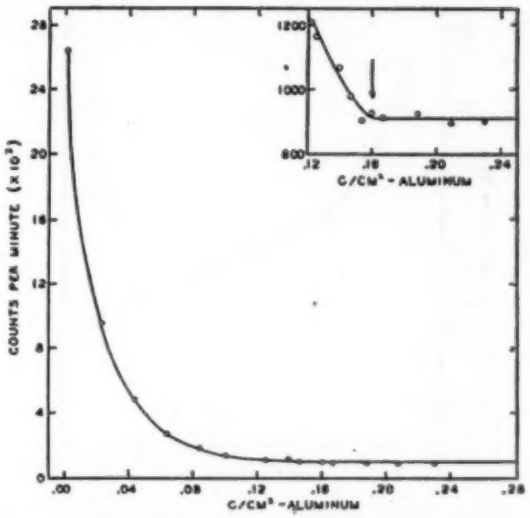

FIG. 6. Absorption in aluminum of the beta-rays of Ir^{192}.

that, on the average, each beta-ray is followed by 0.6 Mev of gamma-radiation. This seems reasonable since the most energetic gamma-ray emitted by Ir^{192} has been shown to have an energy of 0.63 Mev.[5,12] A gamma-gamma coincidence rate of $(0.23\pm0.01)\times10^{-3}$ coincidence per gamma-ray recorded in the gamma-ray counter was also detected.

4. LANTHANUM (140)

The 40-hour activity was induced in La_2O_3, irradiated by slow neutrons in the Clinton pile. In order to measure the gamma-ray energies, a coincidence absorption experiment was performed. It was possible to resolve the curve into two components, giving quantum energies of 1.60 Mev and 2.16 Mev, in agreement with the several previous estimates.[13–15]

A thin source of the radioactive material was placed in the standard position in the beta-gamma coincidence counting arrangement. The beta-gamma coincidence rate, as a function of the surface density of the aluminum absorber thickness placed before the beta-ray counter, is plotted in Fig. 9, where it is seen to be 1.63×10^{-3} coincidence per beta-ray recorded in the beta-ray counter, independent of the beta-ray energy. This result is strikingly similar to that obtained by the Indiana University group.[14] Since observation of the beta-gamma coincidence rate as a function of the surface density of the aluminum placed before the beta-ray counter constitutes an integral method, it does not have the sensitivity of the spectrometric measurements of Osborne and Peacock.[13] Their data have indicated three spectra of energies 0.90, 1.40, and 2.12 Mev rather than a simple spectrum.**

However, a few interesting conclusions can be drawn from the measurements of Fig. 9:

(1) All of the beta-ray spectra of La^{140} lead to excited states of the Ce^{140} residual nucleus, since genuine coincidences were observed as far out as 0.64 g/cm², 1.48 Mev as calculated by Feather's equation.[16]

(2) Using the coincidence rates of Sc^{46} as a calibration point, the beta-gamma coincidence rate of Fig. 9, 1.63×10^{-3} coincidence per beta-ray indicates that each beta-ray is followed, on the average, by 2.3 Mev of gamma-radiation.

[12] J. M. Cork, Phys. Rev. **72**, 581 (1947).
[13] R. K. Osborne and W. C. Peacock, Phys. Rev. **69**, 679 (1946).
[14] A. C. G. Mitchell, L. M. Langer, and L. J. Brown, Phys. Rev. **71**, 140 (1947).
[15] C. E. Mandeville, Phys. Rev. **64**, 147 (1943).

** *Note added in proof:* These beta-gamma coincidence data on La^{140} demonstrate that the method cannot be depended upon to reveal the presence of spectra having a low intensity relative to the principal component. This has bearing upon the many interesting experiments which have been conducted to ascertain whether the beta-ray spectrum of Au^{198} is simple or complex. Experiments of this type would give evidence only of a simple spectrum, though a second component might be present with a relative intensity of several percent.

The differential analog of this method, coincidences on a spectrometer, would obviously constitute a more sensitive approach.

[16] N. Feather, Proc. Camb. Phil. Soc. **34**, 599 (1938).

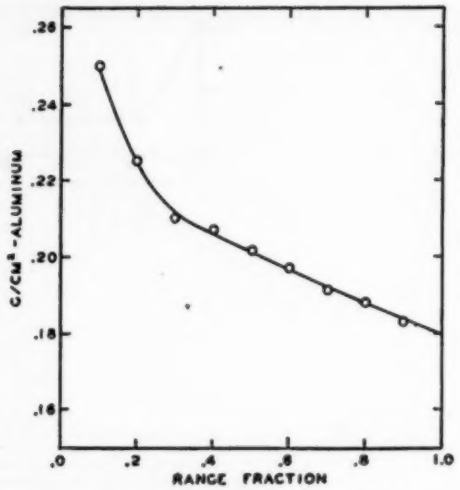

FIG. 7. Feather analysis of the data of Fig. 6.

(3) On considering the statistical probable errors, the beta-gamma coincidence rate can only be represented as a straight line, having a value independent of the beta-ray energy. This would indicate that the 0.90-Mev beta-ray spectrum reported by Osborne and Peacock must be of very low intensity. This is consistent with their report.

A gamma-gamma coincidence rate of $(0.85 \pm 0.03) \times 10^{-3}$ coincidence per gamma-ray recorded in the gamma-ray counter was observed in the disintegration of La^{140}. If the quantum efficiency of the gamma-ray counters is assumed to be constant with energy rather than linear with energy as is actually the case, it is found that two gamma-rays follow each beta-ray.[17] This result also agrees with the Indiana University report.[14]

5. ANTIMONY (124)

The first coincidence experiments in connection with the 60-day activity were carried out by Mitchell, Langer, and McDaniel.[18] Their early data seemed to indicate a simple beta-ray spectrum. Since that time, Meyerhoff and Scharff-Goldhaber[19] have reported a rise in the coincidence rate at low beta-ray energies. This result has been verified by several groups of investigators.[11, 20, 21]

For the sake of completeness, the beta-gamma coincidence rate as a function of the surface density of aluminum before the beta-ray counter is given in Fig. 10. The coincidence rate is seen to decrease from an extrapolated value of 0.92×10^{-3} coincidence per beta-ray at zero absorber thickness to 0.38×10^{-3} coincidence per beta-ray beyond 0.110 g/cm² of aluminum, corresponding to an energy of 0.39 Mev.[8] Beyond this absorber thickness, the calibration point of Sc^{46} indicates that on the average, each beta-ray is followed by 0.55 Mev of gamma-radiation. The gamma-gamma coincidence rate was measured and was found to be $(0.59 \pm 0.03) \times 10^{-3}$ coincidence per gamma-ray.

The radioactive Sb^{124} was prepared when metallic antimony was irradiated for two hours in the pile. The material was aged for three months before the measurements on Sb^{124} were made. No chemical separation was performed.

6. ZIRCONIUM (95)

The long-period zirconium activity has been reported to have a half-life of 63 days.[22] Absorption measurements have indicated beta-rays of energy of 0.29 Mev and gamma-rays of energy 0.94 Mev.[23] Subsequent spectrometric

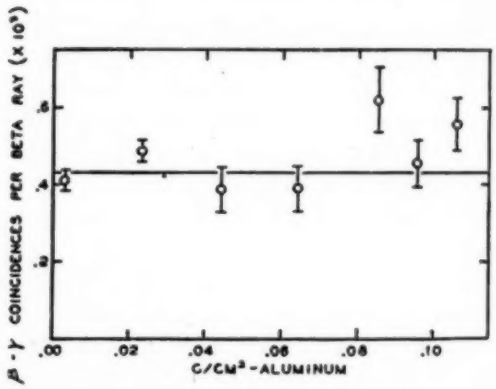

FIG. 8. Beta-gamma coincidence rate for Ir^{192}. This should indicate a simple spectrum.

[17] This result is derived from the following equation:

$$K/(K-1) = \alpha/\beta.$$

α = beta-gamma coincidence rate. β = gamma-gamma coincidence rate. κ = number of quanta per disintegration. For La^{140}, $K = 2.09$.

[18] A. C. G. Mitchell, L. M. Langer, and P. W. McDaniel, Phys. Rev. **57**, 1107 (1940).

[19] W. E. Meyerhof and G. Scharff-Goldhaber, Phys. Rev. **72**, 273 (1947).

[20] E. T. Jurney and A. C. G. Mitchell, Bull. Am. Phys. Soc. **23**, No. 2, 51 (1948).

[21] M. V. Scherb and C. E. Mandeville, Bull. Am. Phys. Soc. **23**, No. 2, 40 (1948).

[22] R. Sagane, S. Kojima, G. Miyamoto, and M. Ikawa, Phys. Rev. **57**, 1180 (1940).

[23] W. N. Moquin and M. L. Pool, Phys. Rev. **65**, 30 (1944).

measurements have given a beta-ray energy of 0.394 Mev and gamma-ray energies of 0.73 Mev and 0.92 Mev.[24] In the course of these latter measurements, a beta-ray spectrum of maximum energy 1.0 Mev and of relative intensity 2 percent was also reported.[24]

Absorption in aluminum of the beta-rays of Zr^{95}, shown in Fig. 11, gives a visual absorption limit of 0.093 g/cm², corresponding to an energy of 0.34 Mev.[8] Analysis of these data by the method of Feather,[16] illustrated in Fig. 12, gives a maximum energy of 0.40 Mev. The coincidence absorption curve of Fig. 13 gives a maximum gamma-ray energy of 0.91 Mev, in good agreement with the measurements already cited. This value for the quantum energy was obtained with the aid of the calibrated coincidence counting arrangement.

The beta-gamma coincidence rate for Zr^{95} is given in Fig. 14, where it is seen to be 0.21×10^{-3} coincidence per beta-ray, independent of the beta-ray energy. The coincidence counting set was calibrated with Sc^{46} for which the beta-gamma coincidence rate was 1.4×10^{-3} coincidence per beta-ray. Miller and Deutsch[25] have shown that 2 Mev of gamma-ray energy follows each beta-ray emitted by Sc^{46}. Since the gamma-ray counter used in the coincidence experiments of this paper had a glass cathode coated with Aquadag and was shielded by a thick aluminum block, the gamma-ray efficiency curve may be assumed to be linear with energy, a good assumption for counters of "low Z" materials. The beta-gamma coincidence rate for Zr^{95} would suggest that each beta-ray is followed by a total gamma-ray energy of about 0.3 Mev. It would seem that the hard gamma-rays are associated with some other decay process such as positron emission or K-electron capture. This view is strengthened by the fact that the gamma-gamma coincidence rate was found to be $(0.29\pm0.02)\times10^{-3}$ coincidence per gamma-ray recorded in the gamma-ray counter, larger than the beta-gamma coincidence rate. K-electron capture or positron emission would lead to the Y^{95} residual nucleus. However, the view has been expressed[24] that Y^{93} and Y^{95} are precedents of isotopes of zirconium. This would suggest a possible confusion of isotopic assignments in the zirconium region. The possibility could also exist that the 0.91-Mev gamma-ray is associated with another zirconium activity of about the same half-period.

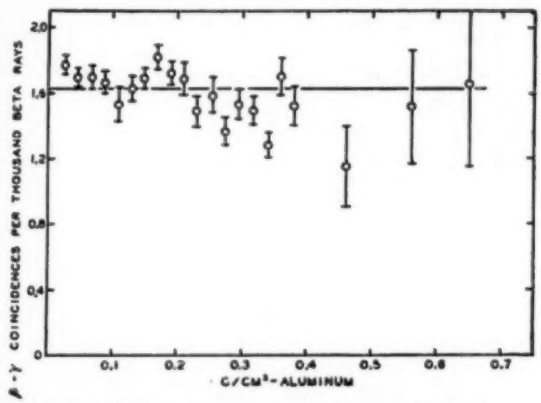

FIG. 9. Beta-gamma coincidence rate for La^{140}.

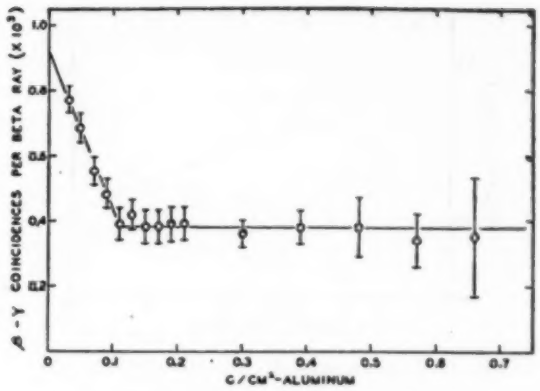

FIG. 10. Beta-gamma coincidence rate for Sb^{124}.

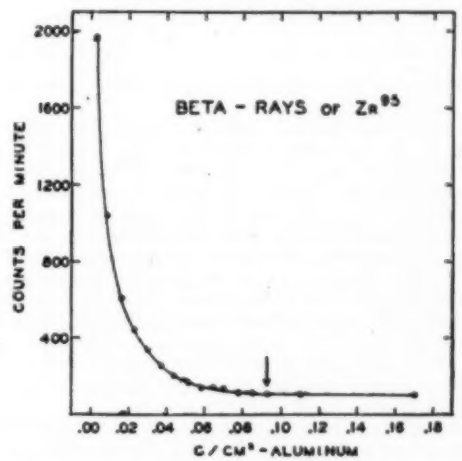

FIG. 11. Absorption in aluminum of the beta-rays of Zr^{95}.

[24] Plutonium Project Report, "Nuclei formed in fission," Rev. Mod. Phys. **18**, 513 (1946).

[25] A. E. Miller and M. Deutsch, Phys. Rev. **72**, 527 (1947).

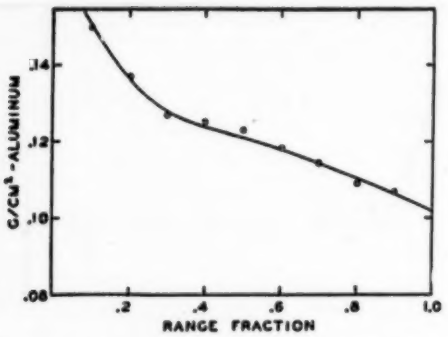

FIG. 12. Feather analysis of the data of Fig. 11.

In observing beta-gamma coincidences, the coincidence resolving time of the circuit was varied from 0.10 microsecond to 12 microseconds. The genuine coincidence rate was found to remain unchanged with the resolving time, so that the low beta-gamma coincidence rate cannot be attributed to coincidence losses arising from a delay in the emission of the gamma-rays which follow the beta-rays. *The role of the 0.91-Mev gamma-ray, and for that matter, of all other gamma-rays emitted by Zr^{95} of energy greater than 0.3 Mev, is unclear.**** It should be added that the coincidence rates were measured immediately after separation of the zirconium activity from its daughter activities of columbium.

7. THE CALIBRATION CURVE FOR COINCIDENCE ABSORPTION MEASUREMENTS OF THE GAMMA-RAY ENERGIES

When coincidence absorption measurements were first undertaken, the coincidence counting arrangement was uncalibrated. Quantum energies were determined by estimating the recoil electron energies from the range-energy relation for homogeneous beta-rays and adding an appropriate amount of energy for collisions in the forward direction. However, as work progressed, many isotopes were investigated upon which spectrometric measurements had already been made. Taking the spectrometric determinations to be correct, the absorption thicknesses (including wall thicknesses of the G-M counters) are plotted against the quantum energies. These data are given in Fig. 15.

The maximum energy of the gamma-rays of As^{76} was recently reported to have a value of 1.98 Mev.[26] The calibration curve of this paper is a revised one, based upon Hayne's value of 2.51 Mev for Ga^{72}. The new value for the maximum energy of the arsenic gamma-rays is then 2.12 Mev.

8. OTHER BETA-RAY SPECTRA

No particular attempt has been made to obtain really high accuracy in the absorption measurements on beta-ray spectra. They were usually made so as to establish the identity of the isotope and to check the validity of the chemical separation. Feather analyses[16] have been made of some data from which end points were previously determined only by visual inspection. The newly determined end points are:

Element	Energy
Sc^{46}	0.32 Mev
Ti^{51}	0.45 Mev
Ta^{182}	0.45 Mev

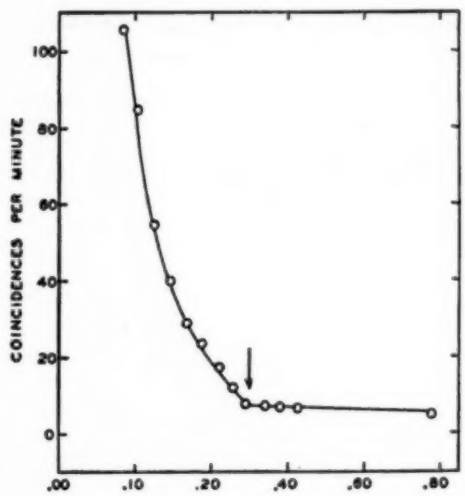

FIG. 13. Coincidence absorption of the secondary electrons of the gamma-rays of Zr^{95}.

*** *Note added in proof May 11, 1948:* The difficulties relating to the presence of the 0.91-Mev gamma-ray are now resolved. A source of the thirty-five day Cb^{95} was separated from the fission fragments of the uranium pile at Oak Ridge. After chemical purification, coincidence and absorption measurements were carried out in the usual manner. A coincidence absorption experiment showed that the 0.91-Mev gamma-ray is emitted by the columbium daughter element, and beta-gamma coincidence measurements indicated that the gamma-ray follows the soft beta-rays emitted by Cb^{95}. Assignment of this gamma-ray to Zr^{95} in the text of this paper apparently resulted from an incomplete chemical separation and from the fact that the 0.91-Mev gamma-ray is very intense.

Gamma-gamma coincidences were found to be 0.28×10^{-3} coincidence per gamma-ray for the fission fragment of Cb^{95}. The gamma-gamma coincidence rate reported in the paper itself for Zr^{95} is therefore probably incorrect.

[26] M. V. Scherb and C. E. Mandeville, Phys. Rev. **73**, 418 (1948).

ACKNOWLEDGMENTS

The writers wish to thank Professor W. B. Keighton of Swarthmore College for having made the chemical separations. They wish also to acknowledge the continued interest of Dr. W. F. G. Swann, Director of the Bartol Research Foundation.

APPENDIX I: CHEMICAL PROCEDURE FOR IRIDIUM

IrO_2, irradiated by neutrons in the pile, was dissolved in HBr. Aqua regia was added, and the solution was evaporated to dryness. Two cc of H_2O were then added, and to this new solution NH_4Cl was added until saturation occurred. After standing for thirty minutes, a precipitate, $(NH_4)_2IrCl_6$, was formed. This was filtered out and washed with a cold saturated solution of NH_4Cl. This procedure should have removed palladium, the outstanding impurity which might have been present.

APPENDIX II: CHEMICAL PROCEDURE FOR LANTHANUM

To 38 mg of irradiated La_2O_3 were added 350 mg of inactive La_2O_3, 10 mg of CaO, 10 mg of BaO, and Na_3PO_4 as carriers for calcium, barium, and phosphorous. This mixture was dissolved in 200 ml of water and a minimum quantity of HCl. Lanthanum hydroxide was precipitated from the boiling solution with ammonia. After washing the precipitate with water containing a small amount of NH_3, the precipitate was dissolved in 0.5*N* HCl, and lanthanum oxalate was precipitated from the boiling solution with oxalic acid. After washing, the precipitate was ignited to La_2O_3.

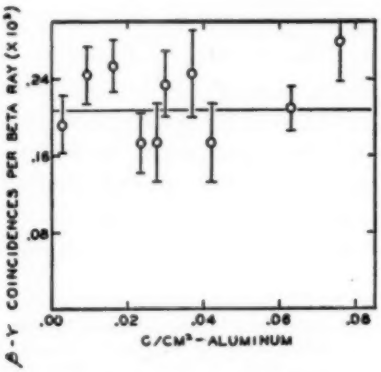

FIG. 14. Beta-gamma coincidence rate for Zr^{95}.

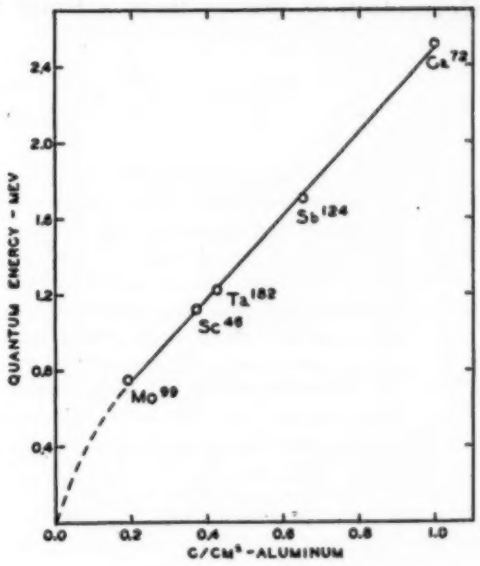

FIG. 15. Calibration curve for the double coincidence counting set used in the coincidence absorption experiments. References:

[1] Ga^{72}—S. K. Haynes, Phys. Rev. **73**, 187 (1948).
[2] Sb^{124}—A. Wattenberg, Phys. Rev. **71**, 497 (1947).
[3] Ta^{182}—W. Rall and R. G. Wilkinson, Phys. Rev. **71**, 321 (1947).
[4] Sc^{46}—A. E. Miller and M. Deutsch, Phys. Rev. **72**, 527 (1947).
[5] Mo^{99}—L. C. Miller and L. F. Curtiss, Phys. Rev. **70**, 982 (1946).

APPENDIX III: CHEMICAL PROCEDURE FOR ZIRCONIUM

To 0.5g of $Zr(OH)_4$ were added 10 mg of CaO, of Fe_2O_3, of KH_2PO_4, and of Ta_2O_5 as carriers for calcium, iron, phosphorous, and columbian, respectively. The mixture was fused with 5g of K_2CO_3 and 100 mg of KNO_3. After cooling, the melt was leached with 10 ml of cold water and filtered. The residue containing ZrO_2 was thoroughly washed with cold H_2O to remove tantalum, phosphorous, and columbium. The residue was fused with $KHSO_4$, and the melt was dissolved in dilute H_2SO_4. Zirconium was precipitated from the acid solutions as $ZrH_2(PO_4)_2$ by an excess of $(NH_4)_2HPO_4$. After washing, the precipitate was ignited to ZrP_2O_7. Immediately before making observations on the zirconium activity, the phosphate precipitate with Ta_2O_5 carrier was again fused with K_2CO_3 and KNO_3 and was leached with cold water to separate out any accumulated columbium.

Refraction of Waves from a Point Source into a Medium of Higher Velocity*

E. GERJUOY
University of Southern California, University Park, Los Angeles, California
(Received February 20, 1948)

A point source is placed in one medium and the fields in a second medium, separated from the first by an infinite plane boundary, are calculated for the case that the wave velocity in the second medium exceeds that in the first medium. Absorption is neglected and the problem is solved both by ray methods and by evaluating, by the method of steepest descents, of an exact solution of the wave equation. The agreement between the solutions by different methods permits a ready and expected interpretation of the wave solution. Rays incident on the boundary at angles exceeding the critical angle are totally reflected; however, directly transmitted energy penetrates to all points in the second medium. At points in the second medium outside the critical angle, near the surface and far from the source, the directly transmitted fields are much smaller than the fields, exponentially decaying from the surface, which result from totally reflected rays. This suggests an experiment to measure quantitatively the penetration of the fields into the second medium in total reflection, easily performable for the case of sound waves penetrating from air into water.

I. INTRODUCTION

IN Fig. 1 a point harmonic source of sound of circular frequency ω is located at P, a height h above an infinite flat water surface. The origin of coordinates O is on the surface directly beneath P, whose rectangular coordinates are $(0, 0, h)$. If the subscripts 1 and 2 refer to air and water, respectively, the sound pressure p in either medium can be found from the relations

$$p_1 = -i\omega\rho_1\varphi_1 e^{-i\omega t}, \qquad p_2 = -i\omega\rho_2\varphi_2 e^{-i\omega t}, \tag{1}$$

where φ_1 and φ_2 satisfy the wave equation in their respective media,

$$\Delta\varphi_1 + k_1^2\varphi_1 = 0, \quad z>0 \qquad \Delta\varphi_2 + k_2^2\varphi_2 = 0, \quad z<0. \tag{2}$$

In these equations ρ denotes density, c sound velocity, and $k=\omega/c$. The boundary conditions determining the solution are: (a) φ_1 and φ_2 each represent outgoing waves of vanishing amplitude at infinity; (b) the solutions are everywhere finite except in the neighborhood of P where, except for an arbitrary multiplicative factor (which we shall ignore),

$$\varphi_1 = e^{ik_1R}/R, \tag{3}$$

R being the distance from the point P; (c) on the bounding plane $z=0$

$$\rho_1\varphi_1 = \rho_2\varphi_2, \quad \partial\varphi_1/\partial z = \partial\varphi_2/\partial z.$$

Formulated in this way this acoustic problem is formally identical with the electromagnetic problem of determining the radiation from a dipole antenna a height h above a plane earth. We have chosen to describe the problem in terms of a point source of sound radiating from air into water merely because we are interested here primarily in the case where the wave velocity in medium 2 is greater than that in medium 1. Sound incident from air to water is, in fact, totally reflected at angles of incidence greater than 13°. The electromagnetic problem was first solved by Weyl,[1] who extended a solution by Sommerfeld[2] of the case $h=0$. The radiation from an antenna located above the earth has since been treated by a number of writers,[3] principally interested, however, in the fields above the earth. Consequently, an evaluation of the fields in the second medium has only been given very recently by Kruger.[4] Kruger solves the electromagnetic problem for the general case that the second medium has a complex index of refraction. His analysis which is long and difficult cannot be applied to the

* This paper is based in part on work done for the Office of Scientific Research and Development.

[1] H. Weyl, Ann. d. Physik u. Chemie **60**, 481 (1919).
[2] A. Sommerfeld, Ann. d. Physik **28**, 665 (1909).
[3] Cf. J. A. Stratton, *Electromagnetic Theory* (McGraw-Hill Book Company, Inc., New York, 1941), pp. 573 ff.
[4] M. Kruger, Zeits. f. Physik **121**, 377 (1943).

problem under consideration for two reasons. Kruger's solution is immediately applicable only when the wave velocity in the second medium is less than the wave velocity in the first medium. Furthermore, Kruger makes the permeability of the second medium unity *ab initio*. With this simplification the analogy to the acoustic problem is no longer exact.[5]

In the following sections expressions are obtained for the sound pressure in the second medium, for the case that the index of refraction is real and less than unity. The solutions are valid at large distances from the source and are derived in two ways, first by solving the wave equation subject to the boundary conditions, next by ray acoustics.

The first solution is accomplished with considerably less effort than Kruger's, the simplification resulting from the fact that absorption is neglected. The solution by ray acoustics is even easier to obtain, and contains the essential features of the wave solution. Energy reaches a point C (Fig. 1), close to the surface and far from the source, in two ways. The ray PD, lying inside the critical angle, OPE, is refracted to C. In addition, the total reflection of a ray PB results in an exponential decrease of sound pressure with increasing depth.

These qualitative results are well known. The quantitative analysis developed below does, however, add to our understanding of the problem. The elementary analysis by ray acoustics gives a surprisingly accurate picture of the transmission.* The method of steepest descents used to evaluate the integrals obtained in the wave solution shows very beautifully that, although according to Huygens' principle wavelets must reach C (Fig. 1) from all points on the surface, actually these waves interfere so that only wavelets from the immediate vicinity of the point D remain to transmit any important amount of energy to C. A further result is that at points C near the surface, sufficiently far from the source and outside the critical angle, the directly transmitted pressure (along the path

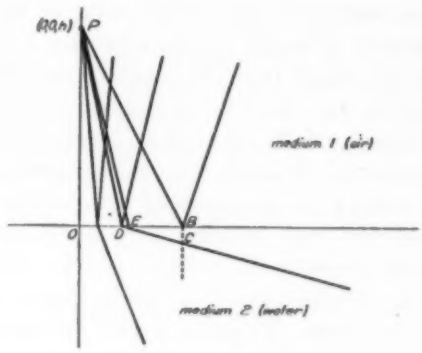

FIG. 1. Ray diagram.

PDC) is proportional to the depth and to the inverse square of the distance from the source, because of the increased divergence of the refracted rays as the incident angle approaches the critical angle. This means that at points C (Fig. 1), within a fraction of a wave-length of the surface, the sound pressure is produced primarily by the exponentially decreasing term, since the pressure at B on the surface varies as the inverse first power of the distance from the source, and the exponential decrease from the pressure at the surface is negligible for depths a fraction of the wave-length.

This result suggests the possibility of a quantitative verification of the theoretical prediction that in total reflection the wave amplitude does penetrate into the second medium. While this penetration is scarcely in doubt, nonetheless it is noteworthy that past optical experiments to test this prediction are all essentially qualitative. That is, they show the presence of some energy in the second medium, but do not quantitatively measure the amount of energy present.[6] The long wave-lengths of sound waves at sonic frequencies make it relatively simple to vary the depth of a hydrophone at points near the surface and outside the critical angle, thereby directly measuring the variation of sound pressure with depth and permitting comparison with the predicted exponential decay. In such an experiment a hydrophone sensitive to pressure rather than to velocity must be used, since the velocity at an

[5] G. Joos and J. Teltow, Physik. Zeits. **40**, 289 (1939).

* A general discussion of the approximations involved in the ray analysis has been given by C. Eckart in a paper "The Approximate Solution of One-Dimensional Wave Equations," soon to appear in the Reviews of Modern Physics.

[6] Cf., for example, R. W. Wood, *Physical Optics* (The Macmillan Company, New York, 1934), pp. 418 ff. A quantitative experiment by C. Schaefer and G. Gross, Ann. d. Physik **32**, 648 (1910), did not directly measure the fields in the second medium.

air-water surface is very small owing to the very great density of water compared to air. It should perhaps be noted that there is no contradiction between the fact that a hydrophone can respond to the exponentially decreasing pressure and the very meaning of total reflection, namely, that all the energy in the incident ray goes into the reflected ray. The presence of a hydrophone in the water introduces a new boundary with new boundary conditions. The result is to permit energy to enter the water from the otherwise totally reflected incident ray in just sufficient amount to energize the hydrophone. Although this assertion is difficult to prove in detail, it must be true because it can be shown directly from the fundamental equations that energy is always conserved.

II. SOLUTION OF THE WAVE EQUATION

If (x, y, z) are the coordinates of a point in medium 1, then[3]

$$\frac{e^{ik_1R}}{R}=\frac{ik_1}{2\pi}\int_0^{2\pi}d\psi\int_0^{(\pi/2)-i\infty}d\theta\,\sin\theta \times e^{ik_1[x\sin\theta\cos\psi+y\sin\theta\sin\psi+(h-z)\cos\theta]}, \quad (5)$$

when $0\leqslant z\leqslant h$.

Write

$$\varphi_1=\frac{e^{ik_1R}}{R}+\frac{ik_1}{2\pi}\int_0^{2\pi}d\psi\int_0^{(\pi/2)-i\infty}d\theta\,\sin\theta f_r \times e^{ik_1[x\sin\theta\cos\psi+y\sin\theta\sin\psi+(z+h)\cos\theta]}, \quad (6)$$

$$\varphi_2=\frac{ik_1}{2\pi}\int_0^{2\pi}d\psi\int_0^{(\pi/2)-i\infty}d\theta\,\sin\theta f_t \times e^{ik_2(x\sin\theta'\cos\psi+y\sin\theta'\sin\psi-z\cos\theta')}, \quad (7)$$

where f_r, f_t, and θ' are as yet undetermined functions of θ, ψ. The boundary conditions at $z=0$ are satisfied when

$$k_1\sin\theta=k_2\sin\theta', \quad (8)$$

$$f_t=\frac{2\rho_1k_1\cos\theta e^{ik_1h\cos\theta}}{\rho_2k_1\cos\theta+\rho_1k_2(1-k_1^2k_2^{-2}\sin^2\theta)^{\frac{1}{2}}}, \quad (9)$$

$$f_r=\frac{\rho_2k_1\cos\theta-\rho_1k_2(1-k_1^2k_2^{-2}\sin^2\theta)^{\frac{1}{2}}}{\rho_2k_1\cos\theta+\rho_1k_2(1-k_1^2k_2^{-2}\sin^2\theta)^{\frac{1}{2}}}. \quad (10)$$

Choose a system of spherical coordinates with the polar axis directed along the positive z axis. The contour in the complex θ plane for the above integrals lies along the real axis from $\theta=0$ to $\theta=\pi/2$, and then in the fourth quadrant to $\theta=\pi/2-i\infty$. For real θ, therefore, the integral (5) represents a system of plane waves moving downward, i.e., outward from the source. The polar angle of the direction of advance of the plane wave defined by ψ, θ in (5) is $\pi-\theta$. Thus θ is the angle of incidence of the wave on the surface. The corresponding wave in (6) is moving upward in the direction whose polar angle is θ, and in (7) is moving in a direction whose polar angle is $\pi-\theta'$. Since (7) must represent an outgoing wave at infinity, the appropriate solution of (8) for real θ' is $\theta'<\pi/2$. Hence θ' is the angle of refraction of a plane wave striking the surface with incident angle θ, and f_r and f_t are, respectively, the reflection and transmission coefficients of the wave amplitude. For real θ', $\cos\theta'$, the square root in (9) and (10), is positive. Along the contour, $\sin\theta$ increases monotonically. Consequently, in order that (7) be finite for negative z,

$$(1-k_1^2k_2^{-2}\sin^2\theta)^{\frac{1}{2}}=i(k_1^2k_2^{-2}\sin^2\theta-1)^{\frac{1}{2}}, \quad (11)$$

when $k_2<k_1\sin\theta$.

If z is now taken as a *positive* depth beneath the surface, $\alpha=c_1/c_2$, $\beta=\rho_2/\rho_1$, (7) can be rewritten as

$$\varphi_2=\frac{ik_1}{\pi}\int_0^{2\pi}d\psi\int_0^{(\pi/2)-i\infty}d\theta\,\sin\theta \times\frac{e^{ik_1(x\sin\theta\cos\psi+y\sin\theta\sin\psi+h\cos\theta+z(\alpha^2-\sin^2\theta)^{\frac{1}{2}})}}{\beta\cos\theta+(\alpha^2-\sin^2\theta)^{\frac{1}{2}}}. \quad (12)$$

For transmission from air to water, $\beta=850$ and $\alpha=0.23$.

Introducing $r^2=x^2+y^2$, letting $\sin\theta=u$, and using Eq. (15) below, it is easily shown that[3]

$$\varphi_2=2ik_1\int_0^{\infty}duuJ_0(k_1ru)(e^{ik_1Q}/P). \quad (13)$$

For sufficiently large k_1ru, J_0 in (13) can be replaced by its asymptotic expansion. Suppose the asymptotic expansion is valid for $|u|>a_0$, where a_0 will be determined later. Then introducing the asymptotic expansion for J_0, with a

a complex number whose magnitude is a_0,

$$\varphi_2=2ik_1\int_0^a duuJ_0(k_1ru)\frac{e^{ik_1Q}}{P}$$
$$+ie^{-(i\pi/4)}\left(\frac{2k_1}{\pi r}\right)^{\frac{1}{2}}\int_a^\infty duu^{\frac{1}{2}}\frac{e^{ik_1A}}{P}$$
$$+ie^{(i\pi/4)}\left(\frac{2k_1}{\pi r}\right)^{\frac{1}{2}}\int_a^\infty duu^{\frac{1}{2}}\frac{e^{ik_1B}}{P}. \quad (14)$$

In (13) and (14)

$$\begin{aligned}P(u)&=\beta(1-u^2)^{\frac{1}{2}}+(\alpha^2-u^2)^{\frac{1}{2}},\\ Q(u)&=h(1-u^2)^{\frac{1}{2}}+z(\alpha^2-u^2)^{\frac{1}{2}},\\ A(u)&=h(1-u^2)^{\frac{1}{2}}+z(\alpha^2-u^2)^{\frac{1}{2}}+ru,\\ B(u)&=h(1-u^2)^{\frac{1}{2}}+z(\alpha^2-u^2)^{\frac{1}{2}}-ru.\end{aligned} \quad (15)$$

The phase of u lies between $-\pi$ and π. Figure 2 shows the complex plane with cuts starting at 1, -1, α, and $-\alpha$, in such directions as to fulfill the required conditions that, on the positive real axis, the expressions $(1-u^2)^{\frac{1}{2}}$ and $(\alpha^2-u^2)^{\frac{1}{2}}$ must be positive real when u is small and positive imaginary when u is large.

For large real u the complex numbers $1-u^2$ and α^2-u^2 have phase π. The contour for each of the infinite integrals in (14) runs from somewhere near the origin to $+\infty$ without crossing any of the cuts. In the various regions of the plane the signs of the real and imaginary parts of $(1-u^2)^{\frac{1}{2}}$ and $(\alpha^2-u^2)^{\frac{1}{2}}$ are negative in the following regions.

$$\begin{aligned}Re(1-u^2)^{\frac{1}{2}}<0&: \textit{ III, V}\\ Re(\alpha^2-u^2)^{\frac{1}{2}}<0&: \textit{ II, III, V, VI}\\ I(1-u^2)^{\frac{1}{2}}<0&: \textit{ I, II, V, VIII}\\ I(\alpha^2-u^2)^{\frac{1}{2}}<0&: \textit{ I, V, VI, VIII.}\end{aligned} \quad (16)$$

Otherwise they are positive. The real and imaginary parts of the radicals change sign discontinuously at the cuts but become zero on the real and imaginary axes if they change sign crossing these axes.

Assume, specifically, $\alpha<1$, $\beta>1$. Then the imaginary parts of both radicals have the same sign at $u=\pm(\beta^2-\alpha^2)^{\frac{1}{2}}/(\beta^2-1)^{\frac{1}{2}}$, the only points where $P(u)$ can possibly be zero. Thus $P(u)$ is never zero and the contours can be deformed without fear of passing through a pole.[7] Asymptotic expressions for the infinite integrals in (14) can be obtained by the method of steepest descents.[8] The saddle points are found from

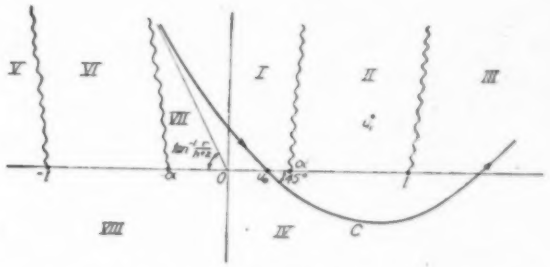

FIG. 2. Regions of the complex plane and contour along which $ReA(u)=A(u_0)$, when $r^2/(r^2+h^2)<\alpha^2$.

$$A'(u)=[-uh/(1-u^2)^{\frac{1}{2}}]-[uz/(\alpha^2-u^2)^{\frac{1}{2}}]+r=0, \quad (17)$$

$$B'(u)=[-uh/(1-u^2)^{\frac{1}{2}}]-[uz/(\alpha^2-u^2)^{\frac{1}{2}}]-r=0. \quad (18)$$

Equation (17) has a root u_0 somewhere on the real axis between 0 and α, and may have a root u_1 somewhere in *II* (Fig. 2). There are no other roots in the right half of the plane nor are there any roots in *VII*. It is necessary to find the contour passing through u_0 along which

$$ReA(u)=ReA(u_0),$$

and along which $IA(u)$ increases as u approaches infinity. Along this contour the phase of e^{ik_1A} in (14) is constant, while the real part of e^{ik_1A} decreases exponentially as infinity is approached. If this contour leads from u_0 to a point at infinity from which the integral to $+\infty$ is zero, the integral involving $A(u)$ in (14) can at once be evaluated. If the contour does not lead to such a point at infinity, it will be necessary to return to $+\infty$ along another path, possibly passing through u_1.

In the vicinity of u_0

$$A(u)=A(u_0)+\tfrac{1}{2}A''(u_0)(u-u_0)^2. \quad (19)$$

$A''(u_0)$ is real and negative. Consequently, the appropriate contour cuts the real axis at u_0 at an angle of $-45°$, as in Fig. 2. Furthermore, $A(u)$ is real and finite on the real axis between $-\alpha$ and α, and has but one maximum in that interval, at u_0. It follows that the extension to

[7] A somewhat lengthier argument shows that P is never zero whatever the value of β.

[8] G. N. Watson, *Treatise on the Theory of Bessel Functions* (The Macmillan Company, New York, 1944), p. 235.

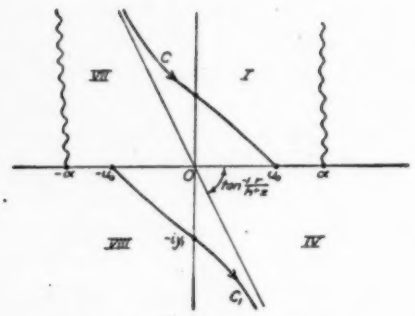

FIG. 3. Contours C and C_1.

the left of the contour $ReA(u)=A(u_0)$ never crosses the real axis again but continues into regions I or VII. In these regions, for large u,

$$(1-u^2)^{\frac{1}{2}}=(\alpha^2-u^2)^{\frac{1}{2}}=-iu. \tag{20}$$

Substituting (20) in (15) with $u=\rho e^{i\varphi}$, ρ approaching infinity, it is seen that $ReA(u)$ can be finite for large u only if φ asymptotically approaches the value $\tan^{-1}-r/(h+z)$. Thus the contour $ReA(u)=A(u_0)$ extends to the left into region VII, and in this region $IA(u)$ approaches $+\infty$ as u becomes infinite. The appropriate contour $ReA(u)=A(u_0)$ has therefore been determined to the left of u_0, as shown in Fig. 2.

The rules (16) and Eqs. (15) show that on the real axis for $-\alpha<u<\alpha$, $B(-u)=A(u)$. Hence $B(u)$ has a saddle point at $-u_0$. Also $A(u)$, u in IV, equals $B(-u)$, $-u$ in VII. $A(u)$, u in I, equals $B(-u)$, $-u$ in $VIII$. The contour C_1, therefore, along which $ReB(u)=B(-u_0)$ and $IB(u)$ increases as $u\to\infty$, leaves $-u_0$ at an angle of $-45°$, as in Fig. 3, and in IV mirrors the contour C in VII, C the contour along which $ReA(u)=A(u_0)$. $P(u)$, u in IV, equals $P(-u)$, u in VII. $IB(u)\to+\infty$ as u becomes infinite anywhere in region IV. Let $-iy_1$ be the point at which C_1 crosses the negative y axis, and choose $a=-ia_0$ in (14). Then in (14)

$$\int_{-ia_0}^{\infty} duu^{\frac{1}{2}}\frac{e^{ik_1B}}{P}=\int_{-ia_0}^{-iy_1} duu^{\frac{1}{2}}\frac{e^{ik_1B}}{P}+\int_{C_1}^{-iy_1} duu^{\frac{1}{2}}\frac{e^{ik_1B}}{P}. \tag{21}$$

In (21) the integral along C_1 proceeds from $-iy_1$ along the direction shown by the arrow (Fig. 3). Furthermore,

$$\int_{C_1}^{-iy_1} duu^{\frac{1}{2}}\frac{e^{ik_1B}}{P}=e^{-i(\pi/2)}\int_{C}^{iy_1} duu^{\frac{1}{2}}\frac{e^{ik_1A}}{P}. \tag{22}$$

In (22) the integral along C proceeds to iy_1 along the direction shown by the arrow (Fig. 3). Substituting Eqs. (21) and (22) in (14) gives, therefore,

$$\varphi_2=2ik_1\int_0^{-ia_0} duuJ_0(k_1ru)\frac{e^{ik_1Q}}{P}+ie^{-(i\pi/4)}\left(\frac{2k_1}{\pi r}\right)^{\frac{1}{2}}\int_{-ia_0}^{ia_0} duu^{\frac{1}{2}}\frac{e^{ik_1A}}{P}+ie^{-(i\pi/4)}\left(\frac{2k_1}{\pi r}\right)^{\frac{1}{2}}\int_{C}^{\infty} duu^{\frac{1}{2}}\frac{e^{ik_1A}}{P}. \tag{23}$$

In (23) the integral along C proceeds from infinity in region VII through u_0 and along the appropriate extension of $ReA(u)=A(u_0)$ in the part of the plane to the right of u_0, arriving finally at infinity on the positive real axis.

On the real axis, between α and 1, $ReA(u)=h(1-u^2)^{\frac{1}{2}}+ru$. Let $r^2/(r^2+h^2)=\gamma^2$. If $\gamma^2<\alpha^2$, $ReA(u)$ decreases monotonically as u varies from α to 1. Therefore, since $ReA(u)$ also decreases as u varies from u_0 to α, if $\gamma^2<\alpha^2$ the contour $ReA(u)=A(u_0)$ cannot cross the real axis between α and 1. Since $ReA(u)$ is constant on the contour, the contour can become parallel to the imaginary axis only when $\partial ReA(u)/\partial y=0$, $u=x+iy$. This means that dA/du is pure real whenever the contour is parallel to the y axis. It is readily shown that in IV the imaginary parts of $u/(1-u^2)^{\frac{1}{2}}$ and $u/(\alpha^2-u^2)^{\frac{1}{2}}$ have the same sign. Thus, from (17), the contour never becomes parallel to the y axis in IV. In III and IV for large u, $(1-u^2)^{\frac{1}{2}}=(\alpha^2-u^2)^{\frac{1}{2}}=iu$. Then, as before, using $u=\rho e^{i\varphi}$, $ReA(u)=A(u_0)$ must approach infinity in III with $\varphi=\tan^{-1}r/(h+z)$. In III $IA(u)\to\infty$ as $u\to\infty$. This completes the determination of the contour C in (23) for the case $r^2/(r^2+h^2)<\alpha^2$ (Fig. 2).

When $\gamma^2>\alpha^2$, the contour may be more complicated. In this case, $ReA(u)$ has a maximum on the real axis at $u=\gamma$, at which point $ReA(u)=(r^2+h^2)^{\frac{1}{2}}$.

If $A(u_0)<(r^2+h^2)^{\frac{1}{2}}$ the contour may cross the real axis between α and 1 and go to infinity in *II*. If $A(u_0)>(r^2+h^2)^{\frac{1}{2}}$, the contour must go to infinity in *III*, as in Fig. 2. When $\gamma^2>\alpha^2$, u_0 approaches α as z approaches zero. In fact, for small z, (17) is solved by

$$u_0=\alpha-z^2/2\alpha b^2, \tag{24}$$

where

$$b=r/\alpha-h/(1-\alpha^2)^{\frac{1}{2}} \tag{25}$$

is positive when $\gamma^2>\alpha^2$. The equation of the contour $ReA(u)=A(u_0)$ becomes in this case

$$ReA(u)=\alpha r+h(1-\alpha^2)^{\frac{1}{2}}+z^2/2b. \tag{26}$$

In the vicinity of $u=\alpha$, for small z, the equation of the contour can be found by letting $u=\alpha+w$, w small, and solving for w. The only question is the choice of sign for $(\alpha^2-w^2)^{\frac{1}{2}}=(-2\alpha w-w^2)^{\frac{1}{2}}$, which is solved by noting from Fig. 2, that the cut through α is so drawn that at $u=u_0$ the phase of w is $-\pi$. Thus $(\alpha^2-u^2)^{\frac{1}{2}}$ is positive real when $u=u_0$ if, for small w, $(\alpha^2-u^2)^{\frac{1}{2}}=i(2\alpha w)^{\frac{1}{2}}$. The solution to (26) is then found to be

$$w=\frac{z^2e^{i\varphi}}{2b^2\alpha(1-\sin\varphi)}. \tag{27}$$

Equation (27) shows that as φ varies from $-\pi$ to 0, u varies continuously from u_0 to a point on the real axis to the right of α. In other words, for small z the contour does cross the real axis into region *II* (Fig. 2), and, in fact, it follows from (27) that it crosses the axis to the right of α at an angle of 45°. For small w

$$A'(u)=\frac{-h\alpha}{(1-\alpha^2)^{\frac{1}{2}}}-\frac{h\alpha^2w}{(1-\alpha^2)^{\frac{1}{2}}}+i\alpha z(2\alpha)^{\frac{1}{2}}w^{-\frac{1}{2}}+r. \tag{28}$$

Or with $w=\rho e^{i\varphi}$

$$\begin{aligned}A'(u)=\alpha b&-h\alpha^2(1-\alpha^2)^{-\frac{1}{2}}\rho\cos\varphi\\&+\alpha z(2\alpha)^{\frac{1}{2}}\rho^{-\frac{1}{2}}\sin\tfrac{1}{2}\varphi\\&+i[-h\alpha^2(1-\alpha^2)^{-\frac{1}{2}}\rho\sin\varphi\\&\qquad+\alpha z(2\alpha)^{\frac{1}{2}}\rho^{-\frac{1}{2}}\cos\tfrac{1}{2}\varphi].\end{aligned} \tag{29}$$

Equation (29) shows that for small ρ and $0<\varphi<\pi$, i.e., for points in *II* near α, $ReA'(u)$ is not zero. On the other hand, $IA'(u)=0$ on a contour which for sufficiently small z lies arbitrarily close to the real axis. This means that for sufficiently small z the contour $ReA(u)=A(u_0)$ does not become parallel to the x axis but necessarily becomes parallel to the y axis in the immediate vicinity of $u=\alpha$. In other words, for small z, the contour $ReA(u)=A(u_0)$ curves around the point $u=\alpha$ and, in *II*, proceeds toward the positive imaginary axis. For small z, at points not near α,

$$A'(u)=-hu(1-u^2)^{-\frac{1}{2}}+r, \tag{30}$$

and it can be shown that the real part of (30) is not zero anywhere along the contour $ReA(u)=A(u_0)$ in *II*.

This completes the proof that for small z and $r^2/(r^2+h^2)>\alpha^2$ the contour C in (23) after passing through u_0 goes to infinity in the extension of region *II* into the second quadrant. To get to $+\infty$ on the real axis, the contour has to return via the saddle point u_1 (Fig. 2). By methods similar to those used above it can be shown that the returning contour goes through u_1 at an angle of $-45°$, for small z, and does in fact proceed to $+\infty$ in region *III* (Fig. 2).

$$\begin{aligned}(d/dz)A(u_0)&=(\alpha^2-u_0^2)^{\frac{1}{2}}+A'(u_0)(du_0/dz)\\&=(\alpha^2-u_0^2)^{\frac{1}{2}}.\end{aligned} \tag{31}$$

Equation (31), which follows from (15) and the definition of u_0, shows that as z increases, for any fixed values of h and r, $A(u_0)$ increases, since $u_0<\alpha$. In fact, for sufficiently large z, (17) shows u_0 approaches zero, and $A(u_0)$ therefore approaches infinity with increasing z. Since the maximum value of $ReA(u)$ on the real axis between α and 1 is $(r^2+h^2)^{\frac{1}{2}}$, the preceding statements mean that as z is increased from zero, with $\gamma^2>\alpha^2$, the contour C in (23), which for small z passes through both u_0 and u_1, somehow deforms with increasing z so that for sufficiently large z the contour after leaving u_0 goes to infinity in *III* without first going to infinity in *II*. The complexity of the algebra makes it difficult to determine explicitly the value of z, as a function of r and h, at which the contour changes abruptly from one which goes through both u_0 and u_1 to a contour which goes only through u_0. However, examination of the contours indicates the transition point probably occurs when $A(u_0)=ReA(u_1)$, and that for values of z such that $A(u_0)$ exceeds $ReA(u_1)$ the contour does not pass through u_1.

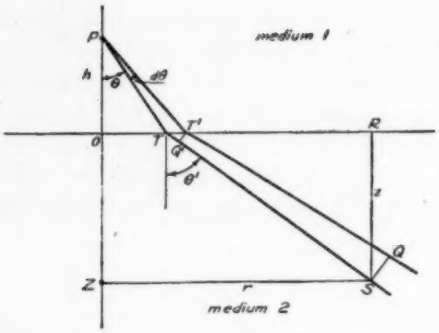

FIG. 4. Divergence of two infinitesimally separated rays.

An asymptotic expansion of the contour integral in (23) can now be obtained[8] by reverting the relation between u and A. The dominant terms of the asymptotic expansion are most simply found by approximating $A(u)$ by (19) in the vicinity of its saddle points, and replacing the contour integral by the integral of a Gaussian function from $-\infty$ to $+\infty$. With this approximation the last term in (23) becomes

$$\frac{2u_0^{\frac{1}{2}}r^{-\frac{1}{2}}e^{ik_1[h(1-u_0^2)^{-\frac{1}{2}}+z\alpha^2(\alpha^2-u_0^2)^{-\frac{1}{2}}]}}{P(u_0)[h(1-u_0^2)^{-\frac{1}{2}}+\alpha^2z(\alpha^2-u_0^2)^{-\frac{1}{2}}]^{\frac{1}{2}}} \tag{32}$$

when the contour does not pass through u_1. When the contour passes through u_1, its contribution must be added to (32). For small z this contribution is

$$\frac{2h(r^2+h^2)^{-1}e^{[ik_1(r^2+h^2)^{\frac{1}{2}}-k_1z(\gamma^2-\alpha^2)^{\frac{1}{2}}]}}{[\beta h(r^2+h^2)^{-\frac{1}{2}}+i(\gamma^2-\alpha^2)^{\frac{1}{2}}]}. \tag{33}$$

The other integrals in (23) can be shown to be negligible compared to (32) and (33) for sufficiently large k_1r. Suppose the asymptotic expansion of $J_0(z)$ represents $J_0(z)$ with sufficient accuracy for $|z|>n$, n some number. Then a_0 in (23) equals n/k_1r. With the substitution $u=w/k_1r$, the first two integrals in (23) are readily seen to be of order $1/k_1r$ compared to (32) and (33). This completes the wave solution of the problem.

III. SOLUTION BY RAY ACOUSTICS

In Fig. 4, PT and PT' are two rays, lying in the same plane with OP, whose angles of incidence on the surface are θ and $\theta+d\theta$. The angles of refraction for these rays are θ' and $\theta'+d\theta'$. θ is assumed less than the critical angle. The ray PT is refracted to a point S, at depth $OZ=z$, and distance $OR=r$ from the axis OP. The amplitude of the pressure at S will now be calculated.

Consider the surfaces formed by rotating Fig. 4 about the line POZ. Energy leaves P in a volume between the cones formed by rotating PT and PT'. Some of this energy is reflected and some refracted. According to ray acoustics, the refracted energy always lies between the cones formed by rotating TS and $T'Q$. The pressure at S can therefore be determined by finding the relation between SQ, which is perpendicular to TS, and $T'Q'$, which is perpendicular to TS at Q'. $T'Q'$ measures the energy density at the point where the energy first enters the water. The relation between the pressure in medium 2 at T, and the pressure in medium 1 at T is obtained from the coefficient f_t, Eq. (9), assuming that the curvature of the incident wave front at T is sufficiently small that the incident wave at T can be regarded as plane. Referring to Fig. 4,

$$\begin{aligned} OT &= h\tan\theta, \\ TT' &= h\sec.^2\theta d\theta, \\ T'Q' &= TT'\cos\theta' = h\sec.^2\theta\cos\theta' d\theta. \end{aligned} \tag{34}$$

The distance SQ to first order in differentials is the perpendicular distance $T'Q'$ at the surface plus the additional distance resulting from the rotation $d\theta'$.

$$SQ = T'Q' + TSd\theta' = T'Q' + z\sec.\theta' d\theta'. \tag{35}$$

From (8) and the definition of α,

$$\sin\theta = \alpha\sin\theta', \quad \cos\theta d\theta = \alpha\cos\theta' d\theta'. \tag{36}$$

Let the pressure in the water at T be $p(T)$ and the pressure at S be $p(S)$. The energy which leaves P between the cones formed by PT and PT', and which enters the water, must pass through a surface of area $2\pi(OT')(T'Q')$ at T, and through a surface of area $2\pi(ZS)(SQ)$ at S. The energy density is proportional to the square of the pressure. Therefore, the ratio of the absolute magnitudes of $p(S)$ and $p(T)$ is given by

$$|(p(S)/p(T))| = \{[(OT')(T'Q')/(ZS)(SQ)]\}^{\frac{1}{2}}. \tag{37}$$

The magnitude of the pressure in the water at T is, from (1), (5), and (7),

$$|p(T)| = \rho_2 p_0 |f_t| / \rho_1 (PT), \tag{38}$$

where p_0 is the magnitude of the outgoing pressure from P at unit distance from P. The phase at S is simply given by the path length from P to S. In other words, from (37) and (38)

$$p(S) = \frac{\rho_2 p_0 |f_t|}{\rho_1 (PT)} \left[\frac{(OT')(T'Q')}{(ZS)(SQ)} \right]^{\frac{1}{2}} e^{ik_1(PT) + ik_2(TS)}. \tag{39}$$

With the aid of Eqs. (9) and (34) to (36), and some elementary trigonometry, Eq. (39) yields

$$p(S) = \frac{2\beta p_0 r^{-\frac{1}{2}} (\sin\theta)^{\frac{1}{2}} e^{ik_1 [h(1-\sin^2\theta)^{-\frac{1}{2}} + \alpha^2 z(\alpha^2 - \sin^2\theta)^{-\frac{1}{2}}]}}{[\beta \cos\theta + (\alpha^2 - \sin^2\theta)^{\frac{1}{2}}][h(1-\sin^2\theta)^{-\frac{1}{2}} + z\alpha^2(\alpha^2 - \sin^2\theta)^{-\frac{1}{2}}]^{\frac{1}{2}}}. \tag{40}$$

The angle θ of the incident ray which reaches S (Fig. 4) is determined by the equation

$$h \tan\theta + z \tan\theta' = r,$$

or

$$[h \sin\theta / (1-\sin^2\theta)^{\frac{1}{2}}] + [z \sin\theta / (\alpha^2 - \sin^2\theta)^{\frac{1}{2}}] = r. \tag{41}$$

Equation (41) in $\sin\theta$ is identical with Eq. (17) which defines u_0. Furthermore, when (33) is of no account the pressure in the water is $\omega\rho_2$ times the expression (32), while the magnitude of the outgoing pressure at unit distance from P is $\omega\rho_1$, according to (1) and (3). Thus the expression (40), derived by ray acoustics, agrees exactly with Eq. (32), obtained by solving the wave equation. Remembering that Eq. (13) was obtained with the substitution $\sin\theta = u$, it appears that the saddle point u_0 simply determines the real angle of incidence contributing primarily to the pressure in the second medium, and this angle is just the angle determined by Snell's law and ray acoustics. The expression (32) thus represents the directly transmitted energy to any point in the second medium, and the approximations made in deriving (32) are apparently equivalent to assuming the curvature of the wave front negligible, the approximation made in deriving (40).

The expression (33) does not contribute to the pressure if $\gamma^2 < \alpha^2$. Evidently, at $z=0$, $\gamma^2 < \alpha^2$ means a point on the surface within the critical angle. Thus any point in the second medium lying directly beneath a point on the surface which is within the critical angle receives only directly transmitted energy. A point near the surface for which $\gamma^2 > \alpha^2$, i.e., a point near the surface outside the critical angle, also is reached by the exponentially decaying term (33). However, for sufficiently large z, for any point such that $\gamma^2 > \alpha^2$, the term (33) no longer contributes to the received pressure. This latter result is a little difficult to interpret. It may be a spurious result of the approximations made, or it may actually be a real effect. If it is real, it may be experimentally verifiable at points in the immediate vicinity of $\gamma^2 = \alpha^2$.

For the case of sound incident from air to water, $\beta \gg 1$, the magnitude of (32) is for small z, using (24)

$$2z\beta^{-1}(\alpha r)^{-\frac{1}{2}}(1-\alpha^2)^{-\frac{1}{4}} b^{-1}. \tag{41}$$

Thus, for small z the directly transmitted pressure is smaller than the exponentially damped term (33) whose magnitude is, for $\beta \gg 1$,

$$2\beta^{-1}(r^2+h^2)^{-\frac{1}{2}} \exp[-k_1 z(\gamma^2 - \alpha^2)^{\frac{1}{2}}]. \tag{42}$$

For very large r, $r \gg z$ and $r \gg h$, the magnitude of (32) becomes

$$2\beta^{-1}\alpha z(1-\alpha^2)^{-\frac{1}{4}}(r^2+z^2)^{-1}. \tag{43}$$

The expression (43) shows that at sufficiently large distances from the source, at any given depth, the increased divergence of the rays causes the pressure to vary as the inverse square of the distance from the source.

I am indebted to Professors Carl Eckart and Otto Halpern for their comments and advice.

On Temperature Dependence of Penetration Depth in Superconductors

JULES DE LAUNAY AND M. C. STEELE
Naval Research Laboratory, Washington, D. C.

(Received February 16, 1948)

By use of the Gorter-Casimir thermodynamic theory of superconductivity, the form of the Sommerfeld relation for the specific heat of electrons, and the form of the acceleration theory expression for penetration depth, the relative number of superconduction electrons and the relative penetration depth are derived as functions of the temperature. When the parabola relationship for threshold magnetic fields is used, comparison with experiment shows good agreement. In the limit of the absolute zero temperature, it is concluded that all of the normal conduction electrons become superconduction electrons in the absence of applied magnetic fields. The parabola relationship for threshold magnetic fields is discussed.

1. INTRODUCTION

IN a paper entitled "Some remarks on supraconductivity and Fermi-Dirac statistics,"[1] Kok has shown how a combination of the Gorter-Casimir equations for the thermodynamics of superconductivity,[2] the Sommerfeld relation for the contribution of normal conduction eletrons to specific heat,[3] and a parabola relationship for magnetic thresholds, leads to an explanation of the specific heats of superconductors in the absence of magnetic fields and in the presence of greater than threshold magnetic fields. It is the purpose of this paper to extend Kok's work to determine theoretically the temperature dependence of the relative number of superconduction electrons and of the relative penetration depth.

2. CALORIMETRIC RELATIONS

In the Gorter-Casimir thermodynamic theory of superconductivity,[2] the difference in the atomic heat of a substance in the superconducting state, C_S, and of the same substance in the normal state, C_N, at a given temperature T°K, is related to the threshold magnetic field H, at that temperature, by

$$\Delta C = C_S - C_N = (JVT/8\pi)[d^2(H^2)/dT^2]. \quad (1)$$

V is the atomic volume at T°K and J is the factor (2.3889×10^{-8}) required to convert ergs to calories.

We shall assume that in the low temperature range of superconductivity, the atomic heat of the substance, when held in the normal state by a magnetic field greater than threshold value, has a T^3 term due to lattice vibrations plus a linear term $\gamma_N T$ due to electron contribution. Then,

$$C_N = D_N T^3 + \gamma_N T. \quad (2)$$

For the atomic heat C_S in the superconducting state, we shall further assume that the lattice contribution also follows a T^3 law and that the electron contribution to the atomic heat is due to those electrons which remain in the "normal" state when the material becomes superconducting. However, whereas γ_N in Eq. (2) was assumed constant, γ_S in the relation below will be a function of the temperature T, since it will be supposed that the number of normal electrons decreases with decreasing T. Thus we write

$$C_S = D_S T^3 + \gamma_S(T) T. \quad (3)$$

Substitution of (2) and (3) into (1) gives

$$(D_S - D_N)T^2 + (\gamma_S - \gamma_N) = (JV/8\pi)[d^2(H^2)/dT^2]. \quad (4)$$

At this point we introduce two relations. The parabola relationship for threshold magnetic fields, with H_0 denoting the value of H at 0°K, is

$$H = H_0(1 - T^2/T_c^2), \quad (5)$$

where T_c is the transition temperature when $H=0$. The second relation is that

$$\gamma_S(0) = 0. \quad (6)$$

From these and the earlier equations, it can be

[1] J. A. Kok, Physica **1**, 1103 (1933–34).
[2] C. J. Gorter and H. Casimir, Physica **1**, 306 (1934).
[3] A. Sommerfeld, Zeits. f. Physik **47**, 1 (1928).

shown that

$$\gamma_N=(JV/2\pi)(H_0^2/T_c^2), \tag{7}$$

$$(\Delta C)_{T_c}=2\gamma_N T_c, \tag{8}$$

and

$$C_S=[D_N+(3\gamma_N/T_c^2)]T^3. \tag{9}$$

Equations equivalent to (7), (8), and (9) were derived by Kok.[1]

The assumption of Eq. (6) is justifiable only if Eqs. (7), (8), and (9) agree with experiment. Thus, these equations have been derived on a semi-empirical basis. However, no assumption was made in this derivation concerning the relation between D_S and D_N. If we put $\gamma_S(T_c)=\gamma_N$ so that the discontinuity in atomic heat at the transition temperature is all ascribed to a lattice atomic heat change, the corresponding change in Debye characteristic temperature for tin would be about 20 percent. The modulus of rigidity for tin and mercury was measured by de Haas and Kinoshita,[4] and no change was observed on passing through the transition temperature. Unpublished results obtained in this laboratory by J. R. Clement on the velocity of sound in tantalum show no discontinuity in the velocity at the transition temperature. This suggests that $D_S=D_N$ and that all of the change in atomic heat is to be attributed to the electrons. Thus, with $D_S=D_N$, it follows that

$$\gamma_S=(3\gamma_N/T_c^2)T^2. \tag{10}$$

3. PENETRATION DEPTH

It will be assumed that those electrons which contribute to $\gamma_N T$ and to $\gamma_S T$ do so in accord with the Sommerfeld relation. Thus the variation of γ_S, with temperature, given by Eq. (10) will be attributed to a decrease in the number of normal conduction electrons with decrease in temperature, accompanied by a corresponding increase in the superconduction electrons. γ has been shown by Sommerfeld[3] to be proportional to the cube root of the number of electrons contributing to the specific heat. The constant of proportionality depends, among other things, on how "free" the electrons are. So we shall not use the relation literally, as Kok[1] did, but limit ourselves to the general form of the Sommerfeld relation. Thus, if k is the constant of proportionality,

$$\gamma=kn^{\frac{1}{3}}. \tag{11}$$

Therefore, if n_N is the number of normal electrons contributing to the atomic heat when the substance is in the normal state, n_S is the number of *normal* electrons remaining when the material becomes superconducting, and the constants of proportionality k_N and k_S are different, Eq. (10) becomes

$$(n_S/n_N)^{\frac{1}{3}}=(3k_N/k_S)t^2, \tag{12}$$

where $t=T/Tc$ is the "reduced" temperature.

Let σ represent that fraction of normal conduction electrons which have become superconduction electrons, that is, which no longer contribute to the atomic heat. Then

$$\sigma=(n_N-n_S)/n_N \tag{13}$$

or, using (12),

$$\sigma(t)=[1-(3k_N/k_S)^3t^6]. \tag{14}$$

When $t=0$, $\sigma(0)=1$. This is the consequence of Eq. (6) and thus the assumption of (6) implies that all of the normal conduction electrons become superconduction electrons at the absolute zero. If at $t=1$, the transition temperature, none of the normal conduction electrons have become superconduction electrons, then $\sigma(1)=0$ and $k_S=3k_N$, corresponding to a sudden change in the state of the normal conduction electrons on passing through the transition temperature. With this condition, $\sigma(1)=0$, (14) becomes

$$\sigma(t)=1-t^6. \tag{15}$$

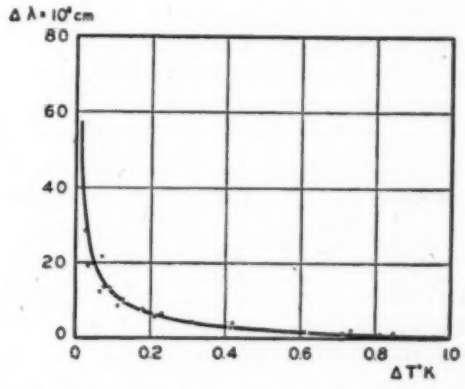

FIG. 1. Results for tin. ○, +, × from Laurmann and Shoenberg (see reference 6). The solid curve is a theoretical plot of Eq. (17) with $\lambda_0=0.75\times10^{-5}$ cm and $T_c=3.711$°K.

[4] W. J. de Haas and M. Kinoshita, Leid. Comm. No. 187 (1927).

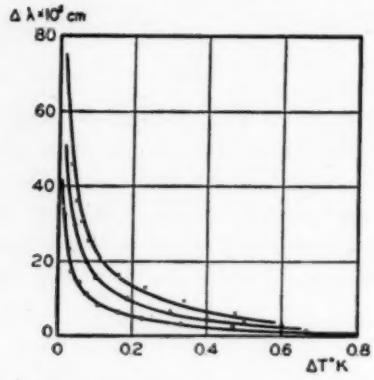

FIG. 2. Results for mercury. ○, Δ, × from Laurmann and Shoenberg (see reference 6). The solid curves are theoretical plots of Eq. (17), using $T_c=4.167°K$ and the following values for λ_0: Upper curve, 1.37×10^{-5} cm; middle curve, 0.95×10^{-5} cm; lower curve, 0.54×10^{-5} cm.

To obtain an expression for the penetration depth λ, we use the *form* of the equation given by the acceleration theory[5] (for similar reasons which led us to use only the form of the Sommerfeld relation, Eq. (11)),

$$\lambda \propto \sigma^{-\frac{1}{2}}. \tag{16}$$

If λ_0 represents the penetration depth at 0°K,

$$\lambda=\lambda_0(1-t^6)^{-\frac{1}{2}}. \tag{17}$$

As the Gorter-Casimir thermodynamic equations were derived neglecting the penetration depth, Eq. (17) holds for those superconducting bodies for which λ is much smaller than the linear dimensions of the body.

4. COMPARISON WITH EXPERIMENT

In a recent article, Laurmann and Shoenberg[6] have collected data on change of penetration depth with change in temperature for tin and mercury. The linear dimensions of the cylinders used were large compared with λ, so that it would be expected that Eq. (17) should apply to their results. The change in penetration depth $\Delta\lambda$ is defined by $\Delta\lambda=\lambda(T)-\lambda(2.1°K)$ and the change in temperature, ΔT, as the temperature difference from the transition temperature. The data for tin are plotted in Fig. 1. The solid curve was computed from Eq. (17) with $T_c=3.711°K$ and $\lambda_0=0.75\times10^{-5}$ cm. In Fig. 2 are shown three sets of data for mercury. The solid curves were computed from Eq. (17) with $T_c=4.167°K$. For the upper curve, $\lambda_0=1.37\times10^{-5}$ cm; for the middle curve, $\lambda_0=0.95\times10^{-5}$ cm; for the lower curve, $\lambda_0=0.54\times10^{-5}$ cm. Laurmann and Shoenberg attribute the differences in the curves for mercury to anisotropy, the middle curve representing polycrystalline mercury.

Although Eq. (17) is not intended to hold for thin films, it is interesting to compare Eq. (17) with the experimental results of Appleyard *et al.*[7] The curve shown in Fig. 3 is a plot of Eq. (17) relating λ/λ_0 with the reduced temperature t. The solid circles represent experimental data obtained from Fig. 6 of the paper by Appleyard *et al.* on the superconductivity of thin mercury films. Their data have been adjusted so that the point corresponding to $t=0.6$ ($T=2.5°K$) is made to fit Eq. (17). The agreement is almost as satisfactory as for bulk materials.

Since Eq. (17) contains the assumption $\sigma(0)=1$, it is important to examine the validity of this assumption in view of reported values ranging from 0.01 to 0.1. If it is assumed that $\sigma(0)=0.1$, it can be shown that γ_N increases by a factor of about 90, while if $\sigma(0)=0.01$, this factor becomes 900. Unfortunately, calorimetric data for γ_N are not available for mercury. However, Keesom and van Laer[8] have made precise

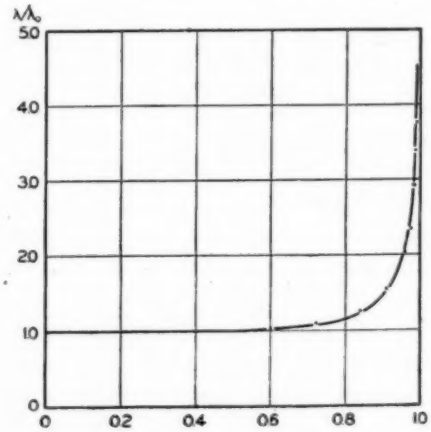

FIG. 3. The curve is a plot of Eq. (17) relating relative penetration depth λ/λ_0 with reduced temperature t. The solid circles are experimental points taken from Appleyard *et al.* (see reference 7).

[5] R. Becker, G. Heller, and F. Sauter, Zeits. f. Physik **85**, 772 (1933).
[6] E. Laurmann and D. Schoenberg, Nature **160**, 747 (1947).
[7] E. T. S. Appleyard, J. R. Bristow, H. London, and A. D. Misener, Proc. Roy. Soc. **170**, 540 (1939).
[8] W. H. Keesom and P. H. van Laer, Physica **5**, 193 (1938).

calorimetric measurements with tin. Their values of γ_N and $(\Delta C)_{T_c}$ are 4.0×10^{-4} and 2.90×10^{-3}, respectively. If we take H_0 for tin to be 300 gauss, as given by de Haas and Engelkes,[9] T_c to be 3.72°K and the atomic volume V to be 15.8, corrected for thermal expansion, Eqs. (7) and (8) give $\gamma_N=3.91\times10^{-4}$ and $(\Delta C)_{T_c}=2.91\times10^{-3}$. The agreement with experiment is very good. Even if there had been a disagreement of 10 percent, $\sigma(0)$ would still be 0.99997 or 1.00004. Calorimetric experiments also show that C_S for tin follows a T^3 law in accord with Eq. (9).

5. DISCUSSION OF THE PARABOLA RELATIONSHIP

If we put $h=H/H_0$ and $t=T/T_c$, the parabola relationship given by Eq. (5) becomes

$$h=1-t^2. \tag{18}$$

Let us examine the experimental results for mercury obtained by independent investigators. In 1934, Kok[1] cites the following empirical formula

$$H=433.0-89.1T^2+60.59T^3 -18.608T^4+1.8774T^5. \tag{19}$$

His accompanying remark is: "For Hg and Pb it is impossible to assume a parabola for the curve of the threshold values." In 1937, Daunt and Mendelssohn[10] give their smoothed data but no empirical formula. Their accompanying remark regarding the equilibrium curves for mercury and the other elements studied is: "None of these curves is a parabola . . . ." In 1940, Misener[11] gives the following empirical formula for mercury

$$H=412.58-19.50T^2-2.133T^3+0.266T^4. \tag{20}$$

Now these polynomial representations, Eqs. (19) and (20) and the data of Daunt and Mendelssohn, can be described by the expression

$$h=(1-t^2)f(t) \tag{21}$$

where $f(t)$ is a "correction factor" to the parabola relationship. For example, $f(t)=1$ for the range $0<t<1$ would indicate that the data could be represented by a parabola, i.e., by Eq. (18). $f(t)$ for the three successive groups of data (in chronological order) is plotted in Fig. 4 and labeled I, II, and III, respectively. Even a cursory inspection will show that the "better" the data the smoother the function $f(t)$. Had a parabola been used to smooth the data for I and II, instead of drawing conclusions concerning the "impossibility" of fitting a parabola to the data, the agreement would have been closer to Misener's results than that which was attained.

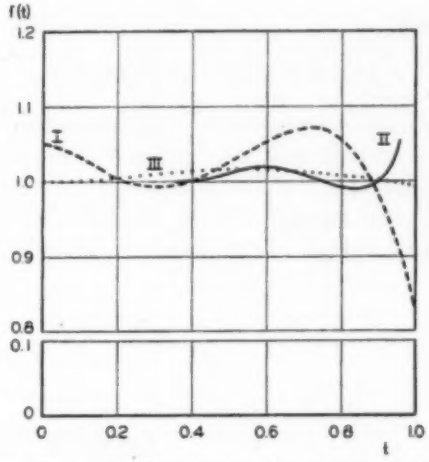

FIG. 4. The correction factor $f(t)$ plotted for Eq. (19) labeled I; Daunt and Mendelssohn's data, II; Eq. (20), III.

In fitting a polynomial of the fourth degree to data, there is a danger in being misled as to the quality of fit of a parabola. To illustrate, Misener's formula for mercury given in Eq. (20) can be written in "reduced" form as

$$h=1-0.82068t^2-0.37407t^3+0.19475t^4. \tag{22}$$

(The last coefficient was changed from 0.19439 to force the polynomial through $h=0$ at $t=1$.) One might at first believe that a parabola could not be fitted because 0.82 is 18 percent less than unity and the other coefficients are certainly not negligible. The drop in the coefficient of the t^2 term is necessary in order to compensate for the t^3 and t^4 terms. In the form of Eq. (21), Eq. (22)

[9] W. J. de Haas and A. D. Engelkes, Physica **4**, 325 (1937).
[10] J. G. Daunt and K. Mendelssohn, Proc. Roy. Soc. **160**, 127 (1937).
[11] A. D. Misener, Proc. Roy. Soc. **174**, 262 (1940). Misener claims that his formulae for Hg, In, and Tl represent his data within 0.3 gauss and 0.001°K. However, it is curious to note that his curve for Tl passes through $H=0$ at 0.013°K below the transition temperature which he gives as 2.392°K. The error in H corresponding to this would be 1.8 gauss or 6 times his allowed error of 0.3 gauss.

becomes

$$h=(1-t^2)[1+0.17932t^2-(0.37407t^2/1+t)]. \quad (23)$$

The last two terms in the parenthesis compensate so well that they scarcely differ by 0.015 at the worst.

σ is very sensitive to the second derivative of H^2. For example, a deviation of only 1.5 percent in H between the parabola relation and the polynomial, given by Misener for indium, causes σ to fluctuate as much as 100 percent from the values computed from Eq. (15). It seems, therefore, that the error which still remains in the best available data is too great for a reliable use of the various polynomials in finding σ, and therefore, λ/λ_0.

PHYSICAL REVIEW VOLUME 73, NUMBER 12 JUNE 15, 1948

Artificially Radioactive Se^{73} and Se^{75}

W. S. COWART,* M. L. POOL, D. A. McCOWN,** AND L. L. WOODWARD***
The Ohio State University, Columbus, Ohio

(Received March 8, 1948)

A radioactive isotope of 7.1-hour half-life has been produced by alpha-particle bombardment of germanium. Assignment of the isotope is made to Se^{73}. Absorption measurements indicate the presence of a positron end point of 1.29 Mev. Aluminum x-ray absorption measurements indicate an x-ray emission with a mass absorption coefficient of 22.1 cm^2/g, corresponding to 1.17A. Bombardment with alpha-particles of Ge^{70}, enriched electromagnetically from 21.2 percent to 90 percent, further confirms the assignment of the activity to Se^{73}. The half-life of Se^{75} is found to be 127 ± 2 days over a decay period of 1000 days. In this activity K-capture and gamma-radiations of 0.22 Mev and 0.43 Mev are observed.

A SELENIUM activity of 160-days half-life has been reported;[1] several electron groups were observed of energies less than 300 kev, corresponding to internally converted gamma-rays. This activity was the result of the bombardment with deuterons of the stable arsenic isotope of mass 75. The decay period of Se^{75}, produced by an (n,γ) reaction of selenium irradiated in the Argonne pile, has been observed[2] to be 115 ± 5 days. This activity was found to decay by K-capture to stable As^{75}, accompanied by a 0.4-Mev gamma-ray. A period of 125 days has also been reported[3] as the half-life of the Se^{75} isotope. The decay is by K-capture with the emission of conversion electrons and gamma-rays of 0.18 Mev and 0.35 Mev.

Inasmuch as the long period in selenium has not been reported in the literature as resulting from alpha-particle bombardment of germanium, such a bombardment was done. As a result of these experiments a strong activity of short half-life was found in selenium in addition to the long period. It is the purpose of this paper to report the characteristic radiations of this short period. Observations, extending over a period of some three years, on the decay and characteristic radiations of the long period will also be described.

I. THE 7.1-HOUR Se^{73} ISOTOPE

The germanium targets were prepared for alpha-particle bombardment by placing finely ground Hilger germanium powder in a thin-bottom copper target holder and carefully heating until a eutectic with the copper was formed.

Figure 1 shows the decay curves of the selenium fraction obtained from the Ge+α-

* Lt. Col., USAF. Research under auspices of Air University, Maxwell Field, Alabama. Now stationed Hqs., USAF, Washington, D. C.
** Captain, QMC, USA. Research under auspices of Air University, Maxwell Field, Alabama.
*** Lt. Col., USAF. Research under auspices of Air University, Maxwell Field, Alabama.

[1] C. V. Kent, J. M. Cork, and W. G. Wadey, Phys. Rev. 61, 389 (1942).
[2] H. N. Friedlander, L. Seren, and S. H. Turkel, Phys. Rev. 72, 23 (1947).
[3] Isotope Committee, Science 103, 697 (1946).

bombardment. The total decay curve represents decay of combined $\beta+X+\gamma$-radiation. This activity decayed initially on a period of 7.1 hours for about 14 half-lives. The gamma-radiation, determined by the insertion of a $\frac{1}{4}$-inch aluminum absorber between the sample and the ionization chamber, shows the same period. Cloud-chamber observations of the radiation were taken at 12-hour intervals throughout the 7.1-hour activity. The total beta-particle activity was found to consist of positrons.

Figure 2 shows aluminum absorption measurements of the activity taken in the 7.1-hour period. The sample was first placed between the poles of an electromagnet with the field adjusted to be neutral. The total activity obtained in the ionization chamber then consisted of $\beta+X+\gamma$-radiation. The curve representing the absorption of this activity is plotted as "total activity" in Fig. 2. A beta-end point of 0.59 g/cm², corresponding to approximately 1.29 Mev as determined by the Sargent range-energy relation, is shown as a result of the absorption measurements.

A magnetic field was then applied between the poles of the electromagnet, of sufficient strength to prevent all beta-particles from entering the ionization chamber, and measurements of only the electromagnetic activity were taken. For purposes of comparison with the total activity absorption curve, the resulting electromagnetic radiation is also shown on Fig. 2, plotted as "electromagnetic radiation."

Figure 3 shows in more detail the results of absorption of the electromagnetic radiation in aluminum. As above, beta-radiations were prevented from entering the ionization chamber by the application of a magnetic field. Electromagnetic radiation was absorbed by the insertion of aluminum foils between the sample and the ionization chamber. The presence of x-ray activity is shown by the subtraction of gamma-emission background from the total electromagnetic activity. The result of the subtraction, as shown in Fig. 3, is a straight line indicating a half-thickness corresponding to an absorption coefficient of 22.1 cm²/g. By use of the ordinary x-ray absorption formula, it is found that this coefficient in aluminum is the result of x-ray emission of a wave-length of 1.17A. Since the

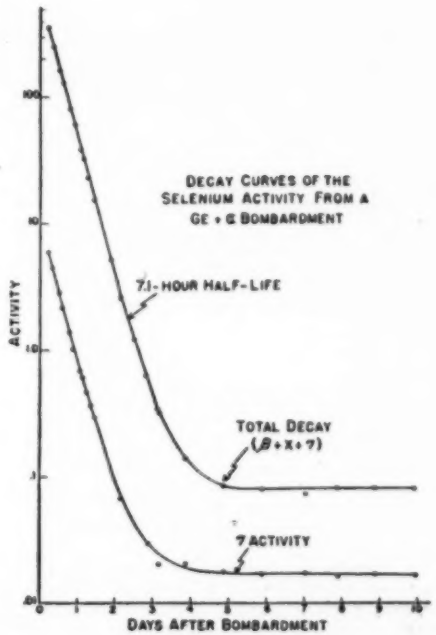

FIG. 1. Decay curves of selenium fraction of a Ge+α-bombardment, showing the 7.1-hour half-life.

$K_{\alpha 1}$ line of arsenic is 1.173A, it is evident that the K-capture process takes place in the activity.

The decay of this x-ray radiation was observed in the following manner. With the field of the electromagnet, as used above, so adjusted as to remove all the beta-particle radiation, a curve representing the decay of the entire electromagnetic radiation was obtained. This radiation consisted of both x-ray and gamma-activity. With a $\frac{1}{4}$-inch aluminum absorber inserted to

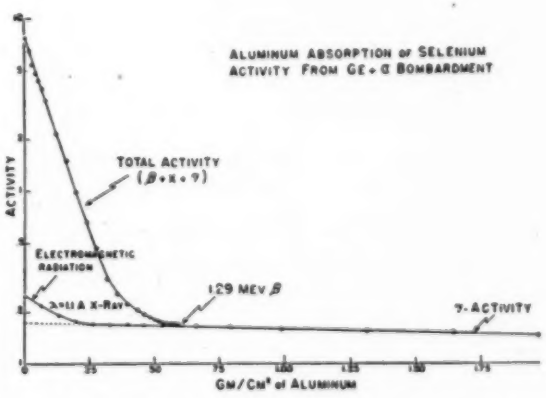

FIG. 2. Aluminum absorption measurements of beta-particle and electromagnetic radiations in a selenium fraction of Ge+α-bombardment. Electromagnetic radiation consists of activity after beta-particle radiations have been removed by a magnetic field.

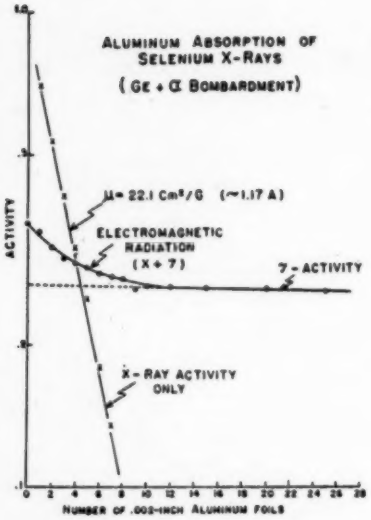
ALUMINUM ABSORPTION OF SELENIUM X-RAYS
(Ge + α BOMBARDMENT)
μ = 22.1 Cm²/G (~1.17 A)
ELECTROMAGNETIC RADIATION (X + γ)
γ - ACTIVITY
X - RAY ACTIVITY ONLY
ACTIVITY
NUMBER OF .003-INCH ALUMINUM FOILS

FIG. 3. Aluminum absorption measurements of x-ray activity in a selenium fraction of Ge+α-bombardment. In obtaining measurements of electromagnetic radiation beta-particle activity was removed by a magnetic field.

remove the x-ray radiation, the decay of the gamma-radiation was simultaneously observed. A subtraction of the two curves gives the decay of the x-ray radiation present. This procedure showed that the x-ray activity decayed in the 7.1-hour period.

Taking into account the relative ionizations produced by x-rays and positrons in the ionization chamber used, it is concluded that the ratio of the number of x-rays to positrons emitted in this period is approximately one.

Lead absorption measurements of the activity showed that the principal gamma-radiation is due to annihilation radiation. Possibly a weak gamma-radiation of higher energy is also present.

Because of the positron emission, the 7.1-hour activity could be placed in mass 73 or 75 of selenium. An attempt was made to produce this short period by bombardment of As^{75} with deuterons. Since this period was not found as a result of such bombardments, mass 73 is most probable.

II. BOMBARDMENT OF ELECTROMAGNETICALLY ENRICHED STABLE Ge^{70}

The stable isotope of germanium of mass 70, enriched electromagnetically from 21.2 percent to about 90 percent,† was also bombarded with alpha-particles. The germanium, in the form of

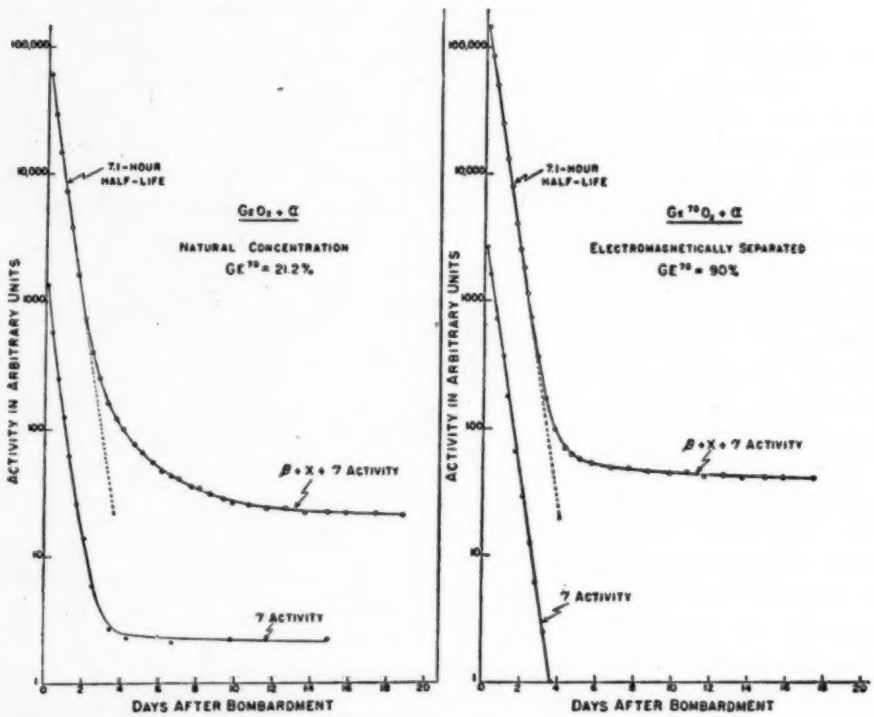

FIG. 4. A comparison of decay curves of germanium of natural isotopic constituency and Ge^{70} enriched electromagnetically to 90 percent. The enriched germanium sample shows a much stronger initial intensity of activity in the 7.1-hour period.

† Supplied by the Y-12 plant, Carbide and Carbon Chemicals Corporation, through the Isotopes Division, U.S.A.E.C., Oak Ridge, Tennessee.

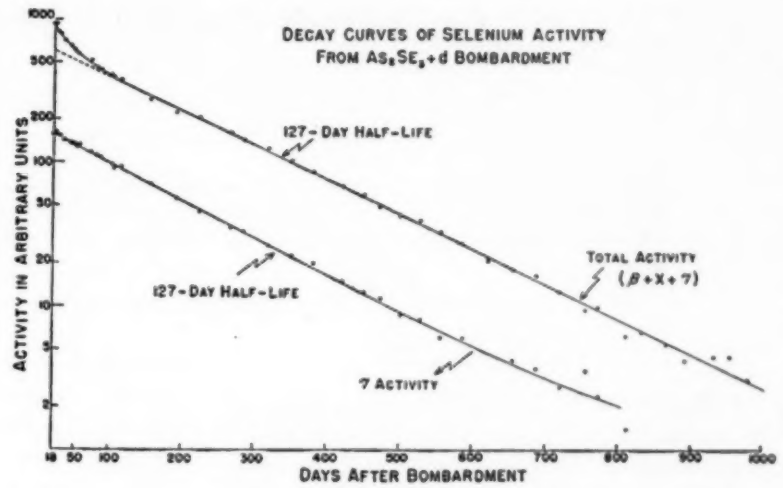

FIG. 5. Decay curves of the selenium fraction from bombardment of arsenic triselenide with deuterons. Decay over 1000 days after bombardment shows a period of 127±2 days.

GeO_2 powder, was prepared for bombardment by pressing the oxide into the bottom of a copper target holder under 5000 pounds of pressure. For comparison purposes germanium oxide of ordinary isotopic constituency and enriched germanium oxide were bombarded simultaneously. This was done by placing the two samples on opposite sides of the cyclotron probe and rotating the probe to obtain equal bombardment times and intensities. Equal amounts of germanium by weight were used in the two samples.

Figure 4 shows a comparison between the decay curves of the ordinary germanium oxide sample and the germanium oxide sample containing the enriched Ge^{70}. Both curves show a strong 7.1-hour activity. However, the initial total activity of the Ge^{70} sample was observed to be about three times that of the ordinary germanium sample. Since this is the order of magnitude of enrichment of the Ge^{70}, and since equal amounts of germanium were used, it may be concluded that the Ge^{70} isotope produces the 7.1-hour selenium activity under alpha-particle bombardment. The assignment of the 7.1-hour activity to Se^{73} is thus confirmed.

III. THE Se^{75} PERIOD

The long period in selenium of mass 75 has also been investigated. Arsenic triselenide was bombarded with deuterons and the selenium activity extracted. Figure 5 shows the total decay curve of this fraction, consisting of beta-particles and electromagnetic radiation, and also the gamma-activity decay curve. Both curves were taken over a period of 1000 days and show a half-life of 127±2 days.

Aluminum absorption measurements of the activity show that x-ray emission is present, with a wave-length corresponding to the arsenic K_α lines. This indicates that the K-capture process occurs in this period and that the active material decays into the stable As^{75} isotope. Decay by means other than K-capture is very improbable. The assignment of the period to Se^{75} is thus confirmed. By absorption measurements in lead, gamma-radiation energies of 0.22 Mev and 0.43 Mev were observed.

IV. ACKNOWLEDGMENTS

It is a pleasure for the authors to acknowledge the support received from The Ohio State University Development Fund and the Graduate School. The assistance received from Mr. H. L. Finston and Miss Joan Gillespie in the performance of the chemical separations is also greatly appreciated.

The Thermionic Properties of Chromium

H. B. WAHLIN
Department of Physics, University of Wisconsin, Madison, Wisconsin
(Received March 4, 1948)

The spectral emissivity, the temperature scale, and the electron work function of chromium have been determined. The emissivity is found to be 0.334 for a wave-length of 6690A and the value found for the electron work function is 4.60 volts with an A for Richardson's equation of 48 amp/cm^2/T^2.

1. INTRODUCTION

CHROMIUM is one of the more common metals that have not been studied thermionically. This is undoubtedly due to the fact that it shows very little ductility and therefore cannot be rolled or drawn into filaments of suitable shapes. Because of this, a new method, described below, had to be used in preparing the samples needed.

2. EMISSIVITY AND TEMPERATURE SCALE

The method used for determining the spectral emissivity and the temperature scale for more ductile metals has been described in earlier work.[1] Briefly, this consists in forming a miniature block body of the metal to be studied by rolling a strip of the metal into the shape of a hollow cylinder about 3 mm in diameter and at least 10 cm long. A hole ½-mm in diameter through the wall of the cylinder at the center serves as a source of blackbody radiation when the cylinder is heated electrically. This radiation can then be compared with that from the outside by means of an optical pyrometer.

In this experiment the cylinder was made by plating a brass tube (using a standard chromium plating bath) ⅛-in. O.D. Before plating, a hole of the size mentioned above was drilled in the side of the tube. After a sufficiently thick plate had been deposited to give the needed strength, the brass was removed with concentrated nitric acid. The strong acid does not attack the deposit. With care the resulting chromium cylinder could be mounted in a tube for evacuation and heat treatment.

It was found that when the cylinder was first heated to a dull red in a vacuum, the chromium showed an excessive volatility. This is probably caused by the fact that the metal as deposited is very fine grained. As the metal evaporated, the emissivity rose. This was noticeable because the contrast between the radiation from the hole and the outside became progressively less sharp. Finally, the radiation from the outside became so nearly like that of a blackbody that the contrast practically disappeared and some difficulty was experienced in locating the hole.

This rise in emissivity results from the fact that electrolytic chromium contains chromium oxide, which is non-volatile. When the metal evaporates the cylinder is left with an oxide surface. It is interesting that at least in the visible part of the spectrum the radiation from the oxide should be nearly the same as that from a blackbody.

To reduce the oxide, hydrogen was introduced and the cylinder was heated for a period of a week at about 1200°C. During this heating a liquid-air trap was kept connected to remove the water vapor formed. This heat treatment gradually lowered the emissivity to a final value of 0.334 for $\lambda = 6690$A. This value was found to be independent of the temperature up to 1550°K, which is the highest temperature at which determinations could be made safely because of evaporation.

The hydrogen was now removed and the heating continued in a vacuum. The emissivity remained unchanged within the limits of error of measurement. The vaporization was also much less than it was initially. If the oxide has not been completely reduced one would expect a rise in the emissivity with time.

It has occurred to the writer that in using the hollow cylinder method for studying emissivity, a temperature gradient through the walls would

[1] H. B. Wahlin and L. O. Sordahl, Phys. Rev. **45**, 886 (1934).

cause too large a temperature difference between the outside and the inside as measured by the radiation from the outside as compared with the radiation from the hole. However, since the emissivity in hydrogen where the conduction losses are superimposed on the radiation losses is the same as in a vacuum, the gradient through the wall must be negligible. This is also shown by the early results reported above where the oxide was exposed. If there had been an appreciable gradient through the wall, the radiation from the outside could not so nearly have matched the radiation from the hole.

For convenience the true *vs.* the apparent temperatures are listed in Table I.

TABLE I.

Apparent Temperature °K	True Temperature °K
1000	1050
1050	1108
1100	1163.5
1150	1220
1200	1276
1250	1333
1300	1390
1350	1447
1400	1504.5
1450	1562.5

3. THERMIONIC EMISSION

Because chromium is brittle it was necessary to use a straight filament with the conventional two-guard ring tube for the thermionic studies. The filament was prepared by coating a brass tube 0.01-in. O.D. with chromium and removing the brass by the method described above. By using care in the plating process, a filament of uniform diameter can be produced and, as a result, one free from temperature gradients when heated. The filaments were heat treated in hydrogen to reduce the oxide before they were mounted in the main tube.

After the thermionic tube was assembled and sealed to the vacuum system it was baked at temperatures up to 450°C until a final pressure of 2×10^{-8} mm was reached with the filament hot. During the baking process the furnace temperature was raised gradually. In this way any reoxidation of the filament was kept to a minimum.

The process in the thermionic measurement was the standard one of measuring the saturation value of the thermionic emission as a function of the temperature and from the Richardson plot determining the work function and the constant.

The values thus determined are $\varphi=4.60$, $A=48.0$. These values represent the average of the stable values obtained after prolonged heat treatment of the filament. Whether they represent the values characteristic of pure chromium depends on the degree to which the oxide is removed by heating in hydrogen and the degree to which reoxidation takes place when the filament is heated in a vacuum of the order of 10^{-8}. The best evidence in support of the contention that such oxidation does not take place comes from the fact that during the emissivity determination there was no progressive increase in the emissivity with time when the cylinder was heated in a vacuum after it had been heated in hydrogen. The fact that A has reasonable value would also indicate that the surface was clean.

The A given above is somewhat less than that for tungsten (75) found by the writer. Reimanns[2] explains the deviation of A from the theoretical value 120 as being caused by a change in the zero-point energy of the electrons due to the thermal expansion causing a decrease in the number density of the free electrons. This change in the zero-point energy would introduce a temperature coefficient of the work function and Richardson's equation would be

$$i=120e^{(-a/k)}T^2e^{(-\varphi_0/kT)}.$$

The experimental value for A is thus $120e^{(-a/k)}$. It is to be expected on this basis that the higher the linear expansion coefficient, the lower the measured value of A. Since chromium has a higher linear expansion than tungsten, A should be less. A more quantitative comparison is impossible since the roughness of the emitting surface makes an accurate determination of the area impossible. The work by Fiske[3] on tantalum supports this explanation.

This work was supported in part by a grant from the Wisconsin Alumni Research foundation.

[2] A. L. Reimann, Nature **133**, 833 (1934).
[3] Milan D. Fiske, Phys. Rev. **61**, 513 (1942).

Mechanical Properties of NaCl, KBr, KCl*

J. K. GALT**
Research Laboratory of Electronics, Massachusetts Institute of Technology, Cambridge, Massachusetts

(Received February 2, 1948)

The pulse method has been applied to measure mechanical properties of NaCl, KBr, and KCl at 10 and 30 Mc/sec. The elastic constants of KBr have been measured in the low temperature region. The strain-optical constants have been measured by a traveling-wave method suggested by Mueller.

I. INTRODUCTION

ONE result of the availability of electrical circuits for pulsing is that pulsed ultrasonic measurements have become practical. This method has some advantages over those previously used to determine the mechanical properties of solids. A traveling plane wave may be propagated through a sample of material in the form of a pulse of ultrasonic vibrations. Simple and direct measurements may be made on the echoes of such pulses as they travel back and forth in a medium in order to determine the elastic constants and the ultrasonic attenuation of the medium. Ultrasonic velocities, and therefore elastic constants, are determined from a direct measurement of the distance traveled by a pulse and the corresponding time. Attenuations are determined from the decrease in signal amplitude of successive echoes. Here again both distance and change in signal level are directly measured. At the start the pulse travels in a beam of finite cross section so that the sample is effectively infinite and no account need be taken of the possible effect of the cross-sectional dimensions of the sample. H. B. Huntington[1] has given a general description of the method used to measure elastic constants and attenuations in solids.

The stresses produced by the wave in the medium may also be determined by measuring the shunt impedance of the crystal and the amplitude of the applied voltage, since these quantities determine the power input during the pulse. The stress is obtained from the well-known relation that the sound intensity (power transmitted per unit area) is given by $X^2/2\rho v$, where X is the peak stress in the sound wave, ρ is the density of the material, and v is the velocity of propagation of the wave.

It is also quite easy to measure the ratios of the strain-optical constants (p_{ik}) of a material by the use of pulsed ultrasonics. These ratios determine the polarization of the light diffracted by ultrasonic waves in a crystal. Mueller[2] has described the method used (his method B). In these cubic crystals we measure p_{12}/p_{11} and $p_{44}/(p_{11}+p_{12})$ this way.

Perhaps the most important advantage of the method, especially for the strain-optical constant measurements where a block of substantial size must be used, is the fact that we are dealing with plane elastic wave fronts. Very nearly plane waves can be produced in a large sample by making the dimensions of the radiating surface many wave-lengths long. Thus the difficulties of producing standing waves with a single set of parallel nodal planes and the influence of the boundary conditions are avoided, and our experimental conditions approach more closely the ideal conditions of the theory than is possible when a block is set in vibration as a resonator.

In order to obtain a short pulse which is still several wave-lengths long, almost all the measurements in the present research were made at a frequency of approximately 10 Mc/sec. Some elastic constant and attenuation measurements were made at 30 Mc/sec also.

II. ELASTIC CONSTANTS

The adiabatic elastic constants c_{ik} of a cubic crystal are determined from the density and the velocities of three plane waves. These are first, a compressional wave propagated along the cube

* This work has been supported in part by the Signal Corps, the Air Materiel Command, and O.N.R.

** Now at H. H. Wills Physical Laboratory, University of Bristol, The Royal Fort, Bristol, England.

[1] H. B. Huntington, Phys. Rev. **72**, 321 (1947).

[2] H. Mueller, Zeits. f. Kristallographie **(A)99**, 122 (1938).

axis, with a velocity of $(c_{11}/\rho)^{\frac{1}{2}}$; second, a shear wave propagated along the cube axis with a velocity of $(c_{44}/\rho)^{\frac{1}{2}}$, and third, a shear wave propagated in the 110 direction with a velocity of $[(c_{11}-c_{12})/2\rho]^{\frac{1}{2}}$.

Measurements of the elastic constants at room temperature have been made on NaCl, KBr, and KCl. The data are presented in Table I along with that obtained by Huntington[1] and Durand.[3]

It is felt that the agreement between the present measurements and those of Huntington illustrates the accuracy obtainable with the present method. These measurements were made on different samples and were otherwise quite independent. The disagreement with the values of Durand for NaCl is larger than the error estimated for the pulsed measurement.

The elastic constants of KBr have been measured over the low temperature range. Refrigeration was obtained with a Collins helium cryostat.[4] The data are shown in Figs. 1 and 2. The data on c_{12} extend only down to 138°K. Cracks occurred in the sample at an angle of 45° to the direction of propagation of the wave and destroyed the echo pattern at temperatures below this. This cracking is the result of stresses produced by the differential thermal contraction between the quartz crystal and the alkali halide. The cleavage planes are parallel to the direction of propagation of the waves used to measure c_{11} and c_{44}, however, so that these measurements could be extended to 4.5°K even though some cracking occurred.

TABLE I. Elastic constants measured at room temperature (units are dynes/cm²).

		NaCl	KBr	KCl
$c_{11}\times10^{-11}$	Galt	4.87	3.46	3.98
	Huntington	4.85	3.45	
	Durand	4.99		4.00 (extrapolated to 300°K)
$c_{12}\times10^{-11}$	Galt	1.24	0.58	0.62
	Huntington	1.23	0.54±0.03	
	Durand	1.31		0.6
$c_{44}\times10^{-11}$	Galt	1.26	0.505	0.625
	Huntington	1.26	0.508	
	Durand	1.27		0.631 (extrapolated to 300°K)

[3] M. A. Durand, Phys. Rev. **50**, 449 (1936).
[4] S. C. Collins, Rev. Sci. Inst. **18**, 157 (1947).

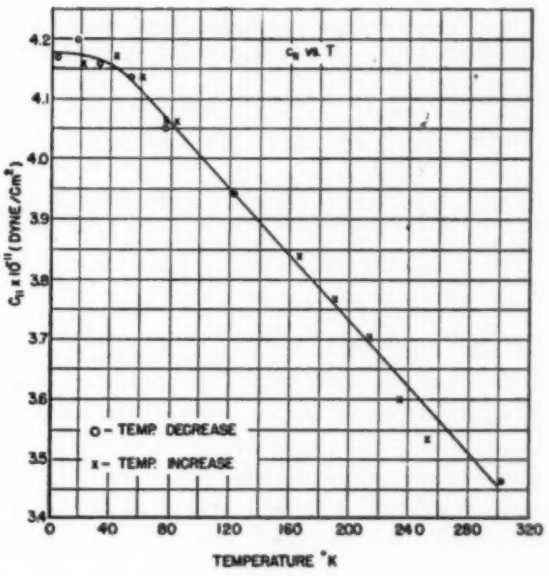

FIG. 1.

The variation in the density of the sample with temperature was corrected for down to 90°K. It was assumed constant below this temperature, as no measurements of expansion coefficient are available there.[5]

For the low temperature measurements the quartz was cemented to the sample with a cement made of a mixture of natural rubber and vaseline.

The zero slope of these curves at 0°K may easily be derived from the Maxwell relation $(\partial X_i/\partial T)_{x_i}=(\partial S/\partial x_i)_T$ (where X_i is a stress, and x_i the strain) and the Nernst theorem in thermodynamics, from which we have $\partial S/\partial x_i=0$ at 0°K.[6]

One source of error in the elastic constant measurements is pulse distortion. At room temperature this is caused by the fact that reflections occur at both sides of the cement film which affixes the quartz crystal to the alkali-halide sample. In the low temperature range it is increased by the adjustments which the film must make to compensate for the differential thermal contraction between the quartz crystal and the alkali halide. A small amount of error may occur in calibrating the sweep of the oscil-

[5] A. Henglein, Zeits. f. physik. Chemie **115**, 91 (1925).
[6] The author is greateful to Professor L. Tisza and Dr. C. Kittel for pointing out these relations to him.

TABLE II. Strain-optical constant ratios.

Substance		p_{12}/p_{11}	$p_{44}/(p_{11}+p_{12})$	p_{44}/p_{11}
NaCl	Galt	1.35±0.03	−0.042±0.004	−0.099
	Pockels	1.30	−0.0343	−0.079
KCl	Galt	0.76±0.01	−0.069±0.004	−0.12
	Pockels	0.74	−0.069	−0.12
KBr	Galt	0.77±0.01	−0.067±0.005	−0.12

loscope used to measure the time required for the mechanical wave to travel through the sample. The largest error in the low temperature measurements is the uncertainty in measuring the temperature of the sample because of temperature gradients in the cryostat. The error in measuring temperature may be as high as several degrees. It is felt, however, that the curves drawn in Figs. 1 and 2 for c_{11} and c_{44} are accurate to better than 1 percent. The c_{12} curve may be in error by a somewhat larger amount since c_{12} is determined by subtracting two larger numbers. The variations indicated by the plots of Figs. 1 and 2 have a much smaller absolute error than the values of the elastic constants themselves, of course.

III. ATTENUATION

The attenuations of all the waves mentioned above were also measured. The attenuation α of a wave, which has traveled a distance x and in which the peak stress is X, may be defined by the relation:

$$X = X_0 e^{-\alpha x}.$$

All shear waves in all crystals have measured α's between 0.004 and 0.005 cm^{-1}. The compressional waves have α-values between 0.001 and 0.002 cm^{-1}. In view of this lack of variation it is felt that these values may only be considered as upper limits. Measurements made on shear waves in NaCl at 30 Mc gave the same value of attenuation.

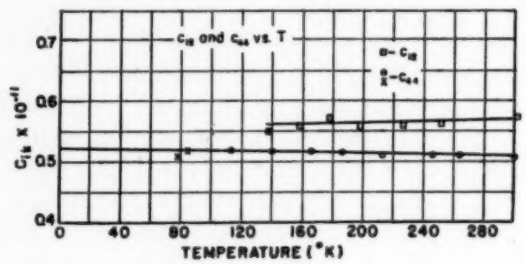

FIG. 2.

IV. STRAIN-OPTICAL CONSTANTS

When light is diffracted by ultrasonic waves in a crystal, its polarization is changed as well. This change can be measured by first crossing analyzer and polarizer while no elastic waves are excited in the crystal, and then noting the change of the analyzer required to extinguish successive diffraction orders of the Debye-Sears pattern when ultrasonic vibrations are excited. If the ultrasonic wave travels vertically along the 100 direction, and the incident light is polarized at +45° to the horizontal, this change in polarization measures p_{12}/p_{11} in a cubic crystal.[2] If the ultrasonic wave travels along the 110 direction and the other conditions are the same, this change in polarization[2] measures $p_{44}/(p_{11}+p_{12})$. Table II gives the strain-optical constants measured and also p_{44}/p_{11}, as determined from p_{12}/p_{11} and $p_{44}/(p_{11}+p_{12})$. For the ratios which were measured, an estimate of the error is given. This estimate is based on the reproducibility of the measurement of the angle at which the diffracted light is crossed out. No large permanent strains were present in the samples and there were no apparent systematic errors. Pockel's data for KCl and NaCl are presented for comparison.

The values in Table II are consistent with the predictions of Mueller's theory.[7] In particular they bear out his prediction that the values for KBr and KCl are the same.

The author wishes to express his gratitude to Professor D. C. Stockbarger for providing the alkali-halide crystals on which the measurements were made. He wishes especially to express his sincerest thanks to Professor H. Mueller, under whose direction this research was carried out.

[7] H. Mueller, Phys. Rev. **47**, 947 (1935).

Resonance Reactions Involving Dirac-Type Incident Particles

G. GOERTZEL
Oak Ridge National Laboratory, Oak Ridge, Tennessee
(Received February 9, 1948)

An investigation has been made to determine whether the results of Wigner and Eisenbud can be extended to include the scattering of a particle which obeys a Dirac-type wave equation. It is found that no additional difficulties arise as a result of the use of Dirac particles, and that the treatment of Wigner and Eisenbud can be carried through step by step with relatively minor changes.

In order to carry out this program, however, it was necessary to determine the appropriate relativistic boundary conditions to be satisfied by the external and internal wave functions at the boundary of the internal region. It is hoped that a comparison of the relativistic and non-relativistic boundary conditions will lead to a clearer understanding of the boundary conditions in the non-relativistic problem.

THE present discussion attempts to show how the treatment of resonance reactions given by Wigner and Eisenbud[1] may be extended to include the scattering cross section (elastic and inelastic) of a neutron obeying a Dirac-type wave function incident on a nucleus of zero spin. The development and notation used in this discussion will closely parallel that of reference 1, which will be referred to as A.

As in A, functions $F_s(r_s, \Omega_s)\psi_s(i_s)$ are defined such that in the external region the most general solutions of the quantum-mechanical equations with a definite energy are linear combinations of these functions. The F_s is a solution of a Dirac-type wave equation where[2] M is the relative mass of the neutron and nucleus.

$$\{c\boldsymbol{\alpha}\cdot\mathbf{p}+\beta Mc^2+E\}F_s(r_s, \Omega_s)=0, \qquad (1)$$

$$\mathbf{p}=-ih\nabla,$$

$\mathfrak{D}$ and $\mathfrak{U}$ type wave functions similar to A (9) but satisfying (1) and the boundary conditions

$$\int_{r=a_s}\mathfrak{D}^*_{sljm}\mathfrak{D}_{sljm}dS=1, \qquad (2a)$$

$$[i\alpha_r\mathfrak{D}_{sljm}]_{r=a_s}=-[\mathfrak{U}_{sljm}]_{r=a_s}, \qquad (2b)$$

may be defined.

The Eqs. (2) do not completely specify the four-component wave functions $\mathfrak{U}$ and $\mathfrak{D}$. This may be done by using the additional condition

$$[(1+\beta)/2](1-i\delta\alpha_r)\mathfrak{U}_{sljm}|_{r=a_s}=0, \qquad (3)$$

where δ is a parameter at our disposal. δ may depend on a_s, l, and j but not on the energy, and α_r is the radial component of $\boldsymbol{\alpha}$.[3]

The R matrix is defined in a manner similar to that of A: (compare A (13)).

$$\varphi_{sljm}=\mathfrak{D}_{sljm}+\sum_{s'l'}R^{(j)}_{sl,\,s'l'}\mathfrak{U}_{s'l'jm}. \qquad (3)$$

R is a real matrix. Now one considers those solutions $X_{\lambda jm}$ of the quantum-mechanical equations in the internal region which satisfy boundary conditions similar to the $\mathfrak{U}_{sljm}$. That is,

$$\int_{r=a_s}dsP_l{}^{m*}[(1+\beta)/2](1-i\delta\alpha_r)X_{\lambda jm}=0. \qquad (4)$$

In A the next step is to apply Green's theorem to the $X_{\lambda\mu}$ and $\varphi_{sl\mu}$. For the present work the following relation is equivalent to Green's

[1] E. P. Wigner and L. Eisenbud, Phys. Rev. **72**, 29 (1947).

[2] The matrices $\boldsymbol{\alpha}$ and β are defined as follows:

$$\alpha_x=\begin{pmatrix}0&0&0&1\\0&0&1&0\\0&1&0&0\\1&0&0&0\end{pmatrix},\quad \alpha_y=\begin{pmatrix}0&0&0&-i\\0&0&i&0\\0&-i&0&0\\i&0&0&0\end{pmatrix},$$

$$\alpha_z=\begin{pmatrix}0&0&1&0\\0&0&0&-1\\1&0&0&0\\0&-1&0&0\end{pmatrix},\quad \beta=\begin{pmatrix}1&0&0&0\\0&1&0&0\\0&0&-1&0\\0&0&0&-1\end{pmatrix}.$$

[3] Explicitly

$$\alpha_r=\begin{pmatrix}0&0&\cos\vartheta&\sin\vartheta e^{-i\varphi}\\0&0&\sin\vartheta e^{i\varphi}&-\cos\vartheta\\\cos\vartheta&\sin\vartheta e^{-i\varphi}&0&0\\\sin\vartheta e^{i\varphi}&-\cos\vartheta&0&0\end{pmatrix},$$

where ϑ and φ are, respectively, the polar and azimuthal angles.

theorem:[4]

$$\int_V dV[\Psi^* H\varphi-(H\Psi)^*\varphi]=i\int_S dS\Psi^* ch\alpha_n\varphi, \quad (5)$$

where S is the bounding surface of the volume V and H is the operator $ich\boldsymbol{\alpha}\cdot\nabla$ added to any function of the space and spin coordinates. α_n is the component of $\boldsymbol{\alpha}$ along the outward normal to S. An application of (5) to φ_{sljm} and $X_{\lambda jm}$ yields, since the $X_{\lambda jm}$ and $\mathfrak{V}_{sljm}$ on the surface $r=a_s$ are orthogonal to the $\mathfrak{D}_{sljm}$,

$$-ch\int_{r=a_s} dSX_{\lambda jm}{}^*\mathfrak{V}_{sljm}$$

$$=(E-E_\lambda)\int dIX_{\lambda jm}{}^*\varphi_{sljm}=-(ch)^{\frac{1}{2}}\gamma_{\lambda slj}. \quad (6)$$

The last relation defines the energy-independent real quantities γ. One may also write for the internal region

$$\varphi_{sljm}=\sum_\lambda A_{sljm}X_{\lambda jm}, \quad (7)$$

whence (6) gives

$$A_{sljm}=(ch)^{\frac{1}{2}}[\gamma_{\lambda slj}/(E_\lambda-E)]. \quad (8)$$

Since φ_{sljm} must be continuous at the surface $r=a_s$ one has further, on S,

$$(ch)^{\frac{1}{2}}\sum_\lambda[\gamma_{\lambda slj}/(E_\lambda-E)]X_{\lambda jm}$$

$$=\mathfrak{D}_{sljm}+\sum_{s''l''}R^{(j)}_{sl,\,s''l''}\mathfrak{V}_{s''l''jm}. \quad (9)$$

If both sides are multiplied by $\mathfrak{V}_{s'l'jm}$ and integrated over the surface S one obtains

$$R^{(j)}_{sl,\,s'l'}=+\sum_\lambda[\gamma_{\lambda slj}\gamma_{\lambda s'l'j}/(E_\lambda-E)]. \quad (10)$$

This is the present result for the R matrix and is identical in form, despite the different wave equation used, with A (23).

The relation between the R matrix and the collision matrix may now be determined. To do this it is necessary to specify the form of the wave functions in the external region. Define

$$\chi_{j-\frac{1}{2},\,j,\,m}=\begin{pmatrix}[(j+m)/2j]^{\frac{1}{2}} & Y_{j-\frac{1}{2}}^{m-\frac{1}{2}}\\ [(j-m)/2j]^{\frac{1}{2}} & Y_{j-\frac{1}{2}}^{m+\frac{1}{2}}\end{pmatrix}, \quad (11a)$$

$$\chi_{j+\frac{1}{2},\,j,\,m}$$

$$=\begin{pmatrix}[(j+1-m)/(2j+2)]^{\frac{1}{2}} & Y_{j+\frac{1}{2}}^{m-\frac{1}{2}}\\ -[(j+1+m)/(2j+2)]^{\frac{1}{2}} & Y_{j+\frac{1}{2}}^{m+\frac{1}{2}}\end{pmatrix}. \quad (11b)$$

It is convenient to use the σ_r matrix

$$\sigma_r=\begin{pmatrix}\cos\vartheta & \sin\vartheta e^{-i\varphi}\\ \sin\vartheta e^{i\varphi} & -\cos\vartheta\end{pmatrix}, \quad (12)$$

and note that

$$\sigma_r\chi_{j\pm\frac{1}{2},\,j,\,m}=\chi_{\mp j\frac{1}{2},\,j,\,m}.$$

Y_l^m is the spherical harmonic normalized to unity.

Incident and emergent waves are then defined as

$$I_{sljm}=\Psi_s(i_s)\frac{1}{(2\epsilon_s)^{\frac{1}{2}}}\frac{e^{-ik_sr}}{r}\times\begin{pmatrix}(\epsilon_s/c)\sigma_r & \chi_{ljm}\\ & \chi_{ljm}\end{pmatrix}, \quad (13a)$$

$$E_{sljm}=\Psi_s(i_s)\frac{1}{(2\epsilon_s)^{\frac{1}{2}}}\frac{e^{ik_sr}}{r}\times\begin{pmatrix}-(\epsilon_s/c)\sigma_r & \chi_{ljm}\\ & \chi_{ljm}\end{pmatrix}, \quad (13b)$$

where

$$k_s=p_s/h, \quad \epsilon_s=p_sc^2/(E_s+Mc^2).$$

One then may further define the quantities A, B, and ω by specifying the asymptotic behavior of the $\mathfrak{D}$'s and $\mathfrak{V}$'s in terms of the I's and E's.

$$\mathfrak{D}_{sljm}\simeq i(c/2)^{\frac{1}{2}}[A_{slj}I_{sljm}-A_{slj}{}^*E_{sljm}], \quad (14a)$$

$$\mathfrak{V}_{sljm}\simeq(c/2)^{\frac{1}{2}}[B_{slj}\omega_{slj}{}^*I_{sljm}+B_{slj}\omega_{slj}E_{sljm}]. \quad (14b)$$

Since $\mathfrak{D}_{sljm}$ and $\mathfrak{V}_{sljm}$ both satisfy (1),

$$\int_s dS\mathfrak{V}_{sljm}{}^*i\alpha_n\mathfrak{D}_{sljm}$$

is a constant for any surface S including the origin, and this constant is seen to be equal to -1 for the surface $r=a_s$ (from (2)). Hence,

$$B\omega A+B\omega^*A^*=2, \quad (15)$$

so that one may also write

$$B\omega A=1-iC, \quad (16)$$

[4] A derivation of (5) is given in the Appendix.

TABLE I.

l	$B\omega$	C
0	$-\left(\frac{\epsilon_s}{c}\right)^{\frac{1}{2}}\left(\frac{1}{1+\delta^2}\right)^{\frac{1}{2}}\left(1+i\left[\frac{1}{k_sa_s}+\frac{c}{\epsilon_s}\delta\right]\right)e^{-ik_sa_s}$	$-\frac{\epsilon_s}{c}\frac{1}{1+\delta^2}\left[\left(\frac{\delta}{k_sa_s}-\frac{c}{\epsilon_s}\right)\left(\frac{1}{k_sa_s}+\frac{c}{\epsilon_s}\delta\right)+\delta\right]$
1	$\left(\frac{\epsilon_s}{c}\right)^{\frac{1}{2}}\left(\frac{1}{1+\delta'^2}\right)^{\frac{1}{2}}\left(\left[\delta'\frac{c}{\epsilon_s}\frac{1}{k_sa_s}-1\right]-i\frac{c}{\epsilon_s}\delta'\right)e^{-ik_sa_s}$	$\frac{\epsilon_s}{c}\frac{1}{1+\delta'^2}\left[\left(\delta'+\frac{c}{\epsilon_s}\frac{1}{k_sa_s}\right)\left(\delta'\frac{c}{\epsilon_s}\frac{1}{k_sa_s}-1\right)-\delta'\frac{c^2}{\epsilon_s^2}\right]$

where C is a real diagonal matrix. Now

$$\varphi_{sljm}=\mathfrak{D}_{sljm}+\sum_{s'l'}R^{(j)}_{sl,\,s'l'}\mathfrak{V}_{s'l'jm}$$
$$=(c/2)^{\frac{1}{2}}\sum_{s'l'}\{(iA+RB\omega^*)_{sl,s'l'}I_{s'l'jm}+(-iA+RB\omega)_{sl,\,s'l'}E_{s'l'jm}\}.$$

Hence, a solution of the quantum-mechanical equation in which only one incident beam occurs may be written

$$(c/2)^{\frac{1}{2}}I_{sljm}+(c/2)^{\frac{1}{2}}\sum_{s'l'}[(RB\omega^*+iA)^{-1}\times(RB\omega-iA^*)]_{sl,\,s'l'}E_{s'l'jm},$$

so that the collision matrix becomes

$$U_{sl,\,s'l'}=-[(RB\omega^*+iA)^{-1}(RB\omega-iA^*)]_{s,\,l,\,s'l'}$$
$$=[\omega(1-iBRB-iC)^{-1}\times(1+iBRB+iC)\omega]_{sl,\,s'l'}. \quad (17)$$

The wave function for a collision experiment is obtained in the usual manner in terms of the U. In fact, a plane wave representing a particle of type s moving along the z axis, with $j_s=\frac{1}{2}$, is given by

$$\Psi_{s,\frac{1}{2}}=(\sqrt{\pi}/k_s)\sum_{l=0}^{\infty}[\{(l+1)^{\frac{1}{2}}E_{s,\,l,\,l+\frac{1}{2},\,\frac{1}{2}}+\sqrt{l}\,E_{s,\,l,\,l-\frac{1}{2},\,\frac{1}{2}}-(-)^l\{(l+1)^{\frac{1}{2}}I_{s,\,l,\,l+\frac{1}{2},\,\frac{1}{2}}+\sqrt{l}\,I_{s,\,l,\,l-\frac{1}{2},\,\frac{1}{2}}\}], \quad (18)$$

so that a continuable solution with the same incident waves as (18) is given by

$$\Psi_{s,\frac{1}{2}}+(\sqrt{\pi}/k_s)\sum_{l,\,s',\,l'}\{(l+1)^{\frac{1}{2}}[(-)^lU^{(l+\frac{1}{2})}_{sl,\,s'l'}-\delta_{sl,\,s'l'}]E_{s',\,l',\,l+\frac{1}{2},\,\frac{1}{2}}+\sqrt{l}[(-)^lU^{(l-\frac{1}{2})}_{sl,\,s'l'}-\delta_{sl,\,s'l'}]E_{s',\,l',\,l-\frac{1}{2},\,\frac{1}{2}}\}. \quad (19)$$

Expressions for the various differential cross sections may be obtained from (19).

The values of B, ω, C as calculated for $j=\frac{1}{2}$ are given in Table I. Note that they contain the energy independent, but otherwise arbitrary, parameters δ and δ'.

The results as given in Table I appear relatively complicated. Nonetheless, for $j=\frac{1}{2}$, $l=1$, the choice $\delta'=0$ gives results no more complex than the non-relativistic formalism. For $j=\frac{1}{2}$, $l=0$, the complication is not so easily removed. However, one must, of course, be able to reduce the present result to the non-relativistic for low energy particles.

The low energy form of the present results is discussed below. For $j=\frac{1}{2}$, $l=1$, $\delta'=0$

$$B_{s,\,1,\,\frac{1}{2}}=-(\epsilon_s/c)^{\frac{1}{2}},$$
$$\omega_{s,\,1,\,\frac{1}{2}}=e^{-ik_sa_s},$$
$$C_{s,\,1,\,\frac{1}{2}}=-(1/k_sa_s).$$

These results agree with those found in reference 1 for $l=1$, except for the B. However, the sign of B is immaterial and in the low energy limit

$$B_{s,\,\frac{1}{2}}\simeq-[\tfrac{1}{2}(\hbar/Mc)]^{\frac{1}{2}}k_s^{\frac{1}{2}},$$

which, except for a difference in normalization, agrees also with reference 1.

For $j=\frac{1}{2}$, $l=0$, one writes

$$-\delta=\tfrac{1}{2}(\hbar/Mc)/a_s$$

and neglects $[\frac{1}{2}(\hbar/Mc)k_s]^2$ with respect to unity, to find, with $\chi_s=k_sa_s$,

$$B_{s,\,0,\,\frac{1}{2}}=-[\tfrac{1}{2}(\hbar/Mc)]^{\frac{1}{2}}k_s^{\frac{1}{2}}[(1+\delta^4\chi_s^2)/(1+\delta^2)]^{\frac{1}{2}},$$
$$\omega_{s,\,0,\,\frac{1}{2}}=\exp-i(\chi_s-\text{arc tan}\,\delta^2\chi_s),$$
$$C_{s,\,0,\,\frac{1}{2}}=\delta^4\chi_s.$$

In addition, one will usually have $k_sa_s<1$, $\delta^2\ll1$, so that

$$B_{s,\,0,\,\frac{1}{2}}=-[\tfrac{1}{2}(\hbar/Mc)]^{\frac{1}{2}}k_s^{\frac{1}{2}},$$
$$\omega_{s,\,0,\,\frac{1}{2}}=\exp-i\chi_s,$$
$$C_{s,\,0,\,\frac{1}{2}}=\delta^4\chi_s,$$

which differs from reference 1 primarily in the non-zero C.

The formal discussion given by Wigner and Eisenbud[1] for the generalized one-level formula may be taken over in toto. We list here for convenience, in the limit where $[\frac{1}{2}(\hbar/Mc)k_s]^2$ is neglected in respect to unity, the partial widths and energy shifts.

$$\Gamma_{\lambda,s,0,\frac{1}{2}}=\frac{\hbar}{Mc}\frac{k_s}{1+\delta^2\chi_s^2}\frac{1+\delta^4\chi_s^2}{1+\delta^2}\gamma^2_{\lambda,s,0,\frac{1}{2}},$$

$$\Delta_{\lambda,s,0,\frac{1}{2}}=\tfrac{1}{2}\delta^4\chi_s\Gamma_{\lambda,s,0,\frac{1}{2}},$$

$$\Gamma_{\lambda,s,1,\frac{1}{2}}=\frac{\hbar}{Mc}\frac{k_s\chi_s^2\gamma^2_{\lambda,s,1,\frac{1}{2}}}{1+\chi_s^2}$$

$$\Delta_{\lambda,s,1,\frac{1}{2}}=-(1/\chi_s)\Gamma_{\lambda,s,1,\frac{1}{2}}$$

where $\chi_s=k_sa_s$

$$-\delta=\tfrac{1}{2}(\hbar/Mc)/a_s.$$

I am greatly indebted to Mr. E. P. Wigner for suggesting this problem and for many helpful discussions. I also wish to thank Dr. M. E. Rose for many valuable discussions. This document is based on work performed under Contract Number W-35-058-eng-71 for the Atomic Energy Project at the Clinton Laboratories.

APPENDIX: DERIVATION OF EQ. (5)

If $H=ich\alpha\cdot\nabla+Q$ and Ψ and φ are four-component wave functions regular on the interior and surface of a volume V, and if Q is an operator such that $\Psi^*(Q\varphi)=(Q\Psi)^*\varphi$, then

$$\int_V d\tau(\Psi^*H\varphi-(H\Psi)^*\varphi)$$

$$=\int_V d\tau(\Psi^*ich\alpha\cdot\nabla\varphi-(ich\alpha\cdot\nabla\Psi)^*\varphi)$$

$$=\int_V d\tau ich[\Psi^*\alpha\cdot\nabla\varphi+(\alpha\cdot\nabla\Psi)^*\varphi]$$

$$=ich\int_V d\tau\nabla\cdot(\Psi^*\alpha\varphi)$$

$$=ich\int_s d\sigma(\Psi^*\alpha_n\varphi),$$

where α_n is the component of α along the outward normal to s.

Letters to the Editor

PUBLICATION of brief reports of important discoveries in physics may be secured by addressing them to this department. The closing date for this department is five weeks prior to the date of issue. No proof will be sent to the authors. The Board of Editors does not hold itself responsible for the opinions expressed by the correspondents. Communications should not exceed 600 words in length.

Compressional Piezoelectric Coefficients of Monoclinic Crystals

HANS JAFFE
*The Brush Development Company, Cleveland, Ohio**
May 8, 1948

IN two recent publications[1,2] Mason has given a complete set of piezoelectric coefficients d_{nm} for the monoclinic polar crystals potassium tartrate hemihydrate (DKT) and ethylene diamine tartrate (EDT). In addition to shear piezoelectric coefficients referring to electric fields perpendicular to the polar axis, crystals of this class have piezoelectric coefficients d_{21}, d_{23}, and d_{25}, relating an electric displacement parallel to the polar (Y) axis with a general stress in the plane perpendicular to this axis, and a coefficient d_{22} relating the same electric displacement with a compressional stress parallel to the Y axis. The sum $d_{21}+d_{22}+d_{23}$ should give the electric displacement parallel to Y caused by hydrostatic pressure.

According to Mason's values for these coefficients,[2] the hydrostatic piezoelectric effect of ethylene diamine tartrate should be the highest known for any crystal. A direct measurement, however, showed an effect only about one-seventh as large as derived from Mason's data. We therefore undertook direct measurements of the piezoelectric coefficients relating to fields parallel to Y by determining the charge developed on the Y face upon removal of a load from the side faces of bars having their length perpendicular to Y at various azimuths. The results are given in Table I.

TABLE I.

	EDT	DKT	DKT*
d_{21}	$+11.3\pm1$	-0.5 ± 0.3	-0.8
d_{22}	-12.3 ± 1	-4.9 ± 0.5	-4.8
d_{23}	-18.4 ± 2	-5.9 ± 2	-6.3
d_{25}	$+1.8\pm0.5$	$+3.4\pm0.5$	$+4.9$
d_{hydro}	1.9 ± 0.2	1.3 ± 0.2	
Temp.	25°C	25°C	20°C

* See reference 3.

The unit in this table is 10^{-12} coulomb/newton ($=3.10^{-4}$ e.s.u.). The values of Spitzer[3] were arranged to conform to our convention on axes which is identical with that of Mason and is based on the standards proposed by the Committee on Piezoelectricity of the I.R.E.[4] The writer has recently been informed by Dr. Mason that new determinations of the signs of the piezoelectric coefficients of EDT and DKT are in agreement with those given in this letter.

I am obliged to Mr. James Mumper for carrying out most of the reported measurements.

* Work supported by U. S. Army Signal Corps under Contract W28-003 sc 1583.

[1] W. P. Mason, Phys. Rev. **70**, 705 (1946).
[2] W. P. Mason, Proc. I.R.E. **35**, 1005 (1947).
[3] F. Spitzer, Dissertation, Goettingen (1938).
[4] Standards on Piezoelectric Crystals (Institute of Radio Engineers, 1948), in print.

Remarks on Diamond Crystal Counters

KATHLEEN LONSDALE
University College, London, England
May 6, 1948

IN a letter with the above title, Robert Hofstadter[1] has quoted the x-ray studies of R. S. Krishnan[2] and G. N. Ramachandran[3] as indicating that ultraviolet opaque (type I) diamonds have an essentially mosaic structure.

This is quite definitely not the case. The diamonds which show "type I" effects *most clearly* are neither mosaic nor laminated; and contrary to my previous opinion, they are not even in a state of strain; they are, in fact, about the nearest approach to a *perfect* crystal that we know. Krishnan and Ramachandran both confirmed this. If a really good type I and a type II diamond are compared under similar conditions, it will be found:

(1) that the diffraction of a narrow pencil of x-rays by the type I diamond is several times less intense than that of the type II;[4,5]

(2) that the absorption pattern given by a divergent beam of x-rays[6] is invisible for the type I diamond, but well-defined for the type II diamond.

Both these observations are evidence of strong primary extinction in type I diamonds and show their near-perfection. It is quite true, on the other hand, that really good type I diamonds are comparatively rare; some diamonds appear to be a mixture of the two types; others intermediate between them.

Good type II diamonds do appear to be laminated; and, if it is this type of diamond that makes the best "gamma-ray counter," then it would seem to be at least possible that the secondary electrons counted are those which move along the boundaries and not through the crystal proper. In this case the reorientation experiment suggested by R. Hofstadter might well show a positive result, but it would neither prove nor disprove Sir C. V. Raman's theory[7] that four kinds of diamond exist.

[1] R. Hofstadter, Phys. Rev. **73**, 631 (1948).
[2] R. S. Krishnan, Proc. Ind. Acad. Sci. **A19**, 298 (1944).
[3] G. N. Ramachandran, Proc. Ind. Acad. Sci. **A19**, 304 (1944).
[4] K. Lonsdale, Proc. Roy. Soc. London **A179**, 315 (1942); Nature, London **153**, 669 (1944).
[5] P. S. Hariharan, Proc. Ind. Acad. Sci. **A19**, 261 (1944).
[6] K. Lonsdale, Nature **153**, 22 (1944); Phil. Trans. Roy. Soc. **A240**, 219 (1947).
[7] Sir C. V. Raman, Proc. Ind. Acad. Sci. **A19**, 189 (1944).

Pair Production by γ-Rays in the Field of an Electron

VÁCLAV VOTRUBA
Institute of Theoretical Physics, Charles University, Prague, Czechoslovakia
May 8, 1948

THE present calculation of the cross section of this process is based on Dirac's theory of positrons as formulated in the quantum theory of wave fields and on the general expression for the matrix element H_{FA}^{III}, which determines the probability of quantum processes of third order.

Summing the contributions of all possible virtual ways in which the process can take place, we get for our specific H_{fa}^{III} the same expression as in the ordinary quantum electrodynamics of electrons (without theory of holes), although the contributions of individual virtual ways are different in both cases.[1] This shows clearly, that the individual sequences of intermediate states of the usual perturbation theory have no unambiguous meaning.

A rather tedious task is the calculation of the spurs (of products of 12th degree in the Dirac matrices), which occur in the expression $W=\frac{1}{4}\Sigma(H_{fa}^{III})^2$, where $\frac{1}{4}\Sigma$ denotes the averaging over the polarizations of the incident photon and spin states of the initial electron and summing over the spin states of the three particles of the final triplet. This can be done by using some "four-dimensional" generalizations of the usual formulas, e.g., expressing the spurs of the form

$$S_p \prod_{m=1}^{3n} \alpha^{i_m}, \quad (i_m=0,\ 1,\ 2,\ 3), \quad \alpha^i \equiv (1,\alpha),$$

in terms of g_{ij}. The resulting complete formula for W is very complicated.

Choosing the polar coordinate system, in which the initial electron is at rest and the photon moves in the direction of the axis, the formula for the differential cross section can be written in the form

$$d\sigma=\frac{r_0^2}{137}\cdot\frac{S}{\pi}\cdot\frac{dE'dE''d\vartheta'd\vartheta''}{\sin\omega_+},$$

where $S=4\pi^3\mu^7c^8E^+E'E''W/h^6\epsilon^6$ and ω_+ is the angle between the planes $(\mathbf{k},\mathbf{p}')$ and $(\mathbf{k},\mathbf{p}'')$. The energies E and the energy k of the photon are measured in units μc^2. μ is the mass, and ϵ the charge of the electron, and $r_0=\epsilon^2/\mu c^2$.

In computing the total cross section $\sigma(k)$, the two final states with $\mathbf{p}'=\mathbf{A}$, $\mathbf{p}''=\mathbf{B}$ and $\mathbf{p}'=\mathbf{B}$, $\mathbf{p}''=\mathbf{A}$ are not to be considered as different. Because the general and exact integration of $d\sigma$ can hardly be performed, the following special cases were discussed in approximation: (1) The case $0\leqq k-4\ll 1$; (2) the case $k\gg 4$, when, further, either (2a) p' is small (*viz.* $2k^{-1}\leqq p'\leqq 1$) and p'', p^+ large (of the order $k\gg 1$), or (2b) p^+ small and p', p'' large, or, at last, (2c) p', p'', p^+ all large. The case of two particles of the triplet receiving momenta $\ll 1$ does not arise.

The results are as follows:

(1) Because in the limit $k=4$ the quantity $S=S_0=1/12$, we obtain the asymptotic formula[2]

$$\sigma(k)=(r_0^2/137)(\pi\sqrt{3}/2^2 3^5)(k-4)^2. \qquad (1)$$

(2a) In this case (of small recoil) the values of S are very large, although only few terms are significant, and the approximate formula for $\sigma(k)$ becomes

$$\sigma(k)=r_0^2/137[(28/9)\log 2k-(102/9)]. \qquad (2a)$$

The approximation involved results in a not entirely accurate value of the additive constant.

(2b) The probability of this case (of a slow positron) is small, because

$$\sigma(k)=(r_0^2/137)\cdot 2k^{-1}\log k. \qquad (2b)$$

Here again the value of the numerical factor[2] is not exact.

(2c) In this last case I was only able to determine the order of magnitude of σ, which is

$$\sigma\sim r_0^2/137\cdot\bar{S}/64, \qquad (2c)$$

where $\bar{S}$ is some constant (independent of k) of the order unity.

The total cross section of the case (2) will now be approximately equal to the sum of the contributions (2a, b, c), i.e. will be in substance given by (2a).[3] This result confirms the formula of Wheeler and Lamb,[4] and their indirect conclusion, that the contribution of the processes connected with a large momentum transfer to the initial electron should be relatively small and enters into the formula for the total cross section only as a part of the constant term.

A more detailed report will be published shortly in the Bulletin international de l'Académie tchèque des sciences, Prague.

I am indebted to Professor G. Wentzel, who suggested this problem, for valuable stimulating discussions about this subject during my stay in Zurich.

[1] In the latter case H_{fa}^{III} can also be computed by using the corresponding formula of Møller, Proc. Roy. Soc. **A152**, 481 (1938) for the (inverse) process of radiative collision between two fast electrons.
[2] See also A. Borsellino, Nuovo Cimento **4**, No. 3–4 (1947). The exponent 3 of $(k-4)$ in Borsellino's formula seems to be a misprint.
[3] Contrary to the opinion of K. M. Watson, Phys. Rev. **72**, 1060 (1947) the contribution of the case p'' small and p', p^+ large should not be counted separately, because the interchange of both electrons of the triplet does not lead to a new final state.
[4] J. A. Wheeler and W. E. Lamb, Jr., Phys. Rev. **55**, 858 (1939).

Magnetic Resonance Absorption in Diluted Chrome Alums*

C. A. WHITMER, R. T. WEIDNER, AND P. R. WEISS
Department of Physics, Rutgers University, New Brunswick, New Jersey
May 5, 1948

THE microwave measurements on the magnetic resonance absorption in single crystals of ammonium chrome alum reported recently[1] have been repeated with refined techniques, and extended to include potassium chrome alum and diluted crystals of both salts. Troublesome drifts in frequency have been greatly reduced by the use of the Pound stabilized oscillator.[2] The absorption was measured again through the off-balance of a magic-tee bridge at a frequency of 9375 mc/sec. The cavity was tuned to a balance at high fields, of about 7200 oersteds. Compared to the previous method of balancing at zero

TABLE I. Observed and calculated magnetic field values of the absorption maxima for $\nu = 9375$ mc/sec.

Undilute Ammonium Chrome Alum $g = 1.99$, $\delta = 0.143$ cm^{-1}							
(111)	1,830	2,780	3,370	3,770	4,910	Calc.	
	1,830	2,720	3,370	Unres.	4,920	exp.	
(100)		3,120		3,540		Calc.	
			3,250			exp.	
(110)	2,390	2,630	3,240	3,580	3,910	4,130	Calc.
	2,380	Unres.	3,220	3,600	Unres.	4,190	exp.
Dilute Ammonium Chrome Alum $g = 1.97$, $\delta = 0.100$ cm^{-1}							
(111)	2,310	2,970	3,400	3,720	4,490	Calc.	
	2,270	2,980	3,400	3,710	4,480	exp.	
(100)		3,280		3,480		Calc.	
		3,300		3,480		exp.	
(110)	2,740	2,860	3,330	3,500	3,830	3,910	Calc.
	2,740	2,880	3,330	3,500	3,820	3,920	exp.

d.c. magnetic field, this procedure shifts the maxima by as much as 100 oersteds in some cases. In the new method, the balance is obtained sufficiently far removed from any resonances so that a minimum of magnetic absorption is balanced out. A recalibration of the d.c. field by comparison with the resonance absorption of the proton moment established the field measurements to within 10 gauss for all field strengths used. The zero field splitting previously reported for ammonium chrome alum (0.15 cm^{-1}) is essentially the same, the changes caused by the new method of balancing being largely compensated by the errors in our previous magnetic field calibration.

The diluted crystals were grown from a solution made up by dissolving 1 part by weight of ammonium chrome alum and 5 parts by weight of aluminum ammonium alum. Chemical analysis of the crystals shows the ratio of the number of chrome ions to aluminum ions to be about 1 to 8.5. The crystals of dilute potassium chrome alum were grown in the same way.

Figures 1, 2, and 3 show the absorption for both dilute and undilute ammonium chrome alum single crystals for the orientations in which the d.c. field is perpendicular to: a 111 face, a 100 face, and a 110 face, respectively.

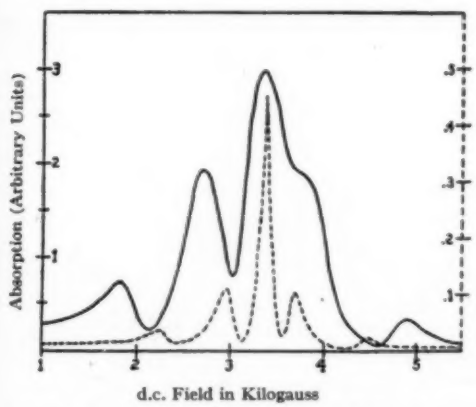

FIG. 1. Relative absorption of ammonium chrome alum with the d.c. field perpendicular to a (111) face. The full line curve refers to the undiluted, the dashed curve to the diluted slat. The scales for the undilute (left) and the dilute (right) salts refer to the same input power.

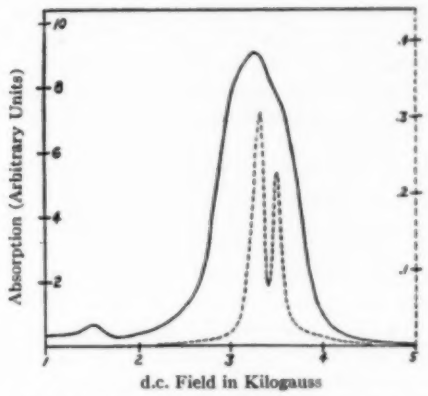

FIG. 2. Relative absorption of ammonium chrome alum with the d.c. field perpendicular to a (100) face. The remarks in the title to Fig. 1 apply here.

The dilution increases the resolution of the peaks by decreasing the widths of the lines. All principal lines predicted by theory[3,4] for the three orientations are resolved. In addition, the dilution decreases the crystalline field splitting. Table I shows the magnetic field strengths of the resonances as observed and as calculated from the theory using the g-values and the zero field splittings shown there. The discrepancies are probably caused by the interference between overlapping resonances.

If the width of the lines were attributed to spin-spin interaction alone the peak absorptions of the lines would be unaffected by the dilution. The measurements show a marked diminution of the peaks with dilution. The ratio of the magnitudes of the peaks vary with the orientation of the d.c. field. This effect is most marked in the (100) orientation, where the ratio can be seen to be about 30. This factor cannot be accounted for by overlapping of the lines, by volume differences of the crystals used, or by changes in the Q of the cavity on account of dielectric absorption. No saturation effects were observed at the power level used. This anomaly is being investigated further.

A comparison of the ammonium and the potassium salts shows that the splitting is smaller in the potassium than

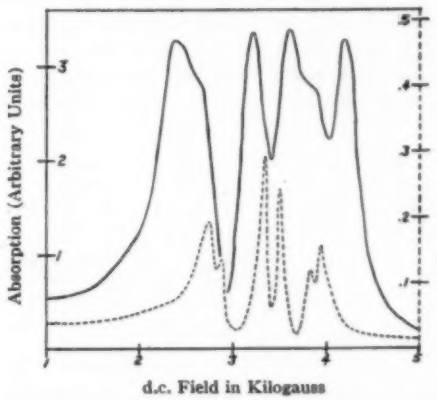

FIG. 3. Relative absorption of ammonium chrome alum with the d.c. field perpendicular to a (110) face. The remarks in the title to Fig. 1 apply here.

in the ammonium salt. This applies to both the undiluted and the diluted salts. The splitting $\delta=0.13$ cm^{-1} for the undilute potassium salt ($\delta=0.091$ for the diluted salt) is somewhat less than the value quoted above for the corresponding ammonium salt. Bagguley and Griffiths[5] report a value of $\delta=0.12$ cm^{-1} for chrome alum. The general appearance of their curves indicates that they refer to the potassium salt. Halliday and Wheatley[6] obtained values of 0.12 cm^{-1} for potassium chrome alum and 0.13 cm^{-1} for ammonium chrome alum. The difference between their values and ours for the undiluted salts appears to be greater than the experimental error in measuring the peak positions. It appears that the interference effects mentioned above shift the positions of the maxima in a different way than do the interference effects in the method used by Halliday[6] and by Griffiths.[5]

A detailed report of this investigation will be given in a forthcoming paper.

* This work was supported by the Rutgers University Research Council, the Research Corporation, and the Office of Naval Research.
[1] P. R. Weiss, C. A. Whitmer, H. C. Torrey, and Jen-Sen Hsiang, Phys. Rev. **72**, 975 (1947).
[2] R. V. Pound, Rev. Sci. Inst. **17**, 490 (1946).
[3] P. R. Weiss, Phys. Rev. **73**, 470 (1948).
[4] C. Kittel and J. M. Luttinger, Phys. Rev. **73**, 162 (1948).
[5] D. M. S. Bagguley and J. H. E. Griffiths, Nature **160**, 532 (1947).
[6] D. Halliday and J. Wheatley, Bull. Am. Phys. Soc. **23**, No. 3, 13 (1948).

Violet Asymmetry of Potassium Resonance Lines under High Rubidium Vapor Pressure

CH'EN SHANG-YI
Institute of Physics, National Academy of Peiping, Peiping, China
May 3, 1948

IT is not surprising at all to conceive that alkali vapors of higher vapor pressure can be used as perturbing atoms, as foreign gases do, on the absorption lines of other alkalis of relatively lower vapor pressure. Because of experimental difficulties, however, experimental research has very seldom been accomplished.

The chief difficulty lies first in the fact that before the discovery of the corrosion-resistant optical windows, it was impossible to get an absorption tube of an alkali vapor in high pressure. Secondly, when the alkali vapor pressure is high, not only its own absorption lines will be extensively broadened but also its molecular absorption bands will be added to the spectrum. Thus the spectral lines of the alkali to be studied will be badly obscured. Füchtbauer and Heimann[1] studied the effects of caesium vapor on the high series lines of sodium by mixing Cs in the discharge lamp of Na. Their pressure was very, very low.

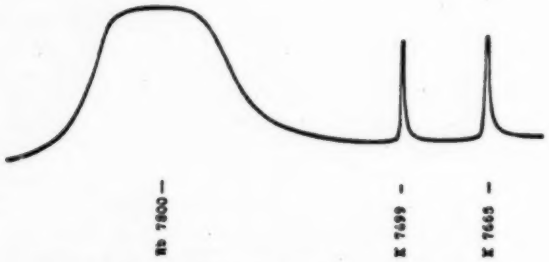

FIG. 1. K resonance lines and the λ7800 of Rb at 426 C. (Rb vapor pressure 19.86 mm; tube length 2 mm.)

If the corrosion resistant MgO windows[2] are used to construct an absorption tube of only 2-mm length,[3] the width of the absorption lines can be considerably narrowed. When the absorption tube of Rb with a trace of K is heated to temperatures as high as 556 C the resonance lines of Rb, λλ7800.29 and 7947.64, with a separation of 147A, are so much broadened that, even when the 2-mm tube is used, they begin to overlap. The pressure of Rb vapor under that temperature would be not less than 150 mm if one extrapolated from the empirical formula of temperature *vs.* Rb vapor density.[4] Fortunately, the region for the λλ7664.94, 7699.01 lines of potassium presented as impurity in the Rb metal are not yet masked, rendering observations feasible.

The microphotometer curve shown in Fig. 1 shows clearly the violet asymmetry of the K lines and the broadened Rb 7800.29. The asymmetry becomes appreciable when the vapor pressure of Rb amounts to about 15 mm or up for the 2-mm tube. When the tube length is increased to 7.5 cm, the asymmetry appears at a Rb vapor pressure of about 2 mm. It is also to be noted that the K impurity lines are narrower than they ought to be if the absorption lines of pure potassium[5] are taken. There is no measurable shift.

This sort of research not only can give more extended data on the investigation of the pressure effects on spectral lines, but also suggests a way to investigate quantitatively the variation of the vapor pressure and the line intensities of one element in the presence of other element or elements. By the measurement of the area under the line contour in terms of the absolute absorption coefficients, it should be possible to estimate the concentration of the absorbing atoms in the absorption column.

[1] Füchtbauer and Heimann, Zeits. f. Physik **110**, 8 (1938).
[2] J. Strong and R. T. Brice, J. Opt. Soc. Am. **25**, 207 (1935).
[3] Ch'en Shang-yi, Phys. Rev. **58**, 884 (1940).
[4] T. J. Killian, Phys. Rev. **27**, 578 (1926).
[5] D. S. Hughes and P. E. Lloyd, Phys. Rev. **52**, 1215 (1937).

Production of New Tc Activities from Separated Mo Isotopes*

E. E. MOTTA AND G. E. BOYD
Oak Ridge National Laboratory, Oak Ridge, Tennessee, and Department of Terrestrial Magnetism, Carnegie Institution, Washington, D. C.
April 30, 1948

DURING the past 10 months, a series of 35 bombardments with 15–20 Mev deuterons on the different enriched Mo isotopes has yielded several new Tc activities (element 43). In addition, data on previously uncertain activities have been obtained. In each case the Tc was separated chemically from the bombarded Mo isotopes by means of a highly efficient volatility separation method developed in our chemical studies on the element, and where necessary, the Tc was prepared as a thin sample for counting by co-precipitation with platinum sulfide. All counting was done with mica end-window, bell-type

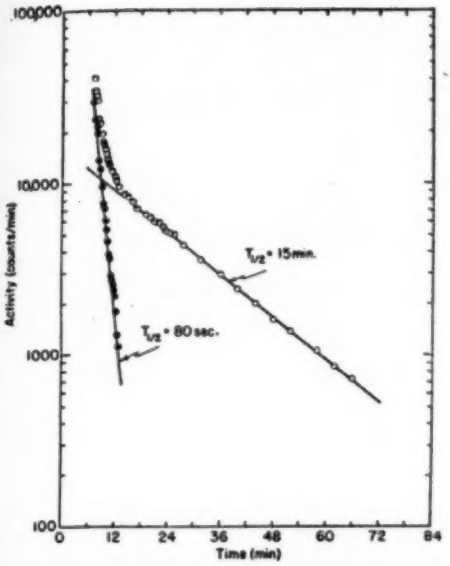

FIG. 1. Decay curve of the 80-second Tc activity produced by the deuteron bombardment of Mo enriched in Mo^{100}.

Geiger-Müller tubes. A preliminary series of deuteron bombardments was carried out in order to see what new activities might be present. This was followed then by a second series using bombardment periods and measuring techniques which served to emphasize the desired radioactivity. Whenever several activities were present together, aluminum and lead absorption curves for the particular Tc activity being studied were obtained by the method of isochrons, i.e. by taking decay curves through each of a set of selected absorbers.

80-second Tc. Short deuteron bombardments on Mo^{100} produced a new short-lived Tc activity which decayed with a half-life of 80±10 seconds (Fig. 1) and which emitted charged particles having an energy of 2.3±0.5 Mev. A gamma-ray of 0.6±0.1-Mev energy was also found associated with this period. The decay curve also shows the previously known[1] 14–15 min. Tc^{101} period as a longer lived component. The new activity is probably Tc^{100} or Tc^{101} produced by $(d,2n)$ or (d,n) reactions, respectively. If it is the latter, it represents an independent isomer of Tc^{101}, of which the 15-min. activity may be the ground state.

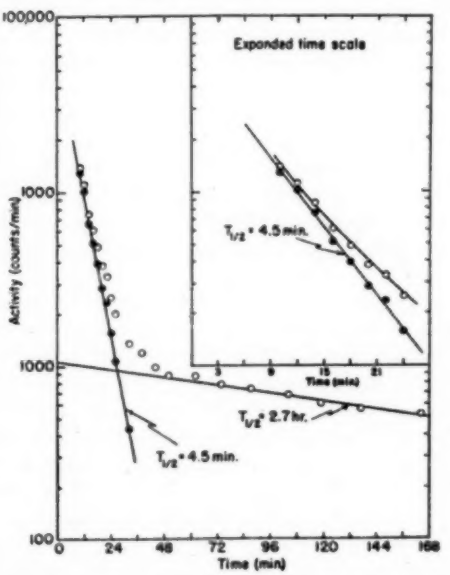

FIG. 2. Decay curve of the 4.5-min. Tc activity produced by the deuteron bombardment of Mo enriched in Mo^{92}.

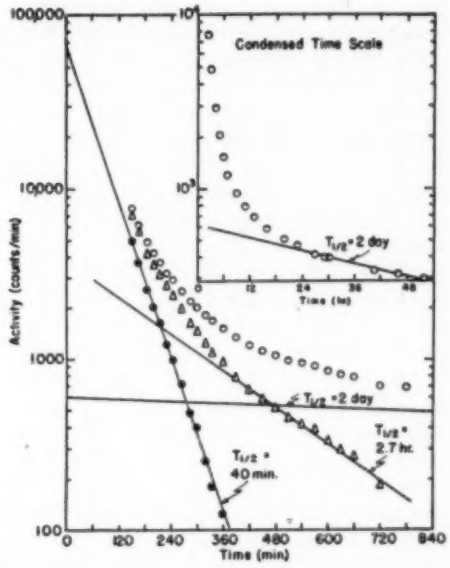

FIG. 3. Decay curve of the 40-min. Tc activity produced by the deuteron bombardment of Mo enriched in Mo^{98}, and of Mo enriched in Mo^{96}.

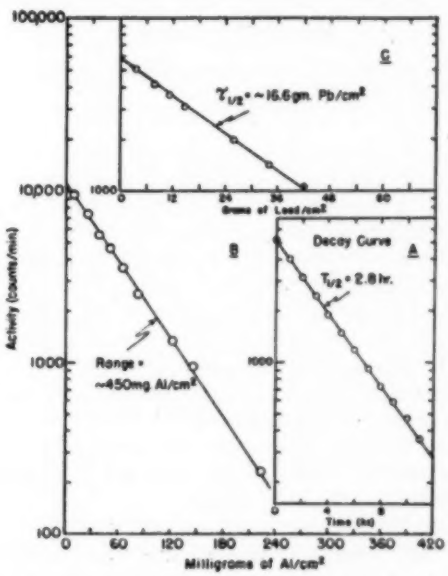

FIG. 4. *A*. Decay curve of the 2.8-hr. Tc activity produced by the deuteron bombardment of Mo enriched in Mo^{96}. *B*. Aluminum absorption curve for the 2.8-hr. Tc. *C*. Lead absorption curve for the 2.8-hr. Tc.

4.5-minute Tc. Five-minute deuteron bombardments of Mo^{92} gave rise to a new positron emitter with a half-life of 4.5±0.5 min. and a positron energy of 4.3±0.5 Mev. A gamma-ray of 1.3±0.3 Mev energy was also present. The decay curve (Fig. 2) showed a longer lived period with a 2.7-hr. half-life, the existence of which has already been indicated.[2] As a result of its mode of production, this 4.5-min. Tc activity is probably Tc^{92} or Tc^{93}.

40-minute Tc. Bombardment of Mo^{97} and Mo^{98} gave rise to a 40±5 min. Tc radioactivity (Fig. 3) emitting charged particles having an energy of 2.0±0.5 Mev. The decay curves show the presence of the previously known 2.7 hr. and ~2 day Tc activities.[3]

2.8-hour Tc. Although a 2.7-hr. activity had been previously observed in a Mo target,[2] no work had been done on the character and energies of its radiations or on its unambiguous chemical identification. Bombardments of Mo^{92} gave good yields of a 2.7±0.1-hr. Tc which was shown to be a positron emitter by magnetic deflection. A positron energy of 1.2±0.2 Mev, and a hard gamma-ray of 2.4±0.5 Mev were determined by absorption measurements. This activity is probably Tc^{92} or Tc^{93}.

This note reports only a part of the results from a general program for the characterization and assignment of the various radioactivities of element 43 produced by deuteron bombardments with the enriched Mo isotopes. The complete data and discussion will appear in a forthcoming article.

* This document is based on work performed under Contract Number W-7405 eng 26 for the Atomic Energy Project at Oak Ridge National Laboratory.

[1] Sagane, Kojima, Miyamoto, and Ikawa, Phys. Rev. **57**, 750 (1940).
[2] Delsasso, Ridenour, Sherr, and White, Phys. Rev. **55**, 113 (1939).
[3] G. T. Seaborg and E. Segrè, Phys. Rev. **55**, 808 (1939).

Identification of Beta-Rays with Atomic Electrons

M. GOLDHABER AND GERTRUDE SCHARFF-GOLDHABER
Department of Physics, University of Illinois, Urbana, Illinois
May 8, 1948

THE old question whether beta-rays are identical with atomic electrons was recently reviewed by Crane.[1] When this problem was much discussed about ten years ago, experiments by Zahn and Spees[2] set doubts at rest by showing that the value of e/m for beta-rays does not differ from the value found for atomic electrons by more than 1.5 percent. While this and other indirect evidence support the assumption that beta-rays and atomic electrons are identical, the question remains ". . . whether or not experiments can exclude the possibility that, for example, the spin of the beta-particle is different from one-half unit, with only a slight effect upon the mass. This kind of question should be answered as precisely as possible for the record. . . ."[3]

As long as experiments show only that a particular property of beta-rays has the same value, within the attainable experimental error, as the corresponding property of atomic electrons, some doubts whether beta-rays and atomic electrons are identical might persist. We have carried out an experiment which is based on the well-founded assumption that Pauli's exclusion principle would not hold for a pair of particles if they differed in any property whatsoever. In this way we have been able to answer the question raised with a degree of certainty which could not be attained by determining the value of any single property of beta-rays and electrons.

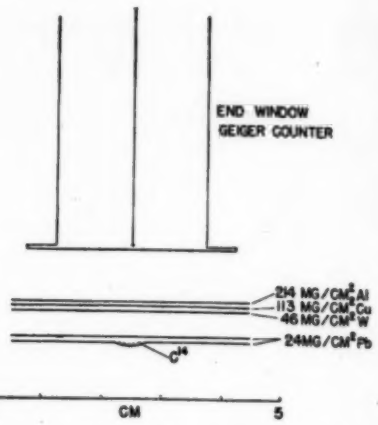

FIG. 1. Arrangement used in search for photons from beta-rays stopped in lead.

The experiment is based on the following consideration: when beta-rays are stopped in matter, their final fate will depend on whether or not they are identical with atomic electrons. If they were not identical with atomic electrons, they would not obey Pauli's exclusion principle and could therefore be captured into bound orbits "filled" with atomic electrons. Their transition to the lowest orbit would take place within an extremely short time and would be accompanied by K x-rays, slightly longer in wavelength than the K x-rays characteristic of the capturing atom, because of the additional screening. A test for the absence or presence of these x-rays can thus decide whether or not beta-rays are identical with electrons.

To carry out the experiment, it is convenient to use a source which emits soft beta-rays and no gamma-rays It is also desirable that the source have high specific activity and that the beta-rays be stopped in a heavy element. We have used as a source of beta-rays C^{14} in the form of $BaCO_3$, with 3–5 percent of the carbon consisting of C^{14}. This source emits beta-rays of 155 kev maximum energy and no gamma-rays.[4] The experimental arrangement is shown in Fig. 1. The C^{14} source was deposited on lead. The bare source emitted "in the direction" of the Geiger counter approximately 5×10^5 beta-rays per min. This was estimated by measuring the counting rate with 7.55 mg/cm² Al absorbing the beta-rays. This absorber was found to reduce the intensity of a weak C^{14} source to 15 percent. Corrections for absorption in the air and the mica window (~3 mg/cm²) were also made. To search for x-rays the source was covered by a lead foil (24.0 mg/cm²) which absorbed practically all beta-rays. When soft photons and secondary electrons were filtered out by 113 mg/cm² of Cu and 214 mg/cm² of Al, approximately 10 counts per minute above background were detected.

This weak radiation is probably caused by internal and external bremsstrahlung as well as excitation of characteristic lead x-rays by the fast beta-rays.

An upper limit for the number of photons for which we were searching was derived in the following way. Our Geiger counter had an average efficiency $\gtrsim 10^{-3}$ for detecting photons of this energy region if they passed through it. A tungsten foil (46 mg/cm²) reduced the counting rate by 2.4±1.5 counts per minute. If we assume that tungsten would absorb the x-rays with an absorption coefficient of 10 cm²/g, and allow for the absorption in the lead foil and in the copper and aluminum filters, we find that less than $(8\pm5)10^3$ photons per min. are emitted "in the direction" of the Geiger counter. Assuming a fluorescence yield close to unity we obtain the result that less than 3 percent of the beta-rays stopped in lead are captured into the K-shell. One can conclude from this experiment that beta-rays, at the end of their path, are identical with atomic electrons.

The C^{14} source was produced in Oak Ridge and allocated by the Atomic Energy Commission. This work was supported by the Office of Naval Research under Contract No. N6-ori-71.

[1] H. R. Crane, Rev. Mod. Phys. **20**, 278 (1948).
[2] C. T. Zahn and A. H. Spees, Phys. Rev. **53**, 365 (1938).
[3] H. R. Crane, Rev. Mod. Phys. **20**, 279 (1948).
[4] S. Ruben and M. D. Kamen, Phys. Rev. **59**, 349 (1941); P. W. Levy, *ibid.* **72**, 248 (1947); W. E. Stephens and Margaret N. Lewis, *ibid.* **72**, 526; G. L. Berggren and R. K. Osborne, Bull. Am. Phys. Soc. **23**, No. 3, 46 (1948).

An Excited State of Be^9 by Inelastic Scattering of Protons

K. E. Davis and E. M. Hafner
University of Rochester, Rochester, New York
April 25, 1948

THE spectrum of protons emitted in the reaction $Be^9(p,p')Be^9$ has been studied in order to locate low lying excited states of Be^9 in the region 0–5.2 Mev. Incident beams of 4.5 and 7.1 Mev were provided by the 27-inch Rochester cyclotron, and observations were made at an angle of 37° using 180-degree magnetic focusing and Eastman NTA photographic plates. The target was a thin evaporated foil of 99.9 percent purity. The resolution of the method, as measured by the energy width of elastically scattered protons, is about 0.15 Mev, and the background is such that a differential cross section 10^{-28} cm² leads to an observable yield.

The results, shown in Fig. 1, indicate no bound states above the ground state, a virtual state at 2.41 Mev (0.78 Mev above the dissociation energy), and no other states up to about 5.2 Mev. The possibility that the tracks were made by deuterons or alpha-particles from the reaction $Be^9(p,d)Be^8$ or $Be^9(p,a)Li^6$ was removed by observing that the count was not reduced when the plate was covered with a foil thick enough to stop the heavier particles. The cross section for excitation of the level is about 3×10^{-27} cm² at these energies. The experimental width is not significantly greater than the width of the elastic peak, suggesting an actual width less than 0.10 Mev.

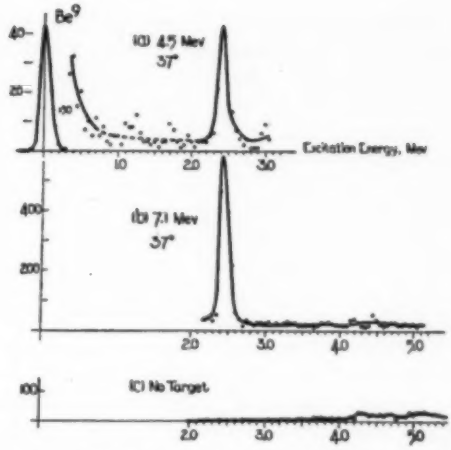

FIG. 1. Energy distribution of protons scattered by Be^9, plotted as number of tracks per 50 kev interval.

Calculations based on the model for Be^9 used by Caldirola[1] account for this state in a qualitative way, giving a value for the position which is in approximate agreement with experiment. However, the indicated width is too great by at least a factor of two. The absence of other states in the neighborhood is confirmed, but the model does not include the effect of the spin dependence of the forces. This model allows one to predict the excitation function and angular distribution for the scattering process; these calculations are being made and the corresponding experiments are under way.

[1] P. Caldirola, Nuovo Cimento **IV**, No. 1–2, 39 (1947).

The Effect of the Composition of the Gas Mixture in Self-Quenching Geiger-Müller Tubes on Their Plateau Characteristics

S. J. du Toit
Nuclear Physics Section, National Physical Laboratory, Council for Scientific and Industrial Research, Pretoria, South Africa
May 8, 1948

THE effect of the composition of the gas mixture in self-quenching G-M counters on the properties of these counters has been described by a number of authors.[1–4] Weisz[2] using ethyl-ether at room temperature and Rochester and McCusker[4] using alcohol at 40°C found the interesting result that at a pressure of 6 cm of Hg of the quenching gas the plateau of a given tube vanishes completely.

This result has been explained in two ways. Weisz[2] suggested that at the higher densities of ethyl-ether the photons formed during the primary discharge near the wire are so strongly absorbed by this vapor that the discharge has difficulty in spreading along the whole length of the wire. One would thus expect the region of limited proportionality to be extended at the cost of the

Geiger-Müller region. Rochester and McCusker on the other hand think that the effect may be caused by the fact that the threshold voltage increases linearly with the alcohol pressure, and that ions in the positive sheath may thus reach the cathode with sufficient energy to cause a liberal emission of electrons.

To test the last hypothesis three tubes, 1, 2, and 3, with wire diameters 0.1 mm, 0.25 mm, and 0.5 mm, respectively, and 3 cm outside diameter, were placed in an incubator together with an argon reservoir, alcohol tube, and manometer and the plateaus determined for various alcohol and argon pressures at 40°C.

The field strength at the cathode is determined by the relation $F=V/(b\log b/a)$ (V=voltage, b=cathode radius, a=wire radius). Thus at the same voltage the counters 3, 2, and 1 will have field strengths at their cathodes in the proportion 0.163:0.142:0.117. If Rochester and McCusker's hypothesis is correct, counter 3 would loose its plateau at a lower voltage, and thus also at a lower alcohol pressure than 2, and 2 at a lower voltage than 1. The plateaus were determined with the help of an oscillograph, the threshold being taken as the voltage that makes all the pulses of equal amplitude, and the end of the plateau as that region where multiple pulses come fairly regularly. The tubes used were made according to the evaporation technique,[5,6] gold being evaporated instead of the copper previously used as this gives a more permanent cathode, and photoelectric threshold of shorter wavelength. These advantages were also independently realized by Ramm.[7] The results of the measurements may be summarized as follows:

(1) On increasing the density of a filling of pure alcohol, the plateaus disappear at more or less the same pressure, and with a very much higher voltage on tube 3 than on 2, and a higher voltage on 2 than on 1.

(2) The addition of as little as 0.5 cm of argon changes the phenomenon. On adding increasing pressures of alcohol vapor to 0.5 cm of argon, the plateau of tube 1 vanishes at 0.5 cm argon+7.5 cm alcohol, that of tube 2 at 0.5 cm argon+5 cm alcohol and of tube 3 at 0.5 cm argon+3.1 cm alcohol. With 16 cm of argon added to various pressures of alcohol the result is in general the same, the plateaus of tubes 1, 2, and 3 being again reduced to nil when the alcohol pressure rises to 7.5, 5.8, and 3 cm, respectively.

In case (1) it thus looks as though the disappearance of the plateau is not caused by the positive ions striking the cathode with too high an energy, but more probably by the photon absorption becoming too high (Weisz) whereas in case (2) it looks as though secondary emission from the cathode at the threshold voltage is responsible for the plateau becoming zero (Rochester and McCusker).

The South African Council for Scientific and Industrial Research is thanked for permission to publish this note.

[1] A. Trost, Zeits. f. Physik **105**, 399 (1937).
[2] P. Weisz, Phys. Rev. **62**, 477 (1942).
[3] G. D. Rochester and L. Jánossy, Phys. Rev. **63**, 52 (1943).
[4] G. D. Rochester and C. B. A. McCusker, Nature **156**, 366 (1945).
[5] P. J. G. de Vos and S. J. du Toit, Rev. Sci. Inst. **16**, 270 (1945).
[6] P. J. G. de Vos, K. Gürgen, and S. J. du Toit, Rev. Sci. Inst. **17**, 516 (1946).
[7] C. A. Ramm, J. Sci. Inst. **24**, 320 (1947).

The Emission of Alpha-Particles from Different Faces of a Radioactive Crystal

K. B. Mather and F. N. D. Kurie
Department of Physics, Washington University, St. Louis, Missouri
April 25, 1948

SEVERAL authors, many years ago, sought to find a difference in the number of α-particles emitted from the various faces of a crystal of a substance containing radioactive nuclei. It is almost unthinkable that the direction of emission of α-particles would bear any relation to the lattice in which the atom containing the radioactive nucleus is situated. However, considering the credence with which the results of Mühlestein were regarded by Rutherford[1] it seemed worth while to examine this point again. Mühlestein,[2] using a crystal of uranium nitrate, found differences between the numbers of α-particles from the various faces of as much as 15 percent when using electrical methods and 32 percent when counting scintillations.

Having at hand a crystal of $ThSO_4$, originally prepared by Boltwood, an examination of the rate of emission of α-particles from its several faces was made. The crystal is a parallelepiped about 2 mm on a side, and thus has three crystallographically different sides. The crystal was laid on a thin piece of plastic through which a 0.04-in. hole had been drilled and this assembly was set on an Ilford C2 nuclear emulsion plate for a given time. This was repeated, on the same plate, for each of the other two faces. Many α-particle tracks were observed going into the emulsion. When counted, under the microscope, the differences in tracks per unit area among the three faces were within the statistical errors caused by the finite number of tracks counted (about 800). It is therefore concluded that the observations of Mühlestein must have been somehow in error. Our thanks are due to Mrs. K. B. Mather who did the actual track counting. This work was supported by a grant from the Research Corporation to one of us (FNDK) and by the Office of Naval Research under Contract N6ori-117.

[1] Rutherford, Chadwick, and Ellis, *Radiations from Radioactive Substances* (Cambridge University Press, 1930), paragraph 34e, p. 175.
[2] Mühlestein, Arch. d. Sci. **2**, 240 (1920).

The D+D Cross Section at Low Energies

A. P. French
Atomic Energy Research Establishment, Harwell, Berkshire, England
May 3, 1948

IN a paper recently published,[1] measurements are described of the thick target yield of the $D(d,p)$ reaction between 15 and 105 kev. In order to derive cross sections from these observations, use is made of an energy-range relation for deuterons in D_2O, arrived at from a synthesis of published data. By an unfortunate oversight, the work of Crenshaw[2] in this field was not included in our survey. If the results of his experiments are taken into consideration, the D+D cross section at any energy becomes approximately 10 percent lower than is stated in our paper.

[1] Bretscher, French, and Seidl, Phys. Rev. **73**, 815 (1948).
[2] Crenshaw, Phys. Rev. **62**, 54 (1942).

Ferromagnetic Domain Observation

L. MARTON
National Bureau of Standards, Washington, D. C.
April 13, 1948

THE visual representation of ferromagnetic domains on the surface of magnetized materials is usually done by means of ferromagnetic colloids. The patterns produced by spreading such colloids give valuable information about the "shape" and distribution of the domains. A few years ago an attempt was made[1] to use the electron microscope for the observation of the orientation of the colloidal particles in the patterns formed on the domains and to gain added knowledge of the distribution of the fringe field. At that time, because of pressure of other work, the attempt was abandoned, and only now has it been resumed by using an entirely different approach.

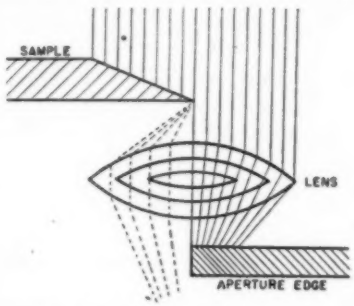

FIG. 1. Arrangement of the sample and of the optical system.

Experiments have been carried out for the observation of the fringe field from ferromagnetic domains by using the electron optical "Schlieren" effect, the description of which appears elsewhere.[2] For this purpose a thin laminar material, like steel shimstock, provided with a fine feather edge, or razor blades were used. After magnetizing to saturation the samples parallel to the edge, they were inserted in an electron microscope at the normal position for the specimens, and first a bright-field image was observed at a magnification of about 6000 diameters. After proper focusing of the bright-field image, the objective lens was slightly misaligned in order to bring in one edge of the objective aperture parallel to the observed edge but in the opposite direction (see Fig. 1). In this manner the direct rays are intercepted by the objective aperture and only the scattered or deflected electrons can reach the final image plane.

Figure 2 shows a typical observation of this kind. The bright line corresponds to a dark-field image produced by the scattered electrons on the edge. This line, however, is not continuous but is interrupted at irregular intervals. Whenever the line is interrupted, close observation shows a washed-out pattern at right angles to the edge. The spacing of this washed-out pattern is on the average equal to a few tenths of a micron. It is reasonable to assume that this pattern is produced by the fringe field of individual ferromagnetic domains and by the fringe field created on grain boundaries. Such a pattern is produced only if the edge is thin enough so that on the average we have no more than one domain in the direction of the electron beam (at right angles to the plane of the sample).

FIG. 2. "Schlieren" effect on magnetized steel edge.

To gather further evidence a similar observation was repeated with the objective aperture at an angle to the observed edge of the sample. In this case part of the image is dark-field and part of it shows a bright-field image of the magnetized edge. When overexposing the bright-field part of the image, a washed-out pattern at right angles to the edge corresponding to that of the dark-field image can be observed also in the bright-field image.

The collaboration of Mr. Max Swerdlow in taking the micrographs is gratefully acknowledged.

[1] L. Marton, Phys. Rev. **65**, 353 (1944).
[2] L. Marton, J. App. Phys. (to be published).

Optimum Conditions for a Beta-Ray Solenoid Spectrometer

E. PERSICO
Université Laval, Québec, Canada
April 30, 1948

IN any beta-ray spectrometer a compromise must be made, as is well known, between the resolving power and the luminosity. A theoretical investigation of the optimum conditions obtainable with a magnetic lens spectrometer of the solenoid type, with uniform field and a baffle system utilizing ring focus (which eliminates the main part of the spherical aberration[1]), has given the following results.

Let us put $D=2p/(He)$ (p=momentum of the electrons, H=intensity of the field, e=electronic charge in e.m.u.) and suppose that the baffle system admits the rays leaving the center of the source at an angle $\alpha\pm\Delta\alpha$ with the field. For a *point source*, one finds that the value of α giving the best resolution for a given luminosity (i.e. a given solid angle ω) is $\alpha=42°\,20'$. Then the inverse resolving power is $\Delta p/p=0.032\omega^2$ (in good agreement with the approximate evaluation given by Frankel[2] for $30°<\alpha<60°$).

However, a case of greater practical importance is that of a source of low specific activity, so that its dimensions cannot be made negligible. Supposing the source to be a disk of diameter S perpendicular to the field, it limits the resolution in two ways: (a) because the rays leaving the source with a given α cross the plane of the final slit in a ring-shaped zone of width S; (b) because the rays coming from excentrical points of the source cover a wider interval of α than those coming from the center, which results (owing to the spherical aberration) in a supplementary

width of the ring-shaped zone. If, neglecting the effect (b), one calculates the values of S and α giving the best resolution for a given luminosity (product of the solid angle ω by the area of the source) one finds that the optimum conditions are $\alpha=40°\ 25'$, and $S/D=11.4(\Delta\alpha)^2=0.172\omega^2$ ($\Delta\alpha$ in radians, ω in steradians). The inverse resolution is then given by $\Delta p/p=0.156\omega^2$ (so that, approximately, $S/D=\Delta p/p$). Under these conditions, $\frac{2}{3}$ of the Δp are produced by the width of the source and $\frac{1}{3}$ by the residual spherical aberration. The radius of the ring focus is $0.544D$ and the distance of its plane from the source is $1.63D$.

The relative importance of the neglected (b) effect may be roughly evaluated by saying that its contribution to the width of the ring-shaped zone (if the first limiting diaphragm is at the point of maximum distance of the rays from the axis) is about $0.17\omega^2$ of the total width—e.g., for $\Delta\alpha=2°$ (that is a solid angle $\omega=0.572$, more than 4.5 times that of Witcher) this contribution is only 1.4 percent.

It would seem that a spectrometer made on such a design and having the same resolving power as that of Witcher should have a luminosity more than 7 times greater.

[1] C. M. Witcher, Phys. Rev. 60, 32 (1941).
[2] S. Frankel, Phys. Rev. 73, 804 (1948).

Measurements of Radio Frequency Resistance of a Piece of Columbium Nitride through the Transition

J. V. LEBACQZ
Department of Electrical Engineering, The Johns Hopkins University, Baltimore, Maryland
May 8, 1948

THE purpose of this investigation was to ascertain the relationship between DC resistance and RF resistance of columbium nitride through the transition from a normal state to a superconducting state. The DC resistance has been measured accurately by potentiometer methods, but the actual RF resistance has not been ascertained up to now.

The first method of approach to measure the RF resistance was to build an oscillating circuit including the strip of columbium nitride under test and measure the decay time of oscillations once built up in the tank circuit. If then the resistance of the CbN changes abruptly over the transition range, one would expect a correspondingly large change in the losses of the circuit and hence in its ringing time. This method, however, had to be abandoned because it was found that at low temperatures the losses in the condenser of the tank circuit change in an unpredictable fashion and overshadow the change in CbN resistance.

Accordingly the following method has been used to determine the RF resistance of CbN over the transition range. The Q of a coil with and without the strip of CbN in series was measured both above and below the transition temperature of the CbN. Assuming all the losses in the circuit to be series losses, the difference between the measurements with and without the CbN gives them the additional resistance introduced by the CbN at the frequency considered. Within the limits of experimental error the RF resistance of the CbN strip was found to be exactly equal to the DC resistance measured at the same temperatures. This holds true at frequencies of from 600 to 1000 kc.

This result was to be expected because of the relatively large ohmic resistance per cm length of CbN above the transition. For such a high value of resistance the skin effect is essentially negligible. The apparatus as used was not delicate enough to measure the differences in resistance when the strip of CbN is almost completely superconducting. Theoretical computations, however, have indicated that a change in resistance can be expected when the d.c. resistance of the strip falls down to approximately 10^{-2} ohm or below. However, the absolute magnitude of the difference is too small to be noticeable, if curves of resistance *vs.* temperature are plotted for varying frequencies up to 1 mc. It can thus be assumed, that, for all practical purposes, the DC and RF transition curves of the CbN are identical.

Variation of Penetrating Showers with Altitude

JOHN TINLOT
Physics Department and Laboratory for Nuclear Science and Engineering, Massachusetts Institute of Technology, Cambridge, Massachusetts
April 30, 1948

PRELIMINARY results have been obtained from an experiment designed to determine the dependence on altitude of penetrating showers. The equipment used as a detector of these showers is similar in principle to the various arrangements used in recent experiments of Broadbent and Janossy,[1] and Jason and George.[2,3] Five trays of Geiger-Mueller counters are arranged as shown in the accompanying figure (Fig. 1); each counter has an active length of ten inches, and is one inch in diameter. There is a thickness of four inches of lead over tray A, between trays A and B, and between trays B and C, and a thickness of three inches on the sides of trays D. The eight counters in trays D are effectively connected in parallel, while fast addition circuits are used in the other trays to select coincident discharges of two or more counters in each tray.

The events recorded can be represented by the following symbols: $A_1B_1C_1$, $A_1B_1C_1D_1$, $A_2B_2C_2$, $A_2B_2C_1$, $A_1B_2C_2$, $A_2B_2C_2D_1$, $A_1B_2C_2D_1$, where, for example, $A\alpha B\beta\cdots$ indicates a simultaneous discharge of α or more counters in tray A, β or more counters in tray B, and so on.

The equipment was operated on the ground at Lexington, Massachusetts (altitude: 300 ft.) and in a B-29 airplane flying at altitudes of 15,000, 20,000, 25,000, and 30,000 feet; all measurements were taken at a geomagnetic latitude of about 53°. The rates of coincidences of the types $A_1B_1C_1D_1$, $A_2B_2C_2$, $A_2B_2C_1$, and $A_1B_2C_2$ are plotted as a function of atmospheric depth in g cm^{-2}; the standard deviations have been indicated wherever they exceed 5 percent.

In interpreting the results, one may make the following assumptions:

(1) Chance coincidences are completely negligible. This follows from the fact that the resolving time for selection of coincidences is less than 2 μsec.

(2) Ordinary air showers have a negligible effect. This is to be expected in consequence of the thick lead shielding. The fact that the observed events vary with altitude much more rapidly than air showers is a good indication that this assumption is valid.

(3) Triple knock-on processes of mesons contribute only a small amount to the observed rate of $A_2B_2C_2$. This needs to be demonstrated only at sea level, since the meson intensity increases with altitude much more slowly than the observed rate of $A_2B_2C_2$. At sea level, an upper limit for the number of events $A_2B_2C_2$ caused by triple knock-on processes can be computed by assuming that the rates of $A_2B_2C_1$ (or $A_1B_2C_2$) are entirely due to double knock-on processes. Under this assumption, and considering the rate of $A_1B_1C_1$ (1180 per hour), one calculates a triple knock-on rate of 0.03 per hour, as compared with the observed rate of 0.2 per hour for the event $A_2B_2C_2$. Since, as pointed out below, it is probable that only one-half of the events $A_2B_2C_1$ (or $A_1B_2C_2$) are caused by double knock-on processes, the knock-on contribution to the rate of $A_2B_2C_2$ is probably less than that given above.

The experimental results are then interpreted in the following way: At all altitudes, the event $A_2B_2C_2$ is the result of nuclear interactions in which penetrating particles are produced. The experimental points indicate an exponential variation with depth corresponding to an absorption thickness for the primary agent of about 120 g cm^{-2}. It appears quite significant that (at all altitudes) the rate of the event $A_2B_2C_2D_1$ (not shown in Fig. 1) is found to be only about 8 percent less than the rate of $A_2B_2C_2$. This suggests large multiplicity and large angular divergence in the production of secondary penetrating particles.

The rates of $A_2B_2C_1$ and $A_1B_2C_2$ at high altitudes follow roughly the same exponential dependence on depth as the rate of $A_2B_2C_2$, but deviate from this exponential behavior near sea level. One explains this result by assuming that for these events double knock-on processes become relatively important in the lower atmosphere. This is confirmed by the observation that the ratio of the rate of $A_2B_2C_1D_1$ to the rate of $A_2C_2B_1$ is over 0.9 at high altitudes, but only about 0.5 on the ground. Since double knock-on processes have a negligible probability of discharging trays D, one may conclude that about half of the counts recorded on the ground in the case of $A_2B_2C_1$ are due to double knock-on processes. The situation is similar in the case of $A_1B_2C_2$.

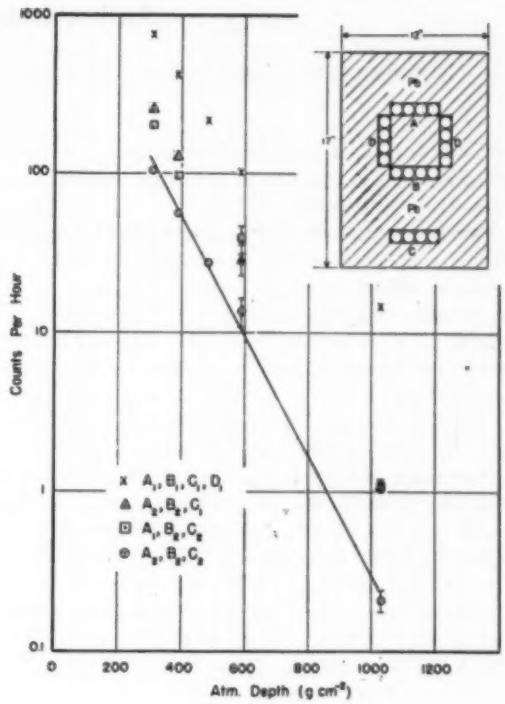

FIG. 1.

It is interesting to note that, at high altitudes, the event $A_1B_1C_1D_1$ varies with depth almost as rapidly as the event $A_2B_2C_2$. This indicates that, at least at high altitudes, most of the events $A_1B_1C_1D_1$ are also caused by nuclear interactions.

While it is believed that most of the events observed are produced by penetrating showers originating in the lead block, it is not possible, from the data presented here, to ascertain the contribution of penetrating showers from the atmosphere. This question has recently been studied by Jason and George,[3] and the writer is planning to investigate it further.

The writer is greatly indebted to Dr. B. Rossi for his guidance and interest in the course of this research. He also received valuable assistance and suggestions from Dr. O. Piccioni. The research described in this letter was supported partially by the Office of Naval Research, U. S. Navy Department. The B-29 used for the measurements at high altitude was provided by the U. S. Army Air Force.

[1] D. Broadbent and L. Janossy, Proc. Roy. Soc. 190, 497 (1947).
[2] E. P. George and A. C. Jason, Nature 160, 327 (1947).
[3] E. P. George and A. C. Jason, Nature 161, 248 (1948).

Author Index to Volume 73

References with (A) are to abstracts of papers presented at meetings of the American Physical Society ,and those with (T) designate title only. References with (L) are to Letters to the Editor.

Adams, Edward N., II (see Hirschfelder, Joseph C.)—863
Adams, Raymond V. (see Lloyd, Paul E.)—650(A)
—— (see Rau, R. Ronald)—534(A)
——, **Paul E. Lloyd, R. Ronald Rau, and Carl D. Anderson.** Distribution in energy of cosmic-ray mesotrons and protons at 30,000 foot elevation—650(A)
Adler, Robert (see Cherry, Walter L., Jr.)—1230(A)
Ahearn, A. J. Conductivity induced in diamond by alpha particle bombardment and its variation among specimens—1113(L)
—— Conductivity pulses induced in single crystals of zinc sulfide by alpha particle bombardment—524(L)
Alba, Fernando. Motion of a particle on the axis of a rotating ring in Birkhoff's theory of gravitation—651(A)
Albert, R. (see Wu, C. S.)—1259(A)
Alburger, David E. Absorption of Na^{24} gamma-radiation in lead, copper, and aluminum—344.
—— Gamma-rays from alpha-particle reactions—1014, 1241(A)
Aldrich, L. T. (see Fairbank, Henry A.)—729, 1263(A)
—— (see Lane, C. T.)—256(L)
Allis, W. P. Electrical phenomena in gases at microwave frequencies—1239(T)
Allison, S. K. and L. del Rosario. Performance of an electron multiplier tube counting alpha-particles—1224(A)
Alpher, R. A., H. Bethe, and G. Gamow. Origin of chemical elements—803(L)
Althaus, E. J. (see Sard, R. D.)—1276(A)
Anderson, Carl D. Cosmic-ray effects at thirty thousand feet—1238(T)
—— (see Adams, Raymond V.)—650(A)
—— (see Leighton, R. B.)—650(A)
—— (see Lloyd, Paul E.)—650(A)
—— (see Rau, R. Ronald)—534(A)
Anderson, Herbert L. Magnetic exchange moment for He^3 and H^3—919(L)
—— **and A. Novick.** Magnetic moment of He^3—919(L)
Andrews, R. D., N. Hofman-Bang, and A. V. Tobolsky. Elasto-viscous properties of polyisobutylene I: Relaxation of stress in whole polymer of different molecular weights at elevated temperatures—1221(A)
Antonoff, George, Alexis Yakimac, and Duncan Randall. Fluctuations in properties of liquids and the effect of radiations on them—1230(A)
Apker, L. Spectral distribution of the external photoelectric yield from semi-conductors—1238(T)
——, **E. Taft and J. Dickey.** Energy distribution of photoelectrons from polycrystalline tungsten—46
Arnold, G. and A. H. Weber. Crystal orientation in Al by slow neutron diffraction—1385
Arnold, Robert D. (see Kip, Arthur F.)—1247(A)
—— **and Arthur F. Kip.** Paramagnetic resonance absorption in copper sulphate—1247(A)
Arnott, E. G. F. Some discharge phenomena in fluorescent lamps—1239(T)
Arons, A. B. Selection of adiabatic parameters in the theory of oscillation of gas globes from underwater explosions—1253(A)
—— (see Yennie, D. R.)—1253(A)
Ashkin, Julius (see Szilard, L.)—1307
—— (see Wu, Ta-You)—986
—— **and Ta-You Wu.** Neutron-proton and proton-proton scattering at high energies—973
Astheimer, Robert W. (see Hawkes, John B.)—520(L)
Aten, A. H. W., Jr. Isotopic composition of xenon—1206(L)
Auger, Pierre (see Maze, Roland)—418(L)
Austern, N. (see Mack, J. E.)—1233(A)

Bacher, R. F. The physicist and the future development of atomic energy—1238(T)
Baez, A. V. (see Kirkpatrick, Paul)—535(A), 1234(A)
Bailey, Carl L., George Freier, and John H. Williams. Neutron and gamma-ray yields from deuterons on carbon—274
Baker, W. O. (see Mason, W. P.)—1074
Baker, W. R., J. V. Franck, and J. D. Gow. Linear accelerator oscillator and coupling system—535(A)
Baldwin, G. C. and G. S. Klaiber. X-ray yield curves of $\gamma-n$ reactions—1156, 1266(A)
Baldwin, J. H. (see Shepherd, M., Jr.)—1229(A)
Ballam, Joseph (see Turner, Clarence)—534(A)
Ballou, N. E. Considerations on the existence of element 61 in nature—630(L)
Balseiro, José A. Transformation theory applied to a radiation field—1346
Band, William and Lothar Meyer. Second sound and the heat conductivity in helium II—226
Baños, Alfredo, Jr., H. Gruen, and David S. Saxon. Propagation characteristics in a coaxial structure with two dielectrics—531(A)
Barajas, Alberto. On the hypotheses underlying any theory of gravitation—651(A)
Barbour, Ian (see Carr, Thomas D.)—1419
Bardeen, J. (see Pearson, G. L.)—1256(A)
—— **and C. H. Townes.** Calculation of nuclear quadrupole effects in molecules—97, 1204(L)
—— **and C. H. Townes.** Second order corrections to quadrupole effects in molecules—627(L), 1204(L)
Barnes, John R. (see Shapiro, Maurice M.)—1243(A)
Barnett, S. J. Magnetization and rotation—530(T)
Barrett, C. S. Low-temperature transformations in lithium and some of its alloys—1218(T)
Barschall, H. H. (see Bockelman, C. K.)—1218(A)
——, **C. K. Bockelman, and L. W. Seagondollar.** Total cross section of Fe, Ni, and Bi for fast neutrons—659
Beams, J. W. (see McQueen, J. H.)—260(L)

Beck, Paul A., M. L. Holzworth, and Hsun Hu. Instantaneous rates of grain growth—526(L)
Becker, G. E. and P. Kusch. On the hyperfine structure of gallium—531(A), 584
Beeck, O., J. W. Otvos, D. P. Stevenson, and C. D. Wagner. Catalytic isomerization of propane containing C^{13}—537(A)
Beers, R. F. Seismic travel paths at Bikini Atoll—646(T)
Beiduk, R. M. and E. J. Konopinski. Shaped field for 180° spectrograph—1229(A)
Belinfante, Frederick J. On different form for the interaction between Dirac's electron field (Ψ) and Maxwell's electromagnetic field (Φ, A)—641(L)
Bell, P. R. Use of anthracene as a scintillation counter—1405(L)
Benedict, D. L. Ballistic treatment of the traveling wave amplifier—1246(A)
Bennett, G. S. Multiple excitation of an elastic system—1270(A)
Benson, Bruce B. Proton-gamma-ray coincidence counting with cyclotron bombardment—7
Benton, Arnold and E. L. Kinsey. Effect of water of crystallization on absorption bands of neodymium bromate crystals—536(A)
Benzer, S. Photoelectric effects and their relation to rectification at metal-semiconductor contacts—1256(A)
Berlin, T. H. Note on the Milne problem for a sphere—437
Bernardini, G., B. N. Cacciapuoti, and R. Querzoli. Electronic component of cosmic rays in the low atmosphere. I. Theoretical—328; II. Experimental—335
Bernstein, R. B. and T. I. Taylor. Countercurrent gaseous exchange method for the enrichment of isotopes—1263(A)
Bernstein, S. Search for a resonance absorption of neutrons in graphite—956
—— (see Szilard, L.)—1307
Berry, Chester Ridlon. A study of lubricating wax coatings by electron diffraction—1117(L)
Beth, Eric. Theoretical considerations of ambient temperature measurements of the upper atmosphere—1218(T)
Beth, Richard A. and J. S. Krohmer. Rectangular analogs of Helmholz coils—94(T), 94(A)
Bethe, H. A. Electromagnetic level shift—1271(A)
—— (see Alpher, R. A.)—803(L)
—— (see Camac, M.)—191
Beyer, Robert T. (see Smith, Myron C.)—654(A)
Biehl, A. T., R. A. Montgomery, H. V. Neher, W. H. Pickering, and Wm. C. Roesch. New measurements on the variation with latitude of the cosmic-ray intensity at the vertical at high altitudes—533(A)
Birks, L. S. (see Friedman, H.)—186(L)
Blair, J. M. (see Sleator, William, Jr.)—1241(A)
Blatt, John M. On the interpretation of data on large air showers—1252(A)
Bleuler, E. (see Lark-Horovitz, K.)—1256(A)
—— **and H. L. Bradt.** Correlation between the states of polarization of the two quanta of annihilation radiation—1398(L)
Blewett, John P. Introduction accelerator for a proton synchrotron—1258(A)
—— (see Moore, Wm. H.)—1258(A)
Bloembergen, N., E. M. Purcell, and R. V. Pound. Relaxation effects in nuclear magnetic resonance absorption—679
Bloomenthal, S. Bridge values of β for non-ohmic disks—1231(A)
Blunt, Robert F. A.c. magneto-resistance of bismuth—654(A)
Bockelman, C. K. (see Barschall, H. H.)—659
——, **L. W. Seagondollar, and H. H. Barschall.** Total cross sections of Fe, Ni, and Bi for fast neutrons—1218(A)
Bohr, Aage. On the hyperfine structure of deuterium—1109(L)
Bonner, T. W. Resonances in the disintegration of fluorine by protons—646(T)
—— (see De Benedetti, S.)—1266(A)
—— (see Evans, J. E.)—649(A)
—— (see Harris, J. C.)—649(A)
—— **and J. E. Evans.** Resonances in the disintegration of fluorine and lithium by protons—666
——, **J. E. Evans, C. W. Malich, and J. R. Risser.** Study of the break-up of Li^8—884
Bottoms, A. M. (see Stephens, William E.)—1269(A)
Bowe, J. C., M. Goldhaber, R. D. Hill, W. E. Meyerhof, and O. Sala. Short lived metastable state in an "even-even" nucleus—1219(A)
Boyd, G. E. (see Motta, E. E.)—1470(L)
Bozorth, R. M. (see Williams, H. J.)— 1246(A)
Bradner, Hugh, Richard Crawford, Hayden Gordon, and John R. Woodyard. Physical design of the Berkeley linear accelerator—534(A)
Bradt, H. L. (see Bleuler, E.)—1398(L)
—— (see Seliger, H. H.)—1408(L)
—— **and Fred L. Mohler.** Mass spectrometer analysis of mercury made by neutron attachment to gold—925(L)
Brady, Edward L. and Martin Deutsch. Angular correlation of γ-rays—1266(A)
Bragg, J. K. Interaction of nuclear quadrupole moments with molecular rotation in asymmetric rotor molecules—1250(A)
Bratenahl, A., R. H. Hildebrand, and B. J. Moyer. Scattering of high energy neutrons—540(A)
Breckenridge, R. G. Low frequency dispersion in ionic crystals—1261(A)
Breit, G. Erratum: Does the electron have an intrinsic magnetic moment—1410(L)
——, **A. A. Broyles, and M. H. Hull.** Sensitivity of proton-proton scattering to potentials at different distances—870, 1242(A)
Bretscher, E., A. P. French, and F. G. P. Seidl. Low-energy yield of D (D, p) H^3 and the angular distribution of the emitted protons—815
Bridge, H., W. E. Hazen, and B. Rossi. Further results on burst production by penetrating cosmic-ray particles—179(L)
Bridgman, P. W. Recent experiments at high pressures—542(T)
Brode, R. B. Apparatus for mesotron mass measurements at high altitudes—533(A)
—— (see Moore, Donald C.)—532(A)

—— (see Retallack, J. G.)—532(A)
Brown, F. C. Temperature-pressure-conductivity relations in semiconductors—1257(A)
Brown, Harrison. New tables of absolute nuclear abundances—1242(A)
Brown, Sanborn C. Detection of ionizing radiation by ultra high frequency gas-discharge counters—1240(A)
—— (see Herlin, Melvin A.)—1245(A)
Brown, S. Leroy. Graphical solution of network impedances with a mechanical harmonic synthesizer—646(A)
—— (see Packard, Robert G.)—646(A)
—— (see Sharp, James M.)—646(A)
—— **and Mary Gowen Foulks.** Graphical evaluation of Jacobi polynomials—539(A)
—— **and James M. Sharp.** Use of mechanical synthesizer to determine characteristics of non-dissipative electric wave-filters—1267(A)
Broyles, A. A. (see Breit, G.)—870, 1242(A)
Buckingham, R. A. (see Massey, H. S. W.)—260(L)
Budó, A. and I. Kovács. On the fine structure of $^4\Sigma$ states of diatomic molecules—1120(L)
Buerger, M. J. Phase determination with the aid of implication theory—927(L)
Bull, H. B. Hydrolysis of proteins—1225(T)
Bundy, F. P. Measurements of rocket flame velocity by doppler shift—1267(A)
Burger, E. E. (see Hull, A. W.)—1228(A)
Burhop, E. H. S. (see Massey, H. S. W.)—1403(L)
Burkhart, L. E., W. F. Peed, and B. G. Saunders. X-ray spectrum of element 43—347
Burnight, T. R. Ionosphere experiments utilizing rockets—1218(T)
Burnstein, E., P. L. Smith, and B. Henvis. Photoelastic constants of cubic crystals—1262(A)
Burwell, J. T., Jr. Dependence of dry friction on the bulk properties of metals—542(T)

Cacciapuoti, B. N. (see Bernardini, G.)—328, 335
Cahn, A. (see Hughes, D. J.)—111
Calderon, F. E. Prieto. Captura de mesotrones negativos por protones—650(A)
Callen, Herbert B. Application of Onsager's reciprocal relations to thermoelectric, thermomagnetic and galvanomagnetic effects—1349
—— Existence of relations among the thermomagnetic and galvanomagnetic coefficients—1248(A)
Camac, M. and H. A. Bethe. Scattering of high energy neutrons by protons—191
Carr, Thomas D. (see Schein, Marcel)—1227(A)
——, **Marcel Schein, and Ian Barbour.** Cosmic-ray investigations on Mt. McKinley—1419
Carter, Robert L. and William V. Smith. Saturation effect in microwave absorption of ammonia—1053
Casmir, H. B. G. and D. Polder. Influence of retardation on the London-van der Waals forces—360
Cerrillo, Manuel. Inversion of a family of Laplace transforms associated to the propagation of electromagnetic waves in cylinders—647(A)
Chandrasekhar, S. On the exact solution to the problem of light scattering by a plane-parallel atmosphere in accordance with Rayleigh's laws—1233(A)
Chelius, L. G. and C. P. Keim. Electromagnetic separation of bromine and chlorine isotopes—813(L)
Ch'en, Shang-yi. Violet asymmetry of potassium resonance lines under high rubidium vapor pressures—1470(L)
Cherry, Walter L., Jr. and Robert Adler. Piezoelectric effect in polycrystalline barium titanate—1230(A)
Chew, Geoffrey F. Production of cosmic-ray mesons—1128(L)
—— **and M. L. Goldberger.** High energy neutron-proton scattering—1409(L)
Christy, R. F. (see Lauritsen, T.)—536(A)
—— (see O'Reilly, J.)—536(A)
Chupp, Warren W., Eugene Gardner, and T. B. Taylor. Energy distribution of protons from a target bombarded by 190-Mev deuterons—742
Claesson, Ingrid and Stig Claesson. Absorption analysis of high molecular substances—1221(A)
Claesson, Stig (see Claesson, Ingrid)—1221(A)
Clark, K. C. Absorption by N_2 and O_2 of solar wavelengths in the extreme ultraviolet—1250(A)
Clearman, Harold E., Jr. Some aspects of the solar spectrum between 3000A and 2300A—1218(T)
—— (see Hopfield, John J.)—876
Cleveland, Forrest F. (see Mitchell, Richard W.)—653(A)
Cobas, A. (see Korff, S. A.)—1010
Cobine, J. D. and C. Gallagher. Cathode phenomena in the electric arc—1239(T)
Cohen, Nathaniel L. (see Goldstein, Ladislas)—83(L)
Colby, M. Y. (see Hatfield, T. N.)—652 (A)
—— **and L. F. Connell, Jr.** X-ray determination of thermal expansion coefficients of crystals—653(A)
Collins, George B. and Rosalie C. Hoyt. Detection of beta-rays by scintillations—1259(A)
Conklin, L. and William Ogle. Further evidence for a $\gamma - p$ process in Be^9—648(A)
Connell, L. F., Jr. (see Colby, M. Y.)—653(A)
Cook, C. Sharp and Lawrence M. Langer. Beta- and gamma-radiation of antimony—1268(A)
—— **and Lawrence M. Langer.** Beta-spectra of Cu^{64} as a test of the Fermi theory—601, 1219(A)
—— **and Lawrence M. Langer.** Energies of the beta- and gamma-rays from antimony—1149
——, **Lawrence M. Langer, and H. Clay Price, Jr.** Beta-spectrum of S^{35} and the mass of the neutrino—1395(L)
Coor, T. and G. A. Snow. Ionization chamber bursts at high altitudes—1252(A)
Copeland, L. E. and M. Mooney. Thermodynamics of a strained elastomer. III. Thermal coefficient of modulus and the statistical theory of elasticity—1224(A)
Copeland, Paul L. (see DeLany, B. Pearson)—1232(A)
—— (see Eggenberger, Delbert N.)—1228(A)
Corben, H. C. Simplified notation in classical mechanics—1270(A)
Cork, Bruce (see Turner, Clarence)—534(A)
Cork, J. M., R. G. Shreffler, and C. M. Fowler. Note on gamma-radiation from europium—78(L)

—, **R. G. Shreffler, and C. M. Fowler.** Gamma-radiation from scandium, cerium, and terbium—1220(A)
Corson, E. M. Note on the Dirac character operators—57
Cowan, Robert D. Use of photo-tubes in the ultraviolet region by fluorescence—1234(A)
Cowart, William S. and M. L. Pool. Radioactive selenium 73 and 75—1223(A)
—, **M. L. Pool, D. A. McCown, and L. L. Woodward.** Artificially radioactive Se^{73} and Se^{75}—1454
Cox, E. F. Upper-atmosphere temperatures from remote sound measurements—1239(T)
Cranberg, L. and J. Halpern. Positron-electron ratios in Cu^{64}—1269(A)
— **and J. Halpern.** Ratio of positive to negatives in Cu^{64}—259(L)
Crawford, Richard (see Bradner, Hugh)—534(A)
Critchfield, Charles L. Phase-shift analysis of the scattering of photons by deuterons—1
Crittenden, E. C., Jr. Properties of thin ferromagnetic films—94(T)
Crossley, Walter (see Jacobs, Harold)—1244(A)
Crowe, M. O'L. and A. Walker. Chromatographic and fluorescence analysis for the isolation and purification for spectroscopic studies of pigments synthesized by micro-organisms—96(T)
Cullington, E. H. (see O'Day, M. D.)—543(A)
Cunningham, B. B. (see Hopkins, H. H., Jr.)—1406(L)
Curtis, B. R., Louis Rosen, and J. L. Fowler. Differential $D(d, n)$ He^3 cross section for 10-Mev deuterons—648(A)
Cyr, R. R. (see Schaaf, S. A.)—1253(A)

Dabbs, J. (see Hughes, D. J.)—111
Danforth, W. E. (see Ramsey, W. E.)—1246(A)
—, **E. L. Hudspeth, C. E. Mandeville, and C. P. Swann.** Compact electrostatic generator for the production of of positive ions—1413
— **and W. E. Ramsey.** Decay of thermionic emission of barium-strontium oxide cathodes during space-charge-limited operation—1244(A)
Danielson, G. C. Orientation of domains in polycrystalline $BaTiO_3$—1248(A)
Daunt, J. G., R. E. Probst, and H. L. Johnston. Experiments on the isotopic properties of helium in the liquid phase—1263(A)
—, **R. E. Probst, and H. L. Johnston.** New isotopic effect in liquid helium—638(L)
Davidson, W. L. (see Shull, C. G.)—262(L), 842
— **and I. G. Geib.** Effects of pile bombardment on uncured elastomers—1225(A)
Davis, Kenneth E. and Everett M. Hafner. Inelastic scattering of protons by light nuclei—1242(A)
— **and Everett M. Hafner.** Excited state of Be^9 by inelastic scattering of protons—1473(L)
Davis, L., Jr., B. T. Feld, C. W. Zabel, and J. R. Zacharias. Hyperfine structure and nuclear moments of chlorine—525(L)
Davis, Leverett, Jr. Stellar electromagnetic fields—536(A)
Davis, Luther, Jr. and Jerrold R. Zacharias. Hyperfine structure of K^{40}—1222(A)
Davis, R. (see Lark-Horovitz, K.)—1256(A)
Davison, Perry W. Proton groups from deuteron bombardment of sulfur—1241(A)
— (see Pollard, Ernest)—1241(A)
Davisson, J. W. Breakdown directions in lithium halide crystals—1196, 1261(A)
Dearnley, I. H., C. L. Oxley, and J. E. Perry, Jr. Proton-proton scattering at 7 Mev—1290
DeBenedetti, S. (see McGowan, F. K.) 1269(A)
—, **J. E. Francis, Jr., W. M. Preston, and T. W. Bonner.** Angular dependence of coincidences between fission neutrons—1266(A)
—, **F. K. McGowan and J. E. Francis, Jr.** Self-delayed coincidences with scintillation counters—1404(L)
de Bretteville, A., Jr. Anomalous effects in hysteresis loops of a single crystal of $BaTiO_3$—807(L)
deHoffman, F., B. T. Feld, and P. R. Stein. Delayed neutrons from U^{235} after short irradiation—636(L)
deLany, B. Pearson and Paul L. Copeland. Studies of the glow discharge in mercury vapor contained in cylindrical tubes with glass walls—1232(A)
de Launay, Jules and M. C. Steele. On temperature dependence of penetration depth in superconductors—1450
del Rosario, L. (see Allison, S. K.)—1224(A)
Dempster, A. J. Alpha-ray emitting isotope in samarium—1125(L)
— Mass-spectrographic identification of radioactive isotopes—1218(T)
Der Mateosian, E., M. Goldhaber, C. O. Muehlhause, and M. McKeown. Multiple nuclear isomerism—1219(A)
Dery, R. J. Development of a combustion wave in a flowing gas—1267(A)
de Toledo, Paulo Saraiva and Gleb Wataghin. On the relative abundances of nuclei in the universe—79(L)
Deutsch, Martin. High efficiency, high speed scintillation counters for beta- and gamma-rays—1240(A)
— (see Brady, Edward L.)—1266(A)
— (see Siegbahn, Kai)—410(L)
Deutsch, Murray L. (see Strandberg, M. W. P.)—188(L)
Dickey, Fred P. and Harald H. Nielsen. Infra-red spectrum of heavy water vapor—1164
Dickey, J. (see Apker, L.)—46
Dienes, G. J. and Frederick Seitz. Activation energy for the migration of paired vacancies in KCl—1260(A)
Dirac, P. A. M. Quantum theory of localizable dynamical systems—1092
Dixit, K. R. Superconductivity and Debye characteristic temperature—182(L)
Donoghue, J. J., E. Gerjuoy, and R. E. Vollrath. Measurement of tensile strengths of liquids by centrifuge method—538(A)
Doty, Paul and S. J. Stein. Depolarization of light scattered by macromolecular solutions—1221(A)
Dow, W. G. Measurement of atmospheric pressure between the altitudes of 65 and 110 km—1218(T)
DuBridge, L. A. Electron emission from metal surfaces: A review—1238(T)
Duckworth, H. E. Design of double-focusing mass spectrographs—543(A)

DuMond, Jesse W. M., David A. Lind, and Bernard B. Watson. Precision wave-length and energy measurement of gamma-rays from Au^{198} with a focusing quartz crystal spectrometer—1392(L)
Dunning, J. R. (see Havens, W. W., Jr.)—963
—— (see Melkonian, E.)—1399(L)
—— (see Rainwater, L. J.)—733
du Toit, S. J. Effect of the composition of the gas mixture in self-quenching Geiger-Mueller tubes on their plateau characteristics—1473(L)
Dyson, F. J. Electromagnetic level shift—1272(A)
—— Electromgnetic shift of energy levels—617
—— Interactions of nucleons with meson fields—929(L)

Eaton, V. E. The demonstration lecture—art or craft?—542(T)
Eckart, Carl. Thermodynamics of irreversible processes. IV. Theory of elasticity and anelasticity—373
—— Vortices and streams caused by sound waves—68
Edwards, H. D. (see Gilliam, O. R.)—635(L)
Edwards, James W., Rudolph Speiser, and Herrick L. Johnston. High temperature x-ray diffraction camera—1251(A)
Eggenberger, Delbert N. and Paul L. Copeland. Transit time of electrons between electrodes—1228(A)
Eggler, C. (see Hughes, D. J.)—809(L), 1248(A)
Eisenbud, L. Neutron-proton scattering formula—1407(L)
Eisenstein, Julian and Fritz Rohrlich. Neutron-proton scattering at 100 Mev—641(L), 1411(L)
Ekstein, H. Response of a linear system to an input with uniformly increasing frequency—1228(A)
—— **and S. Siegel.** Achromatization of Debye-Scherrer lines—1207(L)
Elder, F. K., Jr. Thermal diffusion with neon—1263(A)
Elder, F. R. (see Pollock, H. C.)—1238(T)
Eldridge, John A. Force between magnets in a medium—1229(A)
Eldridge, John E. (see Ferry, John D.)—1225(A)
Ellickson, R. T. (see Thompson, R. H.)—185(L)
Elliott, N. (see Hutchison, C. A.)—1229(A)
Elvey, C. T. Physics of the upper atmosphere—530(T)
Emrich, R. J. and F. B. Harrison. Measurement of velocity loss of shocks traveling in a shock tube—1255(A)
English, W. N. Water drop corona at reduced pressures—532(A)
—— (see Loeb, L. B.)—532(A)
Epstein, Saul T. Remarks on H. W. Lewis' paper "On the reactive terms in quantum electrodynamics"—177(L), 630(L)
——, **R. J. Finkelstein, and J. R. Oppenheimer.** Note on stimulated decay of negative mesons—1140
Estermann, I. Physics of rarefied gases—1239(T)
Evans, J. E. (see Bonner, T. W.)—666, 884
—— (see Harris, J. C.)—649(A)
—— (see Whaling, Ward)—648(A)
—— **and T. W. Bonner.** The 440-kev resonance of Li^7+H^1—649(A)

Fahy, E. F. and Marcel Schein. Burst production at an altitude of 11,200 feet—1227(A)
Fairbank, Henry A. (see Lane, C. T.)—256(L)
——, **C. T. Lane, L. T. Aldrich, and Alfred O. Nier.** Distribution of He^3 between liquid and vapor He^4—729, 1263(A)
Falkoff, David L. Polarization correlation of successive gamma-ray quanta—518(L)
—— (see Wang, C. S.)—1220(A)
—— **and G. E. Uhlenbeck.** Directional correlation between successive beta- and gamma-emissions—649(A)
Fano, U. and R. D. Huntoon. Theoretical analysis of the effect of imperfections in diffraction gratings—1233(A)
Farley, B. G. Pulse transformer technique for application to coincidence counting—1240(A)
Farwell, H. W. Willard Leslie Severinghause—642(L)
Fay, C. H. Bridged double T network—647(A)
Feenberg, E. and H. Primakoff. Interaction of cosmic-ray primaries with sunlight and starlight—449
Feld, B. T. (see Davis, L., Jr.)—525(L)
—— (see deHoffman, F.)—636(L)
—— (see Szilard, L.)—1307
Fermi, E. Interactions between elementary particles—1218(T)
Fernandez, Carlos Graef. Foundation of Birkhoff's theory of gravitation on particle mechanics—651(A)
Ferry, John D. (see Smith, Thor L.)—1233(A)
—— **and John E. Eldridge.** Studies of the melting points, rigidities, and optical activities of gelatin gels—1225(A)
Feshbach, H. (see Lax, M.)—1271(A)
—— (see Rarita, W.)—1272(A)
Fett, G. H. (see Shepherd, M., Jr.)—1229(A)
Fields, R. (see Russell, B.)—545
Fillmore, Franklin, Arthur Hudgins, and Morris Jeppson. Ion source equipment for Berkeley electrostatic generator—534(A)
Finck, J. L. Second law of thermodynamics from the standpoint of the equation of state—655(A)
—— Work, heat, and temperature concepts in thermodynamics and an examination of the temperature scale—1267(A)
Finkelstein, R. J. (see Epstein, S. T.)—1140
Fisher, E. Energy levels of sodium chloride—36
Flügge, S. and E. Hückel. Neutron-proton scattering formula—520(L)
Foley, H. M. Theory of the pressure broadening of spectral lines: A reply—259(L)
—— **and P. Kusch.** On the intrinsic moment of the electron—412(L)
—— (see Wu, Ta-You)—1117(L)
Forrester, A. Theodore (see Gerjuoy, Edward)—922(L)
Forstat, Harold (see Jesse, William P.)—926(L)
Foulks, Mary Gowen. Analytical solution of electrical networks for resonant and antiresonant frequencies—646(A)
—— (see Brown, S. Leroy)—539(A)
Fowler, C. M. (see Cork, J. M.)—78(L), 1220(A)
Fowler, J. L. (see Curtis, B. R.)—648(A)
Fowler, W. A. (see Lauritsen, T.)—636(L)
——, **C. C. Lauritsen, and T. Lauritsen.** Gamma-radiation from light nuclei under proton bombardment—181(L)
—— (see Thomas, R. G.)—536(A)

Fowles, G. R. Structure of the ionized helium line λ1640—639(L)
Francis, J. E., Jr. (see DeBenedetti, S.)—1404(L), 1266(A)
Franck, James. Memorial address in honor of Max Planck—1238(T)
Franck, J. V. (see Baker, W. R.)—535(A)
Frankel, Stanley. A beta-ray spectrometer design of quadratic resolution-solid angle relationship—804(L)
Frauenfelder, H., P. C. Gugelot, O. Huber, H. Medicus, P. Preiswerk, P. Scherrer, and R. Steffen. The 7-second Au^{197} isomer—1270(A)
Freier, George (see Bailey, Carl L.)—274
French, A. P. (see Bretscher, E.)—815
—— $D+D$ cross section at low energies—1474(L)
Fréon, André (see Maze, Roland)—418(L)
Fretter, W. B. Penetrating showers in lead—41
Friedland, S. S. and A. D. Krumbein. On the insensitive and recovery times of self-quenching counters—1227(A)
Friedlander, G. and M. L. Perlman. Relative yields of some x-ray induced nuclear reactions—1266(A)
Friedman, H., L. S. Birks, and H. P. Gauvin. Ultraviolet transmission of "counting" diamonds—186(L)
Furry, W. H. Theory of isotope separation in geological processes—1264(A)

Galginaitis, S. V. Electric fields in the cathode dark space of an abnormal hydrogen discharge—1245(A)
Gallagher, C. (see Cobine, J. D.)—1239(T)
Galt, J. K. Mechanical properties of NaCl, KBr, and KCl—1460
Gamow, G. (see Alpher, R. A.)—803(L)
Gardner, Eugene (see Chupp, Warren W.)—742
—— **and Vincent Peterson.** Stars in photographic emulsions. Part I. Experimental—533(A)
Garwin, R. L. (see Shrader, E. F.)—94(T)
Gast, P. F. Errata: Uncertainty principle and the yield of nuclei formed in fission—529(L)
Gauvin, H. P. (see Friedman, H.)—186(L)
Gehman, S. D. Creep, recovery, and permanent set for GR-S and Hevea—1224(A)
Geib, I. G. (see Davidson, W. L.)—1225(A)
George, M. S. (see Korff, Serge A.)—1133(L)
George, Waller. Further studies of the rupture of metal foils—1262(A)
—— **and George Irwin.** Rupture of metal foils under constand load—1230(A)
Gerjuoy, E. Refraction of waves from a point source into a medium of higher velocity—1442
—— Stability of gas bubbles in water—538(A)
—— (see Donoghue, J. J.)—538(A)
——, **A. Theodore Forrester, and William E. Parkins.** Signal to noise ratio in photoelectrically observed beats—922(L)
Germer, L. H. and F. E. Haworth. A low voltage discharge between very close electrodes—1121(L)
Geyer, Charles J., Jr., C. H. Reichardt, and George Halsey. Theory of commercial yarn testing—1224(A)
Ghoshal, S. N. Excitation curves of (α, n); $(\alpha, 2n)$; $(\alpha, 3n)$ reactions on silver—417(L)
Gibbs, Thomas E. and Arthur E. Lockenvitz. Comparison of the relative molecular stopping power of some hydrocarbon isomers for alpha-particles from Po—652(A)
Gill, P. S. and G. H. Vaze. Azimuthal effect of cosmic rays at Bombay (magnetic latitude 9.5°N)—1395(L)
Gilliam, O. R., H. D. Edwards, and Walter Gordy. Anomalies in the hyperfine structure of CH_3I and ICN—635(L)
Gilvarry, John J. Einstein's equivalence principle and the problem of blind navigation—1409(L)
Glatt, Leonard. Near infra-red dichroism involving aligned CH_2 groups—535(A)
—— Near infra-red dichroism involving hydrogen bonds—541(A)
Glendenin, L. E. (see Solomon, A. K.)—415(L)
Goble, A. T. Simple x-ray intensity meter—96(T)
Goeckermann, R. H. and I. Perlman. Characteristics of bismuth fission with high energy particles—1127(L)
Goeppert-Mayer, M. and R. G. Sachs. On the binding energy of the triton—185(L)
Goertzel, G. Resonance reactions involving Dirac-type incident particles—1463
Goldberg, Leo (see McMath, Robert R.)—1203(L)
Goldberger, Marvin L. Note on zero-zero transitions—1119(L)
—— (see Chew, G. F.)—1409(L)
Golden, S., T. Wentink, R. Hilliger, and M. W. P. Strandberg. Stark spectrum of H_2O—92(L)
Goldhaber, M. (see Bowe, J. C.)—1219(A)
—— (see Der Mateosian, E.)—1219(A)
—— **and Gertrude Scharff-Goldhaber.** Identification of beta-rays with atomic electrons—1472(L)
Goldstein, Ladislas and Nathaniel L. Cohen. Radiofrequency conductivity of gas discharge plasmas in the microwave region—83(L)
Goodman, Clark (see Tittle, C. W.)—1264(A)
Gordon, Hayden (see Bradner, Hugh)—534(A)
—— (see Turner, Clarence)—534(A)
—— (see Gilliam, O. R.)—635(L)
—— (see Simmons, James W.)—713
—— (see Smith, A. G.)—633(L)
Goss, N. P. Continuous casting of metals—94(T)
Gow, J. D. (see Baker, W. R.)—535(A)
Green, Alex E. S. Higher order field equations—519(L)
—— On infinities in generalized meson-field theory—26
Green, C. K. Ion orbit control for a proton synchrotron—1258(A)
Greenstein, Jesse P. Viscosity and streaming birefringence of nucleic acid—1225(A)
Gregg, E. C., Jr. Design of a 30-Mev betatron—94(T), 95(A)
Gregory, Christopher. Note on quantized space—806(L)
Greisen, Kenneth I. On heavy mesons and the cosmic rays far underground—521(L)
—— On neutral mesons in cosmic rays—521(L)
Greuling, E (see Levy, Paul W.)—83(L)
Griffin, L. R. A note on the paper "On the possibility of observing beat frequencies between lines in the visible spectrum"—922(L)

Grimm, G. (see Wu, C. S.)—1259(A)
Gross, S. T. Geometric disorder in linear polymers—1233(A)
Gruen, H. (see Baños, Alfredo, Jr.)—531(A)
Gugelot, P. C. (see Frauenfelder, H.)—1270(A)
Gutenberg, Benno. Microseisms and hurricanes—646(T)

Hadley, J., E. L. Kelly, C. E. Leith, E. Segrè, C. Wiegand, and H. F. York. Angular distribution of $n-p$ scattering with 90-Mev neutrons—1114(L)
——, **C. Leith, H. York, E. Kelly, and C. Wiegand.** 90-Mev neutron-proton scattering angular distribution—541(A)
Hafner, Everett M. (see Davis, Kenneth, E.)—1242(A), 1473(L)
Hagen, G. E. and D. H. Loughridge. Rebuilding of metal Geiger counting tubes—1131(L)
Hale, D. R. Artificial growing of quartz crystal—94 (T)
Hale, Donald H. Breakdown of gases in high frequency electrical fields—1046
Hall, D. (see Hughes, D. J.)—111
Hall, Harvey (see Halpern, Otto)—477
Hall, Leonard. Origin of ultrasonic absorption in water—775
Halpern, J. (see Cranberg, L.)—259(L), 1269(A)
Halpern, Otto. Small-angle diffraction in lattices—653(A)
—— **and Harvey Hall.** Ionization loss of energy of fast charged particles in gases and condensed bodies—477
Halpern, W. (see Sommers, H. S., Jr.)—1243(A)
Halsey, George (see Geyer, Charles, J., Jr.)—1224(A)
Hammermesh, Morton. Interconversion of ortho and paradeuterium due to the deuteron quadrupole moment—638(L)
Hamilton, J. G. Metabolism of the fission products and the heaviest elements—530(T)
Hammond, A., J. Michener, J. Koehler, E. Salkovitz. Damping capacity of anodized aluminum—1230(A)
Hansen, James W. Dust electrostatics—532(A)
Hansen, W. H. Linear electron accelerators—530(T)
Hanson, A. O. (see Klema, E. D.)—106
—— (see Laughlin, J. S.)—1223(A)
—— (see Skaggs, L. S.)—420(L)
Harris, J. C. (see Philips, G. C.)—649(A)
——, **T. W. Bonner, J. E. Evans, and G. C. Phillips.** Study of the narrow resonance at 1430 kev in the reaction $C^{12}+H^2$—649(A)
Harrison, F. B. (see Emrich, R. J.)—1255(A)
Hartman, L. M. Theory of high frequency gas discharges. III. High frequency breakdown—316
—— (see Margenau, H.)—309
Harvalik, Zaboj V. Electronic eyepiece for spectroscopy of near infra-red—1233(A)
Hatfield, T. N. (see Schmitt, Roland W.)—652(A)
—— **and M. Y. Colby.** Measurement of the relative molecular stopping power of gases for Po alphas—652(A)
Havens, R. J. Pressure and temperature of the upper atmosphere—1218(T)
Havens, W. W., Jr. (see Melkonian, E.)—1265(L)
—— (see Rainwater, L. J.)—733, 1265(A)
—— (see Wu, C. S.)—1259(A)
——, **L. J. Rainwater, and C. S. Wu.** Slow neutron velocity spectrometer studies: crystal interference and molecular binding effects at low energies—1265(A)
——, **L. J. Rainwater, C. S. Wu, and J. R. Dunning.** Slow neutron velocity spectrometer studies of Cu, Ni, Bi, Fe, Sn, and calcite—963
Hawkes, John B. and Robert W. Astheimer. Fluctuations in the refractivity of water—520(L)
Haworth, F. E. (see Germer, L. H.)—1121(L)
Hayden, Richard J. (see Inghram, Mark G.)—180(L)
Haynes, J. R. Behavior of photoelectrons in silver chloride crystals exhibited by colloidal silver produced at electron traps—646(T)
—— Production of high velocity mercury vapor jets in spark discharge—891
—— Use of the print-out effect in studying the motion of electrons in silver chloride crystals—542(T)
Haynes, S. K. Beta- and gamma-spectra of Ga^{72}—187(L), 1269(A)
Hazen, W. E. (see Bridge, H.)—179(L)
Heckrotte, W. and Peter Wolff. Excitation function of the reaction C^{12} $(n, 2n)$ C^{11} at high energies—265(L)
—— Excitation function of the reaction C^{12} (p, pn) C^{11} at high energies—264(L)
Hees, George (see Jacobs, Harold)—1244(A)
Heineman, M. On the resistance to motion through highly rarified gases—1254(A)
Heiss, J. H. (see Mason, W. P.)—1074
Helliwell, R. A. On the measurement of ionospheric virtual height at 100 kilocycles—77(L)
Helmholz, A. C. and J. M. Peterson. Excitation of Na^{24} and Na^{22} by deuteron and alpha-bombardment of Al—541(A)
Hemmendinger, Arthur. Disintegration of Be^8—806(L)
Henvis, B. (see Burstein, E.)—1262(A)
Hereford, Frank L. Polarization effects in the ionization loss of 1-Mev electrons in carbon—1123(L)
—— Specific primary ionization in hydrogen by a coincidence-counter method—1239(A)
Herlin, Melvin and Sanborn C. Brown. Measurements of breakdown in low pressure helium at microwave frequencies—1245(A)
Herring, Conyers. Some considerations concerning theories of the oxide cathode—1238(T)
Hershberger, W. D. Minimum detectable absorption in microwave spectroscopy and an analysis of the Stark modulation method—1249(A)
Herzfield, K. F. Friction and heat conduction in rarefied gases—1239(T)
Herzog, Gerhard. Industrial applications of radioactivity—646(T)
Hess, David C., Jr. (see Inghram, Mark G.)—180(L)
Hess, Victor Francis and J. Donald Roll, S. J. Identification of the surplus gamma-radiation from granite—912
—— **and J. Donald Roll, S. J.** New experiments concerning the surplus gamma-radiation from rocks—592, 1239(A)
Hessaby, M. Theoretical evidence for the existence of a light charged particle of mass greater than that of the electron—1128(L)

Hewitt, William H., Jr. Microwave resonance absorption in ferromagnetic semiconductors—1118(L)
Heydenburg, N. P., C. M. Hudson, D. R. Inglis, and W. D. Whitehead, Jr. Angular distribution from Li^7 (p, α) α—241
—— **and D. R. Inglis.** Angular distribution of the (d, p) reactions making two low states of O^{17}—230
Hicks, Bruce L. Perturbation of steady uniform flow by localized sources of heat—636(L)
Hildebrand, R. H. (see Bratenahl, A.)—540(A)
Hill, E. L. On the formal extension of Dirac's equation under continuous transformation groups—907
Hill, J. E. and W. E. Shoupp. Excitation function for proton-neutron reaction in lithium (Li^7 (p, n))—931
Hill, R. D. (see Bowe, J. C.)—1219(A)
—— **and W. E. Meyerhof.** Internal conversion electrons from 70-day Ir^{193}—812(L)
Hillger, R. (see Golden, S.)—92(L)
—— (see Strandberg, M. W. P.)—188(L)
—— (see Wentink, T., Jr.)—1249(A)
Hillier, James. Resolution in electron microscopes—1239(T)
Hincks, E. P. and B. Pontecorvo. On the stability of the neutral meson—1122(L)
—— **and B. Pontecorvo.** Search for gamma-radiation in the 2.2-microsecond meson decay process—257(L)
Hirschfelder, Joseph O. and Edward N. Adams, II. Penetration of gamma-radiation through thick layers. Part II. Plane geometry, iron, and lead—862
—— **and J. L. Magee.** Range-energy relations for protons in substances containing C, H, O, A, and Xe—207
——, **J. L. Magee, and M. H. Hull.** Penetration of gamma-radiation through thick layers. Part I. Plane geometry, Klein-Nishina scattering—851
Hodes, I. Metallic carbide lattice energies and the electron affinity of C_2^{--}—539(A)
Hodge, W. F. Method of studying the thermionic emission of oxide-coated cathodes in gaseous conduction devices—95(A)
—— Study of activation of oxide-coated cathodes—94(T)
Hoffmann, Banesh. Gravitational, electromagnetic, and vector meson fields and the similarity geometry—30, 531(A)
—— Trajectories of charged meson test particles in the similarity geometry—1042
Hofman-Bang, N. (see Andrews, R. D.)—1221(A)
Hofstadter, Robert. Remarks on diamond crystal counters—631(L)
Holmes, John R. Isotope shifts in some previously unexplored lines of nitrogen—539(A)
Holstein, T. Imprisonment of resonance radiation in gas discharges—1245(A)
Holton, Gerald J. Further report on high pressure experiments on supersonic propagation—1268(A)
—— Propagation of sound in liquids under high pressure—543(A)
Holtzman, R. H. (see Hughes, D. J.)—1271
Holzworth, M. L. (see Beck, Paul A.)—526(L)
Honig, Richard E. Ionization potentials of some hydrocarbon series—1266(A)
Hoover, J. I. (see Pomerance, H.)—1265(A)
——, **W. H. Jordan, C. D. Moak, L. A. Pardue, H. Pomerance, J. Strong, and E. O. Wollan.** Clinton pile oscillator—1259(A)
Hopfield, J. J. Characteristics of the sun's spectrum obtained from V-2 rockets—1218(T)
—— **and Harold E. Clearman, Jr.** Ultraviolet spectrum of the sun from V-2 rockets—876
Hopkins, H. H., Jr. and B. B. Cunningham. Nuclear reactions of arsenic with 190-Mev deuterons—1406(L)
Hornbostel, J. (see Snyder, Hartland, S.)—440
Horning, Wendell. Stars in photographic emulsions. Part II. Theoretical—533(A)
Horton, C. W. On the dielectric wave guide of circular cross section—647(A)
—— Low energy pair production—266(L)
Hoyt, Rosalie, C. (see Collins, George B.)—1259(A)
Hu, Hsun (see Beck, Paul A.)—526(L)
Hu, Tsi-Ming (see Massey, H. S. W.)—1403(L)
Hubbell, Harry H., Jr. Effect of apparatus geometry on small-angle x-ray scattering curves—1251(A)
—— (see Turkevich, John)—1250(A)
Hubbert, M. King. Field equations of the flow of liquids through porous solids—646(T)
Huber, O. (see Frauenfelder, H.)—1270(A)
——, **P. Marmier, H. Medicus, P. Preiswerk, and R. Steffen.** New isomer of element 43 (Tc) of very small excitation energy—1208(L)
——, **H. Medicus, P. Preiswerk, and R. Steffen.** Decay scheme of 62-day isotope of element 43 (Tc)—1211(L)
—— **and A. Stebler.** Disintegration energy of N^{14} (n, p) C^{14}—85(L)
—— **and A. Stebler.** (n, p) and (n, α) disintegrations of nitrogen by fast neutrons—89(L)
Hückel, E. (see Flügge, S.)—520(L)
Hudgins, Arthur (see Fillmore, Franklin)—534(A)
Hudson, C. M. (see Heydenburg, N. P.)—241
Hudspeth, E. L. (see Danforth, W. E.)—1413
—— (see Swann, C. P.)—648(A)
Hughes, D. J. Neutron polarization and ferromagnetism—1218(T)
——, **J. Dabbs, A. Cahn, and D. Hall.** Delayed neutrons from fission of U^{235}—111
—— **and C. Eggler.** Reaction He^3 (n, p) H^3 and the neutrino mass—809(L), 1242(A)
——, **J. R. Wallace, and R. H. Holtzman.** Neutron polarization—1277
Hughes, D. S., W. L. Pondrom, and G. B. Thurston. An electronic control device for the stabilization of a 10,000-oersted magnetic field—647(A)
Hull, A. W., E. E. Burger, and R. E. Turrentine. Cesium rectifier—1228(A)
Hull, G. F., Jr. and H. Saltzman. Some characteristics of bridges and arcs between separating metallic contacts—1262(A)
Hull, M. H. (see Breit, G.)—870, 1242(A)
—— (see Hirschfelder, J. O.)—851
Hulsizer, Robert L. Altitude variation of large pulses in ionization chambers—1252(A)

—— **and Bruno Rossi.** Search for electrons in the primary cosmic radiation—1402(L),
Huntington, H. B. Ultrasonics in war and in basic research —96(T)
Huntoon, R. D. (see Fano, U.)—1233(A)
Hutchison, C. A. and N. Elliott. Magnetic susceptibility of uranium oxalate—1229(A)
Hutchison, T. S. and James Reekie. Strain sensitivity of magnetic susceptibility—517(L)

Inghram, Mark G. (see Norris, L. D.)—350
——, **David C. Hess, Jr., and Richard J. Hayden.** Isotopic composition of samarium—180(L)
Inglis, D. R. (see Heydenburg, N. P.)—230, 241
Irwin, George (see George, Waller)—1230(A)

Jablónski, Alexander. On the phase shift approximation in the theory of pressure broadening of spectral lines—258(L)
Jacobs, Donald H. New type of dive angle indicator and servo accelerometer—539(A)
Jacobs, Harold, George Hees, and Walter Crossley. Thermionic emission of oxide-coated filaments—1244(A)
—— **and Armand P. LaRocque.** Study of cathode behavior in the inert gases as applied to minimum sparking potentials—1244(A)
Jacobs, James A., Philip R. Malmberg, and John S. Wahl. Gamma-radiation from the bombardment of fluorine, boron, and beryllium by protons—1130(L)
Jacobs, Louis E. and J. R. Platt. Experimental determination of Lorentz-Lorenz correction in ultraviolet absorption—1234(A)
Jacobsen, J. C. and O. Kofoed-Hansen. On the recoil of the nucleus in beta-decay of Kr^{85}—675
Jacobsohn, Boris A. and Roald K. Wangness. Shapes of nuclear induction signals—942
Jaffe, Hans. Electro-optic effects in crystals of the primary phosphate type—94(T), 95(A)
—— Volume electrostriction in barium titanate ceramics—1261(A)
—— Compressional piezoelectric coefficients of monoclinic crystals—1467(L)
Jastrow, Robert. On the Rydberg-Ritz formula in quantum mechanics—60
Jauch, J. M. and K. Watson. Erratum: Interaction with electrons—268(L)
Jen, C. K. Nuclear and molecular magnetic moments in microwave Zeeman spectra—1248(A)
Jenkins, F. A. Spin of C^{14}—639(L)
Jennings, B. (see Shoupp, W. E.)—421, 1223(A)
Jensen, Erling, N., L. Jackson Laslett, and William W. Pratt. Relative energies of the gamma-radiations from Co^{60} and Zn^{65}—529(L)
Jentschke, W. The crystal counter—77(L)
Jeppson, Morris (see Fillmore, Franklin)—534(A)
Jesse, William P. and Harold Forstat. Energies of alpha-particles from Pu^{238} and Pu^{239}—926(L)
Johnson, Gerald W. Ionization currents in divergent fields in hydrogen and in air—284
Johnson, J. B. Secondary electron emission from insulators —1238(T)
—— Secondary electron emission from targets of barium-strontium oxide—1058
Johnson, T. H. and R. P. Shutt. High pressure cloud chamber with intense magnetic field—1240(A)
Johnson, V. A. Calculation of the dielectric constant of tellurium—1231(A)
—— **and K. Lark-Horovitz.** Theory of the Nernst and Ettingshausen effects in semiconductors at high temperature—1257(A)
Johnston, H. L. (see Daunt, J. G.)—638(L), 1263(A)
—— (see Edwards, James W.)—1251(A)
Jones, Lawrence (see Seren, Leo)—1228(A)
Jones, W. (see Shoupp, W. E.)—421, 1223(A)
Jordan, W. H. (see Hoover, J. I.)—1259(A)
Juarez, Antonio Romero. Propagation of waves of finite amplitude—654(A)
Jukoff, David (see Stalder, J. R.)—1239(T)
Jurney, E. T. and Margaret R. Keck. Coincidence experiments on Sc^{46} and Au^{198}—1220(A)
—— **and Allan C. G. Mitchell.** Coincidence experiments in antimony 124—1153, 1269(A)
Justus, Katharine M. (see Yaffe, L.)—1400(L)

Kaplan, Joseph. Active nitrogen—494
—— Collisions of the second kind—530(A)
Kaplan, Nathan. (see Yagoda, Herman)—634(L)
Karplus, Robert. Frequency modulation in microwave spectroscopy—1027
—— Saturation effects in the microwave spectrum of ammonia—1120
—— **and Julian Schwinger.** Note on saturation in microwave spectroscopy—1020
Kê, T'ing-Sui. On the structure of grain boundaries in metals—267(L)
—— Stress-induced interstitial diffusion of carbon and oxygen atoms in tantalum—1231(A)
—— Viscous slip along grain boundaries and diffusion of zinc in alpha-brass—1235(A)
Keck, Margaret R. (see Jurney, E. T.)—1220(A)
Keim, C. P. (see Chelius, L. G.)—813(L)
Keller, Herbert B. and Joseph B. Keller. Reflection and transmission of electromagnetic waves by a spherical shell—1273(A)
—— **and Joseph B. Keller.** Reflection and transmission of sound by a spherical shell—1254(A)
Keller, Joseph. Solitary wave and periodic waves in shallow water—1254(A)
—— Reflection and transmission of electromagnetic waves by thin curved shells—1273(A)
—— (see Keller, Herbert B.)—1254(A), 1273(A)
Kelly, E. L. (see Hadley, J.)—541(A), 1114(L)
—— **and Clyde Wiegand.** Fission of elements from Pt to Bi by high energy neutrons—1135
Kenny, George S. and Sylvan Rubin. Proton scattering by beryllium—536(A)
Kern, Bernard D. (see Mitchell, Allan C. G.)—1220(A), 1424

—, **Daniel J. Zaffarano, and Allan C. G. Mitchell.** Beta- and gamma-radiation from antimony—1268(A)
—, **Daniel J. Zaffarano, and Allan C. G. Mitchell.** Disintegration of antimony (124)—1142
Kerr, J. W. (see Korff, Serge A.)—1133(L)
Ketelle, B. H. and W. C. Peacock. Neutron induced activities in erbium—1269(A)
Keuffel, J. W. Parallel-plate counters and the measurement of very small time intervals—531(A)
Keyes, Kenneth E. Calculation of the binding energy of self-trapped electrons in potassium chloride—1260(A)
Kikuchi, C. Symmetric energy-momentum tensor of Iwanenko-Sokolow field—1271(A)
Kinsey, E. L. (see Benton, Arnold)—536(A)
Kip, Arthur F. (see Arnold, Robert D.)—1247(A)
—— **and Robert D. Arnold.** Ferromagnetic resonance absorption in a single Fe crystal—1247(A)
Kirkham, Don. Two-dimensional potential problem with application to soil drainage—1228(A)
Kirkpatrick, Paul and A. V. Baez. X-ray optical images—1234(A)
—, **A. V. Baez, and Allen Newell.** Geometrical optics of grazing incidence reflectors—535(A)
Kittel, Charles. Domain theory and dependence of the coercive force of fine ferromagnetic powders on particle size—810(L)
—— On the theory of ferromagnetic resonance absorption —155
—— **and J. M. Luttinger.** Crystalline stark splitting and microwave resonance absorption in paramagnetic salts—162
Klaiber, G. S. (see Baldwin, G. C.)—1266(A)
Klema, E. D. and A. O. Hanson. Determination of the S^{32} (n, p) P^{32} cross section for neutrons having energies of 1.6 to 5.8 Mev—106
Klaiber, G. S. (see Baldwin, G. C.)—1156
Knipp, Julian K. Capture of electrons by ions—652(A)
Koehler, J. (see Hammond, A.)—1230(A)
Kofoed-Hansen, O. (see Jacobsen, J. C.)—675
Kohman, Truman P. Limits of beta-stability—16
—— Search for weak natural radioactives by the method of active daughter extraction—1223(A)
Kolstad, G. A., H. L. Schultz, and C. G. Montgomery. Microwave accelerator for production of high intensity gamma-rays—1258(A)
Konopinski, E. J. (see Beiduk, F. M.)—1229(A)
—— **and E. Teller.** Theoretical considerations concerning the $D+D$ reactions—822
Korff, S. A. and A. Cobas. Production of nucleons by the cosmic radiation II—1010
—, **M. S. George, and J. W. Kerr.** Energy distribution of neutrons in the atmosphere—1133(L)
Kotter, R. W. (see Weissler, G. L.)—538(A)
Kovács, I. (see Budó, A.)—1120(L)
Kovasznay, Leslie S. G. Spectrum of locally isotropic turbulence—1115(L)
Kramer, R. L. (see McMillen, J. Howard)—1255(A)
Kraushaar, W. L. On the lifetime of negative mesons—1408(L)
Kraybill, Henry L. Altitude dependence of high energy atmospheric showers—632(L)
—— High energy atmospheric showers—1226(A)
—— (see Schein, Marcel)—928(L)
—— (see Yngve, Victor H.)—1226(A)
Krisberg, N. L. (see Pool, M. L.)—1035
Krohmer, J. S. (see Beth, Richard A.)—94(T), 94(A)
Kruger, P. G. (see Laughlin, J. S.)—197, 649(A)
Krumbein, A. D. (see Friedland, S. S.)—1227(A)
Kundu, D. N. and M. L. Pool. (H^3, p) reaction in Rh and Co and probable evidence of the di-neutron—22
—— **and M. L. Pool.** Introduction of two neutrons into atomic nuclei under H^3 bombardment—1220(A)
Kupferberg, Kenneth M. Hard component of cosmic radiation as affected by the variation in air mass distribution with latitude—804(L)
Kurbotov, J. D. (see Yu, Fu-Chum)—1268(A)
Kurie, F. N. D. On the use of the Kurie-plot—1207(L)
—— (see Mather, K. B.)—1478(L)
Kusch, P. (see Becker, G. E.)—53(A), 584(A)
—— (see Foley, H. M.)—412(L)

Lachenbruch, S. H. Electron motion in deflecting field of magnetic dipole—1244(A)
—— (see Reverdin, D. L.)—1244(A)
Ladenburg, Rudolf, J. Winckler, and C. C. Van Voorhis. Interferometric studies of faster-than-sound phenomena. Part I. Gas flow around various objects in a free homogeneous supersonic air stream—1359
Lal, Lalji. New bands in the second negative or ultraviolet band system of O_2^+ molecule $(^2\pi_g, ^2\pi_g)$—255(L)
Lampi, E. E. (see Sleator, William, Jr.)—1241(A)
Lane, C. T. (see Fairbank, Henry A.)—729, 1263(A)
—, **Henry A. Fairbank, L. T. Aldrich, and Alfred O. Nier.** He^3 separation by a heat flux in liquid helium II—256(L)
Langer, Lawrence M. (see Cook, C. Sharp)—601, 1149, 1219(A), 1268(A), 1395(L)
Langmuir, R. V. (see Pollock, H. C.)—1238(T)
Lanzl, L. H. (see Skaggs, L. S.)—1223(A)
Lark-Horovitz, K. (see Johnson, V. A.)—1257(A)
—— (see Scanlon, Wayne)—1256(A)
—, **E. Bleuler, R. Davis, and D. Tendam.** Deuteron-bombarded semiconductors—1256(A)
LaRocque, Armand P. (see Jacobs, Harold)—1244(A)
Larsen, H. R. Geomagnetic surveying with a new electronic magnetometer—96(T)
Laslett, L. Jackson (see Jensen, Erling N.)—529(L)
Laughlin, J. S. (see Skaggs, L. S.)—420(L), 1223(A)
—— **and P. G. Kruger.** Scattering of neutrons of energy between 12.0 Mev and 13.0 Mev by protons—197, 649(A)
—, **L. S. Skaggs, A. O. Hanson, and J. J. Orlin.** Electrodisintegration of Cu^{63}, Ag^{107}, and Ag^{109}—1223(A)
Lauritsen, C. C. (see Fowler, W. A.)—181(L)
—— (see Lauritsen, T.)—636(L)
—— (see Thomas, R. G.)—536(A)
Lauritsen, T. (see Fowler, W. A.)—181(L)
—— **and R. F. Christy.** Investigation of a lens type β-ray spectrograph—536(A)

——, **W. A. Fowler, C. C. Lauritsen, and V. K. Rasmussen.** Excited states of B^{10}—636(L)
Lax, M. and H. Feshbach. On the method of virtual quanta—1271(A)
Lebacqz, J. V. Measurements of radio frequency resistance of a piece of columbium nitride through the transition—1476(L)
Leffler, J. M. (see Parkins, W. E.)—538(A)
Leighton, R. B. and Carl D. Anderson. Small radial cloud chamber for high altitude operation—650(A)
Leith, C. (see Hadley, J.)—541(A), 1114(L)
Leland, Wallace T. and Alfred O. Nier. Relative abundances of the zinc and cadmium isotopes—1206(L)
Leng, Herta R. Question of the existence of single magnetic poles—96(T)
Leverenz, H. W. General characteristics of phosphors—1238(T)
Levine, Harold and Julian Schwinger. On the radiation of sound from an unflanged circular pipe—383
Levy, M. G. (see Shamos, M. H.)—1396(L)
Levy, Paul W. and E. Greuling. Radiations from 2.70-day Au^{198}—83(L)
Lewis, H. W. On the analysis of extensive cosmic-ray shower data—1341
—— On the reactive terms in quantum electrodynamics—173
——, **J. R. Oppenheimer, and S. A. Wouthuysen.** Multiple production of mesons—127
Lewis, Margaret N. and Miriam Paul. C^{14} beta-ray spectrum—1269(A)
Libby, W. F. (see Naldrett, S. N.)—487, 929(L)
Liebermann, L. N. Bulk viscosity of liquids—537(A)
Liebowitz, Benjamin. Nature of low energy radiation—1274(A)
Lind, David A. (see DuMond, Jesse W. M.)—1392(L)
Lindner, M. and I. Perlman. Neutron deficient isotopes of rhodium and palladium—1202(L)
—— **and I. Perlman.** Neutron deficient isotopes of tellurium and antimony—1124(L)
Lindsay, R. B. Propagation of sound in air at low pressures—1239(T)
Livingston, M. Stanley. Design study for a 10-Bev proton synchroton—1258(A)
Lloyd, Paul E. (see Adams, Raymond V.)—650(A)
—— (see Rau, R. Ronald)—534(A)
——, **R. Ronald Rau, Carl D. Anderson, and Raymond V. Adams.** Electron showers at 30,000-feet elevation—650(A)
Lockenvitz, Arthur E. (see Gibbs, Thomas E.)—652(A)
—— (see Morris, Fred J.)—649(A)
—— (see Schmitt, Roland W.)—652(A)
Lockwood, J. A. (see Schultz, H. L.)—1259(A)
Loeb, Leonard B. Threshold for the positive pre-onset burst pulse corona and the production of ionizing photons in air at atmospheric pressure—798
—— (see Miller, Charles G.)—84(L)
—— **and W. N. English.** Positive and negative point to plane corona—532(A)
Lofgren, E. J. (see Richardson, J. Reginald)—424
London, F. and O. K. Rice. On solutions of He^3 in He^4—1188
Longini, R. L. Effect of atmosphere on the outgassing and evaporation rates of antimony—1231(A)
Lonsdale, Kathleen. Remarks on diamond crystal counters—1467(L)
Lord, Jere J. (see Schein, Marcel)—189(L)
—— **and Marcel Schein.** Production of mesotrons in cosmic-ray stars in the stratosphere—1252(A)
Loughridge, D. H. (see Hagen, G. E.)—1131(L)
Luttinger, J. M. (see Kittel, C.)—162
Lyons, W. James. Statistical theory of the elementary process of plastic deformation—413(L)
—— **and Irven B. Prettyman.** Method for the absolute measurement of dynamic properties of linear structures at sonic frequencies—1232(A)

Mack, J. E. and N. Austern. Fine structure of He II λ4686—1233(A)
MacKenzie, K. R. Cyclotron frequency modulation—540(A)
Madansky, L. and R. W. Pidd. Characteristics of the parallel plate counter—1215(L)
Magee, J. L. (see Hirschfelder, J. O.)—207, 852
Malich, C. W. (see Bonner, T. W.)—884
—— **and J. R. Risser.** Gamma-rays and neutrons from beryllium bombarded by deuterons—648(A)
Malmberg, Philip R. (see Jacobs, James A.)—1130(L)
Man, Edward M., Jr. (see Robinson, Howard A.)—1222(A)
Mandeville, C. E. (see Danforth, W. E.)—1413
—— (see Scherb, M. V.)—418(L), 655(A), 1268(A) 1401(L)
—— (see Swann, C. P.)—648(A)
—— **and Morris V. Scherb.** Beta-rays of antimony (122)—656(A)
—— **and Morris V. Scherb.** Coincidence study of gold (198)—634(L)
—— **and Morris V. Scherb.** On the resolving time and genuine coincidence loss for Geiger-Mueller counters—90(L), 639(L)
—— **and Morris V. Scherb.** Properties of radioactive tantalum (182)—656(A)
—— **and Morris V. Scherb.** Radiations from molybdenum (99) and technetium (99)—847, 1270(A)
—— **and Morris V. Scherb.** Radiations from scandium (46) and titanium (51)—141
—— **and Morris V. Scherb.** Radiations from tantalum (182), antimony (122), and indium (116)—340
—— **and Morris V. Scherb.** 72-day isomer of titanium (51)—654(A)
—— **and Morris V. Scherb.** Some characteristics of scandium (46)—648(A)
—— **and Morris V. Scherb.** Study of the radiations from iridium (194), iridium (192), lanthanum (140), antimony (124), and zirconium (95)—1434
Mann, Alfred K. Thermal diffusion constant of nitrogen—412(L)
Mapother, Dillon and Robert Maurer. Self-diffusion of sodium in sodium chloride—1260(A)

March, A. Decay of negative mesons in light elements—1205(L)
Margenau, H. Theory of high frequency gas discharges. I. Methods for calculating electron distribution functions—297
—— Theory of high frequency gas discharges. IV. Note on the similarity principle—326
—— **and L. M. Hartman.** Theory of high frequency gas discharges. II. Harmonic components of the distribution function—309
Mariani, Jean. On magnetism of celestial bodies—78(L)
Markham, J. J. and F. Seitz. Binding energy for a self-trapped electron in NaCl—1260(A)
Marmier, P. (see Huber, O.)—1208(L)
Marney, M. C. (see Shull, C. G.)—1265(A)
—— (see Wollan, E. O.)—527(L)
Marshak, R. E. On the neutral meson—1226(A)
Marton, L. Electron optical "Schlieren" effect—1244(A)
—— Ferromagnetic domain observation—1475(L)
—— (see Reverdin, D. L.)—1244(A)
Mason, W. P. Piezoelectric or electrostrictive effect in barium titanate ceramics—1398(L)
——, **W. O. Baker, H. J. McSkimin, and J. H. Heiss.** Mechanical properties of long chain molecule liquids at ultrasonic frequencies—1074
——, **H. P. McSkimin, and W. Shockley.** Ultrasonic observation of twinning in tin—1213(L)
Massey, H. S. W. and R. A. Buckingham. Scattering of protons by deuterons—260(L)
——, **E. H. S. Burhop, and Tsi-Ming Hu.** Effect of non-central forces on the collisions of high energy neutrons with protons—1403(L)
Mather, K. B. and F. N. D. Kurie. Emission of alpha-particles from different faces of a radioactive crystal—1474(L)
Matsen, F. A. Molecular orbitals for methane and ethane—653(A)
—— (see Robertson, W. W.)—652(A)
Matthias, B. T. Growth of barium titanate crystals—808(L)
—— **and A. von Hippel.** Domain structure and electric response of barium titanate single crystals—1261(A), 1378
—— **and A. von Hippel.** Structure, electrical and optical properties of barium titanate—268(L)
Mauer, P. B. and H. L. Reynolds. Protective facings on Eastman emulsions—1131(L)
Maurer, Robert (see Mapother, Dillon)—1260(A)
Maze, Roland, André Fréon, and Pierre Auger. High altitude measurements on extensive showers—418(L)
McCarthy, R. L. (see Schultz, H. L.)—1259(A)
McConaghie, Virginia M. and Harald H. Nielsen. Anomalies in the infra-red spectra of phosphine and arsine—1250(A)
McCown, D. A. (see Cowart, W. S.)—1454
McEwen, George F. Dynamics of large horizontal eddies (axis vertical) in the ocean off southern California—538(A)
McGowan, F. K. (see DeBenedetti, S.)—1404(L)
—— **and S. DeBenedetti.** Short-lived isomers in Tm^{169} and Tm^{171}—1269(A)
McKay, K. G. Conductivity induced in insulators by electron bombardment—1238(T)
McKeown, M. (see Der Mateosian, E.)—1219(A)
McLachlan, Dan, Jr. Method for incorporating into the Fourier equations for x-ray studies previously established structural information—539(A)
McMath, Robert R., Orren C. Mohler, and Leo Goldberg. Telluric bands of methane in the Fraunhofer spectrum—1203(L)
McMillan, Edwin M. and Richard D. Miller. Absolute cross section for the reaction C^{12} (p, pn) C^{11} at high energy—80(L)
—— **and Herbert F. York.** Cross section for the reaction C^{12} $(n, 2n)$ C^{11} at 90 Mev—262(L)
McMillen, J. Howard and R. L. Kramer. Spark shadowgrams of spheres at supersonic speeds in water—1255(A)
McNally, J. Rand, Jr. Ratio of g values of the $^2P^0_{\frac{1}{2}}$ and the $^2S_{\frac{1}{2}}$ states in ionized calcium—1130(L)
McQueen, J. H., J. W. Beams, and L. B. Snoddy. Light scattering in supersonic streams—260(L)
McReynolds, Andrew W. Anomalous plastic deformation in brass and aluminum—1262(A)
McSkimin, H. J. (see Mason, W. P.)—1074, 1213(L)
Meaker, C. L., C. S. Wu, and L. J. Rainwater. Characteristics of Geiger counters filled with lead tetramethyl vapor—1240(A)
Medicus, H. (see Frauenfelder, H.)—1270(A)
—— (see Huber, O.)—1208(L), 1211(L)
Meister, Arnold G. Force constants and assignments of the Raman frequencies of methylbromoacetylene and methyliodoacetylene—1234(A)
Melkonian, Edward. Slow neutron cross sections of oxygen, nitrogen, argon, and the proton in methane, ethane, n-butane, ethylene, and 1,3 butadiene, as measured with a neutron beam spectrometer—1265(A)
——, **L. J. Rainwater, W. W. Havens, Jr., and J. R. Dunning.** Slow neutron spectrometer studies of oxygen, nitrogen, and argon—1399(L)
Melvin, M. Avramy. Theory of the damped non-linear oscillator—1274(A)
Merritt, F. R. (see Townes, C. H.)—1334, 1249(A)
—— **and C. H. Townes.** Stark effect in high frequency fields—1249(A)
Meyer, Herbert M. Two ways of aging—1263(A)
Meyer, Lothar (see Band, William)—226
Meyerhof, W. E. (see Bowe, J. C.)—1219(A)
—— (see Hill, R. D.)—812(L)
Michener, J. (see Hammond, A.)—1230(A)
Migeotte, Marcel V. Spectroscopic evidence of methane in the earth's atmosphere—519(L)
Miller, B. L. and J. M. Wolf. On the acceleration of electrons by cylindrical cavities in TM_{01n} modes—657(A)
Miller, P. H., Jr. (see Smith, A. H.)—1256(A)
Miller, Richard D. (see McMillan, Edwin M.)—80(L)
Miley, H. A. Sky brightness—1218(T)
Miller, Charles G. and Leonard B. Loeb. Spark breakdown at atmospheric pressure and above in relation to Paschen's law—84(L)

Miller, Sherman. Dedication of the South Physics Laboratory—96(T)
Miller, William. Frequency spectrum of noise in crystal rectifiers—1257(A)
Millett, Walter E. Focusing in crossed fields of charged particles at relativistic energies—1259(A)
Mitchell, Allan C. G. (see Jurney, E. T.)—1269(A), 1153
—— (see Kern, Bernard D.)—1142, 1268(A)
——, **D. J. Zaffarano and B. D. Kern.** Beta- and gamma-rays of Ga^{72}—1220(A), 1424
Mitchell, Richard W. and Forrest F. Cleveland. Raman spectrum of hexamethylethane—653(A)
Moak, C. D. (see Hoover, J. I.)—1259(A)
Mohler, Fred L. (see Bradt, Paul)—925(L)
Mohler, Orren C. (see McMath, Robert R.)—1203(L)
Montgomery, C. G. (see Kolstad, G. A.)—1258(A)
Montgomery, R. A. (see Biehl, A. T.)—533(A)
Moon, Robert J. Inorganic crystals for the detection of high energy particles and quanta—1210(L)
Mooney, M. Thermodynamics of a strained elastomer. I. General analysis—1224(A)
—— (see Copeland, L. E.)—1224(A)
Mooney, R. C. L. Crystal structure of element 43, technetium—653(A)
Moore, Donald C. and Robert B. Brode. Low energy mesotrons at high altitudes—532(A)
Moore, Wm. H. and John P. Blewett. Magnetic circuit for a proton synchrotron—1258(A)
Morris, Fred, J. and Arthur E. Lockenvitz. Study of the distribution of polonium on thin silver and bismuth films—649(A)
Morris, Peter A., W. F. G. Swann, and H. C. Taylor. Sea level latitude effect of cosmic radiation—1226(A)
Morse, P. M. Plans for the Brookhaven National Laboratory—1238(T)
Morton, G. A. (see Shull, C. G.)—262(L), 842
Moszkowski, S. and R. G. Sachs. Deuteron problem with Gaussian potentials—184(L)
Motta, E. E. and G. E. Boyd. Production of new Tc activities from separated Mo isotopes—1470(L)
Mouzon, J. C. Simple temperature controller—1267(A)
Moyer, B. J. (see Bratenahl, A.)—540(A)
Mrozowski, S. On the structure of ther mercury band λ2540—1233(A)
Muehlhause, C. O. (see Der Mateosian, E.)—1219(A)
Mulliken, R. S. (see Roothaan, C. C. J.)—1234(A)
Munch, Guido. Model solar atmospheres—651(A)
Munk, M. M. On supersonic flow patterns—1254(A)

Nafe, John E. and Edward B. Nelson. Hyperfine structure of hydrogen and deuterium—718, 1243(A)
Naldrett, S. N. and W. F. Libby. Natural radioactivity of rhenium—487, 929(L)
Neher, H. V. Some discharge characteristics of Geiger-Mueller counters—533(A)
Neher, H. V. (see Biehl, A. T.)—533(A)
Nelson, Edward B. (see Nafe, John E.)—718, 1243(A)
Nemenyi, P. and R. Prim. On methods of deriving three-dimensional gas flow patterns from plane flows—1255(A)
Nereson, Norris. Disintegration of positive and negative mesotrons in different absorbers—565
Nesbitt, E. A. and H. J. Williams. Measurement of longitudinal magnetostriction with automatic recording—1246(A)
Newell, Allen (see Kirkpatrick, Paul)—535(A)
Newton, R. R. Ejection of electrons by ions at high fields—1122(L)
—— Transients in Townsend discharges—570
Nicholson, Seth B. (see Wulf, Oliver R.)—1204(L)
Nielsen, Harald H. (see Dickey, Fred P.)—1164
—— (see McConaghie, Virginia M.)—1250(A)
Nier, Alfred O. (see Fairbank, Henry A.)—729, 1263(A)
—— (see Lane, C. T.)—256(L)
—— (see Leland, Wallace T.)—1206(L)
Nierenberg, W. A., I. I. Rabi, and M. Slotnick. Note on the Stark effect in diatomic molecules—1430
Nilsson, S. Bertil. On the calculation of self-energies in quantum theory by analytic continuation—902
Nolle, A. W. Dynamic mechanical properties of rubber-like material—1232(A)
Norris, L. D. and M. G. Inghram. Half-life of carbon 14—350
—— **and Arthur H. Snell.** Radioactive carbon of high specific activity—254(L)
Norton, F. J. Model to illustrate action of mass spectrograph—96(T)
Nottingham, W. B. The M.I.T. electron-physics programme: past, present, and near future—1238(T)
Novick, A. (see Anderson, H. L.)—919(L)

O'Day, Marcus. Use of a beacon to measure ion density in the *E*-layer—1218(T)
—— **and E. H. Cullington.** High frequency corona applications—543(A)
Ogle, William (see Conklin, Richard L.)—648(A)
Opatowski, I. Generalization of a theorem by Larmor in hydrodynamics—1253(A)
Oppenheimer, Frank (see Panofsky, Wolfgang K. H.)—535(A)
Oppenheimer, J. R. (see Epstein, S. T.)—1140
—— (see Lewis, H. W.)—127
Ore, Aadne. Molecular systems containing a positron—1272(A)
—— Note on the stability of systems containing a light positive particle—1313
O'Reilly, J. and R. F. Christy. Rates of the carbon reactions in the sun—536(A)
Orlin, J. J. (see Laughlin, J. S.)—1223(A)
—— (see Skaggs, L. S.)—420(L)
Ossofsky, Eli. Constant temperature operation of the hot wire anemometer at high frequencies—410(L)
Otvos, John W. Ionization by C^{14} radiation in the ionization chamber—537(A)
—— (see Beeck, O.)—537(A)
Ovrebo, Paul J. Periodic variation of ground level count of cosmic-ray air showers—1227(A)
Oxley, C. L. (see Dearnley, I. H.)—1290

Packard, Robert G. and S. Leroy Brown. Graphical solution for the real and complex roots of polynomials with a mechanical harmonic synthesizer—646(A)
Pake, G. E. Fine structure of a proton paramagnetic resonance line in crystalline hydrates—800(A)
Panofsky, Wolfgang K. H., Chaim Richman, and Frank Oppenheimer. Control of the field distribution in the linear accelerator cavity—535(A)
Papapetrou, A. Question of non-singular solutions in the generalized theory of gravitation—1105
Pardue, L. A. (see Hoover, J. I.)—1259(A)
Parker, W. L. Some physical properties of infra-red phosphors—1239(A)
Parkins, William E. (see Gerjuoy, Edward)—922(L)
—— **and J. M. Leffler.** Use of plasma sheaths as variable capacitances—538(A)
Parsegian, V. L., L. V. Titone, and C. W. van der Merwe. Cross-section measurements using fast continuous energy neutrons—1265(A)
Parzen, Philip. Approximate small signal theory of electron beam wave interaction in a wave guide with a filament beam—1268(A)
Pasternack, Simon (see Snyder, Hartland S.)—440
Paul, Miriam (see Lewis, Margaret N.)—1269(A)
Peacock, W. C. (see Ketelle, B. H.)—1268(A)
Pearson, Angus. Temperature coefficient of resistance of sodium-ammonia solutions—655(A)
Pearson, G. L. and J. Bardeen. Electrical properties of pure silicon and silicon alloys—1256(A)
Peck, R. A., Jr. The Al (αn) and Si (dn) neutron spectra—1264(A)
—— Photographic study of the neutron spectra from Al (αn) and Si (dn)—947
Peed, W. F. (see Burkhart, L. E.)—347
Pekeris, C. L. Propagation of a pulse in the atmosphere. Part II—145
Pellam, John R. Wave transmission and reflection phenomena in liquid helium II—608
Pepinsky, R. and H. I. West, Jr. Microphotometer for x-ray diffraction diagrams—1235(A)
Perl, W. Relation between the limiting line phenomenon and the Karman transonic similarity theory—1254(A)
Perlman, I. (see Goeckermann, R. H.)—1127(L)
—— (see Lindner, M.)—1124(L), 1202(L)
—— (see Templeton, D. H.)—1211(L)
Perlman, M. L. (see Friedlander, G.)—1266(A)
Perlow, G. J. Cosmic-ray studies from V-2's—1218(T)
Perry, J. E., Jr. (see Dearnley, I. H.)—1290
Persico, E. Optimum conditions for a beta-ray solenoid spectrometer—1475(L)
Peters, Bernard (see Richardson, J. Reginald)—424
Peterson, J. M. (see Helmholz, A. C.)—541(A)
Peterson, Vincent (see Gardner, Eugene)—533(A)
Philips, G. C. (see Harris, J. C.)—649(A)
—— **and J. C. Harris.** Scattering of fast neutrons by mercury—649(A)
Piccioni, O. On the capture of negative mesons—411(L)
Pickering, W. H. (see Biehl, A. T.)—533(A)
Pidd, R. W. (see Madansky, L.)—1215(L)
Pippard, A. B., G. E. H. Reuter, and E. H. Sondheimer. Conductivity of metals at microwave frequencies—920(L)
Platt, J. R. (see Jacobs, Lois E.)—1234(A)
Polder, D. On the phenomenology of ferromagnetic resonance—1120(L)
—— On the quantum theory of ferromagnetic resonance—1116(L)
—— (see Casimir, H. B. G.)—360
Pollard, Ernest and Perry W. Davison. Energy levels of A^{41}—1241(A)
Pollard, W. G. and R. D. Present. On gaseous self-diffusion in long capillary tubes—762
Pollock, H. C., F. R. Elder, and R. V. Langmuir. Visible radiation from accelerated electrons in 70-Mev synchrotrons—1238(T)
Pomerance, H. and J. I. Hoover. Thermal neutron absorption cross sections of separated isotopes—1265(A)
—— (see Hoover, J. I.)—1259(A)
Pomerantz, Martin A. Absorption in carbon and lead of cosmic-ray particles at very high altitudes—1253(A)
—— Properties of cosmic-rays at very high altitudes—651(A)
—— (see Witmer, Enos E.)—651(A), 1274(A)
Pondrom, W. L. (see Hughes, D. S.)—647(A)
—— **and W. W. Robertson.** Electronic intensity regulator for a hydrogen discharge tube—652(A)
Pontecorvo, B. (see Hincks, E. P.)—257(L), 1122(L)
Pool, M. L. (see Cowart, W. S.)—1223(A), 1454
—— (see Kundu, D. N.)—22, 1220(A)
—— **and N. L. Krisberg.** Radioactive cerium and praseodymium—1035
Porter, R. W. Rocket propulsion (motion pictures of V-2 launching)—96(T)
Posin, D. Q. The microwave spark—496, 1118(L)
—— Results and semitheoretical calculations in micro wave breakdown—1245(A)
Potapenko, G. and D. Wheeler. Anomalous dispersion and absorption of ultra-short electromagnetic waves in some fatty acids—530(A)
Poulter, T. C. Seismic measurements in the antarctic—646(T)
Pound, R. V. Effects of nuclear electric quadrupole moments in nuclear paramagnetic resonance absorption—1247(A)
—— Magnetic moments of Cu^{63} and Cu^{65}—523(L)
—— On the nuclear moments of I^{127}, Ga^{69}, Ga^{71}, and P^{31}—1112(L)
—— (see Bloembergen, N.)—679
Powell, Wilson M. Recoil protons in the neutron beam of the 184-inch cyclotron—540(A)
Power, A. D. Thermal emittance of various materials used as anodes in radio receiving tubes—1246(A)
Pratt, William W. (see Jensen, Erling N.)—529(L)
Preiswerk, P. (see Frauenfelder, H.)—1270(A)
—— (see Huber, O.)—1208(L), 1211(L)
Present, R. D. (see Pollard, W. G.)—762
Preston, W. M. (see DeBenedetti, S.)—1266(A)
Prettyman, Irven B. (see Lyons, W. James)—1232(A)
Price, H. Clay (see Cook, C. Sharp)—1395(L)

Price, William J. Ultrasonic reflections by domains in rochelle salt single crystals—1132(L)
Prim, R. C. Extension of Crocco's theorems to flows having non-uniform stagnation enthalpy—186(L), 1255(A)
—— (see Nemenyi, P.)—1255(A)
Primakoff, H. (see Feenberg, E.)—449
Probst, R. E. (see Daunt, J. G.)—638(L), 1263(A)
Pruett, John R. H^3 and the mass of the neutrino—1219(A)
Purcell, E. M. (see Bloembergen, N.)—679

Quercia, I. F., B. Rispoli, and S. Sciuti. On the positive excess of the penetrating component at 17,000 feet—516(L)
Querzoli, R. (see Bernardini, G.)—328, 335

Rabi, I. I. (see Nierenberg, W. A.)—1430
Radkowsky, Alvin. Temperature dependence of electron energy levels in solids—749
Rainwater, L. J. (see Havens, W. W., Jr.)—963, 1265(A)
—— (see Meaker, C. L.)—1240(A)
—— (see Melkonian, E.)—1399(L)
——, **W. W. Havens, Jr., J. R. Dunning, and C. S. Wu.** Slow neutron velocity spectrometer studies of H, D, F, Mg, S, Si, and quartz—733
——, **W. W. Havens, Jr., and C. S. Wu.** Slow neutron velocity spectrometer studies of Fe, Ni, and Cu—1265(A)
Rall, Wilfrid. Packing fraction of zirconium—1222(A)
Ramsey, Norman F. Effect of large quadrupole interactions on nuclear radiofrequency spectra at twice larmor frequency—1243(A)
Ramsey, W. E. (see Danforth, W. E.)—1244(A)
—— **and W. E. Danforth.** Types of sparking in high vacuum diodes—1246(A)
Randall, Duncan (see Antonoff, George)—1230(A)
Randolph, M. L. Balancing of sedimentation by electrophoresis in the ultracentrifuge—654(A)
Rarita, W. and H. Feshbach. Tensor forces and the binding energy of the triton—1272(A)
Rasmussen, V. K. (see Lauritsen, T.)—636(L)
Rau, R. Ronald (see Adams, Raymond V.)—650(A)
—— (see Lloyd, Paul E.)—650(A)
——, **Carl D. Anderson, Raymond V. Adams, and Paul E. Lloyd.** Heavily-ionizing cosmic-ray particles at 30,000 feet altitude—534(A)
Raymond, Richard C. and Wayne Webb. Antenna current distribution—1248(A)
Reekie, James (see Hutchison, T. S.)—517(L)
Reichardt, C. H. (see Geyer, Charles J., Jr.)—1224(A)
Retallack, J. G. Mesotron decay—921(L)
—— **and R. B. Brode.** Mass of cosmic-ray mesotrons—532(A)
Reuter, G. E. H. (see Pippard, A. B.)—920(L)
Reverdin, D. L., L. Marton, and S. H. Lachenbruch. Application of the electron optical "Schlieren" effect—1244(A)
Reynolds, H. L. (see Mauer, P. B.)—1131(L)
Reynolds, J. M. (see Webber, Robert T.)—640(L), 1264(A)
Rice, O. K. On the λ-transition of liquid helium—1419
—— (see London, F.)—1188
Rice, P. J. (see Schultz, H. L.)—1259(A)
Richards, Paul I. On the Hamiltonian for a particle in an electromagnetic field—254(L)
—— **and Hartland S. Snyder.** Saturation and power broadening of microwave resonance lines—269(L)
—— (see Snyder, Hartland S.)—1178
Richardson, J. M. On the anomalous dielectric behavior of $BaTiO_3$ near 0°K—1261(A)
Richardson, J. Reginald, Byron T. Wright, E. J. Lofgren, and Bernard Peters. Development of the frequency modulated cyclotron—424
Richman, Chaim (see Panofsky, Wolfgang K. H.)—535(A)
Richter, Harold (see Sugerman, Nathan)—1411(L)
Ricker, Norman. Form of the seismic disturbance due to an explosion—654(A)
Ring, Harold (see Smith, A. G.)—633(L)
Rispoli, B. (see Quercia, I. F.)—516(L)
Risser, J. R. (see Bonner, T. W.)—884
—— (see Malich, C. W.)—648(A)
Rittner, Edmund S. Use of photoconductive semiconductors as amplifiers—1212(L)
Roberts, Arthur. Rotational spectrum of $OC^{14}S$, and the nuclear spin of C^{14}—1405(L)
Robertson, W. W. (see Pondrom, W. L.)—652(A)
——, **F. A. Matsen, and A. J. Seriff.** Effect of O-deuteration and substitution on the ultraviolet absorption spectrum of phenol—652(A)
Robinson, Howard A. and Edward M. Man, Jr. Viscosity of glass—1222(A)
Roesch, Wm. C. (see Biehl, A. T.)—533(A)
Rogers, F. T., Jr. Minimization of some effects of scattering in experimental determinations of XR, for high energy particles—656(A)
Rogers, John, Richard J. Watts and Dudley Williams. Comparison of detection methods for microwave spectra—1230(A)
Rogers, Marguerite M. and Paul E. Shearin. Studies in the progress of ductile fracture in a notched steel bar—656(A)
Rohrlich, Fritz (see Eisenstein, Julian)—641(L), 1411(L)
Roll, J. Donald, S. J. (see Hess, Victor Francis)—592, 912, 1239(A)
Ronneberg, Conrad E. Some advantages of English absolute over English gravitational units—94(T)
Roothaan, C. C. J. and R. S. Mulliken. Molecular orbital treatment of the ultraviolet spectra of benzene and borazole—1234(A)
Rose, M. E. Charge distribution in nuclei and the scattering of high energy electrons—279, 1242(A)
Rosen, Louis (see Curtis, B. R.)—648(A)
Rosen, Nathan. Equations of the neutrino—1272(A)
Ross, Arnold E. Type of non-linear random distortion noise in pulse communication—1126(L)
Rossi, B. (see Bridge, H.)—179(L)
—— (see Hulsizer, Robert I.)—1402(L)
—— (see Valley, G. E.)—177(L)
Rothstein, Jerome. Anomalies in the initiation of cold-cathode discharges—1245(A)
—— On the mechanism of electron emission at the cathode spot of an arc—1214(L)

Rowe, Carl E. Direct measurement of the current-voltage relation in charging and discharging a capacitor—94(T)
Ruark, Arthur. Fast modulation effects in the optical region—181(L)
Rubin, Sylvan (see Kenny, George S.)—536(A)
Rubinowicz, A. Dirac's one-electron-problem in momentum representation—1330
Rudenberg, H. Gunther. Some characteristics of a delay-line coupled wide-band pulse amplifier—543(A)
Rush, J. T. Range of Ra$-\alpha-$Be neutrons in water—271
Russell, B., D. Sachs, A. Wattenberg and R. Fields. Yields of neutrons from photo-neutron sources—545

Sachs, D. (see Russell, B.)—545
Sachs, R. G. Interpretation of the triton moment—1222(A)
—— (see Goeppert-Mayer, M.)—185(L)
—— (see Moszkowski, S.)—184(L)
—— (see Wolfenstein, L.)—528(L)
Safford, Richard W. Probability of meson track endings in a high pressure cloud chamber—1241(A)
Sala, O. (see Bowe, J. C.)—1219(A)
Salkovitz, E. (see Hammond, A.)—1230(A)
Saltzman, H. (see Hull, G. F., Jr.)—1262(A)
Salvini, G. and G. Tagliaferri. On the penetrating component of air showers—261(L)
Sands, Matthew. Directional intensity of cosmic rays at several altitudes—1338
San-Tsiang, Tsien. Errata: On the tripartition of heavy elements—529(L)
Sard, R. D. and E. J. Althaus. Test of the hypothesis that the sea-level cosmic-ray meson disintegrates into a photon and an electron—1251(A)
Saunders, B. G. (see Burkhart, L. E.)—347
Saxon, D. Beta spectrum of Au^{198}—811(L)
Saxon, David S. (see Baños, Alfredo, Jr.)—531(A)
Scanlon, Wayne and K. Lark-Horovitz. Galvanomagnetic and thermomagnetic effects in tellurium—1256(A)
Schaaf, S. A. and R. R. Cyr. Response time in vacuum gages—1253(A)
Scharff-Goldhaber, Gertrude (see Goldhaber, M.)—1472(L)
Schein, Marcel. Mesotrons in the stratosphere—1227(A)
—— Nature of the primary cosmic radiation—1239(A)
—— (see Carr, Thomas D.)—1419
—— (see Fahy, E. F.)—1227(A)
—— (see Lord, J. J.)—1252(A)
—— (see Steinberger, J.)—1227(A)
—— (see Ticho, Harold K.)—81(L)
—— (see Yngve, Victor H.)—1226(A)
—— **and Thomas D. Carr.** Absorption curve of mesotrons on Mount McKinley, Alaska—1227(A)
—— **and Jere J. Lord.** On the production of mesotrons in cosmic ray stars in the stratosphere—189(L)
——, **Victor H. Yngve, and Henry L. Kraybill.** East–west asymmetry of the hard component of the cosmic-radiation—928(L)
Scherb, M. V. Photoelectric effect in self-quenching Geiger-Mueller counters—86(L), 650(A)
—— (see Mandeville, C. E.)—90(L), 141, 340, 634(L), 639(L), 648(A), 654(A), 656(A), 847, 1434, 1270(A)
—— **and C. E. Mandeville.** Beta- and gamma-rays from arsenic (76)—418(L)
—— **and C. E. Mandeville.** 54-minute isomer of indium—655(A)
—— **and C. E. Mandeville.** Internal conversion in tungsten and platinum—1401(L)
—— **and C. E. Mandeville.** Radiations from antimony (124)—1268(A)
Scherrer, P. (see Frauenfelder, H.)—1270(A)
Schiff, L. I. Photo-effects in middle-weight nuclei—534(A), 1311
Schild, A. Discrete space-time and integral Lorentz transformation—414(L)
Schmitt, Roland W., T. N. Hatfield, and Arthur E. Lockenvitz. A comparison of the relative molecular stopping power of $_1H^1$ and $_1D^2$—652(A)
Schremp, Frederic W. (see Smith, Thor L.)—1233(A)
Schultz, H. L. (see Kolstad, G. A.)—1258(A)
——, **J. A. Lockwood, R. L. McCarthy, and P. J. Rice.** Preliminary studies of operation of the Yale linear electron accelerator—1259(A)
Schwarzmann, Gertrude. Actual mass and inert mass—1274(A)
—— Light *versus* matter—1273(A)
Schwinger, Julian. On quantum electrodynamics and the magnetic moment of the electron—416(L)
—— On the polarization of fast neutrons—407
—— Recent developments in quantum electrodynamics—1238(T)
—— (see Karplus, Robert)—1020
—— (see Levine, Harold)—383
—— **and Victor Weisskopf.** On the electromagnetic shift of energy levels—1272(A)
Sciuti, S. (see Quercia, I. F.)—516(L)
Scott, W. J. (see Swann, C. P.)—648(A)
Scott, W. T. and H. S. Snyder. Correlated probabilities in multiple scattering—1260(A)
Seaborg, G. T. Nuclear transmutations with high energy particles—530(T)
—— (see Wahl, Arthur C.)—940
Seagondollar, L. W. (see Barschall, H. H.)—659
—— (see Bockelman, C. K.)—1218(A)
Segrè, E. (see Hadley, J.)—1114(L)
Seidl, F. G. P. (see Bretscher, E.)—815
Seifert, Ralph L. Spectral emissivity and total emissivity of beryllium oxide—1181
Seitz, Frederick. Basic principles of operation of crystal counters—1239(T)
—— On the mobility of electrons in pure non-polar insulators—549
—— (see Dienes, G. J.)—1260(A)
—— (see Markham, J. J.)—1260(A)
Seliger, H. H. and H. L. Bradt. Stability of Os^{187} against K-capture—1408(L)
Serber, Robert. Beam dynamics in the linear accelerator—535(A)
Seren, Leo and Lawrence Jones. Further study on direct coupled pentode and decade rings—1228(A)

Seriff, A. J. (see Robertson, W. W.)—652(A)
Shaler, A. J. and J. Wulff. On the rate of sintering of metal powders—926(L)
Shamos, M. H. and M. G. Levy. On the differential energy spectrum of mesons—1396(L)
Shapiro, Maurice M. and John R. Barnes. Application of Li^6 (n, α) and B^{10} (n, α) to slow-neutron monitoring—1243(A)
Sharp, James M. (see Brown, S. Leroy)—1267(A)
—— **and S. Leroy Brown.** Graphical solution of non-linear simultaneous equations—646(A)
Shaw, A. E. An ion source for isotopic mass comparisons—1222(A)
Shearin, Paul E. (see Rogers, Marguerite M.)—656(A)
Shepherd, M., Jr., J. H. Baldwin, and G. H. Fett. Electronic analogy computer for studying servo-mechanism response—1229(A)
Sherwin, Chalmers W. Conservation of momentum in the beta decay of Y^{90}—1173
—— Momentum conservation in the beta-decay of P^{32} and the angular correlation of neutrinos with electrons—216, 1219(A)
Shockley, W. Electronic polarizability of O^{--} in presence of Ti^{+4}—1273(A)
—— Energy calculations for domains—1246(A)
—— Half-dislocations—1232(A)
—— (see Mason, W. P.)—1213(L)
Shoupp, W. E. (see Hill, J. E.)—931
——, **B. Jennings, and W. Jones.** Threshold for the proton-neutron reaction in copper—421, 1223(A)
Shrader, E. F. and R. L. Garwin. Production of axially symmetric magnetic fields—94(T)
Shreffler, R. G. (see Cork, J. M.)—78(L), 1220(A)
Shull, C. G. (see Wollan, E. O.)—527(L), 830
——, **M. C. Marney and E. O. Wollan.** Laue photography of neutron diffraction—1265(A)
——, **E. O. Wollan, G. A. Morton, and W. L. Davidson.** Neutron diffraction studies of NaH and NaD—842
——, **E. O. Wollan, G. A. Morton, and W. L. Davidson.** Range of nuclear forces in the neutron-proton triplet interaction—262(L)
Shutt, R. P. (see Johnson, T. H.)—1240(A)
Sidhu, S. S. Transmission of monoenergetic slow neutrons through solid solutions and mechanical mixtures of TiC and WC—1264(A)
Siegbahn, Kai and Martin Deutsch. Disintegration scheme of Cs^{134}—410(L)
Siegel, S. (see Ekstein, H.)—1207(L)
Siegert, A. J. F. First passage time-moments for certain Markoffian random functions—1271(A)
Simmons, James W. and Walter Gordy. Structure of the inversion spectrum of ammonia—713
Simpson, J. A., Jr. Latitude dependence of neutron densities in the atmosphere as a function of altitude—1389
Skaggs, L. S. (see Laughlin, J. S.)—1223(A)
——, **J. S. Laughlin, A. O. Hanson, and J. J. Orlin.** Electro-disintegration of Cu^{63}, Ag^{107}, and Ag^{109}—420(L)
——, **J. S. Laughlin, and L. H. Lanzl.** Technique of producing an external beam of electrons from the betatron—1223(A)
Sleator, William, Jr., J. M. Blair, E. E. Lampi, and J. H. Williams. Proton-proton scattering at 2.4 and 3.0 Mev—1241(A)
Slotnick, M. (see Nierenberg, W. A.)—1430
Smith, A. G., Harold Ring, W. V. Smith, and Water Gordy. Nuclear quadrupole coupling of nitrogen in ICN and N_2O—633(L)
——**and P. H. Miller, Jr.** Temperature dependence of work function of semiconductors—1256(A)
Smith, Charles G. Arc motion reversal in transverse magnetic field by heating cathode—543(A)
Smith, L. E., Jr. Positive temperature coefficient of the soft component of cosmic rays—540(A)
Smith, Lloyd P. Separation of isotopes in quantity by electromagnetic means—1238(T)
Smith, Myron C. and Robert T. Beyer. Ultrasonic absorption in water as a function of temperature—654(A)
Smith, P. L. (see Burstein, E.)—1262(A)
Smith, Thor L., John D. Ferry, and Frederic W. Schremp. Transducer measurements of the mechanical properties of polymer solutions—1233(A)
Smith, William V. (see Carter, Robert L.)—1053
—— (see Smith, A. G.)—633(L)
Smoluchowski, R. Crystallographic factors in lattice imperfections—1239(T)
Snell, Arthur H. (see Norris, L. D.)—254(L)
Snoddy, L. B. (see McQueen, J. H.)—260(L)
Snow, G. A. (see Coor, T.)—1252(A)
Snyder, Hartland S. Note on relativistic quantum mechanics—524(L)
—— (see Richards, Paul I.)—269(L)
—— (see Scott, W. T.)—1260(A)
——, **Simon Pasternack, and J. Hornbostel.** Angular correlation of scattered annihilation radiation—440
—— **and Paul I. Richards.** Collision and saturation broadening in microwave spectra—1178
Solomon, A. K. and L. E. Glendenin. Range and energy of beta-radiation from calcium (45)—415(L)
Sommers, H. S., Jr., P. R. Weiss, and W. Halpern. Conversion of a d.c. motor-generator into a low noise power amplifier—1243(A)
Sondheimer, E. H. (see Pippard, A. B.)—920(L)
Speiser, Rudolph (see Edwards, James W.)—1251(A)
Spence, R. D. Scattering and transmission cross sections of circular disks and apertures for sound and electromagnetic waves—1267(A)
Spitzer, Lyman, Jr. Temperature of a highly rarefied gas—1239(T)
Squire, C. F. Low-temperature physics programme at the Rice Institute—646(T)
Stalder, J. R. and David Jukoff. Heat transfer to bodies traveling at high speed in the upper atmosphere—1239(T)
Stebler, A. (see Huber, P.)—85(L), 89(L)
Steele, M. C. (see de Launay, Jules)—1450
Steffen, R. (see Frauenfelder, H.)—1270(A)
—— (see Huber, O.)—1208(L), 1211(L)
Stein, P. R. (see de Hoffmann, F.)—636(L)
Stein, S. J. (see Doty, Paul)—1221(A)

Steinberger, J. and Marcel Schein. Calculations on the mesotron distribution at the geomagnetic equator—1227(A)
Stephens, William E. and A. M. Bottoms. Absorption curve of Be^{10} beta-rays—1269(A)
Stevenson, D. P. Analyses of isotopic propanes—537(A)
—— (see Beeck, O.)—537(A)
Storruste, A. and H. Wergeland. On two complementary diffraction problems—1397(L)
Strandberg, M. W. P. (see Golden, S.)—92(L)
—— (see Wentink, T., Jr.)—1249(A)
—— **and T. Wentink.** Microwave absorption spectrum of COSe—1249(A)
——, **T. Wentink, Jr., R. E. Hillger, Gregory H. Wannier, and Murray L. Deutsch.** Stark spectrum of HDO—188(L)
Street, J. C. (see Whittemore, W. L.)—543(A)
Strong, J. (see Hoover, J. I.)—1259(A)
Steuckelberg, E. C. G. Possible new type of spin-spin interaction—808(L)
Sturkey, Lorenzo. Index of refraction for electrons in crystalline media—183(L)
Suess, Hans E. On the radioactivity of K^{40}—1209(L)
Sugarman, Nathan and Harold Richter. Note on the "Natural Radioactivity of Rhenium"—1411(L)
Swann, C. P. (see Danforth, W. E.)—1413
——, **W. J. Scott, E. L. Hudspeth, and C. E. Mandeville.** Thin target yield of the gamma-rays from the disintegration of beryllium by deuterons—648(A)
Swann, W. F. G. Mass-energy relation—1270(A)
—— (see Morris, Peter)—1226(A)
Sydoriak, S. G. Anomalous magnetic susceptibilities of zinc single crystals at 4.2°K—1247(A)
Szilard, L., S. Bernstein, B. Feld, and J. Ashkin. Inelastic scattering of fast neutrons by Fe, Pb, and Bi—1307

Taft, E. (see Apker, L.)—46
Tagliaferri, G. (see Salvini, G.)—261(L)
Tatel, H. E. Cosmic-ray bursts in the upper atmosphere—1218(T)
—— (see Van Allen, J. A.)—245
—— **and J. A. Van Allen.** Cosmic-ray bursts in the upper atmosphere—87(L)
Taub, A. H. Orbits of charged particles in constant fields—786
Taylor, H. C. (see Morris, Peter A.)—1226(A)
Taylor, Paul B. Reflections of radar waves—94(T)
Taylor, T. B. (see Chupp, Warren W.)—742
Taylor, T. I. (see Bernstein, R. B.)—1263(A)
Taylor, W. J. Application of the method of least squares to x-ray crystal structure analysis—1262(A)
Teller, Edward. On the change of physical constants—801
—— (see Konopinski, E. J.)—822
Templeton, D. H. and I. Perlman. Artificial alpha-active bismuth isotopes—1211(L)
Tendam, D. (see Lark-Horovitz, K.)—1256(A)
Terrell, Nelson James, Jr. Pair production spectrometer for gamma-rays—647(A)
Thellung, Armin and Felix Villars. On the magnetic moment of H^3 and He^3 in the Moller-Rosenfeld theory of nuclear forces—924(L)
Thomas, C. D. Pulse shape of self-quenching counters—1227(A)
Thomas, R. G., W. A. Fowler, and C. C. Lauritsen. Beryllium-proton reactions and scattering—536(A)
Thompson, R. H. and R. T. Ellickson. Excitation of infrared phosphors by alpha- and beta-particles—185(L)
Thurston, G. B, (see Hughes, D. S.)—647(A)
Ticho, Harold K. Mean life of negative mesotrons—1226(A)
—— **and Marcel Schein.** Mean life of negative mesotrons in sodium fluoride—81(L)
Tinlot, John. Variation of penetrating showers with altitude—1476(L)
Titone, L. V. (see Parsegian, V. L.)—1265(A)
Tittle, C. W. and Clark Goodman. Neutron diffusion in hydrogenous media—1264(A)
Tobolsky, A. V. (see Andrews, R. D.)—1221(A)
Tomkins, F. S. Hyperfine structure in the spectrum of NP^{237}—1214(L)
Tongiorgi, Vanna. On the presence of neutrons in the extensive cosmic-ray showers—923(L)
Tonks, Lewi. Mechanical model of chain reaction in nuclear fission—96(T)
Tousey, R. Solar ultraviolet spectroscopy from V-2 rockets—1218(T)
Townes, C. H. (see Bardeen, J.)—97, 627(L), 1204(L)
—— (see Merritt, F. R.)—1249(A)
——, **B. D. Wright, and F. R. Merritt.** Pure rotational spectrum of ICl—1334, 1249(A)
Tranter, W. Owen. Diffraction of electromagnetic waves—184(L)
Truesdell, C. On the differential equations for slip flow—1255(A)
—— On the total vorticity of motion of a continuous medium—510
—— On the transfer of energy in continuous media—513
Tsien, Hsue-Shien. Wind tunnel testing problem in superaerodynamics—1239(T)
Turkevich, John and Harry H. Hubbell, Jr. Experimental check on intensity distribution in small-angle x-ray scattering—1250(A)
Turner, Clarence, Bruce Cork, Joseph Ballam, and Hayden Gordon. Berkeley four million volt electrostatic generator—534(A)
Turrentine, R. E. (see Hull, A. W.)—1228(A)

Uhlenbeck, G. E. On the theory of the transport phenomena in rarefied gases—1239(T)
—— (see Falkoff, D. L.)—649(A)
Urry, Wm. D. Gamma-radiation from granite—596

Vallarta, M. S. Certain problems concerning the primary cosmic radiation—646(T)
Valley, G. E. Decay of slow mesons—1251(A)
—— **and B. Rossi.** On the mean life of negative mesons—177(L)

Van Allen, J. A. Direct measurement of the flux charged cosmic-ray primaries—1218(T)
—— Research by rockets—1218(T)
—— **and H. E. Tatel.** Cosmic-ray counting rate of a single Geiger counter from ground level to 161 kilometers altitude—245
—— (see Tatel, H.E.)—87(L)
van der Merwe, C. W. (see Parsegian, V. L.)—1265(A)
Van Dyke, K. S. Properties of quartz crystals—542(T)
Van Vleck, J. H. On the width of r−f absorption lines in solids—1229(A)
—— Theory of the width of microwave lines in cupric salts—1249(A)
Van Voorhis, C. C. (see Ladenburg, R.)—1359
Vaze, G. H. (see Gill, P. S.)—1395(L)
Villars, Felix (see Thellung, Armin)—924(L)
Vollrath, R. E. (see Donoghue, J. J.)—538(A)
von Hippel, A. Structure and conductivity in the VI$_b$ group of the periodic system—1257(A)
—— (see Matthias, B.)—268(L), 1261(A), 1378
Votruba, Václav. Pair production by γ-rays in the field of an electron—1468(L)

Wagner, C. D. (see Beeck, O.)—537(A)
Wahl, Arthur C. and Glenn T. Seaborg. Nuclear properties of 93^{237}—940
Wahl, John S. (see Jacobs, James A.)—1130(L)
Wahlin, H. B. Thermionic properties of chromium—1458
Walker, A. (see Crowe, M. O'L.)—96(T)
Wallace, J. R. (see Hughes, D. J.)—1277
Wang, C. S. and D. L. Falkoff. On the emission of continuous γ-radiation during β-decay—1220(A)
Wangness, Roald K. (see Jacobsohn, Boris A.)—942
Wannier, Gregory, H. (see Strandberg, M. W. P.)—188(L)
Wataghin, Gleb. On the formation of chemical elements inside the stars—79(L)
—— (see de Toledo, Paulo Saraiva)—79(L)
Watson, Bernard B. (see DuMond, Jesse W. M.)—1392
Watson, K. (see Jauch, J. M.)—268(L)
Watson, Kenneth M. Polarizability of the neutron in an electrostatic field—125
Wattenberg, A. (see Russell, B.)—545
Watts, Richard J. (see Rogers, John)—1230(A)
Way, K. and E. P. Wigner. Rate of decay of fission products—1318
Weaver, Paul. Physical-chemical interpretation of a geological problem: rocks from sea water—646(T)
Webb, Wayne (see Raymond, Richard C.)—1248(A)
Webber, Robert T. and J. M. Reynolds. Critical fields of superconducting vanadium—1264(A)
—— Incipient superconductivity in titanium—640(L)
Weber, A. H. (see Arnold, G.)—1385
Weidner, Richard T. Nuclear quadrupole interaction in the ICl rotational spectrum—254(L)
—— (see Whitmer, C. A.)—1468(L)
Weinstein, Alexander. On the linearized supersonic flow through ducts—1255(A)
Weiss, P. R. Microwave spectroscopy of paramagnetic salts; the spectrum of chromic alum—470
—— (see Sommers, H. S., Jr.)—1243(A)
—— (see Whitmer, C. A.)—1468(L)
Weisskopf, Victor (see Schwinger, Julian)—1272(A)
Weissler, G. L. and R. W. Kotter. Workfunction of a gas-coated surface—538(A)
Welton, T. A. Observable effects of the quantum fluctuations of the electromagnetic field—1271(A)
Wentink, T. (see Golden, S.)—92(L)
—— (see Standberg, M. W. P.)—188(L), 1249(A)
——, **M. W. P. Strandberg and R. Hilliger.** Stark effect in the COSe molecule—1249(A)
Wergeland, H. (see Storruste, A.)—1397(L)
West, H. I., Jr. (see Pepinsky, R.)—1235(A)
Westendrop, W. F. Electron accelerators—96(T)
Whaling, Ward and J. E. Evans. Separation of Li isotopes—648(A)
Wheeler, D. (see Potapenko, G.)—530(A)
Wheeler, J. A. Meson induced fission—1252(A)
Whitehead, W. D., Jr. (see Heydenburg, N. P.)—241
Whitmer, C. A., R. T. Weidner, and P. R. Weiss. Magnetic resonance absorption in diluted chrome alums—1468(L)
Whittemore, W. L. and J. C. Street. Silver chloride used as an ionized detector for cosmic rays—543(A)
Wick, G. C. On the magnetic field of a rotating molecule—51
Wiegand, C. (see Hadley, J.)—541(A), 1114(L)
—— (see Kelly, E. L.)—1135
Wigner, Eugene P. On the behavior of cross sections near thresholds—1002
—— (see Way, K.)—1318
Wilchinsky, Zigmond W. On the diffraction of x-rays from coarse powders—1251(A)
Wilkinson, Geoffrey. Some isotopes of platinum and gold—252
Williams, Dudley (see Rogers, John)—1230(A)
—— (see Zimmerman, John R.)—94(T), 94(A)
Williams, Ferd E. Theory of the luminescence of ionic phosphors—1257(A)
Williams, H. J. Ferromagnetic domains—1239(T)
—— (see Nesbitt, E. A.)—1246(A)
—— **and R. M. Bozorth.** New magnetic powder patterns and their interpretation—1246(A)
Williams, John H. (see Bailey, Carl L.)—274
—— (see Sleator, William, Jr.)—1241(A)
Williams, Robert W. Lateral distribution function of cosmic-ray air showers—1252(A)
Williams, Robley C. Use of the electron microscope in exploring the smoothness of surfaces—1222(A)
Wilson, H. A. Scattering of particles by an attractive center of force varying inversely as the cube of the distance—655(A)
—— Spherical shell nuclear model—655(A)
—— Rice Institute Van de Graaff electrostatic generator—647(A)
Wilson, J. G. Secondary electrons produced by mesons—525(L)
Winckler, J. (see Ladenburg, R.)—1359
Wintner, Aurel. On Dirac's theory of continuous spectra—781
—— On the solutions of radial wave equations—91(L)

Witmer, Enos E. Nuclear magnetic moments as integral multiples of a natural unit—1243(A)
—— **and Martin A. Pomerantz.** Effective path length through a vertical cosmic-ray telescope—651(A)
Wolf, J. M. (see Miller, B. L.)—657(A)
Wolfenstein, L. and R. G. Sachs. Note on angular distributions in nuclear reactions—528(L)
Wolff, Peter (see Heckrotte, W.)—264(L), 265(L)
Wollan, E. O. (see Hoover, J. I.)—1259(A)
—— (see Shull, C. G.)—262(L), 842, 1265(A)
—— **and C. G. Shull.** Diffraction of neutrons by crystalline powders—830
——, **C. G. Shull, and M. C. Marney.** Laue photography of neutron diffraction—527(L)
Woodward, L. L. (see Cowart, W. S.)—1454
Woodyard, John R. (see Bradner, Hugh)—534(A)
Worley, R. Edwin. On the absorption spectrum of active nitrogen—531(A)
Wouthuysen, S. A. (see Lewis, H. W.)—127
Wright, B. D. (see Townes, C. H.)—1334, 1249(A)
Wright, Byron T. (see Richardson, J. Reginald)—424
Wrinch, Dorothy. Proteins as polycondensations of amino acids—1225(A)
Wu, C. S. (see Havens, W. W., Jr.)—963, 1265(A)
—— (see Meaker, C. L.)—1240(A)
—— (see Rainwater, L. J.)—733, 1265(A)
——, **W. W. Havens, Jr., R. Albert and G. Grimm.** Helical focusing beta-ray spectrograph—1259(A)
Wu, Ta-You. Neutron-proton scattering and range of nuclear forces—1132(L)
—— Note on second Born approximation and proton-neutron and proton-proton scattering—934
—— (see Ashkin, Julius)—973
—— **and Julius Ashkin.** Elastic and inelastic scattering of 100–200 Mev protons or neutrons by deuterons—986
—— **and Henry M. Foley.** Neutron-proton scattering formula: Remark on the letter by Flügge and Hückel—1117(L)
Wulf, Oliver R. and Seth B. Nicholson. Possible influence of the moon on recurrent geomagnetic activity—1204(L)
Wulff, J. (see Shaler, A. J.)—926(L)

Yaffe, L. and Katharine M. Justus. A rapid method for the determination of the maximum energies of β-emitters with simple spectra—1400(L)
Yager, W. A. Ferromagnetic resonance absorption at microwave frequencies—1247(A)
Yagoda, Herman. Nuclear evaporation recorded in an emulsion near sea level—263(L)
—— **and Nathan Kaplan.** Background eradication of nuclear emulsions by accelerated fading of the latent image—634(L)
Yakimac, Alexis (see Antonoff, George)—1230(A)
Yennie, D. R. and A. B. Arons. Energy partition in underwater explosion phenomena—1253(A)
Yngve, Victor H. (see Schein, Marcel)—928(L)
——, **Marcel Schein and Henry L. Kraybill.** East–west asymmetry of the mesotron component at 35,000 feet—1226(A)
York, H. F. (see Hadley, J.)—541(A), 1114(L)
—— (see McMillan, Edwin M.)—262(L)
Yu, Fu-Chum and J. D. Kurbotov. Disintegration of isomers of Ba^{133}—1268(A)
Yuan, Luke C. L. Precision high voltage vacuum-tube voltmeter—1273(A)

Zabel, C. W. (see Davis, L., Jr.)—525(L)
Zacharias, J. R. (see Davis, L., Jr.)—525(L), 1222(A)
Zachariasen, W. H. Crystal radii of the heavy elements—1104
Zaffarano, Daniel J. (see Kern, Bernard D.)—1142, 1268(A)
—— (see Mitchell, A. C. G.)—1220(A), 1424
Zimmerman, John R. and Dudley Williams. Method of measuring nuclear magnetic moments—94(T), 94(A)

Analytic Subject Index to Volume 73

References with (A) are to abstracts of papers presented at meetings of the American Physical Society. References with (L) are to Letters to the Editor.

Absorption of radiation
- Absorption of Na^{24} gamma-radiation in Pb, Cu, and Al. David E. Alburger—344
- Ferromagnetic resonance absorption in a single Fe crystal, Arthur F. Kip and Robert D. Arnold—1247(A)
- Ferromagnetic resonance absorption at microwave frequencies, W. A. Yager—1247(A)
- Nuclear paramagnetic resonance absorption, electric quadrupole moments, R. V. Pound—1247(A)
- Paramagnetic resonance absorption in $CuSO_4$, Robert D. Arnold and Arthur F. Kip—1247(A)
- Proton paramagnetic resonance, fine structure, G. E. Pake—1248(A)
- r-f absorption lines in solids, J. H. Van Vleck—1229(A)
- Of ultra-short electromagnetic waves in fatty acids, G. Potapenko and D. Wheeler—530(A)

Acoustics
- Diffraction of sound, A. Storruste and H. Wergeland—1397(L)
- In liquids under high pressure, Gerald Holton—543(A)
- Radiation of sound from circular pipe, Harold Levine and Julian Schwinger—383
- Reflection and transmission by spherical shell, Herbert B. Keller and Joseph B. Keller—1273(A)
- Refraction of waves from point source, E. Gerjuoy—1442
- Scattering and transmission cross sections of circular disks and apertures, R. D. Spence—1267(A)
- Second sound in He II and normal sound, William Band and Lothar Meyer—226
- Supersonic propagation, high pressure, Gerald J. Holton—1268(A)
- Transmission and reflection in liquid helium II, John R. Pellam—608
- Ultrasonic absorption in water, Myron C. Smith and Robert T. Beyer—654(A); Leonard Hall—775
- Ultrasonic reflections in rochelle crystals, William J. Price—1132(L)
- Vortices and streams, Carl Eckart—68
- Waves of finite amplitude, Antonio Romero Juarez—654(A)

Activated gases
- Active nitrogen, Joseph Kaplan—494

Adsorption
- Adsorption analysis of high molecular substances, Ingrid Claesson and Stig Claesson—1221(A)

Aerodynamics (see also **Hydrodynamics**)
- Crocco's theorems, flows having non-uniform stagnation enthalpy, R. Prim—1255(A)
- Flow around objects in supersonic air stream, R. Ladenburg, J. Winckler and C. C. Van Voorhis—1359
- Limiting line phenomenon, W. Perl—1254(A)
- Locally isotropic turbulence, Leslie S. G. Kovasznay—1115(L)
- Resistance to motion through rarified gases, M. Heineman—1254(A)
- Supersonic flow patterns, M. M. Munk—1254(A)
- Supersonic flow through ducts, Alexander Weinstein—1255(A)
- Three-dimensional gas flow patterns, P. Nemenyi and R. Prim—1255(A)

Arcs (see also **Discharge of electricity in gases**)
- Electron emission at cathode spot, Jerome Rothstein—1214(L)

Astrophysics
- Change of physical constants, Edward Teller—801
- Formation of elements inside stars, Gleb Wataghin—79(L)
- Magnetism of celestial bodies, Jean Mariani—78(L)
- Methane in the earth's atmosphere, Marcel V. Migeotte 519(L)
- Model solar atmospheres, Guido Munch—651(A)
- Rates of carbon reactions in sun, J. O'Reilly and R. F. Christy—536(A)
- Relative abundances of nuclei in universe, Paulo Saraiva de Toledo and Gleb Wataghin—79(L)
- Spectrum of sun, V-2 rockets, John J. Hopfield and Harold E. Clearman, Jr.—876
- Stellar electromagnetic fields, Leverett Davis, Jr.—536(A)

Atmosphere (see **Meteorology**)

Atomic structure (see also **Energy states of atoms; Spectra**)
- g values of $^2P^\circ_{1/2}$ and the $^2S_{1/2}$ states in Ca II, J. Rand McNalley, Jr.—1130(L)
- Intrinsic moment of the electron, H. M. Foley and P. Kusch—412(L)
- New type of spin-spin interaction, E. C. G. Stueckelberg—808(L)

Biophysics
- Proteins as polycondensations of amino acids, Dorothy Wrinch—1225(A)
- Slow-neutron monitoring, Maurice M. Shapiro and John R. Barnes—1243(A)

Broadening of spectral lines
- Of microwave resonance lines, Paul I. Richards and Hartland S. Snyder—269(L)
- Theory of pressure broadening, Alexander Jablonski—258(L); H. Foley—259(L)
- Width of lines in cupric salts, microwave region, J. H. Van Vleck—1249(A)

Collisions of second kind
- In nitrogen and oxygen, Joseph Kaplan—530(A)

Conductivity, electrical (see **Electrical conductivity; Discharge of electricity in gases**)

Constants, physical, standards
- Changes in values, Edward Teller—801

Cosmic radiation
- Absorption curve of mesotrons at 18,200 feet, Marcel Schein and Thomas D. Carr—1227(A)

Absorption in carbon and lead, Martin A. Pomerantz—1253(A)
Altitude dependence of high energy showers, Henry L. Kraybill—632(L)
Analysis of shower data, H. W. Lewis—1341
Azimuthal effect at Bombay, P. S. Gill and G. H. Vaze—1395(L)
Burst production at an altitude of 11,200 feet, E. F. Fahy and Marcel Schein—1227(A)
Burst production by penetrating particles, H. Bridge, W. E. Hazen, and B. Rossi—179(L)
Bursts in upper atmosphere, H. E. Tatel and J. A. Van Allen—87(L)
Capture of negative mesons, O. Piccioni—411(L)
Cloud chamber for high altitude operation, R. B. Leighton and Carl D. Anderson—650(A)
Detection of radiation by ultra-high frequency gas-discharge counters, Sanborn C. Brown—1240(A)
Directional intensity, Matthew Sands—1338
East-west asymmetry, hard component, Marcel Schein, Victor H. Yngve, and Henry L. Kraybill—928(L)
East-west asymmetry mesotron component at 35,000 feet, Victor H. Yngve, Marcel Schein and Henry L. Kraybill—1226(A)
Effective path length through a vertical telescope, Enos E. Witmer and Martin A. Pomerantz—651(A), 1274(A)
Electronic component, experimental, G. Bernardini, B. N. Cacciapuoti, and R. Querzoli—335; theoretical—328
Electron showers at 30,000 feet, Paul E. Lloyd, R. Ronald Rau, Carl D. Anderson, and Raymond V. Adams—650(A)
Geiger counting rate to 161 kilometers altitude, J. A. Van Allen and H. E. Tatel—245
Ground level of air showers, Paul J. Ovrebo—1227(A)
Hard component, air mass distribution, Kenneth M. Kupferberg—804(L)
Heavily-ionizing particles at 30,000 feet, R. Ronald Rau, Carl D. Anderson, Raymond V. Adams, and Paul E. Lloyd—534(A)
High energy atmospheric showers, Henry L. Kraybill—1262(A)
Interaction of primaries with sunlight and starlight, E. Feenberg and H. Primakoff—449
Interpretation of large air showers, John Blatt—1252(A)
Ionization bursts at high altitudes, T. Coor and G. A. Snow—000(A); Robert L. Hulsizer—1252(A)
Lateral distribution, air showers, Robert W. Williams—1252(A)
Latitude dependence of neutron densities, J. A. Simpson, Jr.—1389
Life of negative mesons, G. E. Valley and B. Rossi—177(L)
Life of negative mesotrons in NaF, Harold K. Ticho and Marcel Schein—81(L)
Mass of mesotrons, J. G. Retallack and R. B. Brode—532(A)
Measurements at 18,100 feet, Thomas D. Carr, Marcel Schein, and Ian Barbour—1419
Meson disintegration into photon and electron, R. D. Sard and E. J. Althaus—1251(A)
Mesons far underground, Kenneth I. Greisen—521(L)
Mesotron distribution at geomagnetic equator, J. Steinberger and Marcel Schein—1227(A)
Mesotron mass measurements, R. B. Brode—533(A)
Mesotrons and protons at 30,000 feet, Raymond V. Adams, Paul E. Lloyd, R. Ronald Rau, and Carl D. Anderson—650(A)
Mesotrons at high altitudes, Donald C. Moore and Robert B. Brode—532(A)
Mesotrons in 'stars' in stratosphere, Marcel Schein and Jere J. Lord—189(L), 1252(A)
Mesotrons in stratosphere, Marcel Schein—1227(A)
Multiple production of mesons, H. W. Lewis, J. R. Oppenheimer, and S. A. Wouthuysen—127
Neutral mesons, Kenneth I. Greisen—521(L)
Neutrons in atmosphere, Serge A. Korff, M. S. George, and J. W. Kerr—1133(L)
Neutrons in showers, Vanna Tongiorgi—923(L)
Nuclear evaporation recorded near sea level, Herman Yagoda—263(L)
Path length through cosmic-ray telescope, Enos E. Witmer and Martin A. Pomerantz—651(A), 1274(A)
Penetrating component at 17,000 feet, I. F. Quercia, B. Rispoli, and S. Sciuti—516(L)
Penertrating component of air showers, G. Salvini and G. Tagliaferri—261(L)
Penetrating showers, variation with altitude, John Tinlot—1476(L)
Primary radiation, Marcel Schein—1239(A)
Probability of meson track endings, Richard W. Safford—1241(A)
Production of mesons, Geoffrey F. Chew—1128(L)
Production of nucleons, S. A. Korff and A. Cobas—1010
Properties of cosmic rays at very high altitudes, Martin A. Pomerantz—651(A)
Sea level latitude effect, Peter A. Morris, W. F. G. Swann, and H. C. Taylor—1226(A)
Search for electrons in primary radiation, Robert I. Hulsizer and Bruno Rossi—1402(L)
Showers at high altitude, Roland Maze, André Fréon, and Pierre Auger—418(L)
Showers in Pb, W. B. Fretter—41
Silver chloride as detector, W. L. Whittemore and J. C. Street—543(A)
Slow mesons, decay of, G. E. Valley—1251(A)
Specific primary ionization in hydrogen, Frank L. Hereford—1239(A)
Surplus gamma-radiation from rocks, Victor Francis Hess and J. Donald Roll, S. J.—592, 1239(A)
Temperature coefficient of soft component, L. E. Smith, Jr.—540(A)
Variation with latitude, A. T. Biehl, R. A. Montgomery, H. V. Neher, W. H. Pickering, and Wm. C. Roesch—533(A)

Cross section, measurements, theory

Behavior near thresholds, Eugene P. Wigner—1002
Capture of electrons by ions, Julian K. Knipp—652(A)

Cross section, measurements, theory (continued)
C^{12} (p, pn) C^{11} at high energy, Edwin M. McMillan and Richard D. Miller—80(L)
C^{12} (n, $2n$) C^{11} at 90 Mev, Edwin M. McMillan and Herbert F. York—262(L)
Differential D (d, n) He^3 cross section, B. R. Curtis, Louis Rosen, and J. L. Fowler—648(A)
For fast continuous energy neutrons, V. L. Parsegian, L. V. Titone, and C. W. van der Merwe—1265(A)
of Fe, Ni, and Bi for fast neutrons, H. H. Barschall, C. K. Bockelman, and L. W. Seagondollar—659; 1218(A)
In neutron proton scattering, M. Camac and H. A. Bethe—191
Neutrons at low energies, crystal interference and molecular binding effects, W. W. Havens, Jr., L. J. Rainwater, and C. S. Wu—1265(A)
Neutrons in Fe, Ni and Cu, L. J. Rainwater, W. W. Havens, Jr., and C. S. Wu—1265(A)
Slow neutron cross section for H, D, F, Mg, S, Si, and quartz, L. J. Rainwater, W. W. Havens, Jr., J. R. Dunning, and C. S. Wu—733
Slow neutron studies of Cu, Ni, Bi, Fe, Sn and calcite, W. W. Havens, Jr., L. J. Rainwater, C. S. Wu, and J. R. Dunning—963
S^{32} (n, p) P^{32} for neutron energies of 1.6 to 5.8 Mev, E. D. Klema and A. O. Hanson—106
Thermal neutron absorption by separated isotopes, H. Pomerance and J. I. Hoover—1265(A)
Of various elements for neutrons, Edward Melkonian—1265(A)

Crystal structure
Achromatization of Debye-Scherrer lines, H. Ekstein and S. Siegel—1207(L)
Breakdown directions in lithium halide crystals, J. W. Davisson—1196, 1261(A)
Diamond, used as counter, Kathleen Lonsdale—1467(L)
Energy levels of NaCl, E. Fisher—36
Grain boundaries in metals, T'ing-Sui Kê—267(L)
Least squares and x-ray crystal structure analysis, W. J. Taylor—1262(A)
Metallic carbide lattice energies, I. Hodes—539(A)
Monoclinic, piezoelectric constants, Hans Jaffe—1467(L)
Phase determination, implication theory, M. J. Buerger—927(L)
Proteins as polycondensations of amino acids, Dorothy Wrinch—1225(A)
Radii of heavy elements, W. H. Zachariasen—1104
Refraction for electrons in crystalline media, Lorenzo Sturkey—183(L)
Of NaH and NaD, neutron diffraction, C. G. Shull, E. O. Wollan, G. A. Morton, and W. L. Davidson—842
Of technetium, R. C. L. Mooney—653(A)
Of Sn, twinning, W. P. Mason, H. J. McSkimin and W. Shockley—1213(L)

Crystalline state
Age hardening, Herbert M. Meyer—1263(A)
Binding energy for an electron in NaCl, J. J. Markham and F. Seitz—1260(A)
Binding energy of electrons in KCl, Kenneth E. Keyes—1260(A)
Damping of anodized aluminum, A. Hammond, J. Michener, J. Koehler, and E. Salkovitz—1230(A)
Diamond crystal counters, Robert Hofstadter—631(L)
Dielectric behavior of $BaTiO_3$ near 0°K, J. M. Richardson—1261(A)
Dislocations, energy of, W. Shockley—1232(A)
Domain structure and electric response of $BaTiO_3$, B. T. Matthias and A. von Hippel—1261(A), 1378
Electrical properties of pure silicon and silicon alloys, G. L. Pearson and J. Bardeen—1256(A)
Electrostriction in $BaTiO_3$ ceramics, Hans Jaffe—1261(A)
Energy for migration of paired vacancies in KCl, G. J. Dienes and Frederick Seitz—1260(A)
Energy levels in solids, temperature dependence, Alvin Radkowsky—749
Ferromagnetic resonance absorption in Fe crystal, Arthur F. Kip and Robert D. Arnold—1247(A)
Ferromagnetic resonance absorption in various materials, W. A. Yager—1247(A)
Growth of $BaTiO_3$ crystals, B. T. Matthias—808(L)
Hysteresis loops for $BaTiO_3$, A. de Bretteville, Jr.—807(L)
Magnetic susceptibilities of single Zn crystals, S. G. Sydoriak—1247(A)
Nuclear paramagnetic resonance absorption, R. V. Pound—1247(A)
Orientation of domains in $BaTiO_3$, G. C. Danielson—1248(A)
Paramagnetic resonance absorption in $CuSO_4$, Robert D. Arnold and Arthur F. Kip—1247(A)
Photoelastic constants of cubic crystals, E. Burstein, P. L. Smith, and B. Henvis—1262(A)
Piezoelectric effect in barium titanate, Walter L. Cherry, Jr. and Robert Adler—1230(A)
Plastic deformation in brass and aluminum, Andrew W. McReynolds—1262(A)
Polarizability of O^{--} in presence of Ti^{+4}, W. Shockley—1273(A)
Properties of $BaTiO_3$, B. Matthias and A. von Hippel—268(L)
Proton paramagnetic resonance, fine structure, G. E. Pake—1248(A)
r-f absorption lines in solids, J. H. Van Vleck—1229(A)
Rates of grain growth, Paul A. Beck, M. L. Holzworth, and Hsun Hu—526(L)
Self-diffusion of Na in NaCl, Dillon Mapother and Robert Maurer—1260(A)
Sintering of metal powders, A. J. Shaler and J. Wulff—926(L)
Slip along grain boundaries, T'ing-Sui Kê—1235(A)
Stress-induced diffusion of C and O atoms in Ta, T'ing-Sui Kê—1231(A)
Structure and conductivity in the VI_b group, A. von Hippel—1257(A)
Superconductivity and Debye characteristic temperature, K. R. Dixit—182(L)
Theory of luminescence, Ferd E. Williams—1257(A)
Ultrasonic reflections by domains in rochelle salt crystals, William J. Price—1132(L)

Dielectric constants (see also **Dielectrics and dielectric properties**)
Dust electrostatics, James W. Hansen—532(A)
Of tellurium, V. A. Johnson—1231(A)
Dielectrics and dielectric properties
Of $BaTiO_3$ near 0°K, J. M. Richardson—1261(A)
Of $BaTiO_3$ single crystals, B. Matthias and A. von Hippel—1378
Low frequency dispersion in ionic crystals, R. G. Breckenridge—1261(A)
Of Te, V. A. Johnson—1231(A)
Diffraction of atoms and neutrons
Crystal orientation in Al, slow neutrons, G. Arnold and A. H. Weber—1385
Small-angle diffraction, Otto Halpern—653(A)
Diffraction of neutrons (see **Neutron diffraction**)
Diffraction of radiation
Small-angle diffraction, Otto Halpern—653(A)
Of sound, A. Storruste and H. Wergeland—1397(L)
Diffusion (see also **Thermal diffusion**)
Gaseous self-diffusion, W. G. Pollard and R. D. Present—762
Mobility of electrons in insulators, Frederick Seitz—549
Self-diffusion of Na in NaCl, Dillon Mapother and Robert Maurer—1260(A)
Discharge of electricity in gases
Arc motion reversal, heating cathode, Charles G. Smith—543(A)
Breakdown in air at microwave frequencies, D. Q. Posin—496, 1245(A)
Breakdown in helium at microwave frequencies, Melvin Herlin and Sanborn C. Brown—1245(A)
Characteristics of bridges and arcs between metallic contacts, G. F. Hull, Jr. and H. Saltzman—1262(A)
Cold-cathode discharges, initiation of, Jerome Rothstein—1245(A)
Ejection of electrons by ions, R. R. Newton—1122(L)
Fields in cathode dark space, S. V. Galginaitis—1245(A)
Glow discharge in Hg vapor, B. Pearson DeLany and Paul L. Copeland—1232(A)
In high frequency electrical fields, Donald H. Hale—1046
High frequency gas discharges, breakdown, L. M. Hartman—316
High frequency gas discharges, components of distribution function, H. Margenau and L. M. Hartman—309
High frequency gas discharges, electron distribution functions, H. Margenau—297
High frequency gas discharges, similarity principle, H. Margenau—326
Mercury vapor jets in spark discharge, J. Richard Haynes—891
Minimum sparking potentials, cathode behavior, Harold Jacobs and Armand P. LaRocque—1244(A)
Point to plane corona, L. B. Loeb and W. N. English—532(A)
Radiofrequency conductivity of plasmas, Ladislas Goldstein and Nathaniel L. Cohen—83(L)
Spark breakdown, Paschen's law, Charles G. Miller and Leonard B. Loeb—84(L)
Threshold for burst pulse corona, Leonard B. Loeb—798
Transients in Townsend discharges, Robert R. Newton—570
Water drop corona, W. N. English—532(A)
Discharge of electricity in high vacua (see also **Thermionic emission; High voltage tubes and machines**)
Charge between close electrodes, L. H. Germer and F. E. Haworth—1121(L)
Sparking in high vacuum diodes, W. E. Ramsey and W. E. Danforth—1246(A)
Time of electrons between electrodes, Delbert N. Eggenberger and Paul L. Copeland—1228(A)
Disintegration and excitation of nucleus (see also **Radioactivity**)
α-particles on Ag, excitation curves, S. N. Ghoshal—417(L)
Angular distribution from Li^7 $(p, \alpha)\alpha$, N. P. Heydenburg, C. M. Hudson, D. R. Inglis and W. D. Whitehead, Jr.—241
Angular distributions in reactions, L. Wolfenstein and R. G. Sachs—528(L)
Of Sb^{124} coincidence experiments, E. T. Jurney and Allan C. G. Mitchell—1153
Of As, with 190 Mev deuterons, H. H. Hopkins, Jr. and B. B. Cunningham—1406
Of Be^8, Arthur Hemmendinger—806(L)
Beta-decay of Kr^{88}, recoil of nucleus, J. C. Jacobsen and O. Kofoed-Hansen—675
Continuous γ-radiation during β-decay, C. S. Wang and D. L. Falkoff—1220(A)
Of Cu^{63}, Ag^{107} and Ag^{109} by electrons, L. S. Skaggs, J. S. Laughlin, A. O. Hanson, and J. J. Orlin—420(L)
Correlation between beta- and gamma-emissions, D. L. Falkoff and G. E. Uhlenbeck—649(A)
Cross section for C^{12} (p, pn) C^{11} at high energy, Edwin M. McMillan and Richard D. Miller—80(L)
Decay of fission products, K. Way and E. P. Wigner—1318
$D+D$ reactions, theoretical considerations, E. J. Konopinski and E. Teller—822
(d, p) reactions, low states of O^{17}, N. P. Heydenburg and D. R. Inglis—230
Disintegration energy of N^{14} (n, p) C^{14}, P. Huber and A. Stebler—85(L)
Electro-disintegration of Cu^{63}, Ag^{107}, and Ag^{109}, J. S. Laughlin, L. S. Skaggs, A. O. Hanson, and J. J. Orlin—1223(A)
Evidence for di-neutron, D. N. Kundu and M. L. Pool—22
Excitation function, $(Li^7$ $(p, n))$, J. E. Hill and W. E. Shoupp—931
Excitation function of reaction C^{12} $(n, 2n)$ C^{11}, W. Heckrotte and Peter Wolff—265(L)
Excitation function of the reaction C^{12} (p, pn) C^{11}, W. Heckrotte and Peter Wolff—264(L)
Excitation of Na^{24} and Na^{22} by deuteron and alpha bombardment of Al, A. C. Helmholz and J. M. Peterson—541(A)
Of F and Li by protons, T. W. Bonner and J. E. Evans—666
$\gamma-p$ process in Be^9, L. Conklin and William Ogle—648(A)

Disintegration and excitation of nucleus (continued)
Gamma-radiation from bombardment of F, B and Be by protons, James A. Jacobs, Philip R. Malmberg and John S. Wahl—1130(L)
Gamma-radiation from light nuclei under proton bombardment, W. A. Fowler, C. C. Lauritsen, and T. Lauritsen—181(L)
Gamma-rays and neutrons from Be bombarded by deuterons, C. W. Malich and J. R. Risser—648(A)
Gamma-rays from alpha-particle reactions, David E. Alburger—1241(A)
Gamma-rays from disintegration of Be by deuterons, C. P. Swann, W. J. Scott, E. L. Hudspeth, and C. E. Mandeville—648(A)
He^3 (n, p) H^3 reaction, neutrino mass, D. J. Hughes and C. Eggler—809(L), 1242(A)
Introduction of two neutrons into nuclei, D. N. Kundu and M. L. Pool—1220(A)
Neutron and gamma-ray yields from deuterons on carbon, Carl L. Bailey, George Freier and John H. Williams—274
Of N by neutrons, P. Huber and A. Stebler—89(L)
Nuclear evaporation recorded near sea level, Herman Yagoda—263(L)
Photo-effects in middle-weight nuclei, L. I. Schiff—534(A), 1311
Proton-gamma-ray coincidence counting, Bruce B. Benson—7
Resonance at 1430 kev in $C^{12}+H^2$, J. C. Harris, T. W. Bonner, J. E. Evans, and G. C. Phillips—649(A)
Resonance of Li^7+H^1, J. E. Evans and T. W. Bonner—649(A)
Stars in photographic emulsions, experimental, Eugene Gardner and Vincent Peterson—533(A)
Stars in photographic emulsions, theoretical, Wendell Horning—533(A)
S^{32} (d, p) S^{33}, proton groups, Perry W. Davison—1241(A)
Threshold for proton-neutron reaction in Cu, W. E. Shoupp, B. Jennings, and W. Jones—421, 1223(A)
Tripartition of heavy elements, erratum, Tsien San-Tsiang—529(L)
X-ray yield curves for $\gamma-n$ reactions, G. C. Baldwin and G. S. Klaiber—1156, 1266(A)
Yield of D (D, p) H^3, distribution of protons, E. Bretscher, A. P. French, and F. G. P. Seidl—815
Yields of x-ray induced reactions, G. Friedlander and M. L. Perlman—1266(A)

Dynamics
Actual mass and inert mass, Gertrude Schwarzmann—1274(A)
Damped non-linear oscillator, M. Avramy Melvin—1274(A)
Multiple excitation of an elastic system, G. S. Bennett—1270(A)
Simplified notation in classical mechanics, H. C. Corben—1270(A)
Symmetric energy-momentum tensor, C. Kikuchi—1271(A)

Elasticity
Age hardening, Herbert M. Meyer—1263(A)
Ductile fracture in notched steel bar, Marguerite M. Rogers and Paul E. Shearin—656(A)
Dislocations, energy of, W. Shockley—1246(A)
Dynamic properties of linear structures, W. James Lyons and Irven B. Prettyman—1232(A)
Effects of pile bombardment on elastomers, W. L. Davidson and I. G. Geib—1225(A)
Elasto-viscous properties of polyisobutylene, R. D. Andrews, N. Hofman-Bang, and A. V. Tobolsky—1221(A)
Of GR-S and Hevea, S. D. Gehman—1224(A)
Long chain molecule liquids, mechanical properties, W. P. Mason, W. O. Baker, H. J. McSkimin and J. H. Heiss—1074
Mechanical properties of rubber-like material, A. W. Nolle—1232(A)
Melting points, rigidities and optical activities of gelatin gels, John D. Ferry and John E. Eldridge—1225(A)
Plastic deformation, statistical theory, W. James Lyons—413(L)
Plastic deformation in brass and aluminum, Andrew W. McReynolds—1262(A)
Rupture of metal foils, Waller George—1262(A)
Rupture of metal foils under constant load, Waller George and George Irwin—1230(A)
Slip along grain boundaries, T'ing-Sui Kê—1235(A)
Of NaCl, KBr, and KCl, J. K. Galt—1460
Stress-induced diffusion of C and O atoms in Ta, T'ing-Sui Kê—1231(A)
Tensile strengths of liquids, J. J. Donoghue, E. Gerjuoy, and R. E. Vollrath—538(A)
Theory of elasticity and anelasticity, Carl Eckart—373
Thermodynamics of strained elastomer, M. Mooney—1224(A); L. E. Copeland and M. Mooney—1224(A)

Electrical circuits
Analytical solution, Mary Gowen Foulks—646(A)
Bridged double T network, C. H. Fay—647(A)
Direct coupled pentode and decade rings, Leo Seren and Lawrence Jones—1228(A)
Graphical solution, S. Leroy Brown—646(A)
Noise in pulse communication, Arnold E. Ross—1126(L)
Response of system, uniformly increasing frequency, H. Ekstein—1228(A)

Electrical conductivity and resistance
Breakdown directions in lithium halide crystals, J. W. Davisson—1196, 1261(A)
Cesium rectifiers, A. W. Hull, E. E. Burger, and R. E. Turrentine—1228(A)
Deuteron-bombarded semiconductors, K. Lark-Horovitz, E. Bleuler, R. Davis, and D. Tendam—1256(A)
Electrical properties of pure silicon and silicon alloys, G. L. Pearson and J. Bardeen—1256(A)
Ferromagnetic semi-conductors, microwave absorption, William H. Hewitt, Jr.—1118(L)
Induced in diamond by alpha-particles, A. J. Ahearn—1113(L)
Magneto-resistance of Bi, Robert F. Blunt—654(A)
Of metals at microwave frequencies, A. B. Pippard, G. E. H. Reuter and E. H. Sondheimer—920(L)
Mobility of electrons in insulators, Frederick Seitz—549

Noise in crystal rectifiers, William Miller—1257(A)
Non-ohmic disks, characteristics of, S. Bloomenthal—1231(A)
Penetration depth in superconductors, Jules de Launay and M. C. Steele—1450
Photoelectric effects, metal semi-conductor contacts, S. Benzer—1256(A)
Pulses in zinc sulfide by alpha particles, A. J. Ahearn—524(L)
r-f resistance of CbN at low temperature, J. V. Lebacqz—1476(L)
Semiconductors as amplifiers, Edmund S. Rittner—1212(L)
Structure and conductivity in the VI_b group, A. von Hippel—1257(A)
Superconducting vanadium, Robert T. Webber and J. M. Reynolds—1264(A)
Superconductivity and Debye characteristic temperature, K. R. Dixit—182(L)
Superconductivity in Ti, Robert T. Webber and J. M. Reynolds—640(L)
Temperature coefficient of $NaNH_2$ solutions, Angus Pearson—655(A)
Temperature-pressure-conductivity relations in semiconductors, F. C. Brown—1257(A)
Two-dimensional potential problem, Don Kirkham—1228(A)
Work function of semiconductors, A. H. Smith and P. H. Miller, Jr.—1256(A)

Electrodynamics (see **Electromagnetic theory**)

Electromagnetic theory
Dielectric wave guide, C. W. Horton—647(A)
Diffraction of electromagnetic waves, W. Owen Tranter—184(L)
Dirac's electron field (Ψ) and Maxwell's electromagnetic field (Φ, A), Frederick J. Belinfante—641(L)
Electron beam wave interaction in a wave guide, Philip Parzen—1268(A)
Electron motion in field of magnetic dipole, S. H. Lachenbruch—1244(A)
Fluctuations of electromagnetic field, T. A. Welton—1271(A)
Force between magnets in medium, John A. Eldridge—1229(A)
Hamiltonian for particle in electromagnetic field, Paul I. Richards—254(L)
Laplace transforms, electromagnetic waves in cylinders, Manuel Cerrillo—647(A)
Light *versus* matter, Gertrude Schwarzmann—1273(A)
Orbits of charged particles, A. H. Taub—786
Propagation characteristics in coaxial structure with two dielectrics, Alfredo Baños, Jr., H. Gruen, and David S. Saxon—531(A)
Reactive terms in quantum electrodynamics, H. W. Lewis—173; Saul T. Epstein—177(L)
Reflection and transmission of waves by a spherical shell, Herbert B. Keller and Joseph B. Keller—1273(A)
Reflections and transmission of waves by curved shells, Joseph B. Keller—1273(A)
Scattering and transmission sections of circular disks and apertures, R. D. Spence—1267(A)
Shift of energy levels, F. J. Dyson—617

Electron affinity
Of C_2, I. Hodes—539(A)

Electron diffraction (see also **Electron optics**)
Of lubricating wax coatings, Chester Ridlon Berry—1117(L)
Refraction for electrons in crystalline media, Lorenzo Sturkey—183(L)
"Schlieren" effect, L. Marton—1244(A)
"Schlieren" effect, applications, D. L. Reverdin, L. Marton, and S. H. Lachenbruch—1244(A)

Electrons (see also **Positrons**)
Charged particle of mass greater than that of electron, M. Hessaby—1128(L)
In atoms, indentity with β-rays, M. Goldhaber and Gertrude Scharff-Goldharber—1472(L)
Intrinsic moment, H. M. Foley and P. Kusch—412(L); Julian Schwinger—416(L)

Electrons, positive (see also **Positive electrons**)

Electrons, secondary
Ejected by ions at high fields, R. R. Newton—1122(L)
Produced by mesons, J. G. Wilson—525(L)
From targets of barium-strontium oxide, J. B. Johnson—1058

Electrons, thermionic (see also **Thermionic emission**)

Electronic tubes
Acceleration of electrons by cylindrical cavities, B. L. Miller and J. M. Wolf—657(A)

Electro-optical effects (see also **Photoelectric effect and properties**)
Crystals of primary phosphate type, Hans Jaffe—95(A)

Electrostriction
In $BaTiO_3$, ceramics, Hans Jaffe—1261(A)

Elements
Absolute nuclear abundances, Harrison Brown—1242(A)
Existence of element 61 in nature, N. E. Ballou—630(L)
Formation of elements inside stars, Gleb Wataghin—79(L)
Origin of elements, R. A. Alpher, H. Bethe, and G. Gamow—803(L)
Relative abundances of nuclei in universe, Paulo Saraiva de Toledo and Gleb Wataghin—79(L)
X-ray evidence for element 43, L. E. Burkhart, W. F. Peed, and B. G. Saunders—347

Energy states of nucleus (see **Nuclear structure**)

Errata
Does the electron have an intrinsic magnetic moment, G. Breit—1410(L)
Interaction of neutrons with electrons, J. M. Jauch and K. Watson—268(L)
Microwave spark, D. Q. Posin—1118(L)
Natural radioactivity of rhenium, S. N. Naldrett and W. F. Libby—487, 929(L)
Neutron-proton scattering at 100 Mev, Julian Eisenstein and Fritz Rohrlich—1411(L)
Reactive terms in quantum electrodynamics, Saul T. Epstein—630(L)

Errata (continued)
Resolving time and genuine coincidence loss for Geiger-Mueller counters, C. E. Mandeville and Morris V. Scherb—639(L)
Second-order corrections to quadrupole effects in molecules, J. Bardeen and C. H. Townes—1204(L)
Tripartition of heavy elements, Tsien San-Tsiang—529(L)
Uncertainty principle and the yield of nuclei formed in fission, P. F. Gast—529(L)
Excitation of nuclei (see **Disintegration and excitation of nucleus; Nuclear structure**)
Explosion phenomena (see also **Shock Waves**)
Energy partition in underwater explosion, D. R. Yennie and A. B. Arons—1253(A)
Oscillation of gas globes, A. B. Arons—1253(A)
Seismic disturbance due to explosion, Norman Ricker—654(A)

Ferromagnetism (see **Magnetic properties**)
Field theory
Gravitational, electromagnetic, and vector meson fields and geometry—Banesh Hoffmann—30, 531(A)
Higher order field equations, Alex E. S. Green—519(L)
Symmetric energy-momentum tensor of Iwanenko-Sokolow field, C. Kikuchi—1271(A)
Films, properties of
Distribution of Po on thin Ag and Bi films, Fred J. Morris and Arthur E. Lockenvitz—649(A)
Fine structure (see **Spectra,** etc. and **Hyperfine structure**)
Fission of nucleus
Of Bi by high energy particles, R. H. Goeckermann and I. Perlman—1127(L)
Coincidences between fission neutrons, S. DeBenedetti, J. E. Francis, Jr., W. M. Preston, and T. W. Bonner—1266(A)
Delayed neutrons from U^{238}, D. J. Hughes, J. Dabbs, A. Cahn, and D. Hall—111; F. de Hoffmann, B. T. Feld, and P. R. Stein—636(L)
Of elements from Pt to Bi, E. L. Kelly and Clyde Wiegand—1135
Meson induced fission, J. A. Wheeler—1252(A)
Of 93^{237}, Arthur C. Wahl and Glenn T. Seaborg—940
Fluid dynamics (see **Hydrodynamics and Aerodynamics**)

Galvanomagnetic effects
Onsager's reciprocal relations, Herbert B. Callen—1349
Semiconductors at high temperature, V. A. Johnson and K. Lark-Horovitz—1257(A)
In tellurium, Wayne Scanlon and K. Lark-Horovitz—1256(A)
Thermionic and galvanomagnetic coefficients, H. B. Callen—1248(A)
Gamma rays (see also **Disintegration and excitation of nucleus; Radioactivity**)
Gases (see also **Kinetic theory**)
Combustion wave in flowing gas, R. J. Dery—1267(A)
Flow around objects in supersonic air stream, R. Ladenburg, J. Winckler and C. C. Van Voorhis—1359
Flows having non-uniform stagnation enthalpy, Crocco's theorems, R. C. Prim—186(L)
Ratio He^3/He^4, Henry A. Fairbank, C. T. Lane, L. T. Aldrich, and Alfred O. Nier—729; 1263(A)
Stability of gas bubbles in water, E. Gerjuoy—538(A)
Geophysics
Gamma-radiation from granite, Victor Francis Hess and J. Donald Roll, S. J.—912
Geomagnetism, effect of moon, Oliver R. Wulf and Seth B. Nicholson—1204(L)
Isotope separation in geological processes, W. H. Furry—1264(A)
Seismic disturbance due to explosion, Norman Ricker—654(A)
Surplus gamma-radiation from rocks, Victor Francis Hess and J. Donald Roll, S. J.—1239(A)
Gravitation
Foundation of Birkhoff's theory, Carlos Graef Fernandez—651(A)
Generalized theory of gravitation, A. Papapetrou—1105
Hypothesis underlying theory, Alberto Barajas—651(A)
Particle on axis of rotating ring, Fernando Alba—651(A)

High voltage tubes and machines (see **Methods and instruments**)
Hydrodynamics
Equations for slip flow, C. Truesdell—1255(A)
Generalization of theorem by Larmor, I. Opatowski—1253(A)
Horizontal eddies in the ocean, George F. McEwen—538(A)
Limiting line phenomenon, W. Perl—1254(A)
Locally isotropic turbulence, Leslie S. G. Kovasznay—1115(L)
Perturbation of steady uniform flow by heat, Bruce L. Hicks—636(L)
Pulse in atmosphere, propagation of, C. L. Pekeris—145
Solitary wave and periodic waves in shallow water, Joseph B. Keller—1254(A)
Spark shadowgrams of spheres at supersonic speeds, J. Howard McMillen and R. L. Kramer—1255(A)
Total vorticity of a continuous medium, C. Truesdell—510
Transfer of energy in continuous media, C. Truesdell—513
Vortices and streams, sound waves, Carl Eckart—68
Wave transmission and reflection in liquid helium II, John R. Pellam—608
Hyperfine structure (see also **Nuclear moments and spin**)
Of chlorine, L. Davis, Jr., B. T. Feld, C. W. Zabel, and J. R. Zacharias—525(L)
Of deuterium, Aage Bohr—1109(L)
Of Ga, G. E. Becker and P. Kusch—531(A), 584
Of hydrogen and deuterium, John E. Nafe and Edward B. Nelson—718, 1243(A)
Of CH_3I and ICN anomalies, O. R. Gilliam, H. D. Edwards, and Walter Gordy—635(L)
Of Np^{237}, F. S. Tomkins—1214(L)
Of K^{40}, Luther Davis, Jr. and Jerrold R. Zacharias—1222(A)
Quadrupole coupling of H in ICN and N_2O, A. G. Smith, Harold Ring, W. V. Smith, and Walter Gordy—633(L)

Instruments (see **Methods and instruments**)
Ionization
By C^{14} radiation in ionization chamber, John W. Otvos—537(A)
Comparison of the relative molecular stopping power of $_1H^1$ and of $_1D^2$, Roland Schmitt, T. N. Hatfield, and Arthur E. Lockenvitz—652(A)
Comparison of the relative molecular stopping power of some hydrocarbon isomers for alpha-particles from Po, Thomas E. Gibbs and Arthur E. Lockenvitz—652(A)
Energy loss in gases and condensed bodies, Otto Halpern and Harvey Hall—477
In divergent fields in H_2 and air, Gerald W. Johnson—284
In Geiger-Mueller tubes, S. J. du Toit—1473(L)
Measurement of the relative molecular stopping power of gases for Po alphas, T. N. Hatfield and M. Y. Colby—652(A)
Polarization effects in carbon, Frank L. Hereford—1123(L)
Ionization potentials
Of hydrocarbon series, Richard E. Honig—1232(A)
Ionosphere
Virtual height at 100 kilocycles, R. A. Helliwell—77(L)
Ions, mobility
Mobility of electrons in insulators, Frederick Seitz—549
Isotopes
Absolute nuclear abundances, Harrison Brown—1242(A)
Of Bi, α-active, D. H. Templeton and I. Perlman—1211(L)
Enrichment of isotopes, gaseous exchange method, R. B. Bernstein and I. I. Taylor—1263(A)
He^3 separation in liquid helium II, C. T. Lane, Henry A. Fairbank, L. T. Aldrich, and Alfred O. Nier—256(L)
Isotopic properties of helium in liquid phase, J. G. Daunt, R. E. Probst, and H. L. Johnston—1263(A)
Hg^{198} from Au, Paul Bradt and Fred L. Mohler—925(L)
Of Mo, Tc activities from bombardment, E. E. Motta and G. E. Boyd—1470(L)
New isotopic effect in liquid helium, J. G. Daunt, R. E. Probst and H. L. Johnston—638(L)
Os^{187} stability against K capture, H. H. Seliger and H. L. Bradt—1408(L)
Of Pl and Au, Geoffrey Wilkinson—252
Ratio of He^3/He^4, Henry A. Fairbank, C. T. Lane, L. T. Aldrich and Alfred O. Nier—729, 1263(A)
Of Rh and Pd, M. Lindner and I. Perlman—1202(L)
Of Sm, Mark G. Inghram, David C. Hess, Jr., and Richard J. Hayden—180(L)
Separation in geological processes, W. H. Furry—1264(A)
Separation of Br and Cl isotopes, L. G. Chelius and C. P. Keim—813(L)
Separation of Li isotopes, Ward Whaling and J. E. Evans—648(A)
Solutions of He^3 in He^4, F. London and O. K. Rice—1188
Of Tc^{43}, isomers, O Huber, P. Marmier, H. Medicus, P. Preiswerk, and R. Steffen—1208(L)
Of Tc^{43}, 62-day, decay scheme, O. Huber, H. Medicus, P. Preiswerk, and R. Steffen—1211(L)
Of Te and Sb, M. Lindner and I. Perlman—1124(L)
Thermal diffusion with neon, F. K. Elder, Jr.—1263(A)
Isotopic composition of xenon, A. H. W. Aten, Jr.—1206(L)
Of Zn and Cd, abundance, Wallace T. Leland and Alfred O. Nier—1206(L)
Isomers, molecular
Analyses of isotopic propanes, D. P. Stevenson—537(A)
Catalytic isomerization of propane containing C^{13}, O. Beeck, J. W. Otvos, D. P. Stevenson, and C. D. Wagner—537(A)
Isomers, nuclear (see **Nuclear structure and Radioactivity**)

Liquids (see also **Hydrodynamics**)
Fluctuations in properties, effect of radiations, George Antonoff, Alexis Yakimac, and Duncan Randall—1230(A); John B. Hawkes and Robert W. Astheimer—520(L)
He^3 separation in liquid helium II, C. T. Lane, Henry A. Fairbank, L. T. Aldrich, and Alfred O. Nier—256(L)
Isotopic properties of helium in liquid phase, J. G. Daunt, R. E. Probst and H. L. Johnston—1263(A)
Long chain molecule liquids, mechanical properties, W. P. Mason, W. O. Baker, H. J. McSkimin, and J. H. Heiss—1074
New isotopic effects in liquid helium, J. G. Daunt, R. E. Probst, and H. L. Johnston—638(L)
Second sound in He II and normal sound, William Band and Lothar Meyer—226
Solutions of He^3 in He^4, F. London and O. K. Rice—1188
Stability of gas bubbles in water, E. Gerjuoy—538(A)
Wave transmission and reflection in liquid helium II, John R. Pellam—608
Luminescence
Of ionic phosphors, Ferd E. Williams—1257(A)

Magnetic fields
Rectangular analogs of Helmholtz coils, J. S. Krohmer and Richard A. Beth—94(A)
Magnetic properties (see also **Nuclear moments and spin**)
Absorption in ferromagnetic semi-conductors, William H. Hewitt, Jr.—1118(L)
Anomalous susceptibilities of zinc crystals, S. G. Sydoriak—1247(A)
Coercive force, particle size, Charles Kittel—810(L)
Energy calculations for domains, W. Shockley—1246(A)
Ferromagnetic domains, L. Marton—1475(L)
Ferromagnetic resonance, D. Polder—1116(L), 1120(L)
Longitudinal magnetostriction, automatic recording, E. A. Nesbitt and H. J. Williams—1246(A)
Magnetic resonance absorption in chrome alums, C. A. Whitmer, R. T. Weidner, and P. R. Weiss—1468(L)
Magneto-resistance of Bi, Robert F. Blunt—654(A)
Nuclear resonance absorption, N. Bloembergen, E. M. Purcell, and R. V. Pound—679
Powder patterns, interpretation, H. J. Williams and R. M. Bozorth—1246(A)
Susceptibility, strain sensitivity, T. S. Hutchison and James Reekie—517(L)
Susceptibility of uranium oxalate, C. A. Hutchison and N. Elliott—1229(A)
Theory of ferromagnetic resonance, D. Polder—1116(L)

Mass Spectroscopy
Beta-ray, design, E. Persico—1475(L)
Mechanics (see **Dynamics**)
Mechanics, quantum—general
Calculation of self-energies, Bertil S. Nilsson—902
Dirac character operators, E. M. Corson—57
Dirac's electron field (Ψ) and Maxwell's electromagnetic field (Φ, A), Frederick J. Belinfante—641(L)
Dirac's one-electron problem, A. Rubinowicz—1330
Dirac's theory of continuous spectra, Aurel Wintner—781
Extension of Dirac's equation, E. L. Hill—907
Influence of retardation on the London-van der Waals forces, H. B. G. Casimir and D. Polder—360
Localizable dynamical systems, P. A. M. Dirac—1092
Nature of low energy radiation, Benjamin Liebowitz—1274(A)
Pair production by γ-rays in electron field, Václav Votruba—1468(L)
Quantized space, Christopher Gregory—806(L)
Reactive terms in quantum electrodynamics, H. W. Lewis—173; Saul T. Epstein—177(L), 630(L)
Relativistic quantum mechanics, Hartland S. Snyder—524(L)
Resonance reactions, Dirac-type incident particles, G. Goertzel—1463
Solutions of radial wave equations, Aurel Wintner—91(L)
Transformation theory applied to radiation field, José A. Balseiro—1346
Virtual quanta, M. Lax and H. Feshbach—1271(A)
Mechanics, quantum—of solid bodies
Theory of ferromagnetic resonance, D. Polder—1116(L)
Mesotrons (see also **Cosmic radiation**)
Absorption curve of mesotrons at 18,200 feet, Marcel Schein and Thomas D. Carr—1227(A)
Capture of mesotrons by protons, F. E. Prieto Calderon—650(A)
Capture of negative mesons, O. Piccioni—411(L)
In cosmic-ray 'stars,' Marcel Schein and Jere J. Lord—189(L), 1252(A)
Decay of negative mesons in light elements, A. March—1205(L)
Differential energy spectrum, M. H. Shamos and M. G. Levy—1396(L)
Disintegration in different absorbers, Norris Nereson—565
East-west asymmetry of the mesotron component at 35,000 feet, Victor H. Yngve, Marcel Schein, and Henry L. Kraybill—1226(A)
Gamma radiation in meson decay, E. P. Hincks and B. Pontecorvo—257(L)
At high altitudes, low energy, Donald C. Moore and Robert B. Brode—532(A)
Infinities in meson-field theory, Alex E. S. Green—26
Life of negative mesons, G. E. Valley and B. Rossi—177(L); W. L. Kraushaar—1408(L)
Mass, J. G. Retallack and R. B. Brode—532(A)
Mean life in NaF, Harold K. Ticho and Marcel Schein—81(L)
Mean life of negative mesotrons, Harold K. Ticho—1226(A)
Meson disintegration into photon and electron, R. D. Sard and E. J. Althaus—1251(A)
Meson induced fission, J. A. Wheeler—1252(A)
Mesons far underground, Kenneth I. Greisen—521(L)
Mesotron decay, J. G. Retallack—921(L)
Mesotrons in stratosphere, Marcel Schein—1227(A)
Multiple production, H. W. Lewis, J. R. Oppenheimer, and S. A. Wouthuysen—127
Negative mesons, stimulated decay, S. T. Epstein, R. J. Finkelstein and J. R. Oppenheimer—1140
Neutral mesons, Kenneth I. Greisen—521(L); R. E. Marshak—1226(A)
Probability of meson track endings, Richard W. Safford—1241(A)
Production in cosmic rays, Geoffrey F. Chew—1128(L)
Slow mesons, decay of, G. E. Valley—1251(A)
Stability of neutral meson, E. P. Hincks and B. Pontecorvo—1122(L)
Trajectories of charged mesons, Banesh Hoffman—1042
Vector meson fields and geometry, Banesh Hoffman—30
Metals (see **Crystalline state**)
Meteorology
Methane in the earth's atmosphere, Marcel V. Migeotte—519(L)
Pulse in atmosphere, C. L. Pekeris—145
Methods and Instruments
Acceleration of electrons by cylindrical cavities, B. L. Miller and J. M. Wolf—657(A)
Amplifiers, use of semiconductors as, Edmund S. Rittner—1212(L)
Analyses of isotopic propanes, D. P. Stevenson—537(A)
Analytical solution of electrical networks, Mary Gowen Foulks—646(A)
Background eradication, fading of latent image, Herman Yagoda and Nathan Kaplan—634(L)
Balancing of sedimentation by electrophoresis, M. L. Randolph—654(A)
Beta-ray spectrography, T. Lauritsen and R. F. Christy—536(A)
Beta-ray spectrograph, helical focusing, C. S. Wu, W. W. Havens, Jr., R. Albert, and G. Grimm—1259(A)
Beta-ray spectrometer, Stanley Frankel—804(L)
Beta-rays detected by scintillations, George B. Collins and Rosalie C. Hoyt—1259(A)
Cesium rectifier, A. W. Hull, E. E. Burger, and R. E. Turrentine—1228(A)
Characteristics of Geiger counters, H. V. Neher—533(A)
Characteristics of non-dissipative electric wave filters, S. Leroy Brown and James M. Sharp—646(A)
Cloud chamber for high altitude operation, R. B. Leighton and Carl D. Anderson—650(A)
Commercial yarn testing, Charles J. Geyer, Jr., C. H. Reichardt, and George Halsey—1224(A)
Conductivity induced in diamond by alpha-particles, A. J. Ahearn—1113(L)
Conductivity pulses in single crystals of zinc sulfide by alpha-particles, A. J. Ahearn—524(L)
Counters, parallel plate, L. Madansky and R. W. Pidd—1215(L)

Counters filled with lead tetramethyl vapor, C. L. Meaker, C. S. Wu, and L. J. Rainwater—1240(A)
Counters, inorganic crystal, Robert J. Moon—1210(L)
Crystal counter, W. Jentschke—77(L)
Cyclotron frequency modulation, K. R. MacKenzie—540(A)
Damping of anodized aluminum, A. Hammond, J. Michener, J. Koehler, and E. Salkovitz—1230(A)
Design for 10-Bev proton synchrotron, M. Stanley Livingston—1258(A)
Detection of radiation by ultra high frequency gas-discharge counters, Sanborn C. Brown—1240(A)
Diamond crystal counters, Robert Hofstadter—631(L); Kathleen Lonsdale—1467(L)
Direct coupled pentode and decade rings, Leo Seren and Lawrence Jones—1228(A)
Distortion in pulse communication, Arnold E. Ross—1126(L)
Dive angle indicator, Donald H. Jacobs—539(A)
Double-focusing mass spectrographs, H. E. Duckworth—543(A)
Electronic analogy computer, M. Shepherd, Jr., J. H. Baldwin, and G. H. Fett—1229(A)
Electronic eyepiece for near infra-red, Zaboj V. Harvalik—1233(A)
Electron multiplier tube for alpha-particles, S. K. Allison and L. del Rosario—1224(A)
Electron optical "Schlieren" effect, D. L. Reverdin, L. Marton, and S. H. Lachenbruch—1244(A)
Electro-optic effects in phosphate crystals, Hans Jaffe—95(A)
Electrostatic generator, W. E. Danforth, E. L. Hudspeth, C. E. Mandeville, and C. P. Swann—1413
Exploring the smoothness of surfaces, Robley C. Williams—1222(A)
External beam of electrons from betatron, L. S. Skaggs, J. S. Laughlin, and L. H. Lanzl—1223(A)
Fast modulation effects in optical region, Arthur Ruark—181(L)
Field distribution in linear accelerator, Wolfgang K. H. Panofsky, Chaim Richman, and Frank Oppenheimer—535(A)
Focusing in cross fields, relativistic energies, Walter E. Millett—1259(A)
Fourier equations for x-ray studies, Dan McLachlan, Jr.—539(A)
Four million-volt electrostatic generator, Clarence Turner, Bruce Cork, Joseph Ballam, and Hayden Gordon—534(A)
Frequency modulated cyclotron, J. Reginald Richardson, Byron T. Wright, E. J. Lofgren, and Bernard Peters—424
Geiger-Mueller tubes, effect of composition of gases, S. J. du Toit—1473(L)
Graphical evaluation of Jacobi polynomials, S. Leroy Brown and Mary Gowen Foulks—539(A)
Graphical solution of non-linear simultaneous equations, James M. Sharp and S. Leroy Brown—646(A)
Grazing incidence reflectors, Paul Kirkpatrick, A. V. Baez, and Allen Newell—535(A)
High frequency corona, M. D. O'Day and E. H. Cullington—543(A)
High pressure cloud chamber, T. H. Johnson and R. P. Shutt—1240(A)
High voltage vacuum-tube voltmeter, Luke C. L. Yuan—1273(A)
Hot wire anemometer at high frequency, Eli Ossofsky—410(L)
Imperfections in diffraction gratings, U. Fano and R. D. Huntoon—1233(A)
Induction accelerator for a proton synchrotron, John P. Blewett—1258(A)
Intensity regulator for hydrogen discharge tube, W. L. Pondrom and W. W. Robertson—652(A)
Ion orbit control for synchrotron, C. K. Green—1258(A)
Ion source equipment for electrostatic generator, Franklin Fillmore, Arthur Hudgins, and Morris Jeppson—534(A)
Ion source for mass comparisons, A. E. Shaw—1222(A)
Least squares and x-ray crystal structure analysis, W. J. Taylor—1262(A)
Light scattering in supersonic streams, J. H. McQueen, J. W. Beams, and L. B. Snoddy—260(L)
Linear accelerator, beam dynamics, Robert Serber—535(A)
Linear accelerator oscillator and coupling system, W. R. Baker, J. V. Franck, and J. D. Gow—535(A)
Linear accelerator, physical design, Hugh Bradner, Richard Crawford, Hayden Gordon, and John R. Woodyard—534(A)
Longitudinal magnetostriction, automatic recording, E. A. Nesbitt and H. J. Williams—1248(A)
Low noise power amplifier, H. S. Sommers, Jr., P. R. Weiss, and W. Halpern—1243(A)
Magnetic circuit for a proton synchrotron, Wm. H. Moore and John P. Blewett—1258(A)
Measurement of small time intervals, J. W. Keuffel—531(A)
Mesotron mass measurements, R. B. Brode—533(A)
Method for determining maximum β-energies, L. Yaffe and Katharine M. Justus—1400(L)
Microphotometer for x-ray diffraction diagram, T. Pepinsky and H. I. West, Jr.—1235(A)
Microwave accelerator, G. A. Kolstad, H. L. Schultz, and C. G. Montgomery—1258(A)
Neutron absorption by Clinton pile oscillator, J. I. Hoover, W. H. Jordan, C. D. Moak, L. A. Pardue, H. Pomerance, J. Strong, and E. O. Wollan—1259(A)
Nuclear magnetic moments, John R. Zimmerman and Dudley Williams—94(T), 94(A)
Outgassing and evaporation of Sb, R. L. Longini—1231(A)
Pair production spectrometer for gamma-rays, Nelson James Terrell, Jr.—647(A)
Path length through cosmic-ray telescope, Enos E. Witmer and Martin A. Pomerantz—651(A)
Photo-tubes in ultraviolet fluorescence, Robert D. Cowan—1234(A)
Plasma sheaths as variable capacitances, W. E. Parkins and J. M. Leffler—538(A)

Methods and Instruments (continued)
Protective facings on Eastman emulsions, P. B. Mauer and H. L. Reynolds—1131(L)
Pulse transformer, coincidence counting, B. G. Farley—1240(A)
Real and complex roots of polynomials, mechanical harmonic synthesizer, Robert G. Packard and S. Leroy Brown—646(A)
Rebuilding of metal counting tubes, G. E. Hagen and D. H. Loughridge—1131(L)
Rectangular analogs of Helmholz coils, Richard A. Beth and J. S. Krohmer—94(T), 94(A)
Resolving time, coincidence loss for counters, C. E. Mandeville and Morris V. Scherb—90(L)
Resolving time for counters, erratum, C. E. Mandeville and Morris V. Scherb—639(L)
Response time in vacuum gauges, S. A. Schaaf and R. R. Cyr—1253(A)
Rice Institute Van de Graaff generator, H. A. Wilson—647(A)
Rocket flame velocity by Doppler shift, F. P. Bundy—1267(A)
Scintillation counters for beta- and gamma-rays, Martin Deutsch—1240(A)
Scintillation counters, self-delayed coincidences, S. DeBenedetti, F. K. McGowan, and J. E. Francis, Jr.—1269(L)
Scintillation counters, use of anthracene, P. R. Bell—1405(L)
Self-quenching counters, M. V. Scherb—86(L), 650(A); C. D. Thomas—1227(A); S. S. Friedland and A. D. Krumbein—1227(A)
Separation of He^3, C. T. Lane, Henry A. Fairbank, L. T. Aldrich, and Alfred O. Nier—256(L)
Separation of Li isotopes, Ward Whaling and J. E. Evans—648(A)
Shaped field for 180° spectrograph, F. M. Beiduk and E. J. Konopinski—1229(A)
Silver chloride as detector, W. L. Whittemore and J. C. Street—543(A)
Slow-neutron monitoring, Maurice M. Shapiro and John R. Barnes—1243(A)
Solution of network impedances with mechanical harmonic synthesizer, S. Leroy Brown—646(A)
Stabilization of 10,000-oersted magnetic field, D. S. Hughes, W. L. Pondrom, and G. B. Thurston—647(A)
Temperature controller, J. C. Mouzon—1267(A)
Tensile strengths of liquids, J. J. Donoghue, E. Gerjuoy, and R. E. Vollrath—538(A)
Thermionic emission of oxide-coated cathodes in gaseous conduction devices, W. F. Hodge—95(A)
30-Mev betatron, E. C. Gregg, Jr.—94(T), 95(A)
Time moments for Markoffian random functions, A. J. F. Siegert—1271(A)
Transducer measurements of the mechanical properties of polymer solutions, Thor L. Smith, John D. Ferry, and Frederic W. Schremp—1233(A)
Traveling wave amplifier, D. L. Benedict—1246(A)
Two-dimensional potential problem, Don Kirkham—1228(A)
Ultraviolet transmission of diamonds, counting characteristics, H. Friedman, L. S. Birks, and H. P. Gauvin—186(L)
Wide-band pulse amplifier, H. Gunther Rudenberg—543(A)
X-ray diffraction camera, high temperature, James W. Edwards, Rudolph Speiser, and Herrick L. Johnston—1251(A)
X-ray optical images, Paul Kirkpatrick and A. V. Baez—1234(A)
Yale linear electron accelerator, H. L. Schultz, J. A. Lockwood, R. L. McCarthy, and P. J. Rice—1259(A)

Microwaves (see also **Electromagnetic theory; electronic tubes; spectra, microwave**)
Absorption in ferromagnetic semiconductors, William H. Hewitt, Jr.—1118(L)
Detection methods, John Rogers, Richard J. Watts, and Dudley Williams—1230(A)
Discharge in gases at high frequencies, H. Margenau—297; H. Margenau and L. M. Hartman—309; L. M. Hartman—316; H. Margenau—326
Ferromagnetic resonance absorption, Charles Kittel—155
Microwave frequencies, electrical phenomena in gases, W. P. Allis—1239(T)
Microwave resonance lines, broadening of, Paul I. Richards and Hartland S. Snyder—269(L)
Microwave spark, D. Q. Posin—496, 1118(L)
Radiofrequency conductivity of plasmas, Ladislas Goldstein and Nathanial L. Cohen—83(L)
Results and semitheoretical calculations in breakdown, D. Q. Posin—1245(A)
R-f absorption lines in solids, J. H. Van Vleck—1229(A)
Spectrum of ammonia, saturation effects—Robert Karplus—1120(L)
Stark splitting, absorption in paramagnetic salts, C. Kittel and J. M. Luttinger—162

Molecular structure and constants (see also **Spectra, molecular,** etc., and **Raman spectra**)
Force constants and Raman frequencies of methylbromoacetylene and methyliodoacetylene, Arnold G. Meister—1234(A)
Interconversion of ortho- and para-deuterium, deuteron quadrupole moment, Morton Hamermesh—638(L)
Magnetic field of a rotating molecule, G. C. Wick—51
Molecular orbitals for methane and ethane, F. A. Matsen—653(A)
States of diatomic molecules, fine structure, A. Budó and I. Kóvacs—1120(L)
Systems containing light positive particle, Aadne Ore—1313

Necrology
Willard Leslie Severinghaus, H. W. Farwell—642(L)

Neutrino (see also **Radioactivity; Scattering of electrons, neutrons and ions**)
Beta-decay of Y 90, Chalmers W. Sherwin—1173
Equations of the neutrino, Nathan Rosen—1272(A)
Mass, actual and inert, Gertrude Schwarzmann—1274(A)
Mass, from β-spectrum of S^{35}, C. Sharp Cook, Lawrence M. Langer, and H. Clay Price, Jr.—1395(L)

Mass from $He^3(n, p)$ H^3, D. J. Hughes and C. Eggler—809(L), 1242(A)
H^3 and mass of neutrino, John R. Pruett—1219(A)
Momentum conservation in the beta-decay of P^{32}, Chalmers W. Sherwin—216, 1219(A)

Neutrons
Al (αn) and Si (dn) spectra, R. A. Peck, Jr.—1264(A)
In atmosphere, Serge A. Korff, M. S. George, and J. W. Kerr—1133(L)
Coincidences between fission neutrons, S. DeBenedetti, J. E. Francis, Jr., W. M. Preston, and T. W. Bonner—1266(A)
Cross sections of H, D, F, Mg, S, Si, and quartz for slow neutrons, L. J. Rainwater, W. W. Havens, Jr., J. R. Dunning, and C. S. Wu—733
Delayed neutrons from U^{238}, D. J. Hughes, J. Dabbs, A. Cahn, and D. Hall—111
Density in atmosphere, latitude dependence, J. A. Simpson, Jr.—1389(L)
Diffusion in hydrogenous media, C. W. Tittle and Clark Goodman—1264(A)
Evidence for di-neutron, D. N. Kundu and M. L. Pool—22
Fast continuous energy neutrons, V. L. Parsegian, L. V. Titone, and C. W. van der Merwe—1265(A)
High energy collisions with protons, H. S. W. Massey, E. H. S. Burhop, and Tsi-Ming Hu—1403(L)
Interaction with electrons, erratum, J. M. Jauch and K. Watson—268(L)
Laue photography, E. O. Wollan, C. G. Shull, and M. C. Marney—527(L), 1265(A)
Neutron absorption by Clinton pile oscillator, J. I. Hoover, W. H. Jordan, C. D. Moak, L. A. Pardue, H. Pomerance, J. Strong, and E. O. Wollan—1259(A)
Neutron-proton scattering formula, L. Eisenbud—1407(L)
Polarizability in electrostatic field, Kenneth M. Watson—125
Polarization in magnetized iron, D. J. Hughes, J. R. Wallace, and R. H. Holtzman—1277
Polarization of fast neutrons, Julian Schwinger—407
Recoil protons in neutron beam of 184-inch cyclotron, Wilson M. Powell—540(A)
Resonance absorption in graphite, S. Bernstein—956
Slow cross sections in O_2, N_2, A, E. Melkonian, L. J. Rainwater, W. W. Havens, Jr., and J. R. Dunning—1399(L)
Slow neutron studies of Cu, Ni, Bi, Fe, Sn, and calcite, W. W. Havens, Jr., L. J. Rainwater, C. S. Wu, and J. R. Dunning—963
Spectra from Al (αn) and Si (dn), R. A. Peck, Jr.—947
Thermal neutron absorption by separated isotopes, H. Pomerance and J. I. Hoover—1265(A)
Transmission through solid solutions, S. S. Sidhu—1264(A)
Of various elements, cross sections, Edward Melkonian—1265(A)
Velocity spectrometer studies, crystal interference and molecular binding effects, W. W. Havens, Jr., L. J. Rainwater, and C. S. Wu—1265(A)
Velocity spectrometer studies of Fe, Ni, and Cu, L. J. Rainwater, W. W. Havens, Jr., and C. S. Wu—1265(A)
Yields from photo-neutron sources, B. Russell, D. Sachs, A. Wattenberg, and R. Fields—545

Neutron Diffraction
By crystalline powders, E. O. Wollan and C. G. Shull—830
In NaH and NaD, C. G. Shull, E. O. Wollan, G. A. Morton, and W. L. Davidson—842
Laue photography of, C. G. Shull, M. C. Marney, and E. O. Wollan—1265(A)

Nuclear moments and spin (see also **Hyperfine structure**)
Of C^{14}, Arthur Roberts—1405(L)
Of chlorine, L. Davis, Jr., B. T. Feld, C. W. Zabel, and J. R. Zacharias—525(L)
Of deuterium, Aage Bohr—1109(L)
As integral multiples of a natural unit, Enos E. Witmer—1243(A)
Interpretation of triton moment, R. G. Sachs—1222(A)
Of I^{127}, Ga^{69}, Ga^{71}, and P^{31}, R. V. Pound—1112(L)
Magnetic exchange moment for He^3 and H^3, Herbert L. Anderson—919(L)
Magnetic moments of Cu^{63} and Cu^{65}, R. V. Pound—523(L)
Magnetic moment of He^3, H. L. Anderson and A. Novick—919(L)
Magnetic resonance absorption in chrome alums, C. A. Whitmer, R. T. Weidner, and P. R. Weiss—1468(L)
Measuring moments, John R. Zimmerman and Dudley Williams—94(T), 94(A)
Microwave Zeeman spectra, C. K. Jen—1248(A)
Moment of H^3 and He^3, Armin Thellung and Felix Villars—924(L)
Nuclear induction signals, Boris A. Jacobsohn and Roald K. Wangness—942
Quadrupole effects in molecules, J. Bardeen and C. H. Townes—97, 1204(L)
Quadrupole moments in asymmetric rotor molecules, J. K. Bragg—1250(A)
Quadrupole coupling of N in ICN and N_2O, A. G. Smith, Harold Ring, W. V. Smith, and Walter Gordy—633(L)
Quadrupole effects, second-order corrections, J. Bardeen and C. H. Townes—627(L)

Nuclear structure (see also **Disintegration of nucleus; Energy states of nucleus; Radioactivity**)
Of Be^9, excited state, K. E. Davis and E. M. Hafner—1473(L)
Binding energy of triton, M. Goeppert-Mayer and R. G. Sachs—185(L)
Of B^{10}, T. Lauritsen, W. A. Fowler, C. C. Lauritsen, and V. K. Rasmussen—636(L)
Charge distribution in nuclei, M. E. Rose—279, 1242(A)
Deuteron problem with Gaussian potentials, S. Moszkowski and R. G. Sachs—184(L)
Energy levels of A^{41}, Ernest Pollard and Perry W. Davison—1241(A)
Formation of elements inside stars, Gleb Wataghin—79(L)
Interactions of nucleons with meson fields, F. J. Dyson—929(L)

Nuclear structure (continued)
Interpretation of triton moment, R. G. Sachs—1222(A)
Isomer of Tc^{43}, O. Huber, P. Marmier, H. Medicus, P. Preiswerk, and R. Steffen—1208(L)
Limits of beta-stability, Truman P. Kohman—16
Of 93^{237}, Arthur C. Wahl and Glen T. Seaborg—940
Polarization correlation of gamma-rays, David L. Falkoff—518(L)
Spherical shell nuclear model, H. A. Wilson—655(A)
Spin of C^{14}, F. A. Jenkins—639(L)
Tensor forces and binding energy of triton, W. Rarita and H. Feshbach—1272(A)
Zero-zero transitions, isomers, Marvin L. Goldberger—1119(L)

Optical constants and properties
Of $BaTiO_3$, B. Matthias and A. von Hippel—268(L)
Dichroism involving aligned CH_2 groups, Leonard Glatt—535(A)
Dichroism involving hydrogen bonds, Leonard Glatt—541(A)
Fluctuations in refractivity of water, John B. Hawkes and Robert W. Astheimer—520(L)
Grazing incidence reflectors, Paul Kirkpatrick, A. V. Baez, and Allen Newell—535(A)
Melting points, rigidities, and optical activities of gelatin gels, John D. Ferry and John E. Eldridge—1225(A)
Streaming birefringence of nucleic acid, Jesse P. Greenstein—1225(A)
Optical instruments (see **Methods and instruments**)

Packing fraction (see also **Isotopes**)
Of zirconium, Wilfrid Rall—1222(A)
Phosphorescence
Excitation of infra-red phosphors by α- and β-particles, R. H. Thompson and R. T. Ellickson—185(L)
Photo-conductivity
Of inorganic crystals, detection of high energy particles, Robert J. Moon—1210(L)
Of semiconductors, use as amplifiers, Edmund S. Rittner—1212(L)
Photoelasticity
Constants of cubic crystals, E. Burstein, P. L. Smith, and B. Henvis—1262(A)
Photoelectric effect and properties; cells
Beat frequencies between visible lines, L. R. Griffin—922(L); Edward Gerjuoy, A. Theodore Forrester, and William E. Parkins—922(L)
Energy distribution from W, L. Apker, E. Taft, and J. Dickey—46
(γ, p) and (γ, m) processes, L. I. Schiff—1311
Metal semiconductor contacts, S. Benzer—1256(A)
Self-quenching counters, M. V. Scherb—86(L)
Photography
Background eradication, fading of latent image, Herman Yagoda and Nathan Kaplan—634(L)
Protective facings on Eastman emulsions, P. B. Mauer and H. L. Reynolds—1131(L)
Piezoelectric effect
Constants of monoclinic crystals, Hans Jaffe—1467(L)
In barium titanate ceramics, W. P. Mason—1398(L)
Piezoelectric effect in barium titanate, Walter L. Cherry, Jr. and Robert Adler—1230(A)
Polarization, electrical (see also **Dielectric constants**)
Neutron polarization, D. J. Hughes, J. R. Wallace, and R. H. Holtzman—1277
Polarization effects in ionization loss, Frank L. Hereford—1123(L)
Polarization of radiation
Of annihilation radiation, E. Bleuler and H. L. Bradt—1398(L)
Light scattered by macromolecular solutions, Paul Doty and S. J. Stein—1221(A)
Polymerization, properties of polymers
Disorder in linear polymers, S. T. Gross—1233(A)
Effects of pile bombardment on elastomers, W. L. Davidson and I. G. Geib—1225(A)
Elasto-viscous properties of polyisobutylene, R. D. Andrews, N. Hofman-Bang, and A. V. Tobolsky—1221(A)
Mechanical properties of polymer solutions, Thor L. Smith, John D. Ferry, and Frederic W. Schremp—1233(A)
Mechanical properties of rubber-like materials, A. W. Nolle—1232(A)
Melting points, rigidities, and optical activities of gelatin gels, John D. Ferry and John E. Eldridge—1225(A)
Surfaces of polymers, Robley C. Williams—1222(A)
Positrons
Low energy pair production, P. V. C. Hough—266(L)
Molecular systems containing a positron, Aadne Ore—1272(A)
Proceedings of the American Physical Society
Oberlin College, Ohio, Meeting November 1, 1947—94
Union College, New York, Meeting November 8, 1947—96
Los Angeles, California, Meeting January 2–3, 1948—530
New England Section, Middletown, Connecticut, Meeting November 1, 1947—542
Rice Institute, Houston, Texas, Meeting November 28–29, 1947—644
Chicago, Illinois, Meeting December 29–31, 1947—1217
New York, Annual Meeting January 29–31, 1948—1237
Protons
Recoil protons in neutron beam of 184-inch cyclotron, Wilson M. Powell—540(A)

Radiation
Annihilation, polarization of quanta, E. Bleuler and H. L. Bradt—1398(L)
Radio (see also **Ionosphere**)
Antenna current distribution, Richard C. Raymond and Wayne Webb—1248(A)
Radioactivity (see also **Disintegration of nucleus**)
Absorption of Be^{10} beta-rays, William E. Stephens and A. M. Bottoms—1269(A)
Absorption of Na^{24} gamma-radiation in Pb, Cu, and Al, David E. Alburger—344
α-particles from faces of radioactive crystals, K. B. Mather and F. N. D. Kurie—1474(L)

Alpha-rays from Sm, A. J. Dempster—1125(L)
Angular correlation of γ-rays, Edward L. Brady and Martin Deutsch—1266(A)
Of Sb^{124}, Bernard D. Kern, Daniel J. Zaffarano, and Allan C. G. Mitchell—1142
Of Sb^{124}, coincidence experiments, E. T. Jurney and Allan C. G. Mitchell—1153, 1269(A)
Of As^{76}, M. V. Scherb and C. E. Mandeville—418(L)
Beta- and gamma-rays from Sb, C. Sharp Cook and Lawrence M. Langer—1149
Beta- and gamma-rays of Ga^{72}, A. C. G. Mitchell, B. D. Kern, and D. J. Zaffarano—1220, 1431(A)
Beta-decay of Kr^{85}, recoil of nucleus, J. C. Jacobsen and O. Kofoed-Hansen—675
Beta-decay of P^{32}, correlation of neutrinos with electrons, Chalmers W. Sherwin—1219(A)
β-emission, Kurie plot, F. N. D. Kurie—1207(L)
Beta-rays detected by scintillations, George B. Collins and Rosalie C. Hoyt—1259(A)
Beta-rays of Sb, C. E. Mandeville and Morris V. Scherb —656(A)
Beta-spectra of Cu^{64} as a test of Fermi theory, C. Sharp Cook and Lawrence M. Langer—601, 1219(A)
Beta-spectrum of Au^{198}, D. Saxon—811(L)
Of Bi isotopes, α-active, D. H. Templeton and I. Perlman—1211(L)
Of B^{10}, T. Lauritsen, W. A. Fowler, C. C. Lauritsen, and V. K. Rasmussen—636(L)
C^{14} beta-ray spectrum, Margaret N. Lewis and Miriam Paul—1269(A)
C^{14} of high specific activity, L. D. Norris and Arthur H. Snell—254(L)
Of Ce and Pr, M. L. Pool and N. L. Krisberg—1035
Coincidence expriments on Sc^{46} and Au^{198}, E. T. Jurney and Margaret R. Keck—1220(A)
Comparison of the relative molecular stopping power of $_1H^1$ and of $_1D^2$, Roland W. Schmitt, T. N. Hatfield, and Arthur E. Lockenvitz—652(A)
Comparison of the relative molecular stopping power of some hydrocarbon isomers for alpha-particles from Po, Thomas E. Gibbs and Arthur E. Lockenvitz—652(A)
Coincidence measurements in Sb^{124}, E. T. Jurney and Allan C. G. Mitchell—1269(A)
Continuous γ-radiation during β-decay, C. S. Wang and D. L. Falkoff—1220(A)
Correlation between beta- and gamma-emissions, D. L. Falkoff and G. E. Uhlenbeck—649(A)
Decay of fission products, K. Way and E. P. Wigner—1318
Disintegration scheme of Cs^{134}, Kai Siegbahn and Martin Deutsch—410(L)
Energies of alpha-particles from Pu^{238} and Pu^{239}, William P. Jesse and Harold Forstat—926(L)
Existence of element 61 in nature, N. E. Ballou—630(L)
54-minute isomer of In, Morris V. Scherb and C. E. Mandeville—655(A)
Of Ga^{72}, β- and γ-rays, Allan C. G. Mitchell, Daniel J. Zaffarano, and Bernard D. Kern—1424
Of Ga^{72}, β- and γ-spectra, S. K. Haynes—187(L), 1269(A)
Gamma-radiation from granite, Victor Francis Hess and J. Donald Roll, S. J.—592, 912; Wm. D. Urry—596
Gamma-radiation from Eu, J. M. Cork, R. G. Shreffler, and C. M. Fowler—78(L)
Gamma-radiation in meson decay, E. P. Hincks and B. Pontecorvo—257(L)
Gamma-radiations from Co^{60} and Zn^{65}, Erling N. Jensen, L. Jackson Laslett, and William W. Pratt—529(L)
Gamma-radiation from Sc, Ce, and Tb, J. M. Cork, R. G. Shreffler, and C. M. Fowler—1220(A)
Gamma-rays from alpha-particle reactions, David E. Alburger—1014
Gamma-rays from Au (198), wave-length and energy measured with x-ray spectrometer, Jesse W. M. DuMond, David A. Lind and Bernard B. Watson—1392
Of Au^{198}, coincidence study, C. E. Mandeville and M. V. Scherb—634(L)
Half-life of C^{14}, L. D. Norris and M. G. Inghram—350
Internal conversion in W and Pt, M. V. Scherb and C. E. Mandeville—1401(L)
Of Ir^{192}, R. D. Hill and W. E. Meyerhof—812(L)
Of Ir^{192}, Ir^{194}, La^{140}, Sb^{124}, Zr^{95}, C. E. Mandeville and M. V. Scherb—1434
Isomers in Tm^{169} and Tm^{171}, F. K. McGowan and S. DeBenedetti—1269(A)
Isomers of Ba^{133}, Fu-Chum Yu and J. D. Kurbotov—1268(A)
Of Li^8, T. W. Bonner, J. E. Evans, C. W. Malich, and J. R. Risser—884
Maximum energies of β-emitters, L. Yaffe and Katharine M. Justus—1400(L)
Measurement of the relative molecular stopping power of gases for Po alphas, T. N. Hatfield and M. Y. Colby—652(A)
Metastable state in "even-even" nucleus, J. C. Bowe, M. Goldhaber, R. D. Hill, W. E. Meyerhof, and O. Sala—1219(A)
Of Mo^{99} and Tc^{99}, C. E. Mandeville and M. V. Scherb—847, 1270(A)
Momentum conservation in the beta-decay of P^{32}, correlation of neutrinos with electrons, Chalmers W. Sherwin—216
Multiple nuclear isomerism, E. Der Mateosian, M. Goldhaber, C. O. Muehlhause, and M. McKeown—1219(A)
Neutron induced activities in Er, B. H. Ketelle and W. C. Peacock—1269(A)
Of 93^{237}, Arthur C. Wahl and Glenn T. Seaborg—940
Polarization correlation of gamma-rays, David L. Falkoff—518(L)
Positron-electron ratio in Cu^{64}, L. Cranberg and J. Halpern—259(L), 1269(A)
Of K^{40}, decay scheme, Hans E. Suess—1209(L)
Properties of Ta^{182}, C. E. Mandeville and Morris V. Scherb—656(A)
Radiations from Sb^{124}, M. V. Scherb and C. E. Mandeville—1268(A); C. Sharp Cook and Lawrence M. Langer—1268(A); Bernard D. Kern, Daniel J. Zaffarano and Allan C. G. Mitchell—1268(A)
Of Re, S. N. Naldrett and W. F. Libby—487; 929(L); Nathan Sugarman and Harold Richter—1411(L)
Of Sc^{46}, C. E. Mandeville and Morris V. Scherb—648(A)

Radioactivity (continued)
Of Sc^{46} and Ti^{51}, C. E. Mandeville and Morris V. Scherb—141
Of Se^{73} and Se^{75}, William S. Cowart and M. L. Pool—1223(A)
Se^{73} and Se^{75}, artificially radioactive, William S. Cowart, M. L. Pool, D. A. McCown, and L. L. Woodward—1454
7-second Au^{197} isomer, H. Frauenfelder, P. C. Gugelot, O. Huber, H. Medicus, P. Preiswerk, P. Scherrer, and R. Steffen—1270(A)
72-day isomer of Ti^{51}, C. E. Mandeville and Morris V. Scherb—654(A)
62-day Tc isotope, O. Huber, H. Medicus, P. Preiswerk, and R. Steffen—1211(L)
Surplus gamma-radiation from rocks, Victor Francis Hess and J. Donald Roll, S. J. —1239(A)
Of Ta^{182}, Sb^{122}, and In^{116}, C. E. Mandeville and Morris V. Scherb—340
Of Tc isotopes, E. E. Motta and G. E. Boyd—1470(L)
Of Te and Sb, M. Lindner and I. Perlman—1124(L)
Of 2.70-day Au^{198}, Paul W. Levy and E. Greuling—83(L)
Weak natural radioactives, Truman P. Kohman—1223(A)
X-ray yield curves for $\gamma-n$ reactions, G. C. Baldwin and G. S. Klaiber—1156(A)
Of Y 90, beta-decay, Chalmers W. Sherwin—1173
Raman spectra
Of hexamethylethane, Richard W. Mitchell and Forrest F. Cleveland—653(A)
Range of particles
Of β-radiation from Ca^{45}, A. K. Solomon and L. E. Glendenin—415(L)
$D+D$ cross sections, A. P. French—1474(L)
Of $Ra-\alpha-Be$ neutrons in water, J. T. Rush—271
Range-energy relations for protons in C, H, O, A, and Xe, J. O. Hirschfelder and J. L. Magee—207
Rectifier (see **Electrical conductivity and resistance**)
Relativity
Discrete space-time and integral Lorentz transformation, A. Schild—414(L)
Equivalence principle and blind navigation, John J. Gilvarry—1409(L)
Extension of Dirac's equation, E. L. Hill—907
Foundation of Birkhoff's theory of gravitation, Carlos Graef Fernandez—651(A)
Generalized theory of gravitation, A. Papapetrou—1105
Mass-energy relation, W. F. G. Swann—1270(A)
Relativistic quantum mechanics, Hartland S. Snyder—524(L)
Resonance radiation
Imprisonment in gas discharges, T. Holstein—1245(A)
Of K, violet asymmetry, Shang-yi Ch'en—1470(L)

Scattering of electrons, neutrons, and ions (see also **Electron diffraction cross section**)
C^{12} $(n, 2n)$ C^{11} at 90 Mev, Edwin M. McMillan and Herbert F. York—262(L)
Correlated probabilities in multiple scattering, W. T. Scott and H. S. Snyder—1260(A)
$D+D$ cross sections, A. P. French—1474(L)
Determinations of XR for high energy particles, F. T. Rogers, Jr.—656(A)
Of fast neutrons by Fe, Pb, and Bi, L. Szilard, S. Bernstein, B. Feld, and J. Ashkin—1307
Of fast neutrons by Hg, G. C. Phillips and J. C. Harris—649(A)
Of high energy electrons, M. E. Rose—279
Of high energy neutrons, A. Bratenahl, R. H. Hildebrand, and B. J. Moyer—540(A)
Inelastic scattering of protons, Kenneth E. Davis and Everett M. Hafner—1473(L)
Ionization loss of fast charged particles, Otto Halpern and Harvey Hall—477
Milne problem for a sphere, T. H. Berlin—437
Monoenergetic neutrons on sulfur, E. D. Klema and A. O. Hanson—106
$N-p$ scattering, angular distribution, J. Hadley, E. L. Kelly, C. E. Leith, E. Segrè, C. Wiegand, and H. F. York—1114(L)
Neutron-proton scattering at high energies, G. F. Chew and M. L. Goldberger—1409(L)
Neutron-proton scattering formula, S. Flügge and E. Hückel—520(L); Ta-You Wu and Henry M. Foley—1117(L)
Neutron-proton and proton-proton scattering at high energies, Julius Ashkin and Ta-You Wu—973
Neutron-proton scattering at 90 Mev, J. Hadley, C. Leith, H. York, E. Kelly, and C. Wiegand—541(A)
Neutron-proton scattering at 100 Mev, Julian Eisenstein and Fritz Rohrlich—641(L), 1411(L)
Neutron-proton scattering formula, L. Eisenbud—1407(L)
Neutron-proton scattering, range of nuclear forces, Ta-You Wu—1132(L)
Of neutrons by protons, J. S. Laughlin and P. G. Kruger—649(A)
Of neutrons by protons, 12–13 Mev, J. S. Laughlin and P. G. Kruger—197
Of neutrons by protons, 20–80 Mev, M. Camac and H. A. Bethe—191
Of neutrons, from protons, high energy, H. S. W. Massey, E. H. S. Burhop, and Tsi-Ming Hu—1403(L)
Of 100–200 Mev protons or neutrons by deuterons, Ta-You Wu and Julius Ashkin—986
Phase-shift analysis, scattering of protons by deuterons, Charles L. Critchfield—1
Proton-neutron and proton-proton scattering, second Born approximation, Ta-You Wu—934
Proton-proton scattering at 2.4 and 3.0 Mev, William Sleator, Jr., J. M. Blair, E. E. Lampi, and J. H. Williams—1241(A)
Proton-proton scattering at 7 Mev, I. H. Dearnley, C. L. Oxley, and J. E. Perry, Jr.—1290
Proton-proton scattering, sensitivity to change in potential, G. Breit, A. A. Broyles, and M. H. Hull—870
Of protons by deuterons, H. S. W. Massey and R. A. Buckingham—260(L)
Of protons, energy distribution, Warren W. Chupp, Eugene Gardner, and T. B. Taylor—742

Of protons, excited state of Be^9, K. E. Davis and E. M. Hafner—1473(L)
Proton scattering by Be, George S. Kenny and Sylvan Rubin—536(A); R. G. Thomas, W. A. Fowler, and C. C. Lauritsen—536(A)
Range of forces, neutron-proton triplet interaction, C. G. Shull, E. O. Wollan, G. A. Morton, and W. L. Davidson—262(L)
Resonance reactions, Dirac-type incident particles, G. Goertzel—1463
Scattering by attractive center varying inversely as cube of distance, H. A. Wilson—655(A)
Sensitivity of proton-proton scattering, G. Breit, A. A. Broyles, and M. H. Hull—1242(A)
Scattering of radiation (see also **Raman spectra**)
Angular correlation of annihilation radiation, Hartland Snyder, Simon Pasternack, and J. Hornbostel—440
Light scattered by macromolecular solutions, depolarization, Paul Doty and S. J. Stein—1221(A)
Penetration of gamma-radiation, Klein-Nishina scattering, J. O. Hirschfelder, J. L. Magee, and M. H. Hull—852
Penetration of gamma-radiation, photoelectric effect, and pair production in Fe and Pb, J. O. Hirschfelder and Edward N. Adams II—863
Scattering by a plane-parallel atmosphere, S. Chandrasekhar—1233(A)
Semiconductors (see **Electrical conductivity and resistance**)
Shock waves (see also **Explosion phenomena**)
Spark shadowgrams of spheres at supersonic speeds, J. Howard McMillen and R. L. Kramer—1255(A)
Velocity loss of shocks traveling in a tube, R. J. Emrich and F. B. Harrison—1255(A)
Solid state (see **Crystalline state**)
Sound (see **Acoustics**)
Spark discharge (see **Discharge of electricity,** etc.)
Spectra, absorption (see also **Absorption of radiation**)
Absorption spectrum of phenol, substitution of deuterium, W. W. Robertson, F. A. Matsen, and A. J. Seriff—652(A)
Of active nitrogen, R. Edwin Worley—531(A)
Of COSe, M. W. P. Strandberg and T.Wentink—1249(A)
Lorentz-Lorenz correction in ultraviolet absorption, Lois E. Jacobs and J. R. Platt—1234(A)
R-f absorption lines in solids, J. H. Van Vleck—1229(A)
Solar wave-lengths in extreme ultraviolet, K. C. Clark—1250(A)
Water of crystallization and absorption bands of neodymium bromate crystals, Arnold Benton and E. L. Kinsey—536(A)
Spectra, atomic
Displacement of energy levels, H. A. Bethe—1271(A); F. J. Dyson—617, 1272(A); Julian Schwinger and Victor Weisskopf—1272(A); T. A. Welton—1271(A)
Fine structure of He II λ4686, J. E. Mack and N. Austern—1233(A)
He line λ1640, G. R. Fowles—639(L)
Of Np^{237}, fine structure, F. S. Tompkins—1214(L)
Of N, isotope shifts in, John R. Holmes—539(A)
Of K, violet asymmetry, Shang-yi Ch'en—1470(L)
Rydberg-Ritz formula in quantum mechanics, Robert Jastrow—60
Structure of Hg band λ2540, S. Mrozowski—1233(A)
Spectra, general
Observing beat frequencies, Arthur Ruark—181(L)
Of the sun; V-2 rockets, John J. Hopfield and Harold E. Clearman, Jr.—876
Spectra, microwave
Absorption spectrum of COSe, M. W. P. Strandberg and T. Wentink—1249(A)
Of ammonia, Robert Karplus—1120(L)
Of chromic alum, P. R. Weiss—470
Collision and saturation broadening, Hartland S. Snyder and Paul I. Richards—1178
Collision broadening absorption, saturation effects, Robert Karplus and Julian Schwinger—1020
Ferromagnetic resonance absorption, Charles Kittel—155
Frequency modulation, Robert Karplus—1027
Inversion spectrum of NH_3, James W. Simmons and Walter Gordy—713
Magnetic field of a rotating molecule, G. C. Wick—51
Of microwave resonance lines, Paul I. Richards and Hartland S. Snyder—269(L)
Minimum detectable absorption, W. D. Hershberger—1249(A)
Nuclear quadrupole effects in molecules, J. Bardeen and C. H. Townes—97
Quadrupole interaction in ICl, Richard T. Weidner—254(L)
Rotational spectrum of ICl, C. H. Townes, B. D. Wright, and F. R. Merritt—1249(A)
Saturation effect of ammonia, Robert L. Carter and William V. Smith—1053
Stark effect in COSe molecule, T. Wentink, Jr., M. W. P. Strandberg, and R. Hilger—1249(A)
Stark splitting, absorption in paramagnetic salts, C. Kittel and J. M. Luttinger—162
Width of lines in cupric salts, theory, J. H. Van Vleck—1249(A)
Spectra, molecular (see also **Molecular structure and constants**)
Anomalies in phosphine and arsine, Virginia M. McConaghie and Harald H. Nielsen—1250(A)
Of heavy water vapor, infra-red, Fred P. Dickey and Harald H. Nielsen—1164
Magnetic field of a rotating molecule, G. C. Wick—51
Of CH_4, in Fraunhofer spectrum, Robert R. McMath, Orren C. Mohler, and Leo Goldberg—1203(L)
Nuclear quadrupole moments in asymmetric rotor molecules, J. K. Bragg—1250(A)
Of $OC^{14}S$, rotational, spin of C^{14}, Arthur Roberts—1405(L)
Quadrupole interactions on nuclear radiofrequency spectra, Norman F. Ramsey—1243(A)
Rotational spectrum of ICl, C. H. Townes, F. R. Merritt, and B. D. Wright—1334, 1249(A)
Stark spectrum of HDO, M. W. P. Strandberg, T. Wentink, Jr., R. E. Hillger, Gregory H. Wannier, and Murray L. Deutsch—188(L)

Spectra, molecular (continued)
Stark spectrum of H_2O, S. Golden, T. Wentink, R. Hilger, and M. W. P. Strandberg—92(L)
Ultraviolet band system of O_2^+, Lalji Lal—255(L)
Ultraviolet spectra of benzene and borazole, molecular orbital treatment, C. C. J. Roothaan and R. S. Mulliken—1234(A)
Spectroscopy, technique
Photo-tubes in ultraviolet fluorescence, Robert D. Cowan—1234(A)
Production of pure Hg^{198}, Paul Bradt and Fred L. Mohler—925(L)
Stark effect
In COSe molecule, T. Wentink, Jr., M. W. P. Strandberg, and R. Hillger—1249(A)
In diatomic molecules, W. A. Nierenberg, I. I. Rabi, and M. Slotnick—1430
In high frequency fields, F. R. Merritt and C. H. Townes—1249(A)
Stark modulation method, W. D. Hershberger—1249(A)
Stark spectrum of HDO, M. W. P. Strandberg, T. Wentink, Jr., R. E. Hillger, Gregory H. Wannier, and Murray L. Deutsch—188(L)
Superconductivity (see **Electrical conductivity and resistance**)
Surface phenomena
Emissivity of beryllium oxide, Ralph L. Seifert—1181

Thermal diffusion
Of nitrogen, Alfred K. Mann—412(L)
Separation of Ne isotopes, F. K. Elder, Jr.—1263(A)
Thermal expansion
X-ray determination of coefficients of crystals, M. Y. Colby and L. F. Connell, Jr.—653(A)
Thermionic emission; Emitting surfaces
Of chromium, H. B. Wahlin—1458
Decay of Ba−Sr oxide cathodes, W. E. Danforth and W. E. Ramsey—1244(A)
Emittance of materials used as anodes, A. D. Power—1246(A)
Of oxide-coated filaments, Harold Jacobs, George Hees, and Walter Crossley—1244(A)
Mechanism of emission at arc cathode, Jerome Rothstein—1214(L)
Thermionic emission of oxide-coated cathodes in gaseous conduction devices, W. F. Hodge—95(A)
Workfunctions of a gas-coated surface, G. L. Weissler and R. W. Kotter—538(A)
Thermodynamics
Of irreversible processes, elasticity and anelasticity, Carl Eckart—373
Second law, equation of state, J. L. Finck—655(A)
Of strained elastomer, L. E. Copeland and M. Mooney—1224(A); M. Mooney—1224(A)
Work, heat, and temperature concepts, J. L. Finck—1267(A)
Thermoelectric effects
Onsager's reciprocal relations, Herbert B. Callen—1349
Thermomagnetic effects
Onsager's reciprocal relations, Herbert B. Callen—1349
Semiconductors at high temperature, V. A. Johnson and K. Lark-Horovitz—1257(A)
In tellurium, Wayne Scanlon and K. Lark-Horovitz—1256(A)
Thermomagnetic and galvanomagnetic coefficients, H. B. Callen—1248(A)

Ultrasonics, (see also **Acoustics**)
In Sn, observation of twinning, W. P. Mason, H. J. McSkimin, and W. Shockley—1213(L)

van der Waals forces
Influence of retardation on the London-van der Waals forces, H. B. G. Casimir and D. Polder—360
Viscosity
Bulk viscosity of liquids, L. N. Liebermann—537(A)
Of glass, Howard A. Robinson and Edward M. Man, Jr. 1222(A)
Of nucleic acid, Jesse P. Greenstein—1225(A)

Wave guide (see **Electromagnetic theory** and **Electrical circuits**)
Wave motion
Refraction of waves from point source, E. Gerjuoy—1442
Waves of finite amplitude, Antonio Romero Juarez, 654(A)
Work function (see **Thermionic emission; Photoelectric effect**)

X-rays, absorption, diffraction, scattering, reflection, refraction, and polarization
Achromatization of Debye-Scherrer lines, H. Ekstein and S. Siegel—1207(L)
Diffraction camera, high temperature, James W. Edwards, Rudolph Speiser, and Herrick L. Johnston—1251(A)
Diffraction from coarse powders, Zigmond W. Wilchinsky—1251(A)
Fourier equations for x-ray studies, Dan McLachlan, Jr.—539(A)
Small-angle scattering, apparatus geometry, Harry H. Hubbell, Jr.—1251(A)
Small-angle scattering, intensity distribution, John Turkevich and Harry H. Hubbell, Jr.—1250(A)
X-rays, emission (see also **X-rays, spectra** and **spectroscopy,** etc.)
Of element 43, L. E. Burkhart, W. F. Peed, and B. G. Saunders—347
X-ray yield, $\gamma-n$ reactions, G. C. Baldwin and G. S. Klaiber—1156
X-rays, spectra and spectroscopy, wave-length measurements (see also **X-rays, emission**)
Wave-length and energies of γ-rays from Au^{198}, Jesse W. M. DuMond, David A. Lind, and Bernard B. Watson—1392(L)
X-rays, tubes, apparatus
Microphotometer for x-ray diffraction diagrams, R. Pepinsky and H. I. West, Jr.—1235(A)
X-ray optical images, Paul Kirkpatrick and A. V. Baez—1234(A)

Zeeman effect
Microwave Zeeman spectra, C. K. Jen—1248(A)

JUN 21 1948

THE PHYSICAL REVIEW

VOLUME 73 Second Series NUMBER 12

JUNE 15, 1948

Published for the

AMERICAN PHYSICAL SOCIETY

by the

AMERICAN INSTITUTE OF PHYSICS

Incorporated

LANCASTER, PA., AND NEW YORK, N. Y.

THE PHYSICAL REVIEW

A journal of experimental and theoretical physics established by E. L. Nichols in 1893

Published by the American Institute of Physics for the

AMERICAN PHYSICAL SOCIETY

Officers

President

J. R. OPPENHEIMER
Institute for Advanced Study
Princeton, New Jersey

Vice-President

F. W. LOOMIS
University of Illinois
Urbana, Illinois

Secretary

K. K. DARROW
Bell Telephone Laboratories
Office:
Columbia University
New York 27, New York

Treasurer

G. B. PEGRAM
Columbia University
New York 27, New York

Local Secretary for the Pacific Coast

J. KAPLAN
University of California at Los Angeles
Los Angeles, California

Editor

JOHN T. TATE
University of Minnesota
Minneapolis, Minnesota

BOARD OF EDITORS

Editor

JOHN T. TATE

Assistant Editor

J. W. BUCHTA

Associate Editors

E. J. KONOPINSKI	H. A. BETHE	S. A. GOUDSMIT
H. H. NIELSEN	L. A. RIENHOUR	E. M. PURCELL
E. C. POLLARD	W. H. ZACHARIASEN	V. F. WEISSKOPF

Manuscripts for publication should be submitted to John T. Tate, University of Minnesota, Minneapolis, Minnesota.

Proof and all correspondence concerning papers in the process of publication should be addressed to the Publication Manager, American Institute of Physics, 57 East 55 Street, New York 22, New York.

Subscription Price

United States and Canada $15.00
Elsewhere $16.50

Back Numbers

Complete set: Series 2,[1] Vol. 1, 1913–Vol. 72, 1947—$630.00
Yearly rate: $20.00
Single copies: $2.00 each, prior to July, 1929;
$1.00 each, July, 1929–December, 1941;
$2.00 each, January, 1942–December, 1946.
Current issues: $1.00 each.

Subscriptions and orders for back numbers should be addressed to Prince and Lemon Streets, Lancaster, Pennsylvania, or to the American Institute of Physics, 57 East 55 Street, New York 22, New York.

Changes of address in the case of members of the American Physical Society should be addressed to the Treasurer; in the case of other subscribers to the Business Manager, American Institute of Physics.

[1] For Series 1 inquire of Physics Department, Cornell University, Ithaca, New York.

The Physical Review is published semi-monthly at Prince and Lemon Streets, Lancaster, Pennsylvania.

Entered as second-class matter March 6, 1947, at the Post Office at Lancaster, Pennsylvania, under the Act of March 3, 1879.

Acceptance for mailing at special rate of postage provided for in paragraph 4, section 538, P. L. & R., authorized January 27, 1933.

THE AMERICAN INSTITUTE OF PHYSICS

INCORPORATED

57 East 55 Street New York 22, N.Y.

MEMBER SOCIETIES:

American Physical Society

KARL K. DARROW, *Secretary*, Columbia University, New York 27, New York.

Optical Society of America

ARTHUR C. HARDY, *Secretary*, Massachusetts Institute of Technology, Cambridge 39, Massachusetts.

Acoustical Society of America

WALLACE WATERFALL, *Secretary*, 350 Fifth Avenue, 64th floor, New York 1, New York.

Society of Rheology

EARL K. FISCHER, *Secretary*, Institute of Textile Technology, Charlottesville, Virginia.

American Association of Physics Teachers

C. J. OVERBECK, *Secretary*, Northwestern University, Evanston, Illinois.

AFFILIATED SOCIETIES:

American Society for X-Ray and Electron Diffraction

Electron Microscope Society of America

Physical Society of Pittsburgh

Physics Club of Chicago

Physics Club of Philadelphia

Cleveland Physics Society

Physics Club of the Lehigh Valley

ASSOCIATES:

Over seventy-five leading industrial enterprises and other institutions which contribute to the support of the Institute.

JOURNALS:

The Physical Review

Reviews of Modern Physics

JOHN T. TATE, *Editor*—J. W. BUCHTA, *Assistant Editor*, University of Minnesota, Minneapolis, Minnesota.

Journal of the Optical Society of America

GEORGE R. HARRISON, *Editor*, Massachusetts Institute of Technology, Cambridge, Massachusetts.

The Journal of the Acoustical Society of America

FLOYD A. FIRESTONE, *Editor*, 3318 Fessenden Street, N.W., Washington, D. C.

American Journal of Physics

DUANE ROLLER, *Editor*—JOSEPH D. ELDER, *Assistant Editor*, Wabash College, Crawfordsville, Indiana.

The Review of Scientific Instruments

GAYLORD P. HARNWELL, *Editor*, Randal Morgan Laboratory of Physics, University of Pennsylvania, Philadelphia, Pennsylvania.

The Journal of Chemical Physics

JOSEPH E. MAYER, *Editor*, Kent Chemical Laboratory, University of Chicago, Chicago 37, Illinois.

Journal of Applied Physics

ELMER HUTCHISSON, *Editor*, Case Institute of Technology, Cleveland 6, Ohio.

Physics Today

DAVID A. KATCHER, *Editor*, American Institute of Physics, 57 East 55 Street, New York 22, New York.

OFFICERS

GEORGE R. HARRISON, *Chairman*
Massachusetts Institute of Technology

WALLACE WATERFALL, *Secretary*
The Celotex Corporation

GEORGE B. PEGRAM, *Treasurer*
Columbia University

JOHN T. TATE,
Adviser on Publications
University of Minnesota

GOVERNING BOARD

LUIS W. ALVAREZ
ROBERT B. BRODE
E. U. CONDON
A. J. DEMPSTER
W. F. FAIR, JR.
HARVEY FLETCHER
R. C. GIBBS
GEORGE R. HARRISON
W. V. HOUSTON
PAUL E. KLOPSTEG
F. W. LOOMIS
PHILIP M. MORSE
GEORGE B. PEGRAM
A. H. PFUND
JOHN T. TATE
WALLACE WATERFALL
M. W. WHITE
A. G. WORTHING

ADMINISTRATIVE STAFF

HENRY A. BARTON, *Director*

CLEVELAND NORCROSS,
Assistant Director

RUTH F. BRYANS,
Publication Manager

THEODORE VORBURGER,
Business Manager

THE American Institute of Physics was founded in 1931 as a federation of leading societies in the field of Physics. It combines into one operating agency those functions on behalf of physics which can best be done by the Societies jointly. Its purpose is the advancement and diffusion of physics and its applications to human welfare. To this end it publishes for itself or the Societies the eight journals listed on this page; promotes unity and effectiveness of effort among all who are interested in physics; renders numerous direct services to physicists and to the public; and cooperates with government agencies, national associations, educational institutions, technical industries, and others in such manner as to realize the opportunities and fulfill the responsibilities of physics as an important and constructive human activity.

CONTENTS

THE PHYSICAL REVIEW SECOND SERIES, VOL. 73, NO. 12 JUNE 15, 1948

Compact Electrostatic Generator for the Production of Positive Ions . . . . . W. E. DANFORTH, E. L. HUDSPETH, C. E. MANDEVILLE, AND C. P. SWANN 1413

Cosmic-Ray Investigations on Mt. McKinley . . . . . THOMAS D. CARR, MARCEL SCHEIN, AND IAN BARBOUR 1419

Beta- and Gamma-Rays of Ga^{72} . . . . . ALLAN C. G. MITCHELL, DANIEL J. ZAFFARANO, AND BERNARD D. KERN 1434

Note on the Stark Effect in Diatomic Molecules . . . . . W. A. NIERENBERG, I. I. RABI, AND M. SLOTNICK 1430

Study of the Radiations from Iridium (194), Iridium (192), Lanthanum (140), Antimony (124), and Zirconium (95) . . . . . C. E. MANDEVILLE AND M. V. SCHEER 1434

Refraction of Waves from a Point Source into a Medium of Higher Velocity . . E. GERJUOY 1442

On Temperature Dependence of Penetration Depth in Superconductors . . . . . JULES DE LAUNAY AND M. C. STEELE 1450

Artificially Radioactive Se^{77} and Se^{81} . . . . . W. S. COWART, M. L. POOL, D. A. MCCOWN, AND L. L. WOODWARD 1456

Thermionic Properties of Chromium . . . . . H. B. WAHLIN 1458

Mechanical Properties of NaCl, KBr, KCl . . . . . J. K. GALT 1460

Resonance Reactions Involving Dirac-Type Incident Particles . . . . . G. GOERTZEL 1463

Letters to the Editor:

Compressional Piezoelectric Coefficients of Monoclinic Crystals . . . . . HANS JAFFE 1467

Remarks on Diamond Crystal Counters . . . . . KATHLEEN LONSDALE 1467

Pair Production by γ-Rays in the Field of an Electron . . . . . VÁCLAV VOTRUBA 1468

Diagnetic Resonance Absorption in Diluted Chromic Alums . . . . . C. A. WHITMER, R. T. WEIDNER, AND P. R. WEISS 1468

Violet Asymmetry of Potassium Resonance Lines under High Rubidium Vapor Pressures . . . . . SHANG-YI CH'EN 1470

Production of New Te Activities from Separated Mo Isotopes . . E. E. MOTTA AND G. E. BOYD 1470

Identification of Beta-Rays with Atomic Electrons . . . . . M. GOLDHABER AND GERTRUDE SCHARFF-GOLDHABER 1472

Excited State of Be^9 by Inelastic Scattering of Protons . . . . K. E. DAVIS AND E. M. HAFNER 1473

Effect of the Composition of the Gas Mixture in Self-Quenching Geiger-Mueller Tubes on Their Plateau Characteristics . . . . . S. J. DU TOIT 1473

Emission of Alpha-Particles from Different Faces of a Radioactive Crystal . . . . . K. B. MATHUR AND F. N. D. KURIE 1474

D+D Cross Section at Low Energies . . . . . A. P. FRENCH 1474

Ferromagnetic Domain Observation . . . . . L. MARSON 1475

Optimum Conditions for a Beta-Ray Solenoid Spectrometer . . . . . E. PERSICO 1475

Measurements of Radio Frequency Resonance of a Piece of Calcareous Fluoride through the Transition . . . . . J. V. LEBACQZ 1476

Variation of Penetrating Showers with Altitude . . . . . JOHN TINLOT 1476

Author Index to Volume 73 1478

Analytic Subject Index to Volume 73 1498

Volume Table of Contents iii

LANCASTER PRESS, INC., LANCASTER, PA.